EBRAINS SUMMIT 2025

Book of Abstracts

Presented during Poster Session
at 17:15 CET on 10 December

EBRAINS Summit 2025: Book of Abstracts

Please note: six abstracts were either withdrawn or rejected during the review process, leading to four entries (numbers 1, 4, 37, 42, 47 and 53) being shown as “N/A” (not applicable).

Contents

EBRAINS 2.0 has received funding from the European Union's Research and Innovation Program Horizon Europe under Grant Agreement No. 101147319

1. N/A

2. Neuroprotective Mechanisms of an Iridoid Glycoside from Rehmanniae Radix in an MPP+-Induced Cellular Model of Parkinson's Disease

Han-Bin Yang[1], Shih-Ya Hung[1,2]

[1]Graduate Institute of Acupuncture Science, China Medical University, Taiwan
[2]Division of Surgery, Department of Medical Research, China Medical University, Taiwan

Introduction:
Parkinson's disease (PD) is a progressive neurodegenerative disorder characterized by dopaminergic neuronal loss in the substantia nigra, mitochondrial dysfunction, and oxidative stress. Current treatments are symptomatic and do not halt disease progression. Catalpol, an iridoid glycoside derived from Rehmannia glutinosa, has shown neuroprotective properties in dementia, but its effects in PD remain unclear. This study aimed to investigate the therapeutic potential and underlying mechanisms of catalpol in a cellular PD model.

Methods:
We employed SH-SY5Y cells treated with 1-methyl-4-phenylpyridinium (MPP^+) to mimic PD-related neurotoxicity. Catalpol was administered at varying concentrations to assess its neuroprotective effects. Cell viability, expression of autophagy-related proteins (Beclin 1, LC3-II, p62), mitophagy analysis, and nuclear translocation of the antioxidant transcription factor Nrf2 were evaluated using immunoblotting and fluorescence microscopy.

Results:
Catalpol treatment dose-dependently reduced MPP^+-induced cytotoxicity and enhanced autophagic activity, as indicated by increased Beclin 1 and LC3-II expression and p62 degradation. Moreover, catalpol restored MPP^+-suppressed mitophagy and promoted Nrf2 nuclear translocation, suggesting activation of antioxidant defenses.

Discussion:
These results indicate that the catalpol protects dopaminergic-like SH-SY5Y cells from MPP^+ toxicity through coordinated modulation of autophagy, mitophagy, and Nrf2-mediated antioxidant pathways. The findings support its potential as a preventive strategy against PD-related neuronal damage. Future work will assess efficacy in animal models to validate translational potential.

Keywords:
Parkinson's disease; Autophagy; Mitophagy; Nrf2; Neuroprotection

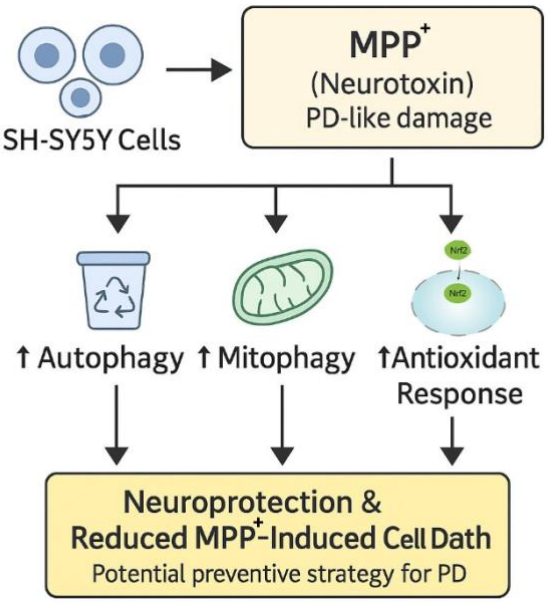

Figure 1. Schematic representation of catalpol's neuroprotective effects in an MPP^+- induced SH-SY5Y cellular model of Parkinson's disease. Catalpol pretreatment attenuates MPP^+-induced cytotoxicity by enhancing autophagy (↑ Beclin 1, ↑ LC3-II, ↓ p62), restoring mitophagy, and promoting Nrf2 nuclear translocation, thereby reducing oxidative stress and preserving dopaminergic-like neuronal integrity.

3. Towards a Multilayer BIDS MoBI Framework for Dance, Music, and Cultural Neuroscience

A. J. Aguilar-Herrera[1], J. L. Contreras-Vidal[1]

[1]IUCRC BRAIN, Cullen College of Engineering, University of Houston

Introduction. Mobile Brain/Body Imaging (MoBI) is transforming neurotechnology by enabling the study of neural dynamics in real-world, embodied, and culturally grounded environments. Unlike traditional laboratory paradigms, it captures brain activity and other physiological and non-physiological variables during naturalistic behaviors, including artistic performance, social interaction, and community-based rituals where movement, emotion, and narrative are deeply interwoven. Yet existing standards such as the Brain Imaging Data Structure (BIDS) and its Hierarchical Event Descriptor (HED) schema remain limited. While BIDS supports conventional EEG and fMRI, it does not capture the multimodal richness of the performing arts. HED encodes events but lacks ontological depth to represent symbolic meaning, choreographic structure, or cultural context. This gap restricts integration of neurophysiological signals with the cultural and emotional dimensions central to dance, music, and theater.

Methods. We propose a multilayer annotation framework that expands BIDS and HED for culturally embedded MoBI research. The framework incorporates synchronized audiovisual data, semantically structured motion tagging, and temporally aligned multimodal streams—including EEG, physiological signals, video, audio, and motion capture. To represent expressive qualities of performance, we embed Laban Movement Analysis (LMA) constructs such as effort, shape, flow, and intention. In addition, OWL-based ontologies (e.g., Labanotation, Motif notation, indigenous gesture taxonomies) and digital humanities standards (e.g., Text Encoding Initiative schemas, narrative timelines) are integrated to enable semantic richness. The framework defines five interpretive layers: (1) physical kinematics/kinetics (movement features), (2) choreographic structure (formal organization), (3)

symbolic meaning (metaphorical or ritual significance), (4) cultural context (community, tradition, intention), and (5) expressive movement quality (affective and intentional dimensions).
Results. The multilayer framework provides modular, interoperable annotation of MoBI datasets, aligning neural, physiological, and behavioral signals with choreographic and cultural semantics. Each interpretive layer can be indexed independently or combined, supporting cross-modal synchronization and comparative analysis. The framework enables fine-grained study of embodied cognition, emotional nuance, and social interaction during group performance. By generating machine-readable metadata with ontological grounding, it supports interoperability across datasets, facilitates machine learning in arts-based neuroscience, and makes cultural and symbolic dimensions visible. Early applications show that choreographic timelines, expressive LMA features, and cultural markers can be represented alongside EEG and motion data thus providing critical contextual information to interpret the data.
Discussion. This framework charts a new standard for MoBI in the arts and humanities, balancing scientific rigor with cultural sensitivity. It addresses technical gaps by enabling audiovisual integration, semantically structured motion tagging, and ontological representation of meaning. Beyond enhancing analysis, it supports respectful engagement with traditional knowledge systems by making cultural context machine-readable without oversimplification. The framework also opens pathways for including marginalized artistic and cultural practices within neurotechnology standards, promoting diversity and inclusivity in neuroscience. To ensure adoption and interoperability, we are working with BIDS, HED, and ontology-development stakeholders so cultural and artistic dimensions are embedded within established standards. This work advances the convergence of neuroscience, digital humanities, and the arts, while contributing practical solutions to current debates on ethics, inclusivity, and cultural representation in neurotechnology.

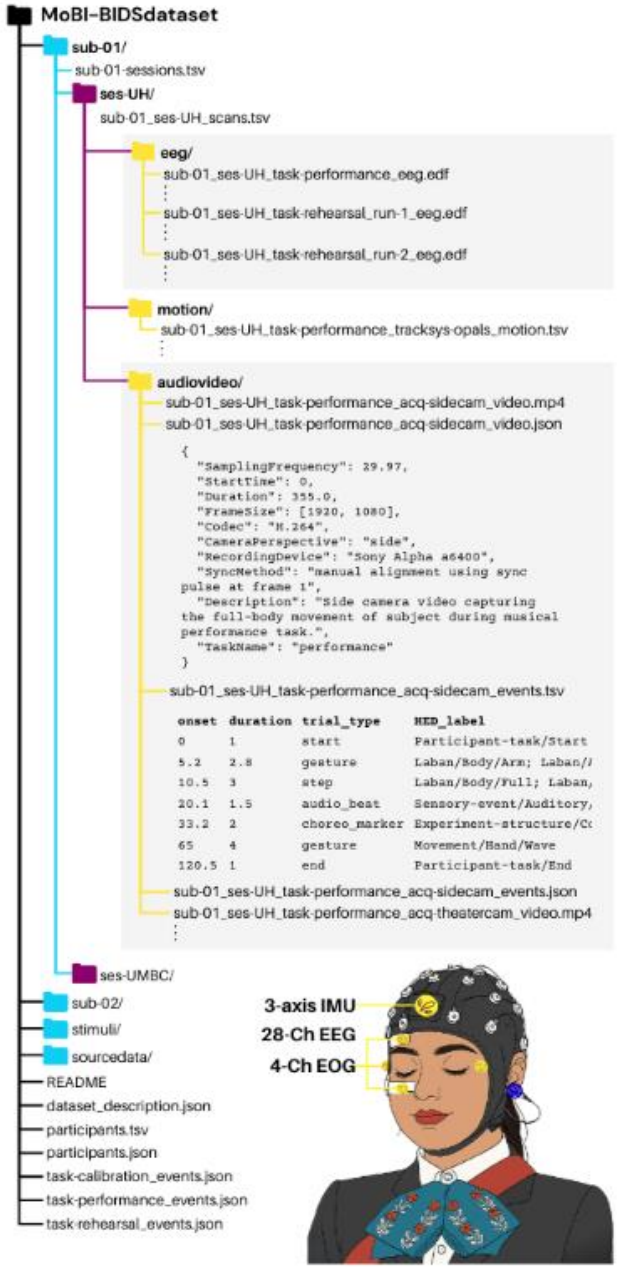

Figure 1. Schematic overview of the proposed multilayer annotation framework extending BIDS and HED for MoBI. The structure aligns multimodal data streams with a five-layer annotation hierarchy, supporting integration of kinematics, choreographic structure, symbolic meaning, cultural context, and expressive qualities. This design establishes a standards-compatible data model for interoperable storage and analysis of complex performance datasets.

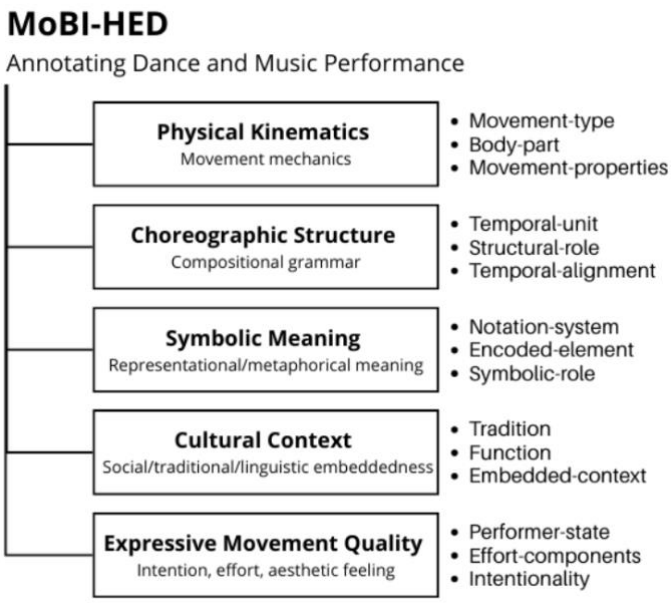

Figure 2. MoBI-HED: Annotating Dance and Music Performance. Implementation of HED extensions for MoBI-specific use cases in dance and music. The schema supports synchronized annotation of discrete and continuous events across multiple modalities, with descriptors spanning movement primitives, choreographic units, symbolic and cultural markers, and expressive dynamics. Encoded in machine-readable form, these annotations facilitate automated parsing, search, and cross-study comparison within the BIDS ecosystem.

References

1. Hermes, D., Pal Attia, T., Beniczky, S. et al. Hierarchical Event Descriptor library schema for EEG data annotation. Sci Data 12, 1448 (2025). https://doi.org/10.1038/s41597-025-05791-2
2. Robbins K, Truong D, Appelhoff S, Delorme A, Makeig S. Capturing the nature of events and event context using hierarchical event descriptors (HED). Neuroimage. 2021 Dec 15;245:118766. doi: 10.1016/j.neuroimage.2021.118766. Epub 2021 Nov 27. PMID: 34848298; PMCID: PMC8925904.
3. Pernet, C.R., Appelhoff, S., Gorgolewski, K.J. et al. EEG-BIDS, an extension to the brain imaging data structure for electroencephalography. Sci Data 6, 103 (2019). https://doi.org/10.1038/s41597-019-0104-8
4. Soumen Paul, Partha Pratim Das, and K. Sreenivas Rao. 2025. Ontology in Dance Domain—A Survey. ACM J. Comput. Cult. Herit. 18, 1, Article 16 (February 2025), 32 pages. https://doi.org/10.1145/3690767
5. Kalita,D; Deka, D (2020) Ontology for Preserving the Knowledge Base of Traditional Dances(OTD), The Electronic Library ,Vol. 38 Issue. 4, pp 785-803 DOI: https://doi.org/10.1108/EL-11-2019-0258
6. Cruz-Garza JG, Hernandez ZR, Nepaul S, Bradley KK and Contreras-Vidal JL (2014) Neural decoding of expressive human movement from scalp electroencephalography (EEG). Front. Hum. Neurosci. 8:188. doi: 10.3389/fnhum.2014.00188

4. N/A

5. Protocol2Publication: An integrated application for data organization, analysis and sharing

Josh Lawrimore[1], Nathanyal Ross[2], Miguel Arenivar2, Dustin Moraczewski[3], Hugo Tejeda[2], Adam Thomas[3*]

[1]Clinical Monitoring Research Program Directorate, Frederick National Laboratory for Cancer Research, Frederick, The United States of America
[2]Unit on Neuromodulation and Synaptic Integration, National Institute of Mental Health, Bethesda, The United States of America
[3]Data Science & Sharing Team, National Institute of Mental Health, Bethesda, The United States of America
*adamt@nih.gov

INTRODUCTION/MOTIVATION

In practice, data sharing involves combining primary data and the original metadata to create datasets that comply with modern FAIR (Findable, Accessible, Interoperable, and Reusable) data standards, such as the Neurodata Without Borders[1] (NWB). Dataset creation is often done after publication, when both the metadata and the primary data are not in active usage. Moreover, metadata is frequently stored separately from the primary data lab notebooks. In preparation for data sharing, users must manually relocate then combine metadata and primary data to create FAIR datasets, a tedious and error-prone process. Recently, electronic lab notebooks (ELNs) have been developed with application programming interfaces (APIs) that allow programmatic access to notebook entries. The Intramural Research Program (IRP) at the National Institutes of Health (NIH) now requires all experiments be recorded using an ELN. These two developments allow for the automated combination of metadata and primary data. Here we present Protocol2Publication (P2P), a graphical user interface application that accesses electronic lab notebook entries to create a predefined directory structure to unify metadata and primary data, organize and monitor data analyses, and automate the creation of FAIR datasets. Here we demonstrate the P2P application with fiber photometry analyses to create an NWB-compliant dataset for upload to the DANDI archive[2].

METHODS

The P2P application parses LabArchives[3] electronic lab notebooks using an open-source Python wrapper for LabArchives' API[4] we developed to automatically access experimental metadata. The P2P application uses the Streamlit[5] web-application development package as the front-end interface but is run on a local machine or high-performance compute cluster. The P2P application uses the metadata to create a pre-defined directory structure. The P2P app then prompts the user to place the primary data into the directory for preprocessing and analysis. The application uses the Python module tdt[6] to parse the fiber photometry data and allows the users to down-sample and smooth the photometry signals, identify signal artifacts, normalize the experimental signal to the isobestic signal to generate the delta F/F curve, align the delta F/F curves to signal cues, perform regression analysis, and exports the processed signal data after alignment to cues. The processed data is exported as a set of CSV files, and the parameters are stored as JSON files. Additionally, the P2P application has a page for tracking experimental progress by monitoring the contents of the directory. The application uses the ndx-fiber-photometry NWB extension[7] to convert the data into an NWB dataset and utilizes the DANDI python client[8] to upload the dataset to the DANDI archive[2].

RESULTS AND DISCUSSION

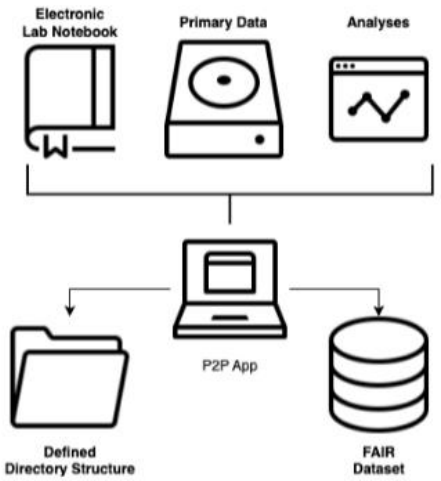

Figure 1. Diagram of Protocol2Publication Workflow
The diagram illustration the Protocol2Publication (P2P) app integrating metadata from an electronic lab notebook, primary data, and analyses to produce a defined directory structure and a FAIR dataset suitable for upload to a data repository.

With the P2P application, we provide an integrated approach to data organization, analysis, and sharing (Figure 1). While the current iteration of the P2P application is limited to fiber photometry, we hope to extend this P2P approach to other modalities as well. The purpose of the application is not just as an analysis tool but as a demonstration of metadata-dictated data organization to enable automated FAIR dataset generation. The P2P approach combines metadata, data, and analyses to facilitate reproducible data analysis, experimental progress tracking, and automate data sharing in a single application. While the current iteration of P2P supports the LabArchives ELN, we hope to extend P2P in the future to include open source ELNs, such as eLabFTW's[9] ELN.

Keywords: <FAIR data>, <Data Sharing>, <NWB>, <Fiber Photometry>, <Streamlit>, <API>, <Electronic Lab Notebook>

ACKNOWLEDGEMENTS
This project was funded by the Intramural Research Program of the NIMH, grant numbers ZICMH002960 and ZIAMH002970, and funded by the NCI Contract No. 75N91019D00024.

REFERENCES
[1] Rübel O, Tritt A, Ly R, et al. The Neurodata Without Borders ecosystem for neurophysiological data science. eLife. 2022;11:e78362. doi:10.7554/eLife.78362
[2] VanDenburgh M, Chiquito D, Nesbitt J, et al. dandi/dandi-archive: v0.12.4. Zenodo. July 2025. doi:10.5281/zenodo.16618503
[3] The Modern Electronic Lab Notebook (ELN) - LabArchives. https://www.labarchives.com/
[4] NIMH-DSST. GitHub - nimh-dsst/labarchives-api: A Python wrapper for the LabArchives Electronic Lab Notebook API. GitHub. https://github.com/nimh-dsst/labarchives-api.
[5] streamlit. PyPI. https://pypi.org/project/streamlit/. Published July 25, 2025.
[6] tdt. PyPI. https://pypi.org/project/tdt/. Published June 11, 2025.
[7] Catalystneuro. GitHub - catalystneuro/ndx-fiber-photometry: This is an NWB extension for storing fiber photometry recordings and associated metadata. GitHub. https://github.com/catalystneuro/ndx-fiber-photometry
[8] Halchenko Y, Wodder JT II, Christian H, et al. dandi/dandi-cli: 0.69.3. Zenodo. Published online June 4, 2025. doi:10.5281/zenodo.15595994
[9] Elabftw. GitHub - elabftw/elabftw: :notebook: eLabFTW is the most popular open source electronic lab notebook for research labs. GitHub. https://github.com/elabftw/elabftw

6. Functional and Metabolic Network Signatures of Mitochondrial Specialization in the Human Brain

Massimiliano Facca[1,2*], Manu S. Goyal[3], Andrei G. Vlassenko[3], Maurizio Corbetta[1,4,5], Michel Thiebaut de Schotten[6,7], Alessandra Bertoldo[1,2*]

[1] Padova Neuroscience Center (PNC), University of Padova (Unipd), Padova, Italy
[2] Department of Information Engineering, University of Padova (Unipd), Padova, Italy
[3] Neuroimaging Laboratories at the Mallinckrodt Institute of Radiology, Washington University School of Medicine, St Louis, MO, USA
[4] Venetian Institute of Molecular Medicine (VIMM), Padova, Italy
[5] Department of Neuroscience, University of Padova (Unipd), Padova, Italy
[6] Brain Connectivity and Behaviour Laboratory, Paris, France
[7] Groupe d'Imagerie Neurofonctionnelle, Institut des Maladies Neurodégénératives-UMR 5293, CNRS, CEA University of Bordeaux, Bordeaux, France

Corresponding authors:
Dr. Massimiliano Facca, massimiliano.facca@unipd.it
Prof. Alessandra Bertoldo, alessandra.bertoldo@unipd.it

INTRODUCTION/MOTIVATION

Despite representing only ~2% of body mass, the human brain consumes about 20% of the body's total energy [1]. Most of this energy fuels spontaneous activity at rest and is produced through oxidative phosphorylation (OxPhos), powered by mitochondria [2]. A recently developed voxelwise atlas of mitochondrial respiratory capacity offers an unprecedented view of this key bioenergetic function [3]. Yet, how this spatial distribution of mitochondrial features aligns with the brain's functional and metabolic network organization remains unknown. Here, we test whether mitochondrial phenotypes are structured according to intrinsic network architecture.

METHODS

We analyzed all gray matter voxels from a biochemically profiled human brain slab (n=249; Figure 1a), each characterized by six mitochondrial features: enzymatic activities of CI, CII, and CIV; mitochondrial density (MitoD); tissue respiratory capacity (TRC); and mitochondrial respiratory capacity (MRC). High-resolution 7T resting-state fMRI (n = 58 subjects) and dynamic [^{18}F]FDG-PET (n = 20 subjects) data were coregistered to the slab's stereotaxic space to derive voxelwise Functional Connectivity (FC) and Metabolic Connectivity (MC) matrices [4] (Figure 1b). For each OxPhos feature, we first computed its correlation across nodes with the FC- or MC-weighted mean in each node's network neighbors (Figure 1c). Significant correlations would suggest network-driven effects in regional variability of mitochondrial features. We then constructed a Mitochondrial Profile Similarity (MPS) matrix by computing Pearson's correlation between the mitochondrial feature profiles of each voxel pair. We applied Louvain community detection to both FC and MC (γ = 0.8–2.0, step 0.1) to identify network modules, and tested whether MPS values were greater within modules than between them (ΔMPS = average MPS within - average MPS between modules, figure 2a-f). All analyses accounted for spatial autocorrelation (SA) and network geometry using SA-preserving and degree- and edge length-preserving null models [5,6].

RESULTS AND DISCUSSION

Across nodes, all mitochondrial features were significantly associated with the MC-weighted neighborhood averages (all $p < 0.01$ vs. both null models). For FC, significant effects were found for CI, CIV, TRC and MRC (all $p<0.05$ vs. both null models), suggesting that

mitochondrial features, particularly oxidative capacity, are shaped by network-level interactions, with stronger effects for MC than FC (Figure 1 c). In the modularity analysis, FC showed higher within-module than between-module MPS across most γ values ($p < 0.001$), with effects strengthening at higher γ and pointing to increased mitotype coherence at finer community resolutions (Figure 2 b,c). For MC, significant effects were observed only at the finest resolutions, peaking at $\gamma = 1.6$ ($p = 0.006$), suggesting a higher degree of scale specificity (Figure 2 e,f).

Our findings show that mitochondrial specialization is closely embedded within the brain's functional and metabolic networks. Connectivity modules appear to act as bioenergetic niches, harboring distinct mitotypes. Regional differences in oxidative capacity are influenced by network-level interactions, suggesting that mitochondrial organization is not merely a local property but also reflects systems-level constraints. Together, these results provide a mechanistic link between intrinsic connectivity and energy metabolism, offering a framework for understanding how mitochondrial phenotypes support human brain function.

Keywords: mitochondria, metabolism, connectomics, networks, functional connectivity, metabolic connectivity, fMRI, PET

FIGURES

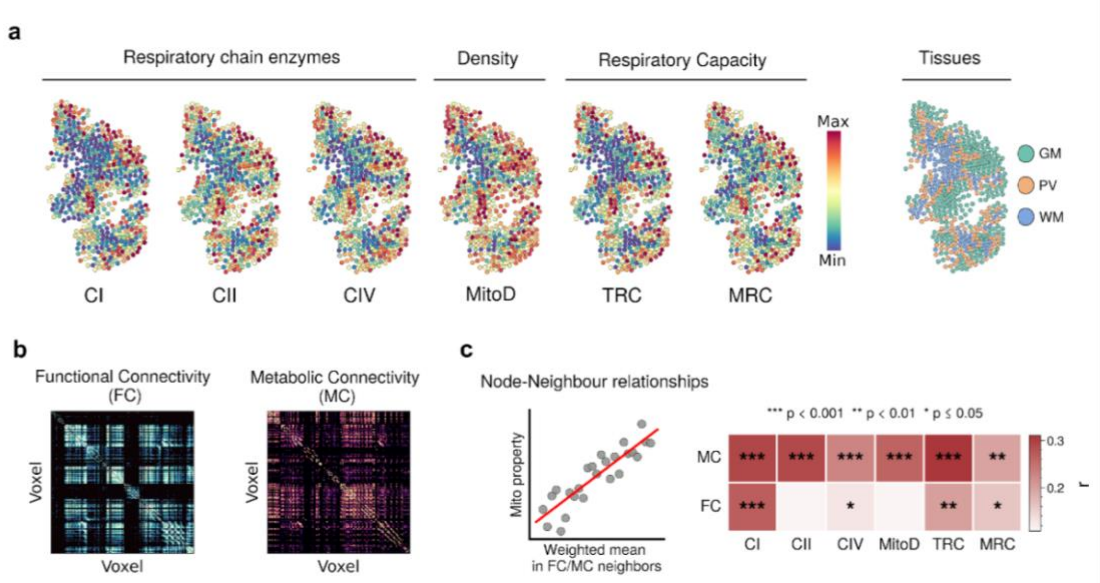

Figure 1. a) Mitochondrial Activity Atlas [3] comprising regional measures of enzymatic activity of respiratory chain complexes CI, CII, and CIV, mitochondrial density (MitoD), tissue respiratory capacity (TRC), and mitochondrial respiratory capacity (MRC) from grey matter, white matter, and partial volume voxels. Analyses were restricted to 249 grey matter voxels. **b)** Voxel-level functional connectivity (FC) and metabolic connectivity (MC) matrices were constructed from rs-fMRI and dynamic [^{18}F]FDG-PET data, registered to the slab's stereotaxic space. **c)** Network-driven effects on the regional distribution of mitochondrial features. Each feature was correlated with the connectivity-weighted mean across network neighbors, defined by either FC or MC. Statistical significance was assessed against two null models: one preserving spatial autocorrelation (SA) and one preserving degree and edge-length distributions [5,6]. A correlation was deemed significant only if surpassing both null models. The heatmap reports, for each feature, the higher p-value across the two tests. Significant network-driven effects were observed for all mitochondrial features with MC and for selected OxPhos features with FC.

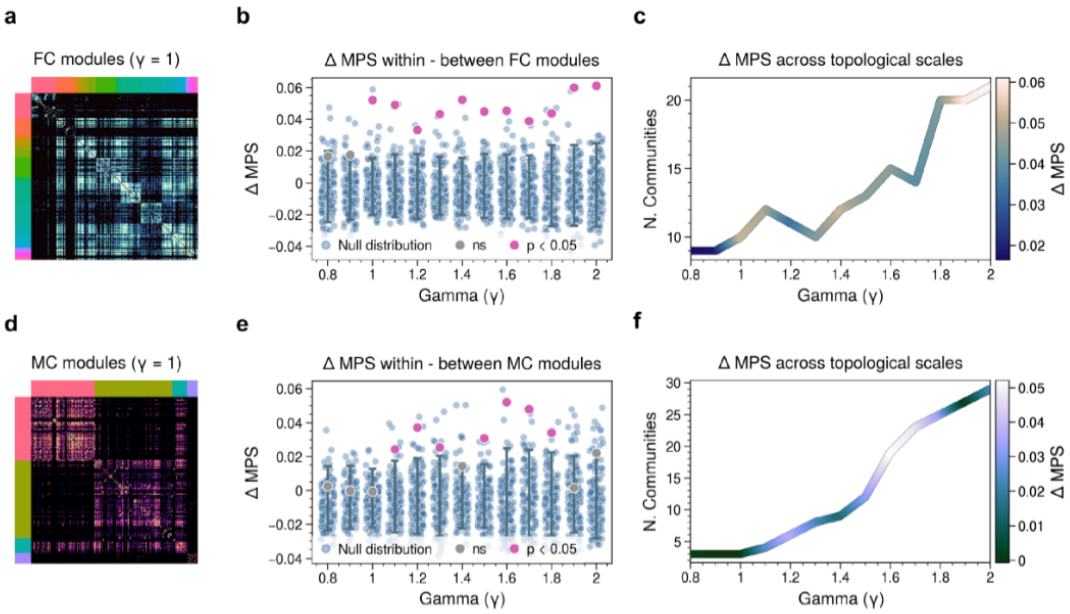

Figure 2. a) Example of a functional connectivity (FC) matrix with its community structure highlighted. **b)** Difference (Δ) between mitochondrial profile similarity (MPS) within versus between FC modules across resolution parameter γ. Positive values indicate greater MPS within than between modules. Pink dots denote statistical significance under a permutation test; grey dots indicate non-significance (ns). **c)** Relationship between γ, number of communities, and ΔMPS, showing that ΔMPS is largest at the finest community resolutions (i.e., many modules). **d)** Example of a metabolic connectivity (MC) matrix with its community structure at an example γ. **e)** ΔMPS within versus between MC modules across γ. Unlike FC, the effect for MC emerges only at specific fine-grained resolutions. **f)** Relationship between γ, number of communities, and ΔMPS in the MC network.

ACKNOWLEDGEMENTS

Support for the research was provided by EU EBRAINS 2.0: A Research Infrastructure to Advance Neuroscience and Brain Health (HORIZON-INFRA-2022-SERV-B-01, grant n.101147319).

REFERENCES

[1] Raichle ME. Neuroscience. The brain's dark energy. Science. 2006;314(5803):1249-1250.
[2] Hall CN, Klein-Flügge MC, Howarth C, Attwell D. Oxidative phosphorylation, not glycolysis, powers presynaptic and postsynaptic mechanisms underlying brain information processing. J Neurosci. 2012;32(26):8940-8951. doi:10.1523/JNEUROSCI.0026-12.2012
[3] Mosharov EV, Rosenberg AM, Monzel AS, et al. A human brain map of mitochondrial respiratory capacity and diversity. Nature. 2025;641(8063):749-758. doi:10.1038/s41586-025-08740-6
[4] Volpi T, Vallini G, Silvestri E, et al. A new framework for metabolic connectivity mapping using bolus [18F]FDG PET and kinetic modeling. J Cereb Blood Flow Metab. 2023;43(11):1905-1918. doi:10.1177/0271678X231184365
[5] Burt JB, Helmer M, Shinn M, Anticevic A, Murray JD. Generative modeling of brain maps with spatial autocorrelation. NeuroImage. 2020;220:117038. doi:10.1016/j.neuroimage.2020.117038
[6] Betzel RF, Bassett DS. Specificity and robustness of long-distance connections in weighted, interareal connectomes. Proc Natl Acad Sci U S A. 2018;115(21):E4880-E4889. doi:10.1073/pnas.1720186115

7. BrainCAP: an open-source platform for identifying brain co-activation patterns using functional MRI

Kangjoo Lee[1*], Samuel Brege[1], Jesse Cai[2,3], Zailyn Tamayo[1], Catie Chang[2], Youngsun T. Cho[1,4]

[1] Department of Psychiatry, Yale University School of Medicine, New Haven, Connecticut, USA
[2] Department of Electrical and Computer Engineering, Vanderbilt University, Tennessee, USA
[3] Princeton Neuroscience Institute, Princeton, New Jersey, USA
[4] Child Study Center, Yale University School of Medicine, New Haven, Connecticut, USA
* kangjoo.lee@yale.edu

INTRODUCTION/MOTIVATION

The analysis of co-activation patterns (CAPs) in functional magnetic resonance imaging (fMRI) is useful to track moment-to-moment neural dynamics, providing key insights into the functional organization of the human brain. CAPs have been linked to behavioral, cognitive [1], and clinical outcomes, including schizophrenia [2], [3] and depression [4], [5]. Despite its promise, CAP analysis is computationally demanding, and no standardized, open-source tools currently supports diverse analytic choices in a unified platform [6]. To fill this gap, we developed BrainCAP, an open-source toolkit in Python (>90%), R and bash.

METHODS

BrainCAP provides a complete pipeline for quantifying CAPs from fMRI data in cross-sectional and longitudinal studies (Fig 1). Using resting-state fMRI from the Human Connectome Project [7], we previously identified highly reproducible spatiotemporal features of neural CAPs linked to behavioral phenotypes such as cognition, emotion regulation, alcohol and substance use [1]. Building on this, BrainCAP implements the following steps: (i) Concatenation of resting-state fMRI across sessions, subjects, or groups, (ii) Temporal sampling of concatenated time-series data (e.g. selecting time-points associated with a seed time-course, excluding time-points with motion artifacts), (iii) Clustering fMRI time-frames by spatial similarity to identify CAPs via cluster centroids, (iv) Spatial evaluation of CAPs via cosine similarity with canonical resting state networks, with flexible atlas options, (v) Quantification of temporal CAP metrics, including fractional occupancy and dwell time, (vi) Second-level analyses, including feature selection, dimension reduction (e.g. identifying low-dimensional representations of individual differences), and behavior prediction (e.g. multiple linear regression), while controlling for confounds (e.g. age, sex and motion), and (vii) quality control and reproducibility assessment using permutation [1]. The beta version of BrainCAP is available on our Github repository (https://github.com/Kangjoo/BrainCAP/tree/develop).

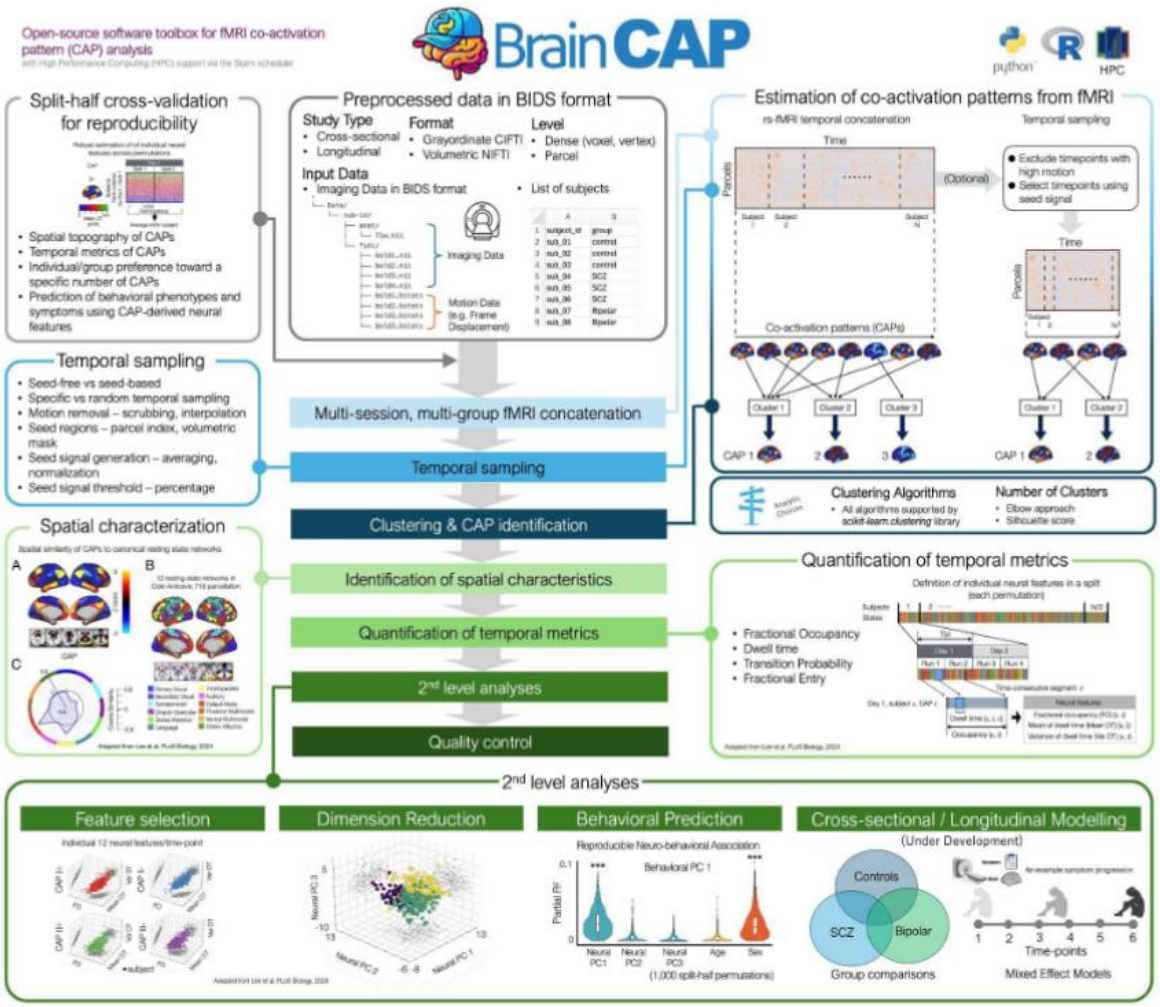

Figure 1. An overview of BrainCAP analytic pipeline.

RESULTS AND DISCUSSION

BrainCAP is distributed by Abbtainer containers based on Github tagged versions. It supports multiple analytic options (e.g. volumetric NIFTI versus grayordinate CIFTI data, network-parcellation atlases, clustering methods), Brain Imaging Data Structure (BIDS) [8], Workbench [7], and HPC systems such as Slurm (Fig 2). Analyses can be conducted at both voxel-wise and parcel levels, with and without temporal sampling. Clustering is performed across all groups (cross-sectional) or time-points (longitudinal), but users may restrict it to specific subsets. After clustering, BrainCAP assigns each time-point to a CAP state and quantifies the temporal profile of state variations [1]. This entire workflow is configured through a single YAML file, allowing users to easily tailor every step to their specific hypothesis. Outputs include quantifiable CAP-derived features, reproducibility statistics, and visualizations in python, R and WorkBench.

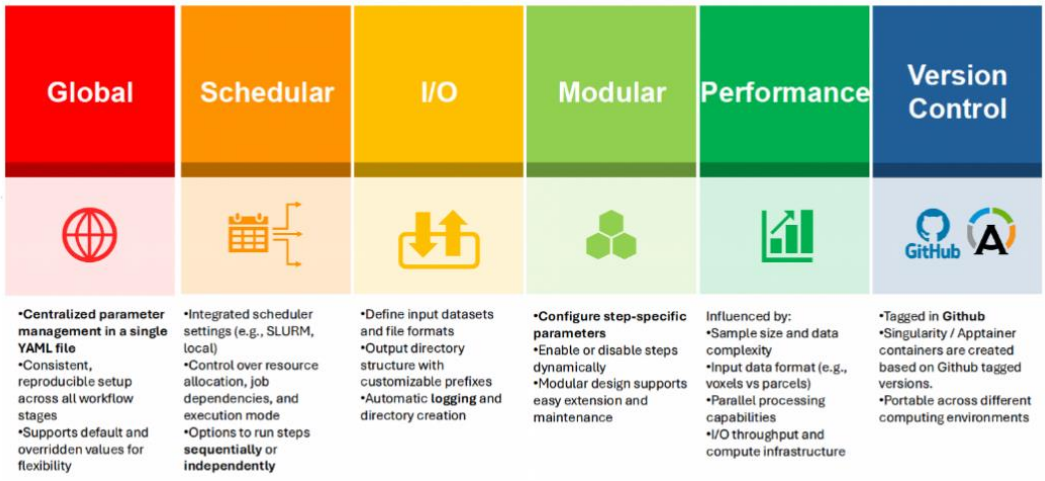

Figure 2. Workflow configuration.

BrainCAP is the first open-source, Python-based toolkit for CAP analysis and a community-driven platform integrating diverse data formats and analytic options with HPC parallel processing. It supports both cross-sectional and longitudinal analyses, allowing for precise mapping of brain-behavior relationships across timescales and clinical phases. By standardizing CAP analysis with robust quality control, BrainCAP addresses a critical need to identify clinically actionable biomarkers and advance precision medicine in psychiatry and neuroscience. Future updates will include integration of additional statistical models (e.g. ANOVA, mixed effect models), brain atlases and analytic metrics to support benchmarking. In parallel, the platform will continue to build community resources including a wiki, and an open GitHub forum to promote open science and collaborative development.

Keywords: Functional MRI, Brain co-activation, Brain dynamics, Functional connectivity, Cross-sectional study, Longitudinal analysis, Python, Open-source software, Open science

ACKNOWLEDGEMENTS
KL and SB are funded by NIH/NIMH U01MH124639 and NIH/NIMH U01MH137298.

REFERENCES
[1] K. Lee et al., “Human brain state dynamics are highly reproducible and associated with neural and behavioral features,” PLOS Biol., vol. 22, no. 9, p. e3002808, Sept. 2024, doi: 10.1371/journal.pbio.3002808.
[2] H. Yang et al., “Reproducible coactivation patterns of functional brain networks reveal the aberrant dynamic state transition in schizophrenia,” NeuroImage, vol. 237, p. 118193, Aug. 2021, doi: 10.1016/j.neuroimage.2021.118193.
[3] T. A. W. Bolton et al., “Triple Network Model Dynamically Revisited: Lower Salience Network State Switching in Pre-psychosis,” Front. Physiol., vol. 11, p. 66, Feb. 2020, doi: 10.3389/fphys.2020.00066.
[4] R. H. Kaiser et al., “Abnormal frontoinsular-default network dynamics in adolescent depression and rumination: a preliminary resting-state co-activation pattern analysis,” Neuropsychopharmacology, vol. 44, no. 9, pp. 1604–1612, Aug. 2019, doi: 10.1038/s41386-019-0399-3.
[5] E. L. Belleau et al., “Resting state brain dynamics: Associations with childhood sexual abuse and major depressive disorder,” NeuroImage Clin., vol. 36, p. 103164, 2022, doi: 10.1016/j.nicl.2022.103164.
[6] T. A. W. Bolton et al., “TbCAPs: A toolbox for co-activation pattern analysis,” NeuroImage, vol. 211, p.116621, May 2020, doi: 10.1016/j.neuroimage.2020.116621.

[7] D. C. Van Essen et al., “The Human Connectome Project: A data acquisition perspective,” NeuroImage, vol. 62, no. 4, pp. 2222–2231, Oct. 2012, doi: 10.1016/j.neuroimage.2012.02.018.
[8] K. J. Gorgolewski et al., “The brain imaging data structure, a format for organizing and describing outputs of neuroimaging experiments,” Sci. Data, vol. 3, no. 1, p. 160044, June 2016, doi: 10.1038/sdata.2016.44.

8. Open Science Metrics

Christoph Li[1], Josh Lawrimore[2], Dustin Moraczewski[1], Adam Thomas[1*]

[1] Data Science & Sharing Team, National Institute of Mental Health, Bethesda, The United States of America
[2] Clinical Monitoring Research Program Directorate, Frederick National Laboratory for Cancer Research, Frederick, The United States of America
* adamt@nih.gov

INTRODUCTION/MOTIVATION
For over 25 years, funders of biomedical science throughout the world have been working to increase data sharing and transparency amongst their grantees using a variety of incentives and mandates. However quantitative bibliometric studies on the rates of transparency practices in biomedical literature continue to show most publications do not contain any information regarding how the source data can be obtained[1]. To help determine which mandates and incentives are successful in increasing data sharing, we present an online dashboard that allows users to compare the proportion of data sharing in open access publications across the ten largest funders of biomedical research in the world.

METHODS
We used the dataset provided by Sergihou et al[1] which contains information on the presence of data sharing statements in 2.75 million publications from PubMed Central's Open Access collection (PMCOA) as well as funder acknowledgments. Using Python scripts[2] we developed, we cleaned and labelled the information from the publications' funder acknowledgements to identify those that included at least one of the ten largest funders of biomedical science in the world. The list of largest funders was assembled using web-based searches to identify funding information from: (1) national governmental research agencies, (2) supranational organizations (e.g.,European Commission), (3) major philanthropic foundations, and (4) independent research institutes. See the legend of figure 1 for a list. We then used this labelled dataset to create an open-source, interactive Streamlit dashboard and deployed it online using GitHub actions and Amazon Web Services (AWS). The code for mining the PMCOA dataset, the dashboard, and the deployment code are publicly available under the Creative Commons 0 (CCO) License on the NIMH-DSST OSM GitHub repository[2].

RESULTS AND DISCUSSION
In our analysis, the National Institutes of Health (NIH) and the National Natural Science Foundation of China (NSFC) stood apart with over 25,000 funded papers from the PMCOA collection in 2019 (the most recent year with complete data). The other eight funders were each below 12,000 (Figure 1). We observed large differences between funders in proportion of papers that contained data sharing statements. For example, despite having a relatively small total number of papers in our dataset, 50% of PMCOA publications that acknowledged HHMI as a funder contained a data sharing statement in 2019 and 2020. No other funder’s data sharing proportion exceeded 30% for these years (Figure 2).
Circa August 2025, of the PMCOA subset for commercial and non-commercial use has grown to approximately 6.7 million publications, more than twice the number available to Sergihou et al1 in 2020. Using the NIH High Performance Compute (HPC) cluster, we are currently processing this

expanded set of publications using the pipeline from Sergihou et al[1] to explore if differences in rates of data availability statements across funders persist in recent years. We intend to update the dashboard to include the current 6.7 million publication PMCOA subset for commercial and non-commercial use prior to the EBRAINS summit in December and maintain it as an open-source resource to the community to monitor data sharing reporting differences between funders.

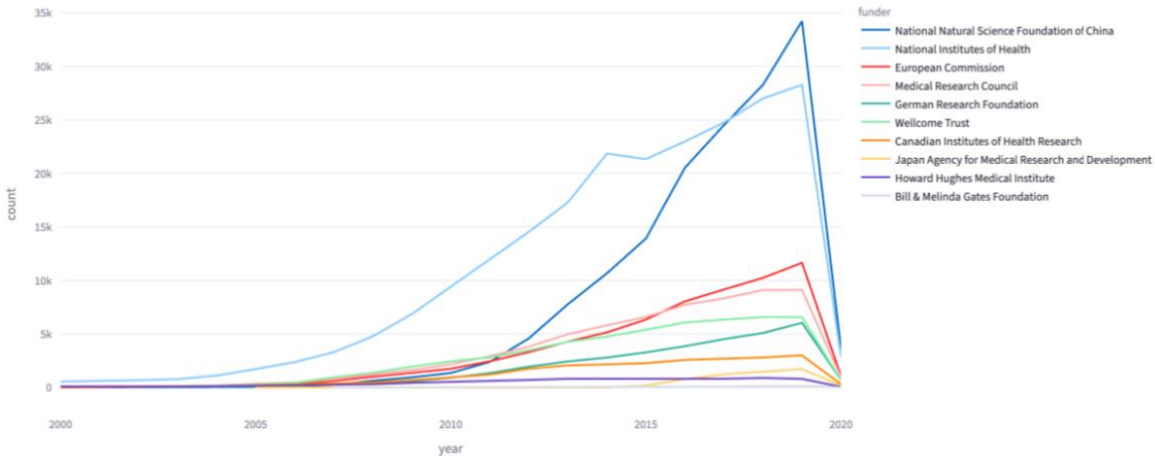

Figure 1. Total PMCOA publications by funder
The graph shows the number of publications in PMCOA that that acknowledge funding from each of the labelled funders from 2000 to 2020.

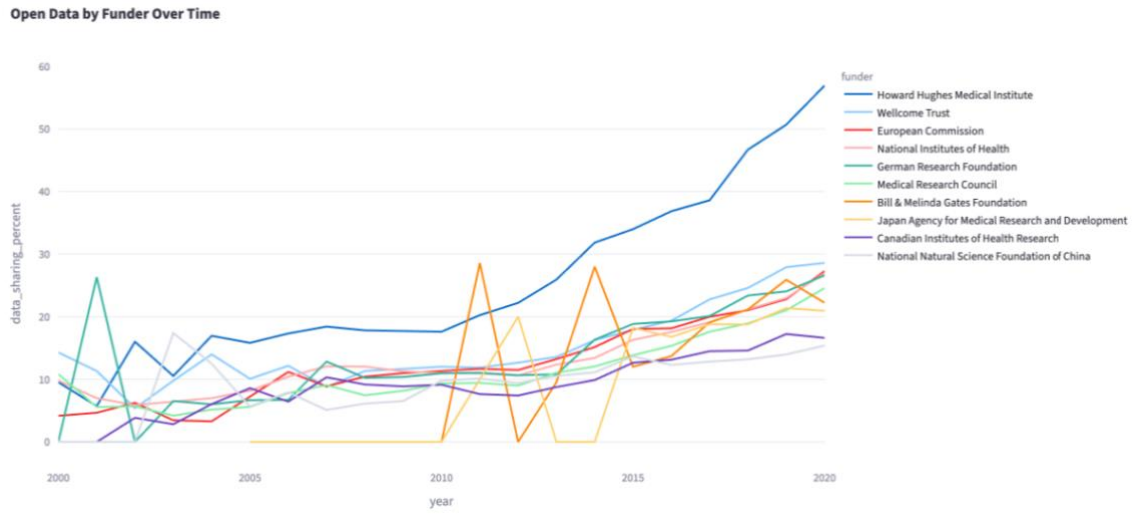

Figure 2. Percent publications with data sharing by funder
For each of the top 10 funders of biomedical science, the graph shows the percentage of publications in PMCOA that contain a data sharing statement as identified by the rtransparent tool from Sergihou et al[1] from 2000 to 2020.

Keywords: <Data Sharing>, <bibliometrics>, <Streamlit>

ACKNOWLEDGEMENTS
Funded by the Intramural Research Program of the NIMH, ZICMH002960. Funded by the NCI Contract No. 75N91019D00024.

REFERENCES

[1] Serghiou, S.; Contopoulos-Ioannidis, D. G.; Boyack, K. W.; Riedel, N.; Wallach, J. D.; Ioannidis, J. P. A. Assessment of Transparency Indicators across the Biomedical Literature: How Open Is Open? PLoS Biol. 2021,19(3),e3001107.
[2] NIMH-DSST. GitHub - nimh-dsst/osm: OpenSciMetrics (OSM) applies NLP and LLM-based metrics and indicators related to transparency, data sharing, rigor, and open science on biomedical publications. GitHub. https://github.com/nimh-dsst/osm/
[3] PMC OA FTP Service - PMC. https://pmc.ncbi.nlm.nih.gov/tools/ftp/

9. Breaking Down Defenses: Autophagy as a Therapeutic Tool to Enhance Chemosensitivity in Neuroblastoma

Sara Ahmed Halawa[1], Yomna Adel Moqidem[1], Ahmed Abdellatif[1] (orcid.org/0000-0003-0486-348X)

[1] Department of Biology, and Biotechnology program, School of Sciences and Engineering. The American University in Cairo, 11835, Egypt.

Abstract

Introduction
Neuroblastoma is the most common type of cancer diagnosed in children aged between one and five years old. Children diagnosed with high-risk neuroblastoma have a 50% 5-year survival rate. Cisplatin is a commonly used treatment for high-risk neuroblastoma, unfortunately, it is often met with chemoresistance due to the induction of autophagy. Autophagy is a double-edged sword; it can either activate cell death and suppress tumor progression or promote cell survival thus promoting tumorigenesis.

Methods
The current study aimed to investigate the role of autophagy inhibition as an adjuvant to chemotherapy on neuroblastoma SK-N-AS cells in vitro. Bafilomycin A1 (200 nM) was used either as a pretreatment or concurrently with Cisplatin. Cell viability was assessed via MTT and Trypan Blue assays, apoptosis was analyzed by flow cytometry, and cell cycle progression was examined. Additionally, autophagy was evaluated using LC3 staining and mRNA expression of pivotal genes such as ATG7 was analyzed via qRT-PCR.

Results
Pretreatment with Bafilomycin A1 significantly enhanced cell death of SK-N-AS cells induced by Cisplatin with an 82% decrease in cell viability compared to only a 31% decrease with Cisplatin alone. Flow cytometry confirmed a higher percentage of apoptotic cells in the pretreatment group, accompanied by G0-G1 phase cell cycle arrest. Furthermore, Bafilomycin A1 pretreatment downregulated mRNA expression of pivotal genes such as ATG7, implying that inhibiting autophagic flux sensitizes neuroblastoma cells to Cisplatin.

Discussion
The current findings highlight the use of Bafilomycin A-1 as an adjuvant treatment with chemotherapy as a promising treatment strategy to overcome autophagy-mediated chemoresistance in high-risk neuroblastoma and improve treatment outcomes in pediatric cancer patients.

Figures

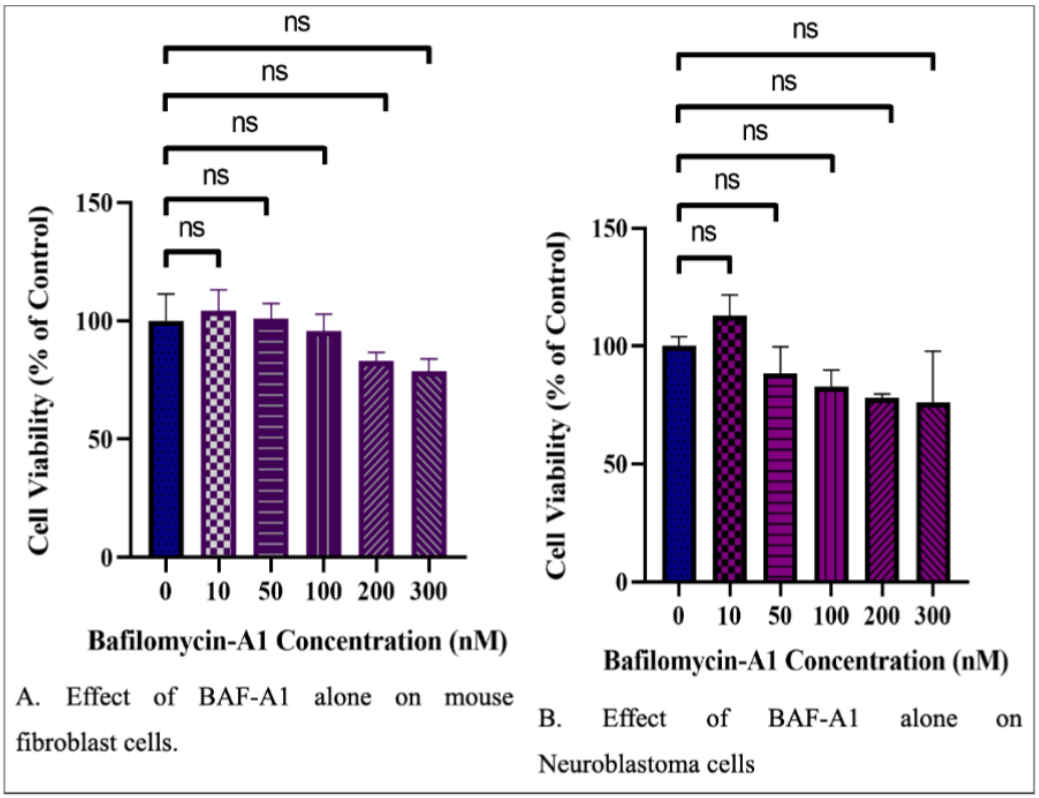

Figure 1. Bafilomycin A-1 is not cytotoxic in fibroblasts and neuroblastoma Cells. Caption: Cell viability assessment following treatment with increasing concentrations of Bafilomycin A1 in L929 fibroblasts and SK-N-AS cells.

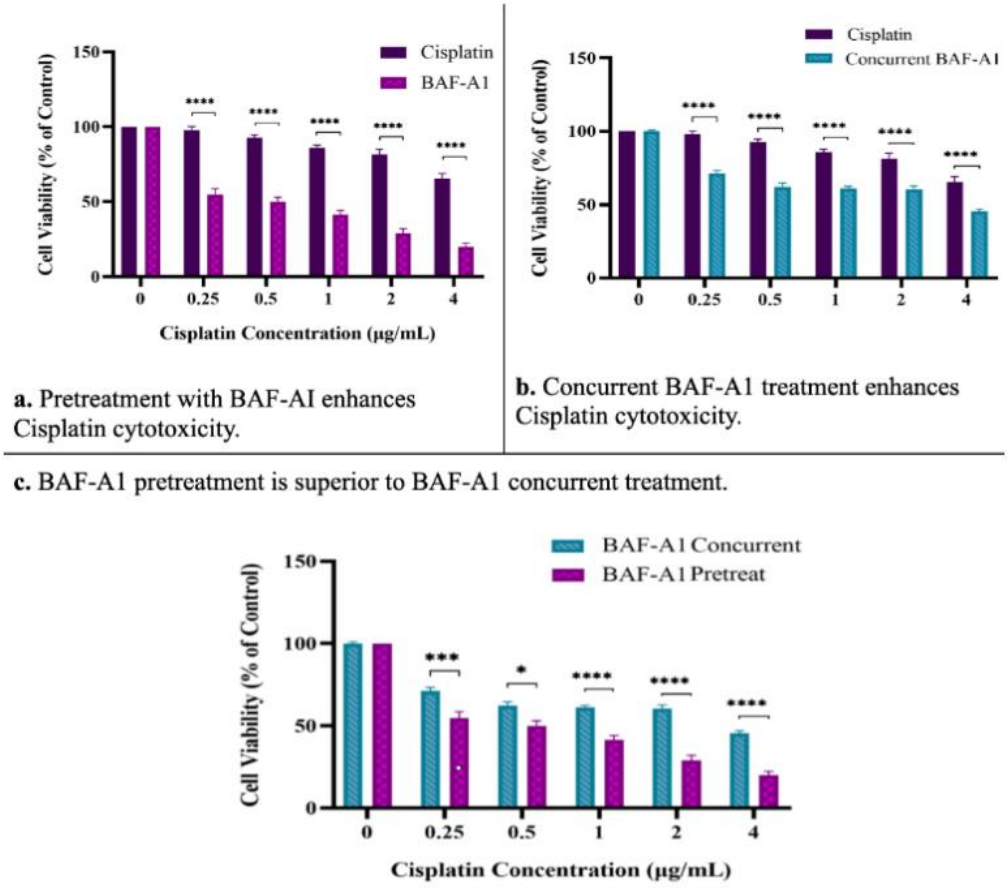

Figure 2. Bafilomycin Enhances Cisplatin Cytotoxicity on Neuroblastoma Cells.
Caption: Cell viability following Cisplatin treatment alone versus pretreatment and concurrent treatment with Bafilomycin A1.

References

1. Aveic S, Corallo D, Porcù E, et al. TP-0903 inhibits neuroblastoma cell growth and enhances the sensitivity to conventional chemotherapy. Eur J Pharmacol. 2018;818:435-448. doi:10.1016/j.ejphar.2017.11.016.
2. Belounis A, Nyalendo C, Le Gall R, et al. Autophagy is associated with chemoresistance in neuroblastoma. BMC Cancer. 2016;16:891. doi:10.1186/s12885016-2906-9.
3. Esposito MR, Aveic S, Seydel A, Tonini GP. Neuroblastoma treatment in the post-genomic era. J Biomed Sci. 2017;24(1):14. doi:10.1186/s12929-017-0319-y.
4. Li, Yue, Yang Yin, Tong Zhang, Jinhua Wang, Zeqi Guo, Yuyun Li, Ya Zhao, Ruihong Qin, and Qian He. 2024. "A Comprehensive Landscape Analysis of Autophagy in Cancer Development and Drug Resistance." Frontiers in Immunology 15 (August). https://doi.org/10.3389/fimmu.2024.1412781.
5. Liao, Yu-Xin, Hai-Yang Yu, Ji-Yang Lv, Yan-Rong Cai, Fei Liu, Zhi-Min He, and Shi-Sheng He. 2019. "Targeting Autophagy Is a Promising Therapeutic Strategy to Overcome Chemoresistance and Reduce Metastasis in Osteosarcoma." International Journal of Oncology 55 (6): 1213–22. https://doi.org/10.3892/ijo.2019.4902.
6. Maris JM. Recent advances in neuroblastoma. N Engl J Med. 2010;362(23):2202-2211. doi:10.1056/NEJMra0804577.

Keywords
Neuroblastoma; Autophagy; Bafilomycin A1; Cisplatin; Chemoresistance; Apoptosis; Cell cycle arrest; Pediatric oncology; Gene expression; Adjuvant therapy

10. Vitamin B12 as an Epidrug for Epigenetic Modulation in Long Covid and Neurodegeneration

Roney Coimbra[1], Leonardo Silva-Contigli[1], Natália Hojo-Souza[1], Marina Oliveira[1], Daniela Rosa[2], Dayane Naves[1], Larissa Cassiano[1], David Langlais[3], Ricardo Gazzinelli[1], Jonas de Paula[2], Débora Miranda[2], Marco Romano-Silva[2*]

Affiliations:; [1]Neurogenômica/Imunopatologia, Fiocruz Minas, Belo Horizonte, Brazil; [2]Centro de Tecnologia em Medicina Molecular, Universidade Federal de Minas Gerais, Belo Horizonte, Brazil; [3]Department of Human Genetics and Microbiology & Immunology, McGill University, Montreal, Canada
*romano-silva@ufmg.br

INTRODUCTION/MOTIVATION
Long Covid is characterized by persistent symptoms following SARS-CoV-2 infection [1] and is associated with chronic inflammation and neuropsychiatric sequelae [2]. Epigenetic mechanisms, particularly DNA methylation [3,4] play a key role in immune regulation. Vitamin B12 is an essential cofactor [4,5] in the methionine cycle and has been shown to modulate gene expression in inflammatory and neurodegenerative conditions. Our group previously demonstrated visuoconstructive deficit (VCD) [5]—a potential early marker of neurodegeneration—in 25% of young adults after mild Covid-19, correlated with neuroinflammatory plasma signatures. This study investigates the epigenetic and neuroprotective actions of vitamin B12 in whole blood cultures from human subjects and a pre-clinical hamster model of Long Covid.

METHODS

We analyzed 12 female participants from a longitudinal cohort (initiated in 2021): four with persistent VCD and eight controls after mild Covid-19. VCD was assessed using the Rey–Osterrieth Complex Figure test at 3–30 months post-infection. Whole blood cultures were incubated with 1 nM B12 or excipient for 24h, followed by RNA-Seq and DNA methylome profiling.

In parallel, 90 golden Syrian hamsters (45 males, 45 females, 8 weeks old) were infected intranasally with SARS-CoV-2 Omicron (10^5 PFU). Animals received B12 (6.25 mg/kg) daily or every three days starting day 1 post-infection until day 15. Behavioral outcomes were weight loss and food intake. Post-mortem analyses assessed plasma and brain Ccl11 (ELISA), microgliosis (Iba1 immunohistochemistry), neurodegeneration and protein aggregation (α-synuclein, NeuN immunofluorescence), and transcriptomes from leukocytes and hippocampal/cortical tissue.

RESULTS AND DISCUSSION

In humans, persistent VCD was associated with transcriptional signatures [7] indicating reduced $CD8^+$ naïve T cells, increased immature dendritic cells, and activation of oxidative phosphorylation, Parkinson's, neurodegeneration, and oxidative stress pathways. Epigenomic scars at CpG sites were detected in regulatory regions of dysregulated genes. Vitamin B12 modulated these methylation patterns, attenuated inflammatory transcriptional signatures, and enhanced autophagy [6]. A machine-learning classifier based on epigenetic signatures achieved robust predictive performance for VCD.

In hamsters, Covid-19 produced acute weight loss and sex-dimorphic brain sequelae. Females displayed elevated hippocampal Ccl11, microgliosis (CA1–CA2), and neurodegeneration (CA1, CA3); males exhibited microgliosis in the supra-hippocampal cortex and perinuclear α-synuclein accumulation in CA1 mature neurons. Administration of B12 every three days prevented acute symptoms and mitigated late neuropathological changes. In females, B12 reversed Covid-induced activation of Parkinson's and oxidative phosphorylation pathways in the hippocampus and reduced spliceosome activation in leukocytes. In males, B12 inhibited immune pathways but paradoxically enhanced neurodegeneration-related transcripts.

Our findings demonstrate that vitamin B12 exerts epigenetic and transcriptomic modulation relevant to Long Covid-associated neuroinflammation and visuoconstructive deficit. Converging human and pre-clinical evidence supports B12 as a sex-specific epidrug with neuroprotective potential [7]. While B12 showed protective effects in females, adverse transcriptomic responses in males highlight the importance of sex as a biological variable. These results strengthen the rationale for clinical trials to validate B12 as a therapeutic strategy for Long Covid and related neurodegenerative processes.

Keywords: Long Covid, visuoconstructive deficit, neurodegeneration, CCL11, epigenetics, DNA methylation, vitamin B12, transcriptomics, neuroinflammation, sex differences

ACKNOWLEDGEMENTS

This research was supported by CNPq, CAPES and FAPEMIG, INOVA Fiocruz

REFERENCES

[1]. Nalbandian A, Sehgal K, Gupta A, et al. Post-acute COVID-19 syndrome. Nat Med. 2021;27(4):601-615. doi:10.1038/s41591-021-01283-z

[2]. Taquet M, Geddes JR, Husain M, Luciano S, Harrison PJ. 6-month neurological and psychiatric outcomes in 236,379 survivors of COVID-19. Lancet Psychiatry. 2021;8(5):416-427. doi:10.1016/S2215-0366(21)00084-5

[3]. Pellegrini C, Pirazzini C, Sala C, et al. A meta-analysis of brain DNA methylation across sex, age, and Alzheimer's disease points for accelerated epigenetic aging in neurodegeneration. Front Aging Neurosci. 2021;13:639428. doi:10.3389/fnagi.2021.639428

[4]. Cacabelos R, Torrellas C. Epigenetics of aging and Alzheimer's disease: implications for pharmacogenomics and nutrigenomics. Pharmacol Ther. 2015;149:41-91. doi:10.1016/j.pharmthera.2014.11.002
[5]. de Paula JJ, Paiva RERP, Souza-Silva NG, et al. Selective visuoconstructional impairment following mild COVID-19 with inflammatory and neuroimaging correlation findings. Mol Psychiatry. 2023;28(2):553-563. doi:10.1038/s41380-022-01632-5
[6]. Cassiano LMG, Cavalcante-Silva V, Oliveira MS, et al. Vitamin B12 attenuates leukocyte inflammatory signature in COVID-19 via methyl-dependent changes in epigenetic markings. Front Immunol. 2023;14:1048790. doi:10.3389/fimmu.2023.1048790
[7]. Klein SL, Flanagan KL. Sex differences in immune responses. Nat Rev Immunol. 2016;16(10):626-638. doi:10.1038/nri.2016.90

11. PublicnEuro: a GDPR compliant data sharing platform for EU data

Introduction:
Data sharing using web-platform is becoming an integral part of the research life cycle. Not only sharing data allows to reproduce analyses, a tenet of experimental research, but it also allows deepening analysis of exist datasets, combine data, meta-anlayse and also ask outright new questions on existing data. Because neuroimaging data can be seen as personal data, this activity is challenging for EU-based researchers who have to comply with the General Data Protection regulation - the law that protects EU citizens on misusing their personal data. Here we introduce Public nEUro (https://public-neuro.github.io/index.html), a platform for EU-regulation-compliant data sharing.

Methods:
(1) We developped a legal framework allowing data providers to share their neuroimaging data using institition-specific data user agreements (figure 1)
(2) We created a governance framework ensuring fair, legal and secure data sharing
(3) Leveraging Denmark national life science super-computing facility (computerome) we can offer sovereign and secured hosting of datasets
(4) Using DataLad (Halchenko et al., 2021) data catalogue (https://docs.datalad.org/projects/catalog/en/latest/) we are develipping tools to share Publicly metadata, making EU datset findable
(5) Using verified user registration, we can make EU neuroimaging data accessible.

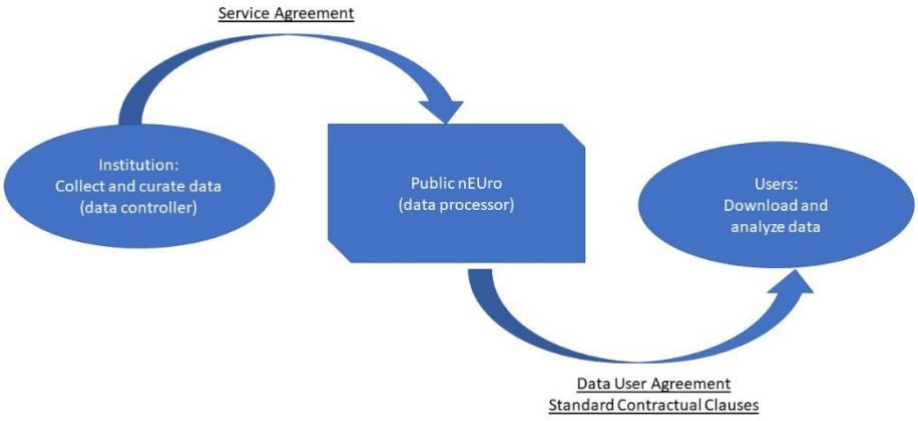

Figure 1: schematic overview of the legal framework allowing EU data sharing

Results:
(1) We have successfully established connections with several institutions who found the 'terms and conditions' acceptable to share EU data.
(2) Datasets are being uploaded and processed for data sharing. Each dataset must be BIDS (Gorgolewski et al., 2016) compliant (https://bids.neuroimaging.io/) ensuring interoperability and Reusability.

Conclusions:
The sharing of EU protected neuroimaging data is possible, without the need od data lakes thereby bringing users to the data. Instead, by allowing data creator to use institution specific data user agreements, verifying users identities and controlling data access, the can bring data to users, a model we believe to be more relevant in many cases, as proven by the success of OpenNeuro. Public nEUro aims to achieve more than just providing data access, but to also make data public, that is create a public record of metadata to enhance findablity.

12. Neurophysiological Assessment for Experimental Immersive Enhancement of Learning in the Humanities

Rebeca Romo-De León[1], Mei Li L. Cham-Perez[1], Veronica Andrea Elizondo-Villegas[1], Alejandro Villarreal-Villarreal[1], Alexandro Antonio Ortiz-Espinoza[1], Carol Stefany Velez-Saboyá[1], Jorge de Jesús Lozoya-Santos, Manuel Cebral-Loureda[1*], and Mauricio A. Ramírez-Moreno[1]

[1]Mechatronics Department, School of Engineering and Sciences, Tecnologico de Monterrey, Ave. Eugenio Garza Sada #2501, Tecnologico, Monterrey, MX.
[2]Schoool of Humanities and Education, Tecnologico de Monterrey, Ave. Eugenio Garza Sada #2501, Tecnologico, Monterrey, MX.
*manuel.cebral@tec.mx .

INTRODUCTION/MOTIVATION
While educational innovation has focused on science and engineering with notable technological advancements improving learning outcomes[1], the Arts and Humanities have seen less empirical research into new pedagogical approaches[2]. Humanities foster critical thinking, empathy, and creativity, vital for innovation across domains[2], necessitating improved teaching methods to engage students. Technology in education can enhance learning and engagement[1,3]. Tools such as online platforms, virtual reality, and neurotechnology could play a significant role in this enhancement[4,3].

METHODS
This study is continuation of a previous one[5] and using a developed EEG emotion detection model[6]. It was done with 24 Spanish-speaking adults aged 18-25, not undergoing medical treatment for mental conditions. Participants were divided into two groups completing 4 tasks or Scenes in two different environments: traditional classroom and immersive, based on Descartes' book "The Passions of the Soul" (Fig. 1). EEG signals from the Open BCI cap and Electro Dermal Activity (EDA), Blood Volume Pulse (BVP) signals from the Empatica E4 Bracelet were analysed. EEG data was collected at 250 Hz and pre-processed to remove noise. Clean EEG signals were processed with machine learning (ML) algorithms to distinguish between learning experiences. Features like total power and power spectral density (PSD) were extracted, creating a feature matrix. Three ML models were trained and tested to find the best model. EDA (4 Hz) data was processed using a Gaussian filter, while BVP signal was analysed in its raw form. Skin conductance response (SCR) was calculated using the Bio-SP tool. The phasic component of the EDA signal was obtained by differentiation and convolution, comparing baseline and Scene values. Heart rate (HR) was estimated from the BVP signals (64 Hz) to calculate maximum points and time intervals between peaks.

RESULTS AND DISCUSSION

Key features distinguishing between control and experimental groups were identified. Engagement levels from EEG were significant in differentiating class distinctions, linking engagement to immersion and presence[1,7]. Scene-specific engagement values showed the experimental group generally had higher engagement. Dipole fitting localized brain sources, revealing active Brodmann Areas (BAs) during tasks. BA 10, 18, and 19 were common across Scenes, linked to higher cognitive functions and visual processing (Fig. 2). Unique activations in the experimental group included BA 7 and BA 1, associated with sensory stimuli and somatic sensations, indicating a multi-sensory experience in the immersive environment. Clusters in BA 6, 10, and 18 were present in both groups in Scene 4, indicating similar engagement in promoter cortex, anterior prefrontal cortex, and secondary visual cortex. The control group also showed activity in BA 19, related to complex visual processing during painting interpretation. Average SCRs during each Scene showed higher SCR peaks for both groups compared to baseline, indicating increased engagement. Notably, Scene 4 showed more SCR peaks in the control group compared to the experimental group, suggesting differences in engagement levels. HR increased more in the control group, indicating a higher presence level in the immersive experience.

The results provide preliminary evidence supporting the effectiveness of immersive technologies in teaching Humanities. Future work may scale this to fully virtual reality environments (not employed in this study) and consider using emotion detection algorithms in medical applications, like therapy for mental disorders. Ethical considerations are crucial, ensuring biometric data like EEG, heart rate, and emotions are anonymized and protected. For medical uses, stricter regulations, such as encryption and controlled access, are necessary to prevent data misuse and harm to patients.

Keywords: Immersive Technologies, Neurohumanities, Learning Environments, Electroencephalography, Human in the Loop.

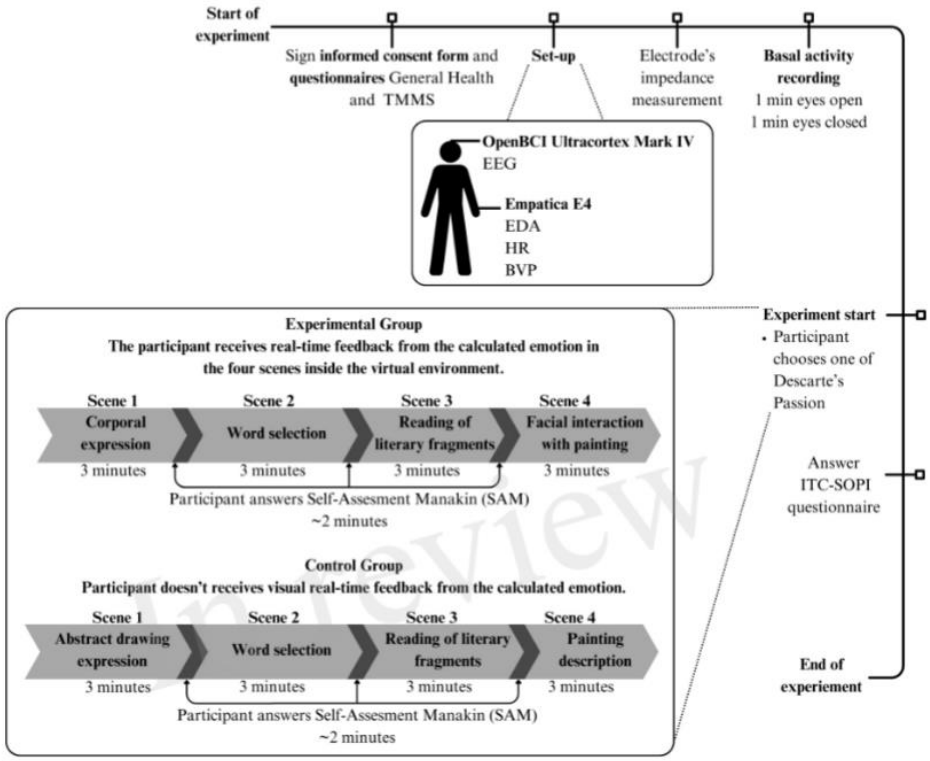

Figure 1. Methodology overview of the experimental protocol used for both groups. Diagram shows the process from start (top left) to end (bottom right).

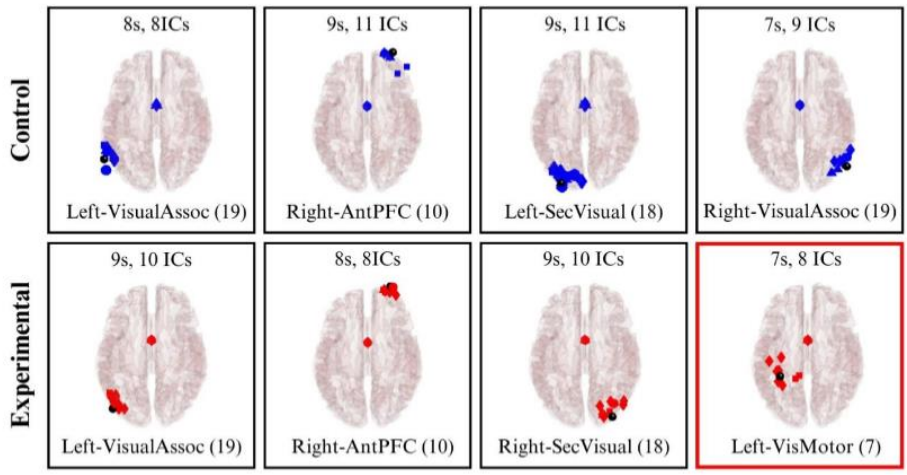

Figure 2. Brodmann Areas found during the dipole fitting and clustering analysis for Scene 1 (experimental and control groups). Colored boxes show unique BA activations in one particular group.

ACKNOWLEDGEMENTS

This research is part of the project Neurohumanities Lab: Engaging Experiences for Human Flourishing, which has been awarded by the grant Ciencia de Frontera of Secihti (Mexico), number CF-2023-G-583. It is also part of the AccelNet Network, Movement, Music and Brain Health, funded by the National Science Foundation (US) with the award number #2412731.

REFERENCES

1.
Bond M, Buntins K, Bedenlier S, Zawacki-Richter O, Kerres M. Mapping research in student engagement and educational technology in higher education: a systematic evidence map. Int J Educ Technol High Educ. 2020;17(1):2. doi:10.1186/s41239-019-0176-8
2.
Hutson J, Olsen T. Digital Humanities and Virtual Reality: A Review of Theories and Best Practices for Art History. IJTE. 2021;4(3):491-500. doi:10.46328/ijte.150
3.
Pradeep K, Sulur Anbalagan R, Thangavelu AP, Aswathy S, Jisha VG, Vaisakhi VS. Neuroeducation: understanding neural dynamics in learning and teaching. Front Educ. 2024;9:1437418. doi:10.3389/feduc.2024.1437418
4.
Collins J, Regenbrecht H, Langlotz T, Said Can Y, Ersoy C, Butson R. Measuring Cognitive Load and Insight: A Methodology Exemplified in a Virtual Reality Learning Context. In: 2019 IEEE International Symposium on Mixed and Augmented Reality (ISMAR). IEEE; 2019:351-362. doi:10.1109/ISMAR.2019.00033
5.
Romo-De León R, Cham-Pérez MLL, Elizondo-Villegas VA, et al. EEG and Physiological Signals Dataset from Participants during Traditional and Partially Immersive Learning Experiences in Humanities. Data. 2024;9(5):68. doi:10.3390/data9050068
6.
Blanco-Ríos MA, Candela-Leal MO, Orozco-Romo C, et al. Real-time EEG-based emotion recognition for neurohumanities: perspectives from principal component analysis and tree-based algorithms. Front Hum Neurosci. 2024;18:1319574. doi:10.3389/fnhum.2024.1319574
7.

Debener S, Thorne J, Schneider TR, Viola FC. 3.1 Using ICA for the Analysis of Multi-Channel EEG Data. In: Ullsperger M, Debener S, eds. Simultaneous EEG and fMRI. 1st ed. Oxford University PressNew York; 2010:121-134. doi:10.1093/acprof:oso/9780195372731.003.0008

13. GreenDIGIT: Project and Initiative to Lower environmental Impact of the Future Digital Research Infrastructures

GreenDIGIT's propositions

1. Framework for managing the full digital RI lifecycle from the environmental impact perspective:
    - For status assessment, Design, Implementation, Operation, Decommissioning
2. Software tools for power usage efficiency:
    - Metrics infrastructure, Schedulers, Reproducibility frameworks, Resource managers (VMs, containers, workflows, AI/ML models, Data, etc.)
3. Develop skills and collaborations
    - Training resources, events, courses, forums

Sustainable RI and IT refers to the integration of environmental considerations into the design, manufacturing, use, and disposal of ITC products and services.

1. Software/Applications Sustainability: Building and using software applications in a manner that requires fewer resources
    - Efficient coding practices that use less computational power.
    - Cloud-based services that optimize server loads.
    - Sustainable Architecture Design principles to ensure durable technical solutions
2. Energy Efficiency: Designing and using IT systems and infrastructure that consume less energy
    - Energy-efficient data centers, Power-saving modes on devices.
    - Energy-efficient cloud computing solutions.
3. Reducing Carbon Footprint: Minimizing the greenhouse gas emissions associated with IT activities:
    - The energy sources of data centers (e.g., transitioning to renewable energy).
    - The carbon impact of IT supply chains.
4. Resource Management and Waste Reduction: Reducing the use of non-renewable resources in IT products and minimizing e-waste
5. Awareness, green practices and education and training
    - GreenComp – Green competences framework for researchers published by EC in 2022

14. Extending EEG Microstate Analysis to Real-World Settings for Characterizing Creativity in the Arts

Yoshua E. Lima-Carmona[*1], Maxine A. Pacheco-Ramírez[1], Aime J. Aguilar-Herrera[1], Lianne Sánchez-Rodríguez[1], Debolina Das[1], Roscoe Ferguson[2], Jose L. Contreras-Vidal[*1]

[1] Laboratory for Non-Invasive Brain-Machine Interface Systems, IUCRC BRAIN, University of Houston, Houston, TX, USA.
[2] Ferguson Control Systems, Houston, TX, USA
* yelimacarmona@uh.edu; jlcontreras-vidal@uh.edu

INTRODUCTION/MOTIVATION

EEG microstates are brief, quasi-stable configurations of scalp electrical activity that provide a unique framework to investigate large-scale brain dynamics and potential biomarkers in neuropsychological

processes[1]. Most research has concentrated on resting-state, consistently revealing 4 to 7 canonical topographies[2]. However, microstate analysis has remained largely absent from cognitive and behavioral tasks in ecologically valid contexts. Of 10 task-related microstate reports identifying more than 7 microstates, 9 focused on event-related potentials and only 1 on continuous EEG[3], highlighting the need for approaches that identify microstates in naturalistic behavior. With Mobile Brain-Body Imaging (MoBI) and adaptive noise cancelling algorithms[4,5], it is now possible to acquire and interpret brain activity in real-world environments, including artistic domains such as music[6], acting[7], and dance[8,9]. Based on this, we developed a pipeline adapting established EEG microstate methods to extend analysis to continuous MoBI EEG during artistic performance. This represents the first application of EEG microstates to complex ecological tasks, enabling study of higher-order functions such as creativity and social interaction beyond resting state.

METHODS

Three public MoBI datasets in artistic contexts, comprising 10 participants, were analyzed: 6 student actors (3 males, 3 females) in live theater (Closer[7]), 2 professional female butoh dancers (The Slowest Wave[8]), and 2 contemporary dancers (1 male, 1 female) across rehearsals and performances (Livewire[9]). All datasets included 28 EEG channels (1kHz), 4 EOG channels (1kHz), and head motion data via Inertial Measurement Units (IMU-128Hz). Preprocessing combined bandpass filtering, adaptive H-Infinity filters for eye blinks[4] and motion[5] artifacts removal, Artifact Subspace Reconstruction, Independent Component Analysis, and Dipole Fitting. Denoised EEG was downsampled to 250Hz and analyzed with MICROSTATELAB[10] to estimate microstate topographies at Global Field Power peaks. The optimal number of clusters was selected via the metacriterion. Temporal parameters of the identified microstates were quantified: mean duration (average stability), occurrence (frequency), and coverage (percentage of total time).

RESULTS AND DISCUSSION

Preliminary analysis revealed 9 microstates optimally fit the data, explaining 76.16% of variance. The 7 canonical microstates (A-G) were consistently observed, while 2 novel topographies (H-I) emerged. Temporal metrics varied across artistic contexts. In Livewire, microstates had shorter mean durations (~17ms) but higher occurrence, reflecting rapid switching. In acting and butoh dance, microstates showed longer durations (~20-27ms) and greater coverage, showing more stable brain configurations. Microstate C in acting had the longest duration overall (~27ms). Microstate D was the most frequent in Livewire, where it also had the highest coverage. In butoh, microstate C showed the highest coverage (21%), suggesting task-specific stability.

These results demonstrate the feasibility of extending EEG microstate to real-world MoBI data. Canonical microstates were robustly identified, while novel topographies (H–I) reflect additional neural states engaged in creative tasks. Dataset-specific dynamics highlight functional differences: prolonged engagement of microstate C in acting may reflect sustained processing of emotional states, while dominance of microstate D in Livewire points to heightened working memory and sensorimotor coordination. In butoh, broad coverage of microstate C suggests a sustained emotional or affective involvement during slow, meditative movement. Future work is needed to determine the functions of novel microstates and their role in naturalistic brain dynamics. Overall, this pioneering work demonstrates that microstate temporal parameters can serve as sensitive markers of the neural dynamics underlying creativity, emotion, and cognition in naturalistic artistic performance.

Keywords: EEG Microstates, Mobile Brain-Body Imaging, Creativity, Arts, Social Neuroscience

ACKNOWLEDGEMENTS

This work was supported by National Science Foundation (NSF) IUCRC BRAIN Award #2137255, NSF AccelNet Award #2412731, NSF REU Award #1757949, and NIH NSAP Award #R25HD106896

REFERENCES

[1] SA A, C S, P D, et al. Analysis of EEG microstates as biomarkers in neuropsychological processes – Review. Computers in Biology and Medicine. 2024;173:108266. doi:10.1016/j.compbiomed.2024.108266

[2] Custo A, Van De Ville D, Wells WM, Tomescu MI, Brunet D, Michel CM. Electroencephalographic Resting-State Networks: Source Localization of Microstates. Brain Connectivity. 2017;7(10):671-682. doi:10.1089/brain.2016.0476

[3] Schiller B, Sperl MFJ, Kleinert T, Nash K, Gianotti LRR. EEG Microstates in Social and Affective Neuroscience. Brain Topogr. 2024;37(4):479-495. doi:10.1007/s10548-023-00987-4

[4] Kilicarslan A, Grossman RG, Contreras-Vidal JL. A robust adaptive denoising framework for real-time artifact removal in scalp EEG measurements. Journal of Neural Engineering. 2016;13(2):026013. doi:10.1088/1741-2560/13/2/026013

[5] Kilicarslan A, Vidal JLC. Characterization and real-time removal of motion artifacts from EEG signals. Journal of Neural Engineering. 2019;16(5):056027. doi:10.1088/1741-2552/ab2b61

[6] Ramírez-Moreno MA, Cruz-Garza JG, Acharya A, et al. Brain-to-brain communication during musical improvisation: a performance case study. F1000Research. 2023;11:989. doi:10.12688/f1000research.123515.4

[7] Hendry MF, Cruz-Garza JG, Delgado-Jiménez EA, et al. Mobile Brain-Body imaging and visual data of theatrical actors during rehearsal and performance. PubMed. 2025;12(1):1421. doi:10.1038/s41597-025-05713-2

[8] Theofanopoulou C, Paez S, Huber D, et al. Mobile brain imaging in butoh dancers: from rehearsals to public performance. BMC Neuroscience. 2024;25(1). doi:10.1186/s12868-024-00864-1

[9] Pacheco-Ramírez MA, Ramírez-Moreno MA, Kukkar K, et al. Neural dynamics of creative movements during the rehearsal and performance of “LiveWire". Scientific Data. 2024;11(1). doi:10.1038/s41597-024-04010-8

[10] Kalburgi SN, Kleinert T, Aryan D, Nash K, Schiller B, Koenig T. MICROSTATELAB: The EEGLAB toolbox for Resting-State Microstate analysis. Brain Topography. 2023;37(4):621-645. doi:10.1007/s10548-023-01003-5

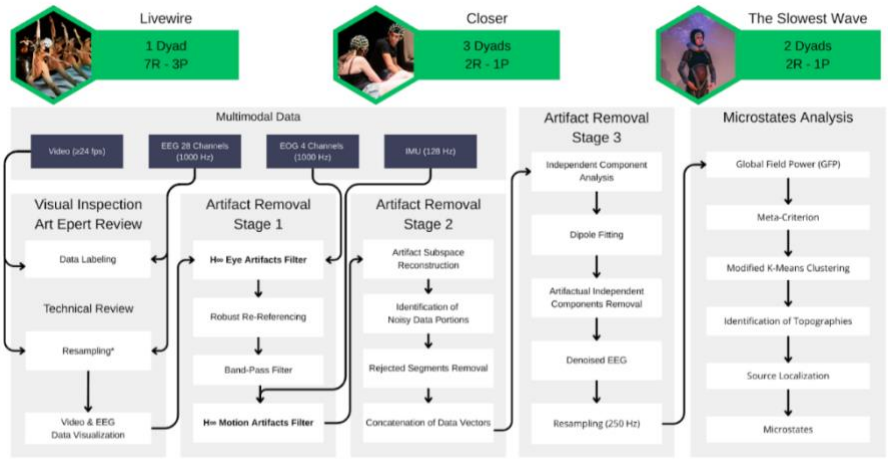

Figure 1. Preprocessing and EEG microstate analysis pipeline. Data included all recordings from the Livewire and Closer datasets, and two participants from The Slowest Wave dataset.

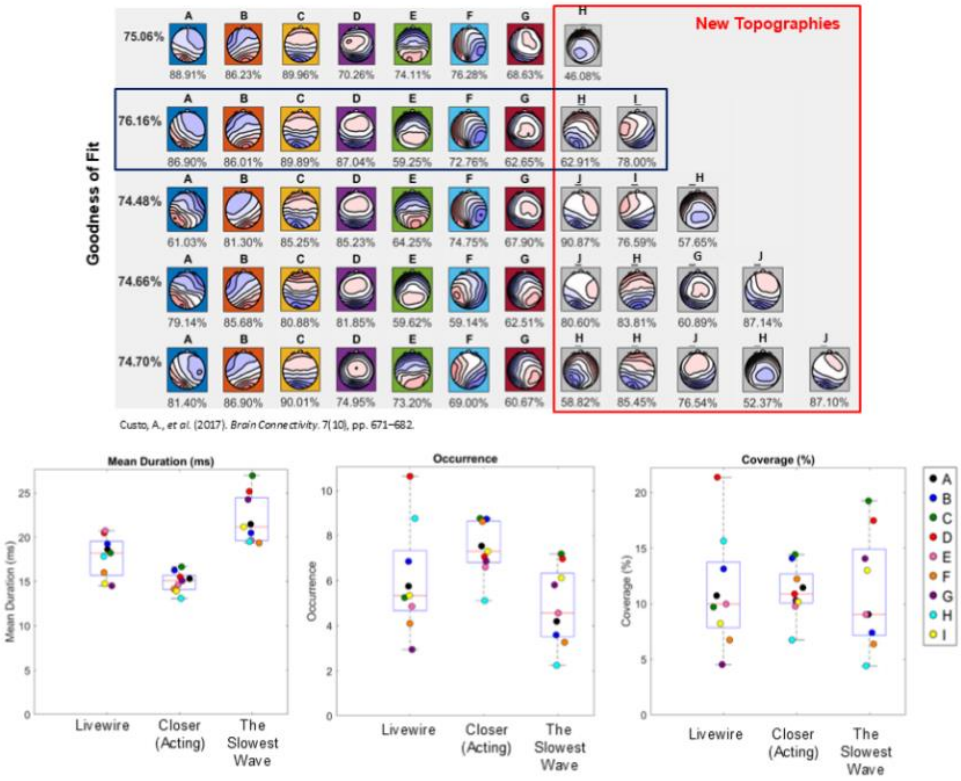

Figure 2. EEG microstate and temporal dynamics across MoBI artistic datasets

15. Hippocampal Immaturity in CaMKII-a-htKO Mice: Characterization of Social Behavior and Neuronal Marker Expression

Maria Queiroz[1], Natalia Turrini[1], Henning Ulrich[1]

[1]Department of Biochemistry, Chemistry Institute – University of São Paulo, São Paulo, Brazil

Keywords: social behavior, hippocampus, CaMKII-a, immunofluorescence

Introduction:
Schizophrenia and bipolar disorder are severe psychiatric conditions involving dysfunctions in brain regions related to cognition and social behavior. The purinergic system, which regulates cellular signaling through nucleotides such as ATP and adenosine, has been implicated in both disorders. Heterozygous CaMKII-α knockout (htKO) mice represent a model of hippocampal immaturity and may mimic social and emotional alterations observed in neuropsychiatric diseases. This study aimed to analyze the social behavior of htKO mice and investigate the expression of purinergic receptors (A2A, P2X7, A3) and neuronal maturation markers (MAP2, β3-tubulin, calbindin, calretinin).

Methods:
Male and female C57BL6/J wild-type (WT) and htKO mice (n = 10 per group) underwent behavioral testing, including habituation-dishabituation, sociability, social novelty, and emotional discrimination. Sessions were video-recorded and analyzed by one- and two-way ANOVA. Procedures were approved by the Institute of Chemistry of the University of São Paulo Ethics Committee (No. 310), following COBEA and NIH guidelines. After testing, animals were divided into two cohorts for tissue collection. One cohort was perfused with 4% formaldehyde, cryoprotected, and stored at -80 °C for immunofluorescence using antibodies against calretinin, calbindin, and CaMKII-α to confirm genotype.

Results:
In the habituation-dishabituation test, htKO females showed reduced interaction time between sessions 2 and 4, and 2 and 5 ($p < 0.01$). In sociability and social novelty tasks, all groups maintained preference for the social stimulus, with no significant differences between genotypes or sexes. Similarly, no differences were observed in emotional discrimination ("relief" and "stress") tests.
Discussion:
These findings suggest that heterozygous CaMKII-α loss does not markedly affect social interaction, novelty preference, or emotional discrimination. Ongoing immunofluorescence analyses will determine whether WT mice exhibit higher expression of neuronal maturation markers in the dentate gyrus compared to htKO animals, providing further insight into CaMKII-α's role in hippocampal development and social behavior.

References:
1. YANAGI, M. et al. Animal Models of Schizophrenia. Progress in Molecular Biology and Translational Science, p. 411–444, 2012. DOI: 10.1111/j.1476-5381.2011.01386.x
2. HARRISON, P. J.; GEDDES, J. R.; TUNBRIDGE, E. M. The Emerging Neurobiology of Bipolar Disorder. Trends in Neurosciences, v. 41, n. 1, p. 18–30, jan. 2018. DOI: 10.1016/j.tins.2017.10.006
3. TARUNO, A. ATP Release Channels. International Journal of Molecular Sciences, v. 19, n. 3, p. 808, 11 mar. 2018. DOI: 10.3390/ijms19030808
4. ORTIZ, R. et al. Purinergic system dysfunction in mood disorders: a key target for developing improved therapeutics. Progress in Neuro-Psychopharmacology and Biological Psychiatry, v. 57, p. 117–131, mar. 2015. DOI: 10.1016/j.pnpbp.2014.10.016
5. MALEWSKA-KASPRZAK, M.; PERMODA-OSIP, A.; RYBAKOWSKI, J. Disturbances of purinergic system in affective disorders and schizophrenia. Psychiatria Polska, v. 53, n. 3, p. 577–587, 30 june 2019. DOI: 10.12740/PP/97335
6. HAGIHARA, H. et al. Immature Dentate Gyrus: An Endophenotype of Neuropsychiatric Disorders. v. 2013, p. 1–24, 1 jan. 2013. DOI: 10.1155/2013/318596
7. YAMASAKI, N. et al. Alpha-CaMKII deficiency causes immature dentate gyrus, a novel candidate endophenotype of psychiatric disorders. Molecular Brain, v. 1, n. 1, 10 set. 2008. DOI: 10.1186/1756-6606-1-6
8. ANDREJEW, R. et al. Post-weaning social isolation impairs purinergic signaling in rat brain. Neurochemistry International, v. 148, p. 105111, sept. 2021. DOI: 10.1016/j.neuint.2021.105111

Acknowledgments: FAPESP and CNPq for grant and fellowship support.

16. Robust Multi-Class EEG Emotion Recognition Via Trial-Level Validation & Supervised Feature Selection

Maxine Annel Pacheco-Ramírez[1*], Jose L. Contreras-Vidal[1*]

[1] Laboratory for Non-Invasive Brain-Machine Interface Systems, IUCRC BRAIN, University of Houston, Houston, TX, USA. *mpachec4@cougarnet.uh.edu; jlcontreras-vidal@uh.edu

INTRODUCTION/MOTIVATION
Emotion recognition from electroencephalography (EEG) is an important research area in human-computer interaction and brain-computer interfacing (BCI), with applications in mental healthcare, education and entertainment[1-3]. Despite progress, the field faces persistent methodological limitations. Many works evaluate performance at the window level, where overlapping windows from the same trial appear in both training and test sets, introducing leakage and inflating accuracy estimations[4]. Others rely on unsupervised dimensionality reduction such as principal component analysis, which does not guarantee preservation of class-discriminative information[5]. Moreover, most

prior studies restrict classification to 2 or 3 broad emotional categories, limiting ecological validity and translation to real-world applications. This study addresses these limitations by employing trial-level leave-one-out (LOTO) cross-validation, supervised feature selection, and classification of 5 discrete emotions.

METHODS

Using the SEED-V dataset[6] in order to set some testing parameters and pipelines (1 subject, 3 sessions, 5 emotion classes), preprocessing was implemented using filter designs optimized for prospective real-time applications, including a high-pass filter to attenuate slow drifts, an H-infinity adaptive filter for robust elimination of ocular artifacts[7], and a low-pass filter at 20 Hz cutoff to restrict the spectrum to conventional EEG bands while minimizing contamination from muscular activity. Preprocessing variants with and without Artifact Subspace Reconstruction and Independent Component Analysis were also evaluated, and results indicated that the best approach for this analysis was to exclude these steps. Signals were segmented into overlapping windows of 1s with a 0.1s step, and feature extraction consisted of differential entropy across canonical frequency bands, hemispheric asymmetry indices (DASM and RASM), alpha-band asymmetry for valence, and beta/alpha power ratios for arousal. This process produced 446 candidate features per window. To ensure strict separation of training and testing, features were aggregated per trial using mean and standard deviation, resulting in one feature vector per trial. For classification, Linear Discriminant Analysis (LDA), Support Vector Machine (SVM), Logistic Regression, Random Forest, and Extra Trees were analyzed. Supervised feature selection was applied using ANOVA F-tests to retain the top 40% most discriminative features. Model evaluation followed a LOTO cross-validation strategy at the trial level, ensuring that no windows from the same trial appeared simultaneously in both training and test sets.

RESULTS AND DISCUSSION

Under the five-emotion setting, LDA achieved the highest performance: accuracy = 77.8%, precision = 0.777, recall = 0.778, and F1 score = 0.764. Logistic Regression followed with ~68.9% accuracy, ensemble methods (Random Forest, Extra Trees) achieved ~60–62%, and SVM ~57.8%. A consistent advantage of LDA across all evaluation metrics underscores that, when supervised feature selection is combined with trial-level LOTO validation, the resulting feature space favors linear separability over more complex non-linear approaches.

These results are significant because they demonstrate that EEG emotion decoding with five emotional categories is feasible under strong validation constraints. Achieving ~78% accuracy with trial-level LOTO indicates performance that is both reliable and generalizable. The usage of supervised feature selection preserves discriminative information and helps avoid the pitfalls of unsupervised methods. Given that LDA is relatively simple and computationally efficient, this pipeline is promising for future real-time applications, such as BCIs or adaptive affective computing, where latency and interpretability are key. This benchmark provides a useful standard for emotion recognition research pushing toward more ecologically valid, robust, and reproducible systems.

Keywords: Electroencephalography (EEG), Emotion recognition, Brain–computer interfaces (BCI), Artificial intelligence (AI), Machine learning (ML), Feature extraction, Signal processing

ACKNOWLEDGEMENTS

This work was supported by National Science Foundation (NSF) IUCRC BRAIN Award #2137255 and the NSF AccelNet Award #2412731.

REFERENCES

[1] Alarcao SM, Fonseca MJ. Emotions Recognition Using EEG Signals: A survey. IEEE Transactions on Affective Computing. 2017;10(3):374-393. doi:10.1109/taffc.2017.2714671
[2] Zheng NWL, Lu NBL. Investigating Critical Frequency Bands and Channels for EEG-Based Emotion Recognition with Deep Neural Networks. IEEE Transactions on Autonomous Mental Development. 2015;7(3):162-175. doi:10.1109/tamd.2015.2431497
[3] Zhang Z, Fort JM, Mateu LG. Mini review: Challenges in EEG emotion recognition. Frontiers in Psychology. 2024;14. doi:10.3389/fpsyg.2023.1289816

[4] Khan NN, Sweet T, Harvey CA, Knapp C, Krusienski DJ, Thompson DE. The Role of Review Process Failures in Affective State Estimation: An Empirical Investigation of DEAP Dataset. arXiv Preprint. 2025. arXiv:2508.02417.
[5] Martinez AM, Kak AC. PCA versus LDA. IEEE Transactions on Pattern Analysis and Machine Intelligence. 2001;23(2):228-233. doi:10.1109/34.908974
[6] Liu W, Qiu JL, Zheng WL, Lu BL. Comparing recognition performance and robustness of multimodal deep learning models for multimodal emotion recognition. IEEE Transactions on Cognitive and Developmental Systems. 2022;14(2):715-729. doi:10.1109/tcds.2021.3071170
[7] Kilicarslan A, Grossman RG, Contreras-Vidal JL. A robust adaptive denoising framework for real-time artifact removal in scalp EEG measurements. Journal of Neural Engineering. 2016;13(2):026013. doi:10.1088/1741-2560/13/2/026013

17. An interoperability pipeline for sharing FAIR non-human primate data through EBRAINS

Reema Gupta[1*], Thomas Wachtler[2]

[1]Faculty of Biology, Ludwig-Maximilians-Universität, Munich, Germany
[2]Faculty of Biology, Ludwig-Maximilians-Universität, Munich, Germany
*gupta@biologie.uni-muenchen.de

INTRODUCTION/MOTIVATION
Neural data from non-human primates (NHP) are essential for understanding function and dysfunction of the human brain, but sharing and re-use of such data is hampered by the complexity and diversity of data formats and custom processing workflows. We address these challenges in the context of the EU training network In2PrimateBrains (http://In2PrimateBrains.eu), which investigates neural processing in NHP brain networks, and the EBRAINS open call project NHP-BRAINS. Here we present a processing pipeline that is built on open tools and standards to harmonise NHP data from different laboratories and to share them via the EBRAINS RI.

METHODS
We developed a processing and curation pipeline to create structured and comprehensively annotated datasets compliant with EBRAINS (RRID:SCR_019260) and community standards such as the Brain Imaging Data Standard (BIDS) (RRID:SCR_016124) with its extension for animal microelectrode electrophysiology (BEP032). The pipeline systematically converts heterogeneous data formats into standardized NIX (RRID:SCR_016196) and NWB (RRID:SCR_015242) files using the Neo (RRID:SCR_000634) representation for electrophysiological data. Metadata is collected using researcher-friendly tools including the web-based CEDAR metadata workbench (RRID:SCR_016270) and spreadsheet-based odML tables (RRID:SCR_016228), utilizing controlled vocabularies aligned with the openMINDS (RRID:SCR_023173) metadata schemas. Our data collection comprises 1.16 TB of resting state recordings from 20 subjects across 13 European laboratories, spanning multiple brain regions including prefrontal, motor (M1, PMd), parietal (AIP, 7A, DP), visual (V1, V2, V4), cingulate cortex, and thalamus. Data were recorded with state-of-the-art multi-site probes including Neuropixels, Primatepixels, SiNAPS, TREC MiniMatrix, and Utah arrays, supplemented with behavioral data such as eye tracking and EMG recordings. The data is stored as DataLad (RRID:SCR_003931) datasets on the version-controlled GIN platform (RRID:SCR_015864) and made findable through the EBRAINS KnowledgeGraph (RRID:SCR_017612) and registered to the EBRAINS macaque atlas (MEBRAINS).

RESULTS AND DISCUSSION
The pipeline yields unified data collections that can be integrated into EBRAINS with minimal curation effort and that are seamlessly compatible with EBRAINS analysis tools. A key component of this

workflow includes metadata templates developed using CEDAR web-forms that systematically map to openMINDS schemas, providing standardized data annotation across the diverse laboratory formats. The datasets, once processed, will serve as the foundation for an extensible open resource of NHP electrophysiological data on EBRAINS. The open-source, configurable pipeline will be re-usable by the neuroscience community for standardising and preparing data for sharing through the EBRAINS RI.

The work presented here demonstrates how EBRAINS RI components and other open-source community tools can be effectively integrated as building blocks to facilitate data harmonisation and curation of rich, multi-laboratory NHP datasets. This approach will result in a comprehensive NHP data collection spanning multiple brain regions and recording modalities that is immediately accessible for analysis with EBRAINS analysis tools, and that can be extended by contributions from the wider community. The combination of standardised workflows and this diverse electrophysiological dataset creates lasting benefit for neuroscience research, facilitates broader adoption of FAIR data sharing practices, and demonstrates how the EBRAINS RI supports creation and re-use of high-quality neurophysiology data.

Keywords: Non-human primate, Electrophysiology, FAIR data, EBRAINS, Data sharing, Interoperability, BIDS, openMINDS, Metadata, Standardization

ACKNOWLEDGEMENTS
This work received funding from the European Union through the In2PrimateBrains project (GA 956669) and through the EBRAINS 2.0 (GA 101147319) Open Call (Project 46).

REFERENCES
[1] Gorgolewski KJ, Auer T, Calhoun VD, et al. The brain imaging data structure, a format for organizing and describing outputs of neuroimaging experiments. Sci Data. 2016;3(1):160044. doi:10.1038/sdata.2016.44
[2] BIDS BEP032. BEP 032: Microelectrode electrophysiology. Accessed August 25, 2025. https://bids.neuroimaging.io/bep032
[3] Garcia S., Guarino D., Jaillet F., Jennings T.R., Pröpper R., Rautenberg P.L., Rodgers C., Sobolev A., Wachtler T., Yger P. and Davison A.P. (2014) Neo: an object model for handling electrophysiology data in multiple formats. Frontiers in Neuroinformatics 8:10: doi:10.3389/fninf.2014.00010
[4] Open Metadata Initiative. openMINDS metadata framework: open metadata initiative for neuroscience data structures. Accessed August 25, 2025. https://github.com/openMetadataInitiative/openMINDS
[5] Rübel O, Tritt A, Ly R, et al. The Neurodata Without Borders ecosystem for neurophysiological data science. eLife. 2022;11:e78362. doi:10.7554/eLife.78362
[6] Gonçalves RS, O'Connor MJ, Martínez-Romero M, et al. The CEDAR Workbench: An Ontology-Assisted Environment for Authoring Metadata that Describe Scientific Experiments. Semant Web ISWC. 2017;10588:103-110. doi:10.1007/978-3-319-68204-4_10
[7] Balan PF, Zhu Q, Li X, et al. MEBRAINS 1.0: A new population-based macaque atlas. Imaging Neurosci (Camb). 2024;2:imag-2-00077. doi:10.1162/imag_a_00077
[8] Halchenko YO, Meyer K, Poldrack B, et al. DataLad: distributed system for joint management of code, data, and their relationship. Journal of Open Source Software. 2021;6(63):3262. doi:10.21105/joss.03262
[9] Stoewer A, Kellner C, Benda J, Wachtler T, Grewe J. File format and library for neuroscience data and metadata. Front Neuroinform. 2014;8. doi:10.3389/conf.fninf.2014.18.00027
[10] Wilkinson MD, Dumontier M, Aalbersberg IjJ, et al. The FAIR Guiding Principles for scientific data management and stewardship. Sci Data. 2016;3(1):160018. doi:10.1038/sdata.2016.18

18. Task-Evoked Functional Connectivity of Object–Location Memory: A Basis for Focal Brain Stimulation

Author names and affiliations:
Mohamed Abdelmotaleb[1*], Harun Kocataş[1], Leonardo M. Caisachana Guevara[1], Filip Niemann[1], Alireza Shahbabaie[1], Robert Malinowski[1], Daria Antonenko[1], Marcus Meinzer[1], Agnes Flöel[1,2]

[1] Department of Neurology, University Medicine Greifswald, Greifswald, Germany
[2] German Center for Neurodegenerative Diseases (DZNE Site Greifswald), Greifswald, Germany

*Mohamed.Abdelmotaleb@med.uni-greifswald.de

Introduction
Object–location memory (OLM) enables us to remember where objects are located in the environment[1], yet its neural mechanisms remain poorly understood despite its clinical relevance and vulnerability to aging and Alzheimer's disease[2]. This gap limits the development of effective neuromodulation strategies: non-invasive brain stimulation (NIBS), including transcranial direct current stimulation (tDCS), has shown mixed results[3–6], likely due to suboptimal targeting[7]. Moving beyond activation mapping, connectivity-based approaches can identify cortical nodes that are both accessible and functionally coupled to memory-critical medial temporal structures, providing evidence-informed stimulation targets[8,9]. Using an established OLM paradigm[3,10] and task-evoked fMRI connectivity analyses, we characterized network interactions underlying OLM and linked them to learning success. Our findings advance mechanistic understanding of OLM and establish a network-guided framework for optimizing future stimulation interventions.

Methods
This preparatory study, part of a larger sham-tDCS controlled crossover study (https://www.memoslap.de/de/home/), mapped task-evoked fMRI connectivity during an OLM task. Twenty healthy, right-handed adults (19 included after quality control; 10 females; mean age = 25 years) completed an intrascanner OLM paradigm and a control task. The OLM task involved learning house–location associations with feedback, while the control task matched perceptual and motor demands without associative learning. To establish a workflow consistent with later project phases involving active tDCS, we targeted the right lateral occipito-temporal cortex (ROTC) with sham tDCS during scanning. MRI data were collected on a 3T scanner with high-resolution functional and anatomical scans. Task-evoked functional connectivity was analyzed with a Generalized Psychophysiological Interaction (gPPI) model in both seed-to-voxel and ROI-to-ROI frameworks. Statistical inference used a voxel-wise threshold of $p < 0.001$, with cluster-level family-wise error correction (FWEc) at $p < 0.05$. Exploratory analyses assessed correlations between connectivity strength and behavioural accuracy.

Results
Participants showed robust learning across four OLM stages, with increasing accuracy and decreasing reaction times confirming successful acquisition of object–location associations. Univariate analyses revealed stronger activation for OLM (vs. control) in hippocampal, parahippocampal, fusiform, temporo-occipital, and lateral occipital regions. Connectivity analyses identified medial temporal and lateral occipito-temporal cortices as key hubs of learning-related functional coupling. ROI-to-ROI analyses demonstrated strengthened hippocampal–fusiform, parahippocampal–occipito-temporal, and temporo-occipital intra- and interhemispheric connections. Exploratory brain–behavior correlations further indicated that stronger medial temporal–ventral visual connectivity predicted higher accuracy, underscoring the functional integration of memory and perceptual networks during OLM.

Discussion

This study provides novel insight into the network-level mechanisms supporting OLM, showing that successful learning emerges from coordinated interactions between medial temporal structures and temporal–occipital cortices, forming an integrated memory–perception network. Our results highlight temporo–occipital cortices as accessible cortical nodes functionally connected to the hippocampus, making them promising targets for NIBS interventions. Importantly, stronger connectivity between medial temporal and ventral visual areas was associated with more pronounced learning success, highlighting their functional relevance. Together, these results provide mechanistic insight into OLM acquisition and establish an evidence-based framework for identifying target networks to enhance ecologically relevant spatial memory through NIBS.

Keywords

Object–location memory, Spatial memory, Episodic memory, Functional Magnetic Resonance Imaging (fMRI), FMRI analysis, Functional connectivity, Generalized Psychophysiological Interaction (gPPI), Non-invasive brain stimulation, Transcranial direct current stimulation (tDCS), Hippocampus.

Acknowledgments

This research was funded by the German Research Foundation (DFG) (project grants: ResearchUnit5429/1 [467143400]; CRC1315-B03 [327654276]; FL379/22-1; FL379/26-1; FL379/34-1; FL379/35-1; FL379/37-1; ME3161/3-1; ME3161/5-1; ME3161/6-1; AN1103/3-1; AN1103/6-1 [539593253]). This study was pre-registered on the Open Science Framework (OSF). The pre-registration protocol is available under OSF Registries (https://osf.io/t37u2). We are grateful to our research coordinators and student assistants for their help with scheduling and testing.

Figure

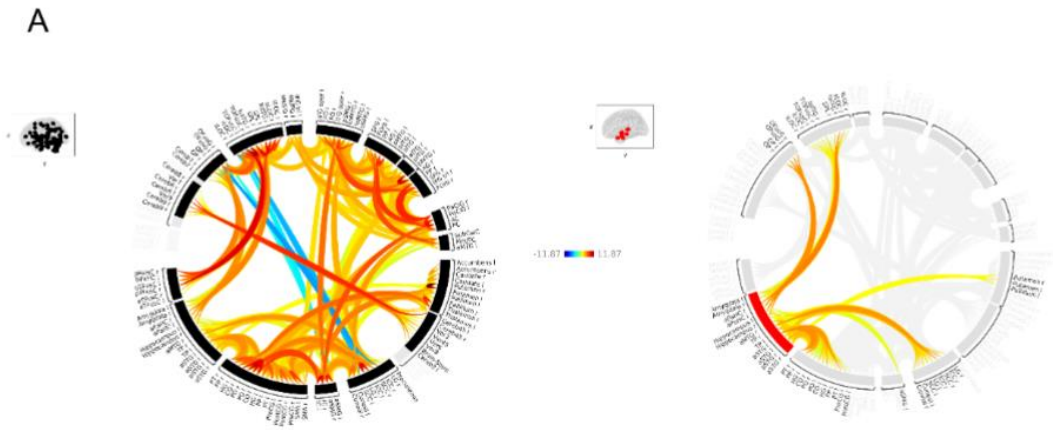

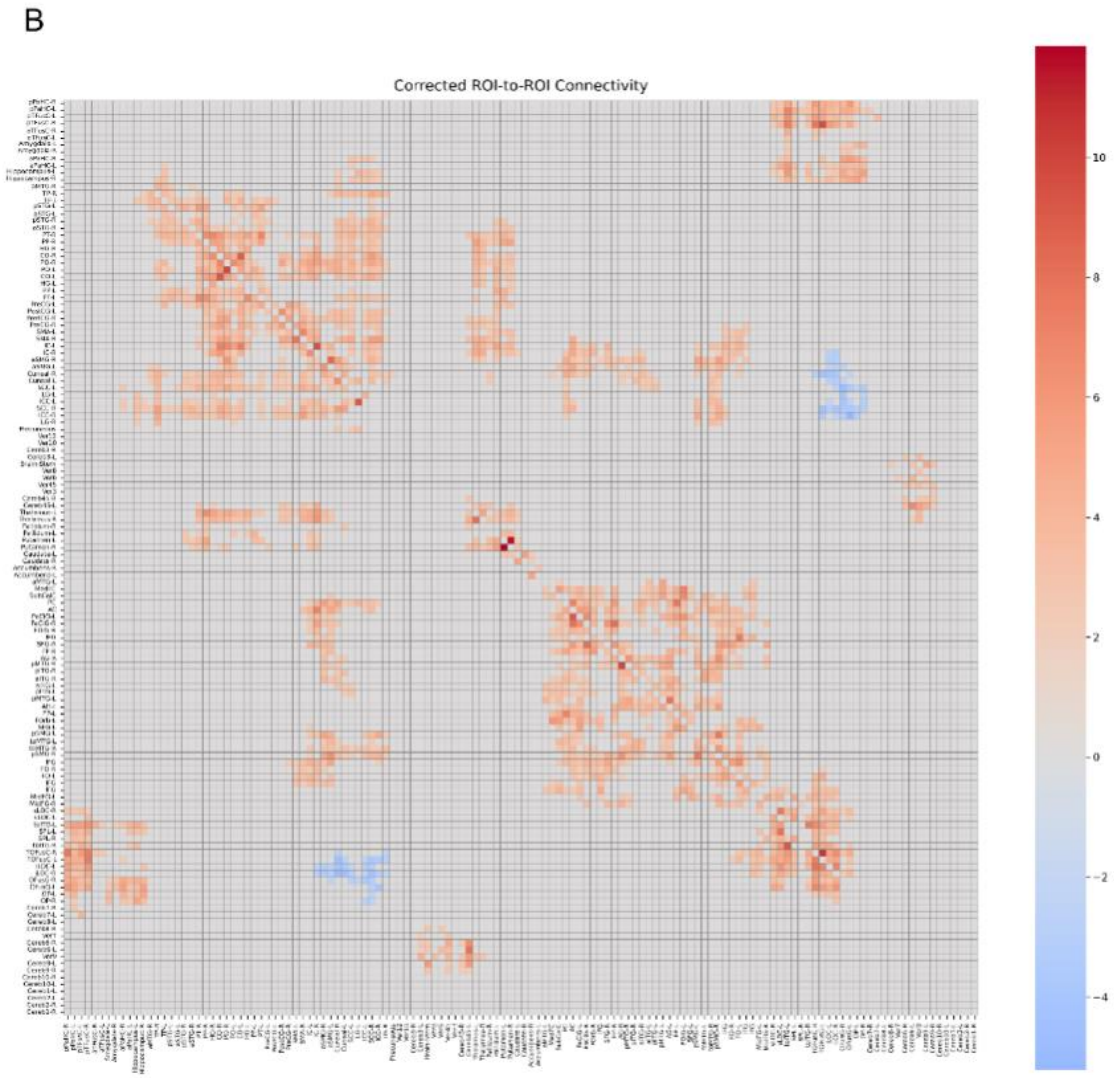

Figure 1. Task-based ROI-to-ROI functional connectivity during object–location learning (N = 19).
(A) Connectome ring plots depicting group-level ROI-to-ROI connectivity derived from generalized psychophysiological interaction (gPPI) analysis for the contrast learning > control using Harvard–Oxford–defined regions of interest (ROIs). The left panel shows the full connectivity matrix, while the right panel highlights connections involving regions previously implicated in object–location memory (OLM), including the hippocampus, parahippocampus, and temporo-occipital cortices. Statistical maps were thresholded at $p < 0.001$ with cluster-level family-wise error correction (FWEc).
(B) Heatmap representations of the same group-level ROI-to-ROI connectivity results. The color scale indicates t-values, with warm colors reflecting stronger connectivity during learning relative to control, and cool colors indicating stronger connectivity during control relative to learning.

References

1. Postma A, Kessels RPC, van Asselen M. The Neuropsychology of Object-Location Memory. In: Human Spatial Memory: Remembering Where. Lawrence Erlbaum Associates Publishers; 2004:143-160.
2. Zimmermann K, Eschen A. Brain regions involved in subprocesses of small-space episodic object-location memory: a systematic review of lesion and functional neuroimaging studies. Memory. 2017;25(4):487-519. doi:10.1080/09658211.2016.1188965
3. Flöel A, Suttorp W, Kohl O, et al. Non-invasive brain stimulation improves object-location learning in the elderly. Neurobiology of Aging. 2012;33(8):1682-1689. doi:10.1016/j.neurobiolaging.2011.05.007

4. England HB, Fyock C, Meredith Gillis M, Hampstead BM. Transcranial direct current stimulation modulates spatial memory in cognitively intact adults. Behavioural Brain Research. 2015;283:191-195. doi:10.1016/j.bbr.2015.01.044
5. Antonenko D, Külzow N, Sousa A, Prehn K, Grittner U, Flöel A. Neuronal and behavioral effects of multi-day brain stimulation and memory training. Neurobiol Aging. 2018;61:245-254. doi:10.1016/j.neurobiolaging.2017.09.017
6. Fromm AE, Grittner U, Brodt S, Flöel A, Antonenko D. No Object–Location Memory Improvement through Focal Transcranial Direct Current Stimulation over the Right Temporoparietal Cortex. Life. 2024;14(5):539. doi:10.3390/life14050539
7. Meinzer M, Shahbabaie A, Antonenko D, et al. Investigating the neural mechanisms of transcranial direct current stimulation effects on human cognition: current issues and potential solutions. Front Neurosci. 2024;18:1389651. doi:10.3389/fnins.2024.1389651
8. Fox MD, Buckner RL, Liu H, Chakravarty MM, Lozano AM, Pascual-Leone A. Resting-state networks link invasive and noninvasive brain stimulation across diverse psychiatric and neurological diseases. Proc Natl Acad Sci U S A. 2014;111(41):E4367-4375. doi:10.1073/pnas.1405003111
9. Nilakantan AS, Bridge DJ, Gagnon EP, VanHaerents SA, Voss JL. Stimulation of the posterior cortical-hippocampal network enhances precision of memory recollection. Curr Biol. 2017;27(3):465-470. doi:10.1016/j.cub.2016.12.042
10. Külzow N, Kerti L, Witte VA, Kopp U, Breitenstein C, Flöel A. An object location memory paradigm for older adults with and without mild cognitive impairment. J Neurosci Methods. 2014;237:16-25. doi:10.1016/j.jneumeth.2014.08.020

19. A proposal for a distributed Local Service Provider Ecosystem for interfacing with a European Digital Infrastructure Consortium for neuroscience research

Roberto Inchingolo[1], Irene Costantini[1], Victoria Barygina[1], Francesco Saverio Pavone[1]

[1]University of Florence, LENS - European Laboratory for Non-Linear Spectroscopy, Sesto Fiorentino, Italy

EBRAINS is a European open research infrastructure that gathers data, tools and computing facilities for brain-related research, and one of the key outcomes of the Human Brain Project, a European Future and Emerging Technologies (FET) Flagship project that ran from 2013 to 2023.

As EBRAINS is expected to transition into its future role as both a European Digital Infrastructure Consortium (EDIC) and a long-term Research Infrastructure (RI), a clear organisational framework is needed to ensure sustainable service delivery and stakeholder engagement. This works proposes a position on structuring a Ecosystem of Local Service Provider (LSPE) to align with EBRAINS' hybrid nature and outlines practical mechanisms to integrate and sustain local service providers (LSPs) in this evolving landscape.

LSPs, typically research institutions or scientific facilities embedded in EBRAINS National Nodes or operating independently, play a key role in complementing EBRAINS' centrally funded core services. These accessory services may include workflow customization, data production and annotation, training and education, on-site technical support, innovation management, and technology transfer.

Given that EBRAINS EDIC services must remain free of charge for final users and will have limited capacity to fund external contributions, the LSPE model proposes a cost-recovery mechanism to allow LSPs to sustain their activities. This includes the possibility of reimbursement for personnel, overhead, and consumables linked to EBRAINS-related tasks. Additionally, services provided by

LSPs to private or industrial stakeholders should be fee-based, as commercial services fall outside the scope of free EDIC offerings.

Beyond direct service provision, participation in the LSPE also offers strategic advantages for LSPs. By being part of an organised, recognized ecosystem, they are better positioned to co-develop proposals for EU research and innovation funding calls. Featuring EBRAINS EDIC as a strategic partner enhances competitiveness and fosters broader scientific collaboration. This framework builds upon the legacy of the Human Brain Project's "Facility Hubs" and "Competence Centers," while establishing a more structured and financially viable model for long-term collaboration.

20. Teacher propagation through space, time, and the brain

Authors: Federico Benitez[1], Paul Haider[1], Benjamin Ellenberger[1], Kevin Max[2], Jakob Jordan[1], Laura Kriener[3], Ben von Hünerbein[1], Mihai A. Petrovici[1]

Affiliations: 1) NeuroTMA Group, University of Bern; 2) OIST, Japan 3) INI, ETH Zurich

Introduction: The way in which physical networks of neurons, bound by spatio-temporal locality constraints, can perform eZicient credit assignment, remains, to a large extent, an open question. In machine learning, the answer is almost universally given by the error backpropagation algorithm, through both space and time. However, this algorithm is well-known to rely on biologically - and, more generally, physically - implausible assumptions, in particular given its manifest violation of spatio-temporal locality. Alternative forward-propagation models such as real-time recurrent learning only partially solve the locality problem, and involving a not inconsiderable scaling cost, due to prohibitive storage requirements.

Methods: We propose that this challenge can be met by taking into account a number of key observations from neuroscience - in particular prospective coding, functional neuronal morphology and error-correcting plasticity – as well as recent developments in neuromorphic engineering. This allows us to build novel neuronal and network models such as Generalized Latent Equilibrium (GLE) and learning methods such as Phaseless Alignment Learning (PAL) and EZicient Learning of Sequences in Structured Networks (ELISE). GLE represents a local and controled approximation to backpropagation through time, yielding a satisfactory answer to the temporal locality problem. In turn, PAL solves the weight transport problem for general network architectures, providing the final piece on the puzzle of spatial locality. Finally, ELISE takes inspiration from biology to implement structured networks that are by design highly eZiceint when learning to reproduce temporal sequences.

Results: With these components and methods, we show how fully local network dynamics can efficiently solve the spatiotemporal credit assignment problem, thereby providing clear blueprints for physical circuits capable of carrying out these computations, both in vivo and in silico. Beyond error backpropagation, we show how our biologically-inspired methods provide an efficient toolkit for learning in temporally non-trivial contexts, such as the learning of complex sequences.

Discussion: Our results point towards a unified thoery of local learning in the brain, with applications neuroscience and in neuromorphic engineering. Adding spikes to these models, for example, is an envisageable extension that is currently under active research.

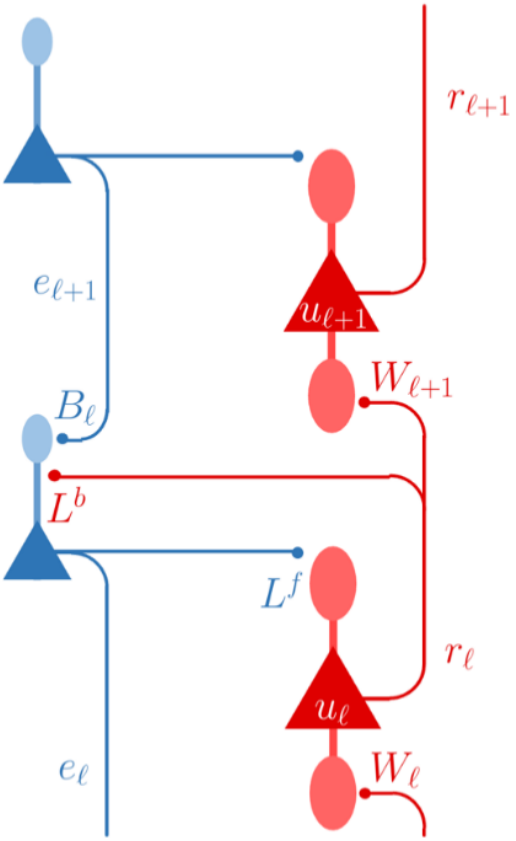

Figure 1: Generalized Latent Equilibrium Network: Mapping of GLE equations to hierarchical, cortical microcircuits with feedforward representation neurons (red) and feedback error neurons (blue). Both classes of neurons are pyramidal, likely located in diAerent layers of cortex. Lateral connections enable information exchange and gating between the two streams. Errors are also represented in dendrites, likely located in the apical tuft of signal neurons, enabling local three-factor plasticity to correc the backpropagated errors.

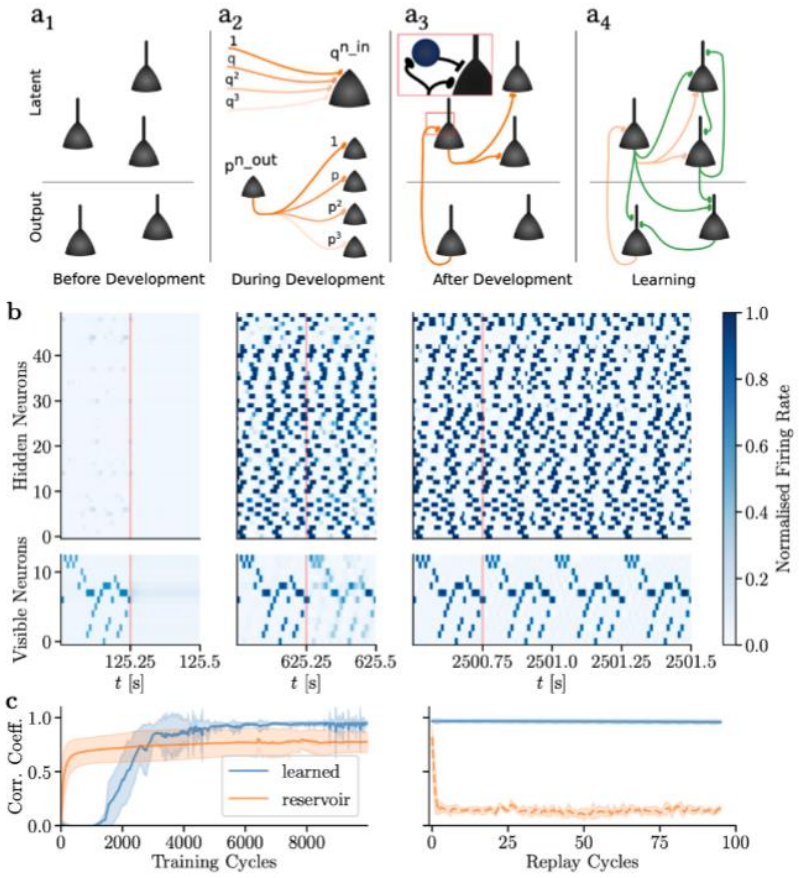

Figure 2: ELISE Model(a) Development and learning in a two-population model of latent and output neurons. Following neurogenesis (a1), axons (orange) extend to form a sparse scaAold of somato-somatic connections between pyramidal neurons. Its structure is controlled by parameters p and q (a2). Inhibition in this scaAold is mediated by interneurons (a3). Following the development phase, somato-dendritic synapses (green) evolve according to a three-factor plasticity rule (a4).
(b) Evolution of network activity during learning. Output neurons are first nudged towards a particular target and then released in order to observe the network's spontaneous activity (as demarcated by the red line). Snapshots during early (left), intermediate (middle) and final (right) stages of training.
(c) Accuracy and stability of sequence replay, measured by the correlation between generated and target activity. Comparison between our model (capable of recurrent learning) and an equivalent reservoir (where only latent-to-output connections are learned). Left: Accuracy during training. Right: Accuracy after repeated replay cycles.

Acknowledgements: We gratefully acknowledge funding from the European Union under grant agreements #945539 (Human Brain Project, SGA3) and #101147319 (EBRAINS 2.0). We would like to express particular gratitude for the ongoing support from the Mandred Stärk Foundation. Our work has greatly benefitted from access to the Fenix Infrastructure resources, which are partially funded by the European Union's Horizon 2020 research and innovation programme through the ICEI project under the grant agreement No. 800858.

References:

Haider, Ellenberger, Kriener, Jordan, Senn, Petrovici. Advances in Neural Information Processing Systems, 34, 17839-17851, 2021
Ellenberger, Haider, Jordan, Max, Jaras, Kriener, Benitez, Petrovici. Nature Communications, in press, 2025
Brandt, Petrovici, Senn, Wilmes, Benitez. ArXiv pre-print arXiv:2405.14810, 2024

Max, Kriener, Pineda García, Nowotny, Jaras, Senn, Petrovici. Nature Machine Intelligence, 6, 619–630, 2024
Max, Jaras, Granier, Wilmes, Petrovici. Biorxiv pre-print 2025.07.11.664263, 2025
Kriener, Völk, von Hünerbein, Benitez, Senn, Petrovici. ArXiv preprint arXiv:2402.16763, 2024

21. Integrating empirical region- and subject-specific hemodynamic response function in The Virtual Brain

Alejandro Veloz[1], Amogh Johri[2], Guorong Wu[3], Daniele Marinazzo[4]

1. University of Valparaiso, Valparaiso, Chile
2. CALTECH, Pasadena, USA
3. Southwest University, Chongqing, China
4. Ghent University, Ghent, Belgium

Introduction
The hemodynamic response function (HRF) greatly influences intra- and inter-subject variability of brain activation and connectivity, presenting a fundamental challenge in personalized brain modeling. The Virtual Brain (TVB) on EBRAINS provides an open-source platform for constructing and simulating personalized brain network models, yet traditional approaches rely on canonical HRF assumptions that fail to capture subject-specific and regional hemodynamic variations. HRF variability across brain regions, individuals and populations substantially confounds connectivity estimates and between-subjects group differences, limiting the accuracy of digital brain twins. This study addresses the critical need to incorporate empirically-derived, subject-specific HRF profiles into large-scale brain simulations.

Methods
We integrated the rsHRF toolbox, which retrieves onsets of pseudo-events triggering hemodynamic responses from resting-state fMRI BOLD signal using point process theory, with TVB's personalized brain modeling pipeline on EBRAINS. The rsHRF method fits a model to retrieve optimal lag between events and HRF onset, as well as HRF shape parameters for each voxel/vertex. We processed multimodal neuroimaging data from healthy subjects and patients through the TVB image-processing pipeline to generate structural and functional connectomes. Subject-specific HRF shapes were extracted using rsHRF and incorporated into TVB's neural mass models, replacing canonical HRF assumptions. Simulated BOLD signals were generated using these personalized HRF profiles and compared against empirical resting-state data using correlation metrics and spectral analysis.

Results
We successfully developed and tested a comprehensive pipeline that seamlessly integrates rsHRF estimation with The Virtual Brain framework on EBRAINS. The pipeline automatically extracts subject-specific HRF parameters from resting-state fMRI data and incorporates them into TVB's personalized brain modeling workflow. Our approach demonstrates improved correspondence between simulated and empirical BOLD signals when using empirically-derived HRF profiles compared to canonical assumptions. The pipeline effectively captures regional and individual HRF variability patterns, leading to enhanced match between empirical and simulated functional connectivity. All components are fully operational within the EBRAINS cloud infrastructure, ensuring compatibility with existing TVB workflows and data standards.

Discussion
This work presents the first ready-to-deploy pipeline for integrating subject-specific HRF estimation into The Virtual Brain ecosystem on EBRAINS. By providing a tested framework that addresses the

fundamental challenge of HRF variability in brain simulation, we enable researchers to build more accurate digital brain twins. The pipeline's integration within EBRAINS infrastructure ensures seamless compatibility with existing neuroimaging processing workflows and facilitates scalable application to large cohort studies. This methodology represents a crucial step toward the Virtual Brain Twin paradigm for personalized medicine, providing the neuroimaging community with practical tools for enhanced brain modeling and improved inference of neural parameters without the HRF confounding. The framework is immediately available for clinical and research applications, supporting improved understanding of neurovascular coupling and advancing personalized approaches to neurological and psychiatric disorders.

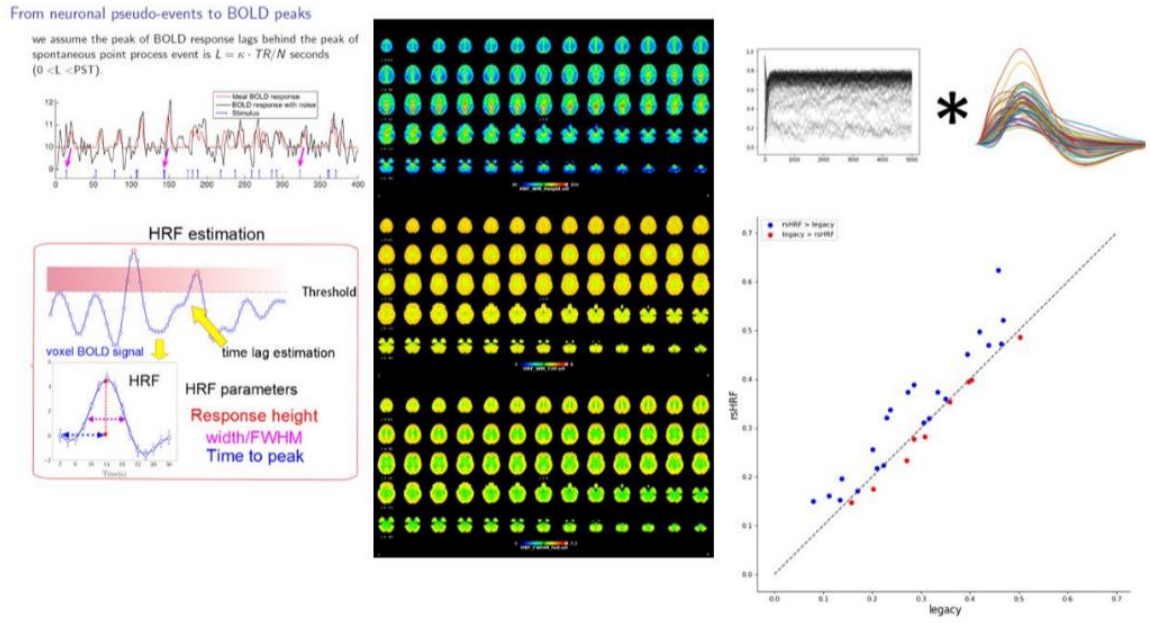

Figure 1. Scheme of the procedure. Left column: BOLD peaks are assumed to be generated by point processes, fitted by GLMs allowing to retrieve rsHRF and shape parameters. Central column: Variability of the shape parameters across the brain. Right column: region-wise rsHRFs are convolved with simulated neural activity, and the approach is compared with the legacy TVB one, showing better.

Acknowledgements
INCF and the Google Summer of Code program; EU Horizon 2020 Grant No. 101147319 (EBRAINS 2.0 Project), Ghent University mobility funds.

References
1. Wu, G. R., Colenbier, N., Van Den Bossche, S., Clauw, K., Johri, A., Tandon, M., & Marinazzo, D. (2021). rsHRF: A toolbox for resting-state HRF estimation and deconvolution. NeuroImage, 244, 118591. https://www.sciencedirect.com/science/article/pii/S1053811921008648
2. https://www.ebrains.eu/tools/rshrf
3. https://www.ebrains.eu/tools/the-virtual-brain

22. EBRAINS: Building a Federated, Transdisciplinary Brain Ecosystem

Victoria Barygina[1], Roberto Inchingolo[2], Francesco Saverio Pavone[1,2,3]

[1]University of Florence, [2]LENS - European Laboratory for Non-Linear Spectroscopy, [3]CNR-National Institute of Optics

Corresponding author: victoria.barygina@unifi.it

EBRAINS 2.0 envisions a sustainable, inclusive, multidisciplinary ecosystem that reaches beyond neuroscience to embrace brain health, public engagement, citizen science, education, and cultural interfaces.

Despite world-class assets, Europe lacks a federated, cross-sector platform that operationalizes global brain strategies and systematically engages diverse stakeholders, limiting translation to healthcare, innovation, and societal benefit.

In EBRAINS 2.0 project (WP7, Task 7.7) we performed a comprehensive stakeholder analysis to position EBRAINS as an open, federated research infrastructure. The approach aligns EBRAINS with WHO's IGAP, the Global Brain Coalition's "One Brain One Health", and the WEF Brain Economy vision, defining priority stakeholder segments, tailored value propositions, engagement pathways, and governance/sustainability levers.

The resulting roadmap strengthens strategic coherence and long-term viability of EBRAINS as a transdisciplinary European and global platform. It accelerates integration of new tools and services for brain research, broadens participation, and enhances downstream impact on brain health, innovation, and human development.

23. QUINT workflow now supports whole brain analysis using the Developmental Mouse Brain Atlas (DeMBA).

Maja Puchades[1], Ingvild E. Bjerke[1], Harry Carey[1], Heidi Kleven[1], Martin Øvsthus[1], Sharon C. Yates[1], Gergely Csucs[1], Simon McMullan[2], Trygve B. Leergaard[1] & Jan G. Bjaalie[1]

1. Neural Systems Laboratory, Institute of Basic Medical Sciences, University of Oslo, Oslo, Norway
2. Macquarie Medical School, Faculty of Medicine, Health & Human Sciences, Macquarie University, Marsfield, NSW, Australia

Abstract

INTRODUCTION: Three-dimensional, open access digital brain atlases are important resources in neuroscience research, opening new possibilities for automated analyses in atlas defined regions of interest. The EBRAINS QUINT workflow [1,2] has been developed to support standardized atlas-based analysis of sectioned tissue without the need for coding ability. It features integrated brain atlases for the adult rat and mouse brain and is increasingly used in the neuroscience community. However, a recurrent request from many QUINT users interested in understanding brain development, has been to include brain atlases representing different developmental ages, to so achieve better spatial registration for brains from young individuals.

METHODS: To meet this need, we have now integrated the novel Developmental Mouse Brain Atlas (DeMBA), a four-dimensional atlas covering every postnatal day from 4 to 56 [3]. This atlas features segmentations from the widely adopted Allen Mouse Brain CCF and the Kim developmental atlases, that have been transformed and interpolated to the same ages, ensuring comparable region definitions across ages [4].

RESULTS AND DISCUSSION: The DeMBA atlas was implemented in the registration software QuickNII and VisuAlign and shared as specific packages together with the atlas itself on EBRAINS [4]. Those versions require usage of the specific Filebuilder utility shared within the packages. Next,

the DeMBA atlas was implemented in a new Nutil Quantifier version (v1.1) and thereby the complete QUINT analysis can now be performed on young mouse brains.

All the software tools and the DeMBA atlas are shared through the EBRAINS Knowledge graph [5]. We here present the updated QUINT workflow and give examples of preliminary developmental data analysis.

Keywords: Brain atlas, developmental ages, cell counting, QUINT, software.

References:
1. Yates, S. et al. (2019) QUINT: Workflow for Quantification and Spatial Analysis of Features in Histological Images From Rodent Brain. Front. Neuroinform. 13, 1–14. https://doi.org/10.3389/fninf.2019.00075
2. Puchades MA, Yates SC, Csucs G, Carey H, Balkir A, Leergaard TB and Bjaalie JG (2025) Software and pipelines for registration and analyses of rodent brain image data in reference atlas space. Front. Neuroinform. 19:1629388. https://doi.org/10.3389/fninf.2025.1629388
3. Carey, H., Ovsthus, M., Kleven, H., Yates, S. C., Csucs, G., Puchades, M. A., Bjaalie, J. G., Leergaard, T. B., & Bjerke, I. E. (2024). Developmental mouse brain atlas (DeMBA) with continuous coverage of postnatal day 4 to 56 (v1) [Data set]. EBRAINS. https://doi.org/10.25493/V3AH-HK7
4. Carey, H., Kleven, H., Øvsthus, M. et al. DeMBA: a developmental atlas for navigating the mouse brain in space and time. Nat Commun 16, 8108 (2025). https://doi.org/10.1038/s41467-025-63177-9
5. https://search.kg.ebrains.eu

Acknowledgements
This work received funding from European Union's Horizon 2020 Framework Program for Research and Innovation under the specific grant agreement no. 945539 (Human Brain Project SGA3); the European Union's Research and Innovation Program Horizon Europe under Grant Agreement no. 101147319 (EBRAINS 2.0); and UNIFOR-FRIMED.

24. Toward Standardization: A Multimodal Pipeline for Mobile Brain-Body Imaging (MoBI)

L. Sánchez-Rodríguez, A. J. Aguilar-Herrera, M. A. Pacheco-Ramírez, Y. E. Lima-Carmona, J. L. Contreras-Vidal

IUCRC BRAIN, University of Houston

Introduction: Studying the social and creative brain in real-world scenarios requires methodological and technical innovations that preserve ecological validity and enhance data quality while capturing neural dynamics in naturalistic settings, including artistic performances. Mobile Brain/Body Imaging (MoBI) has emerged as a transformative approach, integrating mobile electroencephalography (EEG) with motion capture, eye tracking, video, sound, and environmental context to study embodied cognition outside the lab, enabling investigation of neural activity as it unfolds in situ during dance, music, theater, or visual arts or their appreciation by the audience. Yet, recording from free-behaving participants generate extensive artifacts, including eye movements, muscle activity, motion, and ambient noise. Such artifacts often overwhelm the EEG signals of interest, obscuring interpretable dynamics. Moreover, the lack of standardized, community-validated pipelines limits replication, comparability across studies, and clinical translation.

Methods: We propose a multimodal, stepwise methodology for signal acquisition and artifact identification and reduction in MoBI datasets, combining EEG with EOG, motion sensors, and

synchronized video recordings. Careful attention to best practices during acquisition is essential. Proper EEG cap preparation, secure electrode placement, elastic net adjustment and subject familiarization with equipment ensure stable contact and comfort during performances. Electrode impedances are checked before and after sessions to detect potential drifts. Furthermore, Transistor-Transistor Logic (TTL) triggers integrate audiovisual systems and motion sensors to guarantee hardware-based synchronization across modalities and participants, which is critical in hyperscanning protocols were multiple participants are recorded. Consistent use of these practices[1] minimizes artifacts at the source, reduces reliance on aggressive post-hoc corrections, and strengthens interpretability in creative and interactive contexts. The denoising pipeline consists of several stages: (1) Visual inspection aligns EEG with motion signals, recording triggers, and annotated video, ensuring artifacts are identified in their behavioral context while minimizing bias. (2) Two sequential artifact removal steps apply adaptive noise canceling (ANC)[2,3] to identify and remove eye blinks, bias, motion artifacts, drifts, and structured noise while preserving neural activity.

Results: Application across artistic contexts, classical and contemporary dance, live acting, and collaborative music-making, demonstrated robust separation of neural signals from movement noise. The pipeline enabled reproducible detection of creativity-related oscillatory activity, reliable intra- and inter-brain synchrony, and context-dependent mapping of network dynamics otherwise masked by artifacts.

Discussion: The multimodal framework establishes best practices for MoBI EEG denoising in ecological environments, offering a reproducible path from raw recordings to interpretable dynamics. The proposed approach advances the neuroscience of creativity, social interaction and neuroaesthetics. Beyond application, the approach supports FAIR data principles, enabling large-scale and cross-cultural sharing of MoBI datasets. By bridging methodological rigor with ecological validity, this framework advances open, reproducible neuroscience and deepens understanding of artistic expression, its role in cognition, emotion, social interaction, and human well-being.

References

1. Theofanopoulou, C., Paez, S., Huber, D. et al. Mobile brain imaging in butoh dancers: from rehearsals to public performance. BMC Neurosci 25, 62 (2024). https://doi.org/10.1186/s12868-024-00864-1
2. Kilicarslan A, Grossman RG, Contreras-Vidal JL. A robust adaptive denoising framework for real-time artifact removal in scalp EEG measurements. J Neural Eng. 2016;13(2):026013. doi:10.1088/1741-2560/13/2/026013
3. Kilicarslan A, Contreras Vidal JL. Characterization and real-time removal of motion artifacts from EEG signals. J Neural Eng. 2019;16(5):056027. Published 2019 Sep 17. doi:10.1088/1741-2552/ab2b61

25. MarmotGraph v4 – the evolution of the EBRAINS Knowledge Graph

AUTHORS
Annapaola Iolanda Santarsiero[1], Claudio Goffi[1], Oliver Schmid[1]

AFFILIATIONS
1. CSCS, ETH Zurich, Zurich, Switzerland

ABSTRACT
Introduction: The increasing uptake of Knowledge Graph technology in academic and industrial settings causes the importance of graph databases to grow. Tooling and workflows to ensure metadata quality as well as the establishment of fine granular access permissions remain an important aspect and need to follow this evolution. Consequently, we recognized that a major

development step of the EBRAINS Knowledge Graph (KG; RRID:SCR_017612) was required to adopt new capabilities while preserving and enhancing its core functionalities. The combination of these considerations with the learnings from more than six years of productive use in the context of the Human Brain Project (RRID:SCR_002241) and the EBRAINS RI (RRID:SCR_019260) resulted in the “MarmotGraph” solution.

Methods:
To achieve our goals, the following actions have been taken:
• **Semantic separation** between the technology and the deployed service(s)
• Increased **modularization** of the graph related components to make the underlying graph engine exchangeable.
• **Architectural redesign** to improve performance and **usability** with a focus on **accessibility standards.**
• Enhanced functionalities for **mass-manipulation** activities (e.g. for meta-data migrations)
• Preparations for future storage of **sensitive metadata**
• Introduction of **multi-tenancy** capabilities
• Improved **containerized deployment**
• API level **backwards compatibility**

Results:
We have extracted the underlying technology of the “EBRAINS Knowledge Graph” into the software product “MarmotGraph” which stands for “**M**anagement **A**pplications for **R**ich **M**etadata **O**bjec**T**s in a **Graph**”. This semantic split, in combination with the new multi-tenancy capability, allows us to be more precise in communication and to reuse the core technology in multiple contexts. To showcase the adaptability and to prove the domain-agnosticism of the technology, we have established a “CSCS Knowledge Graph” representing a semantic digital twin of the Swiss National Supercomputing Center.

The establishment of a multi-tenancy ready design allows us to adapt the various tools to different use cases and contexts. Thanks to the regular review of usability aspects with heterogenous user groups, the number of perspectives on requirements and features have been extended.

Architectural redesigns and partial replacement of underlying technologies have resulted in significant performance improvements and code maintainability. Thanks to the backwards compatibility of the API, migration efforts for integrated clients can be kept minimal. Mass manipulation operations have been tested with the real-life use-case of openMINDS (RRID:SCR_023173) version migration. Optimizations of operational aspects (semantic versioning, creation of reusable Helm charts, etc.) have simplified the maintenance in both Kubernetes and non-Kubernetes environments on multiple sites.

Discussion:
The separation of the built technology providing the “EBRAINS Knowledge Graph” into the service and the domain-agnostic metadata management product “MarmotGraph” makes the technology reusable. This allows to expand the userbase beyond the neuroscientific community, creates synergies in the development and maintenance process, increases funding possibilities and enables cross-domain integrations (e.g. by linking neuroscientific research data with computing resources of a supercomputer center) which positively affects the sustainability of the solution.

Furthermore, the architectural redesign allows to replace the underlying off-the-shelf graph engine whilst maintaining consistent APIs and tools. This makes the solution future-proof, protects it from a “vendor-lock-in” in case of discontinuation or change of license, and ultimately allows the adaptation to new developments and requirements.

ACKNOWLEDGEMENTS
This open-source software code was developed in part or in whole in the Human Brain Project, funded from the European Union's Horizon 2020 Framework Programme for Research and Innovation under Specific Grant Agreements No. 720270, No. 785907 and No. 945539 (Human Brain Project SGA1, SGA2 and SGA3).

Current funding is provided by the State Secretariat for Education, Research and Innovation SERI Switzerland as part of an associated partner in the project EBRAINS 2.0.

KEYWORDS
1. Knowledge Graph
2. Linked Data
3. FAIR principles
4. MarmotGraph
5. Data management

26. openMINDS SANDS: making brain atlases machine- actionable using Linked Data

Ulrike Schlegel[1*], Heidi Kleven[1], Tom Gillespie[2], Louisa Köhnen[3], Xiao Gui[3], Raphaël Gazzotti[4], Oliver Schmid[5], Timo Dickscheid[3,6], Katrin Amunts[3,4,7], Jan G. Bjaalie[1,4], Trygve B. Leergaard[1,4], Lyuba Zehl[4*]

[1]Institute of Basic Medical Sciences, Faculty of Medicine, University of Oslo, Oslo, Norway
[2]Department of Neurosciences, University of California, San Diego, La Jolla, United States
[3]Institute of Neuroscience and Medicine (INM-1), Research Centre Jülich, Jülich, Germany
[4]EBRAINS AISBL, Brussels, Belgium
[5]CSCS, ETH Zurich, Zurich, Switzerland
[6]Faculty of Mathematics and Natural Sciences, Institute of Computer Science, Heinrich Heine University Düsseldorf, Düsseldorf, Germany
[7]C. and O. Vogt Institute for Brain Research, University Hospital Düsseldorf, Heinrich Heine University Düsseldorf, Düsseldorf, Germany
*ulrike.schlegel@medisin.uio.no; lyuba.zehl@ebrains.eu

INTRODUCTION/MOTIVATION
Brain atlases underpin many branches of neuroscience by providing a spatial scaffold on which multimodal data can be organised and compared. Yet atlas resources are often released as project-specific archives differing in structure, coordinate space, parcellation logic, and nomenclature. This heterogeneity forces developers to write custom loaders, hinders cross-atlas comparison, and propagates inconsistency. To overcome these barriers we introduced **openMINDS SANDS** (RRID:SCR_023498), a Linked Data specification that operationalises the Atlas Ontology Model (AtOM) [1] within the openMINDS metadata framework (RRID:SCR_023173). Our goal is to turn static atlas downloads into interoperable web resources that can be queried and reused by humans and machines alike.

METHODS
SANDS was implemented as an openMINDS extension integrating the four AtOM entities (reference data, coordinate system, annotations, terminology) into the holistic openMINDS model. Schemas were designed to follow the FAIR principles [2] (e.g., licensing, links to other FAIR resources) and to adopt AtOM suggestions (e.g., standardized atlas structures, versioning). To demonstrate

expressiveness, we curated widely used brain atlases in accordance with SANDS for three common atlas types: (i) discrete atlases where the annotation set contains only discretely defined regions, (ii) probabilistic atlases where the annotation set contains regions defined by statistically-weighted composites, and (iii) parcellation models where processive annotation criteria are defined to create specimen-specific atlases by parcellating a single specimen's anatomy and mapping it to a defined terminology. Finally, the SANDS compliant Linked Data descriptions of the curated atlases were shared formatted as JSON-LD files through the openMINDS instance libraries (RRID:SCR_027358) making them serviceable to any software and service developers as standardized atlas representations.

RESULTS AND DISCUSSION

As of today (2025-08-28), we have applied SANDS to 13 commonly used brain atlases and parcellation models from 3 different species. Their Linked Data representations are provided in the openMINDS instances libraries. As evidence, we present one example for each atlas type: (i) the Waxholm Space Rat Brain Atlas (RRID:SCR_017124) [3] as example for a discrete atlas, (ii) the Julich-Brain Atlas (RRID:SCR_023277) [4] as example for a probabilistic atlas, and (iii) the Desikan Killiany Atlas [5] as example for a parcellation model. These examples demonstrate harmonized atlas usage between the EBRAINS Knowledge Graph (RRID:SCR_017612; EBRAINS central data and knowledge platform), and the siibra toolsuite [6] (EBRAINS software for providing interactive multilevel brain atlases) enabled by adopting SANDS.

By integrating AtOM into the openMINDS metadata framework, SANDS converts existing atlases into FAIR, machine-actionable web resources. The resulting Linked Data facilitates side-by-side visualization, pipeline automation, and atlas-driven analysis. Moreover, SANDS instances can be harvested by search engines, enriched with community annotations, and mirrored across repositories. However, the main limitation remains sociotechnical: atlas providers must supply compliant metadata, and developers must replace hard-coded templates with dynamic queries. To ease adoption we are developing open-source converters from other standardization efforts such as BIDS [7] and provide integration support through our GitHub (Open Metadata Initiative). By making brain atlases first-class Linked-Data citizens, openMINDS SANDS removes the final technical barrier to fully FAIR, automation-ready neuroanatomical workflows.

Keywords: Atlas Ontology Model (AtOM), discrete brain atlas, FAIR principles, Linked Data, openMINDS SANDS, parcellation model, probabilistic brain atlas, spatial reference frameworks

ACKNOWLEDGEMENTS

This work has received funding from the European Union's Horizon Europe research and innovation programme under grant agreement No 101147319 (EBRAINS 2.0). It also was supported by the Helmholtz International BigBrain Analytics and Learning Laboratory (HIBALL).

REFERENCES

[1] Kleven H, Gillespie TH, Zehl L, et al. AtOM, an ontology model to standardize use of brain atlases in tools, workflows, and data infrastructures. Sci Data. 2023;10:486. https://doi.org/10.1038/s41597-023-02389-4

[2] Wilkinson MD, Dumontier M, Aalbersberg IJJ, et al. The FAIR guiding principles for scientific data management and stewardship. Sci Data. 2016;3:160018. https://doi.org/10.1038/sdata.2016.18

[3] Kleven H, Bjerke IE, Clascá F, et al. Waxholm Space atlas of the rat brain: a 3D atlas supporting data analysis and integration. Nat Methods. 2023;20:1822-1829. https://doi.org/10.1038/s41592-023-02034-3

[4] Amunts K, Mohlberg H, Bludau S, Zilles K. Julich-Brain: a 3D probabilistic atlas of the human brain's cytoarchitecture. Science. 2020;369(6506):988-992. https://doi.org/10.1126/science.abb4588

[5] Desikan RS, Ségonne F, Fischl B, et al. An automated labeling system for subdividing the human cerebral cortex on MRI scans into gyral based regions of interest. Neuroimage. 2006;31(3):968-980. https://doi.org/10.1016/j.neuroimage.2006.01.021
[6] Dickscheid T, Gui X, Simsek A, et al. Siibra: a software tool suite for realizing a multilevel human brain atlas from complex data resources. bioRxiv. Published online May 20, 2025. https://doi.org/10.1101/2025.05.20.655042
[7] Gorgolewski KJ, Auer T, Calhoun VD, et al. The brain imaging data structure, a format for organizing and describing outputs of neuroimaging experiments. Sci Data. 2016;3:160044. https://doi.org/10.1038/sdata.2016.44

27. From Metadata to Insight: How openMINDS and the EBRAINS Knowledge Graph Accelerate Brain Research

Raphaël Gazzotti[1*], Alix Bonard[2], Laura Morel[2], Sophia Pieschnik[3], Ulrike Schlegel[3], Eivind Hennestad[3], Peyman Najafi[2], Claudio Goffi[4], Annapaola Santarsiero[4], Oliver Schmid[4], Andrew P. Davison[2], Lyuba Zehl[1*]

[1]EBRAINS AISBL, Brussels, Belgium
[2]Institut des Neurosciences Paris-Saclay, Université Paris-Saclay, CNRS, Saclay, France
[3]Institute of Basic Medical Sciences, Faculty of Medicine, University of Oslo, Oslo,Norway
[4]CSCS, ETH Zurich, Zurich, Switzerland
*raphael.gazzotti@ebrains.eu; lyuba.zehl@ebrains.eu

INTRODUCTION/MOTIVATION
Sharing and reusing data, models, and tools is essential for modern neuroscience but remains challenging because resources are scattered, inconsistently described, and hard to connect. For the EBRAINS Research Infrastructure (RI; RRID:SCR_019260), the EBRAINS Knowledge Graph (KG; RRID:SCR_017612) addresses this challenge by providing a curated, searchable platform that links digital research outputs contributed by the community. For this, the KG leverages openMINDS (RRID:SCR_023173), a framework that provides structured, machine- and human-readable Linked Data [1] descriptions of research products, learning resources, and actors (persons, organizations, consortia). Together, openMINDS and EBRAINS KG enable researchers to discover relevant resources, developers to build interoperable tools, and the wider community to contribute to a growing, FAIR [2] ecosystem.

METHODS
openMINDS is an open-source, community-driven metadata framework offering (i) a metadata model composed of interlinked schema specifications, (ii) instance libraries for well-defined terms and constructs (e.g. species, brain atlases), and (iii) supportive tooling for handling schemas and instances in Python, MATLAB, or Java. Product metadata submissions to the EBRAINS RI are curated and validated by the EBRAINS Curation service before being registered in the EBRAINS KG as openMINDS-compliant Linked Data in JSON-LD format. Through this model, the EBRAINS KG connects resources to each other and makes them available via graphical and programmatic interfaces (GUIs and APIs).

RESULTS AND DISCUSSION
The EBRAINS KG currently hosts metadata about over 1100 dataset versions, 270 model versions, 250 software versions, 30 service versions, 250 learning resources, and 2560 contributors. openMINDS links all these entities to capture content, provenance, reusability, and integration potential. For example, workflows can be annotated to track provenance end-to-end; datasets can be linked to services for processing or visualization; computational models can be connected to their

foundational data; software can be linked to compatible inputs and outputs; derived datasets can be connected to their sources; products can reference learning resources that facilitate use; and live papers can be linked to all their components. A forthcoming openMINDS v5.0 release, shaped by user and developer feedback, will extend schema coverage, optimize usability, and enhance integration that further increase the FAIR components of neuroscience resources within the EBRAINS KG and facilitate cross platform integrations.

openMINDS and EBRAINS KG provide a common language for neuroscience resources within and beyond the EBRAINS RI. For developers, adopting openMINDS enhances interoperability and visibility by integrating tools in a linked ecosystem. For users, the EBRAINS KG simplifies discovery and reuse across datasets, models, and software, supporting more transparent and reproducible science. For the community, the open-source, collaborative development of openMINDS is essential to ensure that both tools evolve with scientific needs. By describing their work, integrating their tools, or helping refine schemas, scientists and students contribute to a shared infrastructure that strengthens EBRAINS and accelerates neuroscience.

Keywords: FAIR principle, Linked Data, Interoperability, Metadata, Knowledge Graph

ACKNOWLEDGEMENTS
This work has received funding from the European Union's Horizon Europe research and innovation programme under grant agreement No 101147319 (EBRAINS 2.0).

REFERENCES
[1] Heath T, Bizer C. Linked Data: Evolving the Web into a Global Data Space. Synthesis Lectures on the Semantic Web: Theory and Technology. 2011;1(1):1-136. https://doi.org/10.2200/S00334ED1V01Y201102WBE001
[2] Wilkinson MD, Dumontier M, Aalbersberg IJ, et al. The FAIR Guiding Principles for scientific data management and stewardship. Sci Data. 2016;3:160018. https://doi.org/10.1038/sdata.2016.18

28. Advanced Probabilistic Inference for Causal Discovery

Meysam Hashemi[*1], Nina Baldy[1], Abolfazl Ziaeemehr[1], Amir Esmaeili[1], Lia Domide[2], Pierpaolo Sorrentino[1], Spase Petkoski[1], Marmaduke Woodman[1], Viktor Jirsa[*1]

[1] Aix Marseille Univ, INSERM, INS, Inst Neurosci Syst, Marseille, France
[2] Codemart, Cluj-Napoca, Romania
* Email :Meysam.hashemi@univ-amu.fr/viktor.jirsa@univ-amu.fr

Introduction
Understanding the principles and causal mechanisms underlying complex brain function, dysfunction, and cognition is essential for advancing precision medicine. Dynamic Causal Modeling (DCM [1]) and The Virtual Brain (TVB [2]) represent major steps forward, combining statistical and computational models of brain dynamics with anatomical data to simulate brain activity at the mesoscopic and macroscopic scales, respectively. Causality is central to these approaches, particularly in the context of experimental manipulations such as stimulation and intervention. However, there remains a critical need for automatic and widely available inference tools, despite recent advances in probabilistic machine learning.

Methods
In this work, we aim to bridge this gap by providing efficient and flexible Bayesian inference methods, operating across brain scales. We used the state-of-the-art probabilistic machine learning tools, employing adaptive Markov chain Monte Carlo sampling [3] , and simulation-based inference [4].

Results
We have developed two open-source tools:
1) *Automatic DCM* [5]. This tool enables: (a) algorithmic benchmarking in probabilistic programming frameworks, (b) effective solutions for parameter degeneracy, and (c) comprehensive model comparison in fitting event-related potentials observed in magneto/encephalography data.
2) *Virtual Brain Inference (VBI)* [6]. This tool enables: (a) fast simulations of whole-brain models, (b) a taxonomy of data feature extraction, and (c) deep neural density estimators for inference from various recordings.
These tools are now available on EBRAINS, along with tutorials and demo applications. We have demonstrated their accuracy and reliability using in-silico data. The performance of these methods is then demonstrated for causal inference in multiple sclerosis [7], Parkinson [8], focal intervention [9], and social facilitation [10].

Discussion
This work shows potential to improve causal hypothesis evaluation through uncertainty quantification, contributing to advances in precision medicine. Further integration with EBRAINS datasets is planned for future work.

Acknowledgements
This project/research has received funding from the European Union's Horizon Europe Programme under the Specific Grant Agreement No. 101147319 (EBRAINS 2.0 Project), No. 101137289 (Virtual Brain Twin Project), and government grant managed by the Agence Nationale de la Recherche reference ANR-22-PESN-0012 (France 2030 program).

Keywords: Causal inference, Probabilistic machine learning, Multimodal brain data, Precision medicine

References
[1] Friston, K. J., Harrison, L., & Penny, W. (2003). Dynamic causal modelling. Neuroimage, 19(4), 1273-1302. https://doi.org/10.1016/S1053-8119(03)00202-7
[2] Sanz Leon, P., Knock, S. A., Woodman, M. M., Domide, L., Mersmann, J., McIntosh, A. R., & Jirsa, V. (2013). The Virtual Brain: a simulator of primate brain network dynamics. Frontiers in neuroinformatics, 7, 10. https://doi.org/10.3389/fninf.2013.00010
[3] Hoffman, M. D., & Gelman, A. (2014). The No-U-Turn sampler: adaptively setting path lengths in Hamiltonian Monte Carlo. J. Mach. Learn. Res., 15(1), 1593-1623. https://www.jmlr.org/papers/volume15/hoffman14a/hoffman14a.pdf
[4] Cranmer, K., Brehmer, J., & Louppe, G. (2020). The frontier of simulation-based inference. Proceedings of the National Academy of Sciences, 117(48), 30055-30062. https://doi.org/10.1073/pnas.1912789117
[5] Baldy, N., Woodman, M., Jirsa, V. K., & Hashemi, M. (2025). Dynamic causal modelling in probabilistic programming languages. Journal of the Royal Society Interface, 22(227), 20240880. https://doi.org/10.1098/rsif.2024.0880
[6] Ziaeemehr Abolfazl, Woodman Marmaduke, Domide Lia, Petkoski Spase, Jirsa Viktor, Hashemi Meysam (2025) Virtual Brain Inference (VBI): A flexible and integrative toolkit for efficient probabilistic inference on virtual brain models eLife 14:RP106194 https://doi.org/10.7554/eLife.106194.2
[7] Sorrentino, P., Pathak, A., Ziaeemehr, A., Lopez, E. T., Cipriano, L., Romano, A., ... & Hashemi, M. (2024). The virtual multiple sclerosis patient. Iscience, 27(7). https://doi.org/10.1016/j.isci.2024.11010
[8] Angiolelli, M., Depannemaecker, D., Agouram, H., Régis, J., Carron, R., Woodman, M., ... & Sorrentino, P. (2025). The virtual parkinsonian patient. npj Systems Biology and Applications, 11(1), 40. https://doi-org.proxy.insermbiblio.inist.fr/10.1038/s41540-025-00516-y

[9] Rabuffo, G., Lokossou, H. A., Li, Z., Ziaee-Mehr, A., Hashemi, M., Quilichini, P. P., ... & Bernard, C. (2025). Mapping global brain reconfigurations following local targeted manipulations. Proceedings of the National Academy of Sciences, 122(16), e2405706122. https://doi.org/10.1073/pnas.2405706122
[10] Esmaeili, A., Demolliens, M., Viersen, M., Ziaeemehr, A., Isbaine, F., Huguet, P., ... & Hashemi, M. (2024). Probing other's Presence: Probabilistic Inference Across Brain Scales Reveals Enhanced Excitatory Synaptic Efficacy. bioRxiv, 2024-09. [accepted Communications Biology] https://doi.org/10.1101/2024.09.09.612006

29. Advanced computational pipelines for multiscale brain mapping with light-sheet fluorescence microscopy

Authors and affiliations
Federica Fenizi Caria[a], Irene Costantini[a,b], Michele Sorelli[a,c], Danila Di Meo[a,b], Samuel Bradley[a], Josephine Ramazzotti[a] , Laura Perego[a], Giacomo Mazzamuto[a,d], Paolo Frasconi[a,e], Francesco Saverio Pavone[a,c,d]

[a]European Laboratory for Non-linear Spectroscopy (LENS), Italy; [b]Department of Biology, University of Florence, Italy; [c]Department of Physics and Astronomy, University of Florence, Italy; [d]National Institute of Optics, National Research Council; [e]Department of Information Engineering, University of Florence, Italy

Introduction
Understanding brain architecture across different scales requires imaging and advanced analysis able to capture cellular details, preserve spatial contexts and process large samples. Light-sheet fluorescence microscopy (LSFM) enables fast volumetric imaging of large cleared tissues at subcellular resolution, yielding datasets suitable for 3D reconstructions. Advanced statistical analysis and deep learning methods enable the extraction of quantitative features from large volumes, transforming raw image data into maps of brain organization. In this work, three pipelines that integrate these approaches are presented: LSFM analysis of whole mouse brains, LSFM analysis of human Broca's area both to characterize neuronal organization[1,2,3] and LSFM imaging of DiD-labeled human tissues, to obtain 3D fiber orientation mapping.[4,5]

Materials and Methods
Sample preparation and Pre Processing
Whole murine brains were clarified using iDISCO protocol, imaged at subcellular resolution with LSFM, reconstructed with ZetaStitcher[6] and registered to the Allen Brain Atlas with ANTs.[1,7,8] Human cortical slabs from Broca's area were subjected to SHORT clearing and neuronal immunolabeling to achieve transparency and staining.[2,3] For fiber analysis, human slabs were treated with SHORT combined with DiD lipophilic labeling, enhancing fiber contrast while preserving tissue clarity. Dual-view inverted LSFM was used and raw datasets were corrected by affine transformations and stitched with ZetaStitcher.[4,5]

Computational analysis
Automated cell detection was performed in both mouse and human datasets with BCFind v2.0, a deep-learning framework based on a 3D U-Net architecture trained on manually annotated subvolumes. Soma centroid positions were extracted using DoG-based local maxima detection and indices such as total counts, density and spatial clustering were computed.[1,3] In Broca's area, manually annotated cortical layers were converted into laminar masks that enabled laminar-specific quantification.[3]

For fiber orientation mapping, LSFM volumes were analyzed with the GPU-accelerated Foa3D pipeline, which applies multiscale 3D Frangi filtering to enhance tubular structures. Voxel-level orientation vectors were aggregated into orientation distribution functions (ODFs) and orientation dispersion indices quantified local variability in fiber architecture.[4,5]

Results

In mouse brains, automated centroid detection and statistical analysis produced brain-wide measures supporting quantitative reconstructions of neuronal populations, consistent with anatomical expectations.[1] In slabs from Broca's area, layer-specific density estimates obtained from laminar masks were compared with stereology, confirming the validity of automated detection and highlighting marked laminar heterogeneity in neuronal organization (Figure 1).[3]

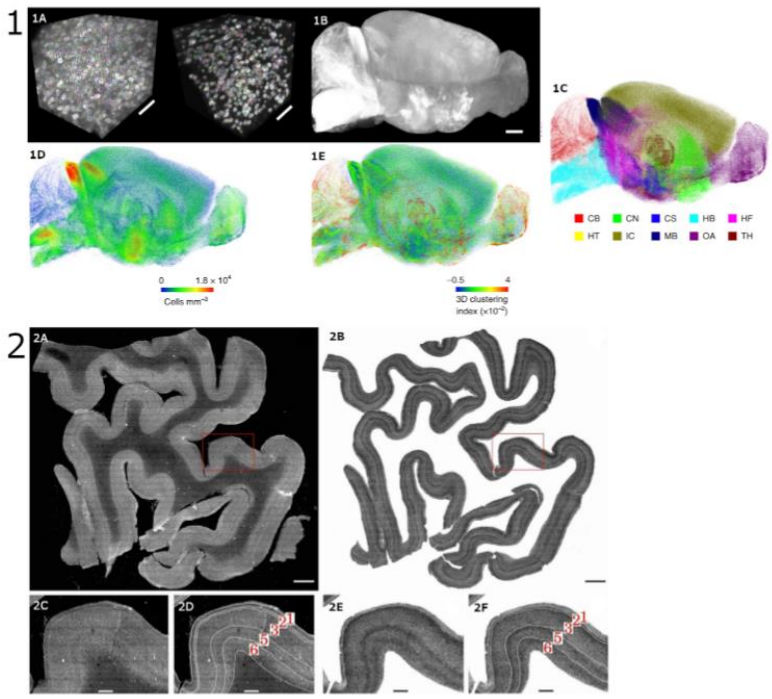

Figure 1. Multiscale brain mapping in mouse models (1A–E) and human tissues (2A–F). (1) Mouse: ground-truth annotations (1A), whole-brain reconstructions (1B), neuron point clouds (1C), and maps of cell density (1D) and 3D clustering (1E). (2)Human Broca's area (LSFM + BCFind-v2): maximum-intensity projection of slab 30 (2A), BCFind-v2 predictions (2B), ROI on raw data without/with layer contours (2C–D), and ROI on predictions without/with layer contours (2E–F). Images adapted from Silvestri et al. (2021)[1] and Checcucci et al. (2024).[3]

Finally, LSFM imaging of DiD-labeled slabs combined with the Foa3D pipeline enabled the reconstruction of 3D myelinated fiber orientations. The resulting orientation colormaps and distribution functions captured the expected architectural differences between gray and white matter and served as histological ground truth for tractography validation (Figure 2). GPU acceleration removed the major computational bottleneck, reducing Frangi filtering runtimes by approximately two orders of magnitude compared to CPU-based processing. [4,5]

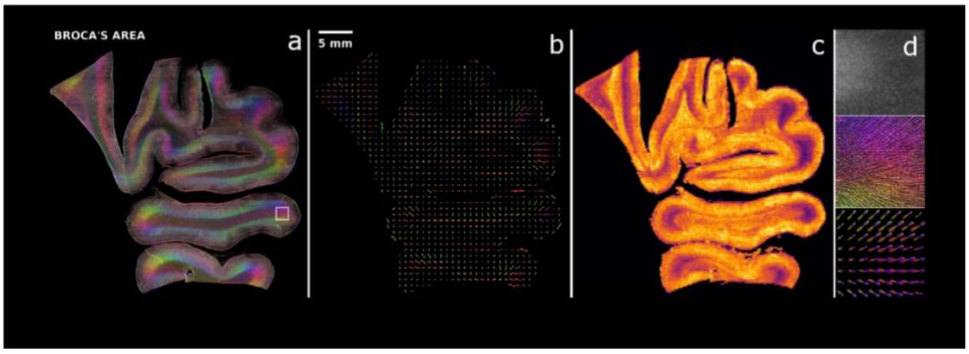

Figure 2. LSFM reconstructions of DiD-labeled human Broca's area for orientation mapping of myelinated fibers, showing direction colormaps (a), voxel-level orientation distribution functions (b), orientation dispersion maps (c), and zoomed examples with raw data, orientation maps, and vector fields (d). Image adapted from Sorelli et al. (2025).[5]

Discussion

These three pipelines illustrate how combining large-scale clearing, advanced microscopy and deep learning-based analysis yields quantitative maps of brain organization across species and scales. Together, these results highlight how optical and computational pipelines can deliver anatomically faithful and computationally tractable maps at both cellular and fiber level. Key challenges remain in making these analyses scalable to whole-brain and large human samples and in developing standardized protocols for comparative studies across cohorts and conditions.

References

[1] Silvestri L, Müllenbroich MC, Costantini I, et al. Universal autofocus for quantitative volumetric microscopy of whole mouse brains. Nat Methods. 2021;18(8):953-958. doi:10.1038/s41592-021-01208-1

[2] Costantini I, Morgan L, Yang J, et al. A cellular resolution atlas of Broca's area. Sci Adv. 2023;9(41):eadg3844. doi: 10.1126/sciadv.adg3844

[3] Checcucci, C., Wicinski, B., Mazzamuto, G. et al. Deep learning-based localization algorithms on fluorescence human brain 3D reconstruction: a comparative study using stereology as a reference. Sci Rep 2024;14:14629. https://doi.org/10.1038/s41598-024-65092-3

[4] Sorelli, M., Costantini, I., Bocchi, L. et al. Fiber enhancement and 3D orientation analysis in label-free two-photon fluorescence microscopy. Sci Rep 2023;13:4160. doi:10.1038/s41598-023-30953-w

[5] Sorelli M, Di Meo D, Bradley S, et al. Myelinated fiber labeling and orientation mapping of the human brain with light-sheet fluorescence microscopy. Preprint. bioRxiv. 2025;2025.03.31.645981. Published 2025 Apr 1. doi:10.1101/2025.03.31.645981

[6] Mazzamuto G, Silvestri L, Sancataldo G, Gavryusev V, Scardigli M, Costantini I, Pavone FS. High-speed light-sheet microscopy imaging and data post-processing using custom hardware and software solutions. In: Brown TG, Wilson T, Waller L, eds. Three-Dimensional and Multidimensional Microscopy: Image Acquisition and Processing XXX. Vol 12385. SPIE; 2023:9. doi:10.1117/12.2650374

[7] Franceschini A, Mazzamuto G, Checcucci C, et al. Brain-wide neuron quantification toolkit reveals strong sexual dimorphism in the evolution of fear memory. Cell Rep. 2023;42(8):112908. doi:10.1016/j.celrep.2023.112908

[8] Silvestri L, Allegra Mascaro AL, Costantini I, Sacconi L, Pavone FS. Correlative two-photon and light sheet microscopy. Methods. 2014;66(2):268-272. doi:10.1016/j.ymeth.2013.06.013

Keywords

Light-sheet fluorescence microscopy; Structural brain analysis; Deep learning methods; Fiber orientation mapping; Whole-brain imaging; Convolutional neural networks; Multiscale image filtering; Tissue clearing

Acknowledgments
This project was supported by the European Union's Horizon Europe research and innovation program under grant agreement No 101147319 (EBRAINS 2.0) and under grant agreement No. 654148 (Laserlab-Europe). From the Italian Ministry for Education in the framework of Euro-Bioimaging Italian Node (ESFRI research infrastructure) and by the European Union – Next Generation EU, Mission 4 Component 1, CUP B53C22001810006, Project IR0000023 SeeLife Strengthening the Italian Infrastructure of Euro-Bioimaging. From the General Hospital Corporation Center of the National Institutes of Health under award number U01 MH117023 and BRAIN CONNECTS (award number U01 NS132181). The content of this work is solely the responsibility of the authors and does not necessarily represent the official views of the National Institutes of Health-USA. The work was also supported by grants to RG from the Tuscany Region Call for Health 2018 (project DECODE-EE), Fondazione Cassa di Risparmio di Firenze (project Human Brain Optical Mapping). The research was also funded by RICTD2025_2026-CUP: B97G24000240005, by LENS and CNR for the technical and scientific support to the Italian National Node FOE 2022 - CUP B53C24004790001. From University of Florence (D.R. n. 464 del 02/04/2024) with the project "Smart hydrogels with enhanced toughness to enable human brain tissue clearing (SMART-brain)," CUP: B97G24000240005.

30. Motor-Cognitive Interaction in Multiple Sclerosis: A cross-sectional study using AI-driven Integration of EEG and Motor Assessment in a dual-task paradigm

Valè N.[1,+], Siviero I.[2,+], Ramos-Murguialday A.[3,4,5,6], Gandolfi M.[2], Menegaz G.[1], Storti S.F[1].

1: Dept. of Engineering for Innovation Medicine, University of Verona, Verona, Italy;
2: Dept. of Neuroscience, Biomedicine and Movement Science, University of Verona, Verona, Italy;
3: Institute of Medical Psychology and Behavioral Neurobiology, University of Tübingen, Tübingen, Germany;
4: TECNALIA, Basque Research and Technology Alliance, San Sebastian, Spain;
5: Dept. of Neurology and Stroke, University of Tübingen, Tübingen, Germany;
6: Athenea Neuroclinics, San Sebastian, Spain.
+: The authors contributed equally to this work.

Background:
Multiple sclerosis (MS) is a chronic, immune-mediated neuro-inflammatory disease that affects approximately 2.2 million people worldwide [1]. MS lesions can appear across the central nervous system (CNS), and a wide range of symptoms and functional impairment can emerge, such as sensorimotor dysfunction (e.g., postural control, balance, and manual dexterity impairment) and cognitive deficits [2]. Falls are one of the most critical events, as they can lead to injuries and reduced mobility with negative effects on quality of life [3]. Among the dysfunctions associated with increased risk of falls in people with MS (PwMS), cognitive and mobility impairments play a key role.

Community ambulation indeed requires cognitive engagement, like conversing while walking. The simultaneous execution of motor and cognitive tasks (dual-tasking) places demand on attentional and memory resources to process information necessary for maintaining balance and completing cognitive activities. Research on people with multiple sclerosis (PwMS) highlights difficulties in dual-task performance, suggesting impairments in motor-cognitive interaction [4]. However, the neural correlates of these impairments remain only partially understood, and the evidence to guide targeted rehabilitation is still limited. This study explores the neural correlates of motor-cognitive interaction in

PwMS using wearable electroencephalography (EEG) and inertial sensors (IMU) in a novel dual-task paradigm.

Methods:
The methodological framework of this study is showed in Figure 1. Thirteen PwMS were enrolled (6 female; age (mean [SD]): 59.3 [11.5] years; EDSS: (median [25th, 75th percentiles]): 5.5 [4.25-6.00]). They performed a cognitive single-task of serial subtraction of 7 for 90 s (STc), and 5 trials of the timed up and go (TUG) in isolation (STm) and in combination with the serial subtraction (DT). Motion and EEG data were recorded via a custom-made IMU placed on the right arm and an 8-channels wearable EEG system. Motion data were used for automatic TUG segmentation using a 1-D convolutional neural network (CNN) with a long short-term memory (LSTM) to extract EEG epochs corresponding to each trial [5]. An inter-session cross-validation approach was adopted. For each participant, data from one task/session was used as the training set, while the other was used as the testing set.

EEG signals were baseline-corrected and filtered using two 5th-order Butterworth filters (high-pass filter: with a cut-off frequency of 3.5 Hz and a low-pass filter with a cut-off of : 30 Hz). Eye blinks and other artifacts, such as those caused by body or head movements during the task, were removed via an independent component analysis (ICA) analysis. The mental workload was quantified using the task load index (TLI), calculated as the ratio of theta (4-8 Hz) and alpha (8-12 Hz) power spectral density (PSD) over Pz and AFz, respectively [6].

Results:
The AI model achieved accurate TUG segmentation, with a root-mean-squared-error (RMSE) of 0.42 s and 0.36 s for STm and DT, respectively. The EEG analysis revealed significant condition effects in the TLI ($\chi2=8.78$, $p=0.012$), frontal PSD in theta band ($\chi2=12.15$, $p=0.002$), and parietal PSD in alpha band ($\chi2=7.53$, $p=0.023$). As shown in Figure 2, STc was associated with lower TLI and alpha parietal PSD compared to the DT condition ($p = 0.006$ and $p=0.003$ respectively) and with lower values of frontal PSD in theta frequency compared to both DT and STm conditions ($p<0.001$ and $p=0.013$, respectively).

Conclusion:
The adoption of a wearable and portable EEG device allowed the recording of prefrontal and parietal cortical activity during walking. Preliminary findings on our small sample of PwMS might be interpreted as in line with previous studies showing excessive prefrontal activity in motor [7]. A larger sample is needed to confirm the results and to design specific rehabilitation strategies aimed at improving motor-cognitive interaction in PwMS.

Acknowledgments:
The work of V. N., M. G., G. M and S. S. F. was supported by NEXTGENERATIONEU (NGEU) and funded by the Ministry of University and Research (MUR), National Recovery and Resilience Plan (NRRP), project MNESYS (PE0000006) – ”A Multiscale integrated approach to the study of the nervous system in health and disease” (DN. 1553 11.10.2022).

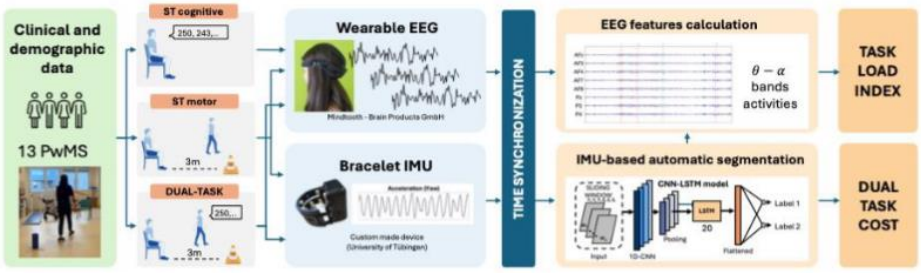

Figure 1: Overview of the methodological framework.

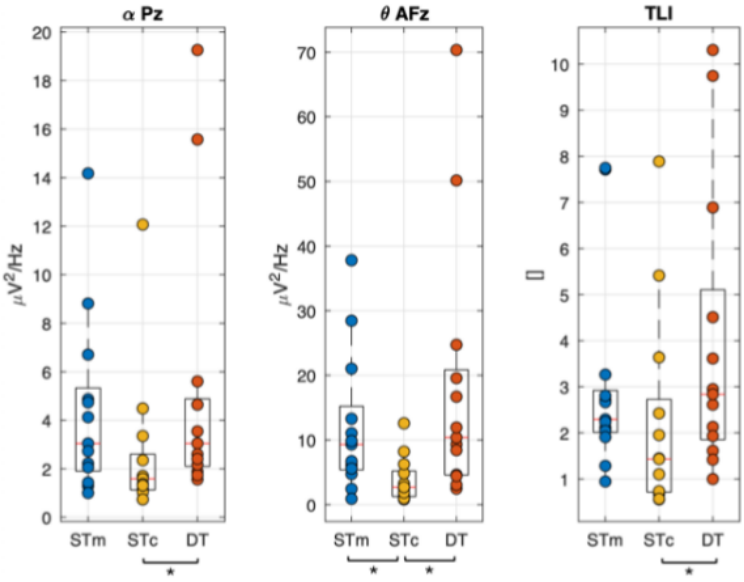

Figure 2: Comparative analysis between STm (light blue), STc (yellow), and DT (orange) of the average α band, θ, and TLI across participants.
**: post-hoc statistically significant differences.*

REFERENCES

[1] H. Lassmann, W. Bruck, and C. F. Lucchinetti, “The immunopathology of multiple sclerosis: an overview” Brain Pathol, vol. 17, no. 2, pp. 210–218, 2007. doi: 10.1111/j.1750-3639.2007.00064.x

[2] N. Koch-Henriksen and M. Magyari, “Apparent changes in the epidemiology and severity of multiple sclerosis” Nat Rev Neurol, vol. 17, no. 11, pp. 676–688, 2021. doi: 10.1038/s41582-021-00556-y

[3] A. Wallin et al., “Effects of balance exercise interventions on balance-related performance in people with multiple sclerosis: A systematic review and a meta-analysis of randomized controlled trials” Neurorehabil Neural Repair, vol. 38, no. 10, pp. 775–790, 2024. doi: 10.1177/15459683241273402

[4] I. Siviero et al., “Remote motor rehabilitation: EMG-IMU based deep learning model improves the estimate of wrist kinematics” in 46th Annu Int Conf IEEE Eng Med Biol Soc (EMBC). IEEE, 2024, pp. 1–4. doi: 10.1109/EMBC53108.2024.10782268

[5] F. Hamilton et al., “Walking and talking: an investigation of cognitive—motor dual tasking in multiple sclerosis” Mult Scler, vol. 15, no. 10, pp. 1215–1227, 2009. doi: 10.1177/1352458509106712

[6] L. E. Ismail and W. Karwowski, “Applications of EEG indices for the quantification of human cognitive performance: A systematic review and bibliometric analysis” PLOS One, vol. 15, no. 12, p. e0242857, 2020. doi: 10.1371/journal.pone.0242857

[7] F. B. Santinelli et al., “Cortical activity and gait parameter characteristics in people with multiple sclerosis during unobstructed gait and obstacle avoidance” Gait amp; Posture, vol. 86, p. 226–232, 2021. doi: 10.1016/j.gaitpost.2021.03.026

31. In-depth metadata curation as an enabler of data reuse in EBRAINS

Alix E. Bonard[1*], Laura Morel[1], Peyman Najafi[1], Lyuba Zehl[2], Andrew P. Davison[1*]

[1]Institut des Neurosciences Paris-Saclay, Université Paris-Saclay, CNRS, Saclay, France

[2]EBRAINS AISBL, Brussels, Belgium
*alix.bonard@cnrs.fr; andrew.davison@cnrs.fr

INTRODUCTION/MOTIVATION

The emergence of cutting-edge high-resolution techniques in neuroscience, combined with the use of algorithms and machine learning, has created fertile ground for an explosion of data and metadata. This expansion, beneficial to the neuroscience field, gives rise to a requirement for an efficient and robust framework for sharing data. Existing data sharing frameworks with basic metadata curation often lack detail for optimal reuse of data. Adding in-depth metadata to curation processes tackles the need of connecting dataset, models and tools in a machine- readable manner to ensure findability and interoperability across services, teams, laboratories and institutes improving collaboration. In-depth metadata enable meaningful reuse and repurposing of data that is required to face the rise of AI-related tools. EBRAINS, a digital research infrastructure developed with funding from the European Union, offers data services such as in-depth curation, which improves basic curation by establishing standardised FAIR procedures[1] for structured and linked metadata by implementing comprehensive guidelines for metadata annotation. In-depth metadata need to become part of the new curation standards to serve as the foundation of interoperability AI-readiness and enable sustainable reuse of neuroscience data.

METHODS

In-depth metadata describing data in detail is one of the pillars that enhances findability and reusability, saving time on finding data and articles, as well as data reuse. With the In-depth curation workflow, curated datasets registered in the EBRAINS Knowledge Graph (KG) are annotated with relevant experimental information improving the understanding of the dataset. This additional information is in-depth metadata. We organise in-depth metadata in dictionaries using Python template scripts corresponding to experimental approach diagrams developed by the curators and based on the openMINDS ephys, specimenPrep, chemicals and stimulation modules. We developed the ebrains_in_depth_curation Python module to convert the in-depth metadata to openMINDS instances, and use the fairgraph[2] library to upload the metadata to the KG, and link the newly created instances with the existing metadata instances in the KG (those that were created during the initial, basic curation of the datasets).

RESULTS AND DISCUSSION

This poster describes the Python-based in-depth curation workflow used to integrate experimental metadata from patch clamp recording, extracellular recording, and two-photon calcium imaging datasets in order to facilitate reproduction of figures from associated publications, as an example of data reuse. We demonstrate the importance of in-depth metadata for data reuse and findability for datasets via the EBRAINS Neural Activity Resource app and Jupyter notebook case studies running in the EBRAINS Lab. The Neural Activity Resource is a user-friendly graphical interface for exploring the in-depth metadata of datasets. Jupyter notebook case studies present how in-depth metadata within the EBRAINS ecosystem facilitates data re-use and data exploration through standardised Jupyter notebook templates.

In-depth metadata adds significant value to published datasets, aligning them to the FAIR principles (Findable, Accessible, Interoperable, Reusable). Providing in-depth metadata increases dataset findability. It also increases interoperability by making analysis workflows more machine-actionable. It facilitates data reuse, which is essential for the development of robust models and analysis pipelines. In the future, the in-depth curation workflow will cover more experimental approaches, such as behaviour and neuroimaging techniques like fMRI and EEG. It will also offer a user-friendly interface, and be compatible with other EBRAINS data sharing tools, aligning with the need to develop visualisation and data exploration tools.

Keywords: FAIR principles, In-depth Metadata, Linked Data

ACKNOWLEDGEMENTS
This work receives funding from the European Union's Research and Innovation Program Horizon Europe under Grant Agreement No. 101147319 (EBRAINS 2.0 project).

REFERENCES
[1] Wilkinson MD, Dumontier M, Aalbersberg IJJ, et al. The FAIR guiding principles for scientific data management and stewardship. Sci Data. 2016;3:160018. doi:10.1038/sdata.2016.18
[2] Davison AP, Ates O, Feld N, Zerlaut Y, Mattheisen G, Najafi P. fairgraph: a Python API for the EBRAINS Knowledge Graph [Internet]. GitHub; 2025. Available from: https://github.com/HumanBrainProject/fairgraph

32. Mulit-scale modelling, from biochemical cascades, to neuron and network level, using Snudda

JJJ. Hjorth[1], W. Thunberg[1,2], A. Kozlov[1,2], O. Eriksson[1], A. Kramer[1], S. Grillner[2], J. Hellgren Kotaleski[1,2]

[1]Royal Institute of Technology (KTH), Stockholm, Sweden, [2]Karolinska Institute, Department of Neuroscience, Stockholm, Sweden

Introduction
Neurons in the brain perform computations on multiple scales. Neurotransmitters and their downstream second messenger systems dynamically modulate the behaviour of synapses and neuronal membrane electrophysiology. Modelling these systems requires integrating formalisms of different scales, from subcellular reaction-diffusion processes, multicompartment Hodgkin-Huxley electrophysiology, and touch detection between neuronal morphologies for network prediction.

Methods
We present an integrated framework that introduces subcellular reaction-diffusion processes into our framework for detailed network topography, "Snudda" (Hjorth et al 2021), by incorporating NEURON's RxD module into network simulations. The framework imports biochemical reaction-diffusion models of receptor induced cascades, defined in SBML, SBtab or JSON and instantiates them in the multi-compartmental NEURON models. The behaviour of the ion channels are modulated as a function of second messenger concentrations that changes maximal conductance or half-activation values for the channel conductances.

Results and Discussion
We apply this framework to investigate the dopamine system of the basal ganglia, by integrating earlier biochemical models of D1R and D2R cascades (Nair et al 2015, 2016, Yapo et al 2017) into our detailed model of the striatal network (Hjorth et al 2020). Here multiple ion channels are modulated in the neurons, and the effect on network scale are studied both in health and disease. These simulations are then run on the super computer Dardel at PDC/KTH at network scale.

Keywords: multi-scale modelling, multi-compartment modelling, biochemical reactions, touch detection

References:

Nair AG, Gutierrez-Arenas O, Eriksson O, Vincent P, Kotaleski JH. Sensing positive versus negative reward signals through adenylyl cyclase-coupled GPCRs in direct and indirect pathway striatal medium spiny neurons. Journal of Neuroscience. 2015 Oct 14;35(41):14017-30.

Nair AG, Bhalla US, Hellgren Kotaleski J. Role of DARPP-32 and ARPP-21 in the emergence of temporal constraints on striatal calcium and dopamine integration. PLoS computational biology. 2016 Sep 1;12(9):e1005080.

Yapo C, Nair AG, Clement L, Castro LR, Hellgren Kotaleski J, Vincent P. Detection of phasic dopamine by D1 and D2 striatal medium spiny neurons. The Journal of physiology. 2017 Dec 15;595(24):7451-75.

Hjorth JJ, Kozlov A, Carannante I, Frost Nylén J, Lindroos R, Johansson Y, Tokarska A, Dorst MC, Suryanarayana SM, Silberberg G, Hellgren Kotaleski J. The microcircuits of striatum in silico. Proceedings of the National Academy of Sciences. 2020 Apr 28;117(17):9554-65.

Hjorth JJ, Hellgren Kotaleski J, Kozlov A. Predicting synaptic connectivity for large-scale microcircuit simulations using Snudda. Neuroinformatics. 2021 Oct;19(4):685-701.

Funding:
This study was supported by the Swedish Research Council (VR-M-2020-01652, VR-M-2024-01995), the Swedish e-Science Research Centre (SeRC), Science for Life Laboratory, KTH Digital Future, EU/Horizon 2020 No. 945539 (HBP 935 SGA3) and No. 101147319 (EBRAINS 2.0 Project), the European Union's Research and Innovation Program Horizon Europe under grant agreement No. 101137289 (the Virtual Brain Twin Project).

33. Tattoo Bioelectronics for Multifunctional Devices and Physiological Sensing

Faheem Ershad[1*] and Cunjiang Yu[2]
[1] Department of Electrical and Computer Engineering, University of Houston, Houston, TX, 77204 USA
[1] Department of Electrical and Computer Engineering, University of Illinois Urbana-Champaign, Urbana, IL, 61801 USA

Introduction: Extraction of physiological and physical signals from human skin is central to health monitoring, disease prevention, and therapy. Recent epidermal wearables have opened pathways for BCI, clinical decision-making, neuroimaging adjuncts, and digital-twin data streams, yet most suffer motion artifacts because they lack durable adhesion and truly conformal skin contact. We introduce ultra-conformal Drawn-on-Skin (DoS) electronics as an on-demand platform for multifunctional, motion-artifact-free sensing and stimulation. Liquid functional inks are traced through stencils with ballpoint pens directly on skin, forming a robust, stretchable, and intimate interface that preserves signal fidelity during movement, potentially enabling stable neurophysiological acquisition for BCI and ambulatory neuroimaging and supplying high-quality inputs to clinical workflows and digital twins.

Materials and Methods:
DoS devices are based on an Ag/poly(3,4-ethylenedioxythiophene)-poly(styrenesulfonate) (Ag-PEDOT:PSS) composite, poly(3-hexylthiophene-2,5-diyl) nanofibrils (P3HT-NF) semiconducting ink, and an ion gel dielectric. Ink drawability, mechanics, skin compatibility, and electrical performance were characterized; devices included transistors, heaters, strain, temperature, hydration, and electrophysiology (EP) sensors (Fig. 1a). A wireless ECG system was implemented for a clinically

relevant stress test and DoS sensors were compared with gel and ultrathin mesh electrodes under motion (Fig. 1b and 1c).

For high-density DoS MEAs, we used Ag-PEDOT:PSS ink, a water/acrylic emulsion insulator, pens, and stencils to hand-fabricate customizable grids. We evaluated uniformity, SNR, and robustness to large muscle deformation; identified motor unit action potentials (MUAPs), tracked propagation, localized innervation zones, and compared against a fixed commercial grid during wrist/finger gestures. Gesture-classification performance and real-time control of a robotic hand were assessed (Fig. 2a-b).

Results and Discussion: DoS lines were drawn with ~300 μm resolution, with stretchability to 30%, no inflammatory response up to 48 h, and low sheet resistance (conductive ink ≈ 1.2 Ω/sq). Devices functioned under deformation, and the wireless system tracked heart-rate changes during stress. Under skin deformation, DoS EP sensors maintained markedly higher ECG SNRs than alternatives - 50 dB vs 20 dB (gel) and 12 dB (mesh) (Fig. 1b); resting muscle potential signals (<250 Hz) remained free of vibration contamination (Fig. 1c).

High-density DoS MEAs exhibited uniform electrical properties and stable EMG during large movements owing to the skin-conformal interface for 3 human subjects. Like commercial grids, DoS MEAs captured MUAPs, propagation across wrist flexors, and an innervation band (Fig. 2a). Unlike commercial grids, reconfigurable DoS arrays could be rearranged *in situ* to match anatomy, extend coverage, and reveal centers of activity missed by the commercial grid during multiple gestures (Fig. 2b). Customized DoS MEAs yielded informative low-dimensional structure (PCA) and improved gesture classification, enabling a subject to control a robotic hand with high fidelity.

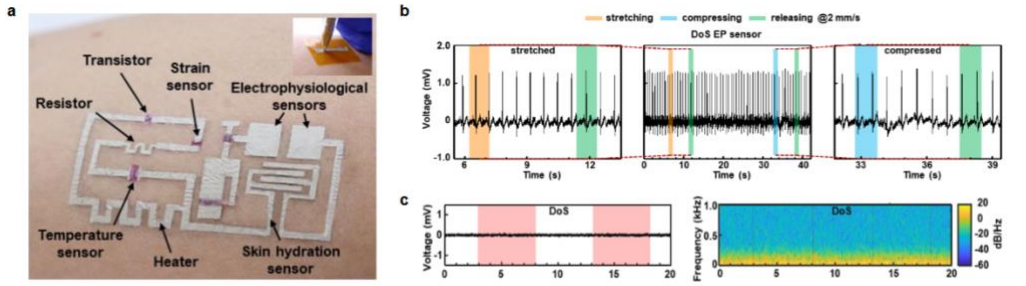

Figure 1. DoS electronics. a) Various DoS devices and sensors that can be fabricated on skin. b) ECG signals show now change in the waveform during various deformations. c) Vibrating the skin (pink sections) does not affect the EMG potentials in the time and time-frequency domains.

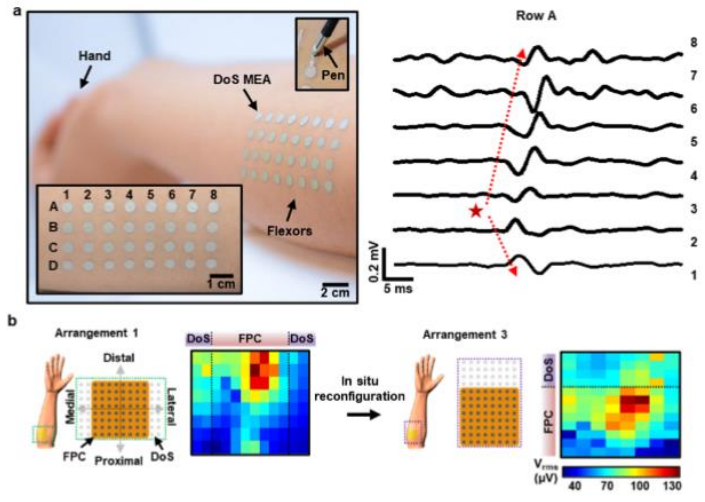

Figure 2. DoS MEAs. a) High-density DoS MEA drawn on the wrist flexors (left) and MUAP propagation shown from one row of the MEA (right). b) Rearrangement of the DoS MEAs relative to a fixed commercial grid to show the center of muscle activity while the subject flexed their closed hand.

Conclusion: Pens, inks, and stencils constitute a rapid, accessible toolkit for personalized DoS bioelectronics on textured, deformable, curvilinear skin-robust to motion without extra hardware or computation. While demonstratd primarily as a proof-of-concept here, by unifying motion-artifact-resistant sensing with high-density, reconfigurable MEAs, DoS bioelectronics provides a practical path to BCI interfaces, clinical monitoring/therapy, neuroimaging-relevant ambulatory recordings, and high-quality streams for digital-twin neurophysiology. Further optimization of ink formulations, device variability, and integrated wireless readout will advance DoS toward scalable, personalized healthcare.

Acknowledgements: F.E. would like to acknowledge the National Science Foundation Graduate Research Fellowship Program (DGE1255832). C.Y. would like to acknowledge the funding support of the Office of Naval Research grants (N—1–2480), the National Institute of Health grant (R21EB026175), and the National Science Foundation grant (CBET-1936151).

34. HOB: A Homeostasis-inspired Optimizer for Bioelectric Models

Wilhelm Thunberg[1,2,3], Jeanette Hellgren Kotaleski[1,2]

1. KTH Royal Institute of Technology, Department of Computer Science, Science for Life Laboratory, Solna, Stockholm, Sweden
2. Karolinska Institutet, Department of Neuroscience, Solna, Stockholm, Sweden
3. Contact: wilhelm.thunberg@ki.se

Introduction
Fitting parameters to detailed multicompartment models is notoriously difficult, typically requiring high-performance computing resources to explore their vast parameter space. Biological neurons, however, control this parameter space to maintain their function across diverse perturbations. Inspired by this phenomenon of homeostatic control, we present an optimization framework, HOB, where model parameters are obtained not only based on fitness metrics, but also the corresponding internal state of the model.

Method
Each free parameter is associated with a transfer function of fitness or state metrics. These functions are thus considered hyperparameters of the algorithm and parameters are iteratively updated using these. A superset of the commonly employed fitness metrics is used to capture spike events, action potential waveform, and subthreshold dynamics, to model a range of striatal, subthalamic, and pallidal neurons, using the NEURON simulation environment. HOB is implemented as a modular, simulator-agnostic Python library, allowing for extension to other domains.

Results
HOB achieves improved fits across all tested neurons and can therefore capture diverse membrane dynamics from striatal cholinergic interneurons to fast-spiking pallidal neurons. A common initial guess and set of hyperparameters was shared across all models. Each model is obtained within 100 (sequential) iterations running on a standard laptop.

Discussion

The current validation results suggest that HOB generalizes across the spectrum of neuronal membrane dynamics, with improved fits and orders of magnitude-increases in speed compared to the state of the art.

Acknowledgements
We thank Drs. Linda Koene, Yvonne Johansson, Maya Ketzef, and prof. Gilad Silberberg for data sharing.

This study was supported by the Swedish Research Council (VR-M-2020-01652), the Swedish e-Science Research Centre (SeRC), Science for Life Laboratory, EU/Horizon No. 101147319 (EBRAINS 2.0 Project), the European Union's Research and Innovation Program Horizon Europe under grant agreement No. 101137289 (the Virtual Brain Twin Project).

35. Interaction between Seizure and Theta Rhythm

Nikabadze N [2] *, Bilanishvili I[1], Barbakadze M[1] *, Balarjishvili K[1], Andronikashvili G[1], Nanobashvili Z.[1] *
[1] Laboratory of Neurophysiology, I. Beritashvili Center of Experimental Biomedicine, Tbilisi, Georgia.
[2] Ilia State University, Tbilisi, Georgia.
*nini.nikabadze.1@iliauni.edu.ge ; maikobarbakadze@yahoo.com ; zaqariananobashvili@gmail.com

Introduction

It is well known, that the hippocampus generates rhythmical slow activity, or theta rhythm. Another important characteristic of the hippocampus is high susceptibility to epileptogenic electrical or chemical agents.

The purpose of this study is to test this proposal by determining the effects on seizures of induction or suppression of hippocampal theta activity.

There were two main goals in our study: 1) Changes in convulsive electrical activity of the hippocampus in different stages of sleep and wakefulness of the animal. 2) Changes in electrographic convulsive reactions during theta-rhythm and/or desynchronization of the electrical activity of the hippocampus caused by stimulation of the hypothalamus.

Hypothesis

Seizure-theta antagonism in our experiments could be interpreted as an adjustment of the inhibitory mechanisms when the theta rhythm is evoked.

Methods

In Wistar albino rats (n = 32) the bipolar stimulating/recording electrodes were implanted bilaterally in the ventral hippocampus and dorso-medial hypothalamus. After at least 10 - 12 days post-surgery rats were electrically stimulated in the hippocampus according to the kindling paradigm.

Experiment 1. After the kindling procedure, spontaneous (larval) seizure dischargers were found in 8 rats. The parameters of these seizure dischargers were examined within the sleep-wakefulness cycle. The field electrical activity of the hippocampus was recorded and processed using a 10-channel analyzer/integrator, ANJEG-81.

Experiment 2. After the lapse of post-operation period in rats (n = 12) we studied the effect of hypothalamic stimulation, using different parameters, on the course of hippocampal theta rhythm and seizure reactions. Electrodes were implanted in the dorsal hippocampus bilaterally. The stimulating electrode was implanted on one side, while the recording one contralaterally.

Results

After the kindling process terminated and also after 8 to 9 days, larval epileptiform activity was noticed composition of fully awake rats. The frequency and amplitude of these discharges increased immediately with the transition from the awake state to drowsiness and a slow-wave sleep phase.

After the animal came from slow- wave sleep to paradoxical sleep, epileptiform activity in the EHG composition completely disappeared (Figure 1).

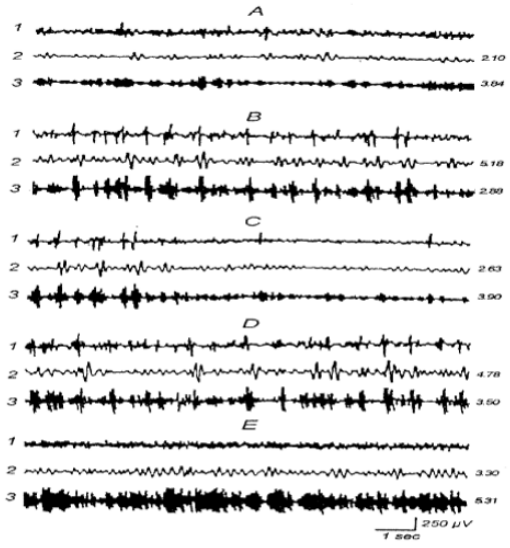

Fig.1. EHG after the kindling procedure. (A) Records in the awake state; (B) (D) Those in the slow-wave sleep state; (C) Transition of slow-wave sleep to awake state. (E) Paradoxal sleep.

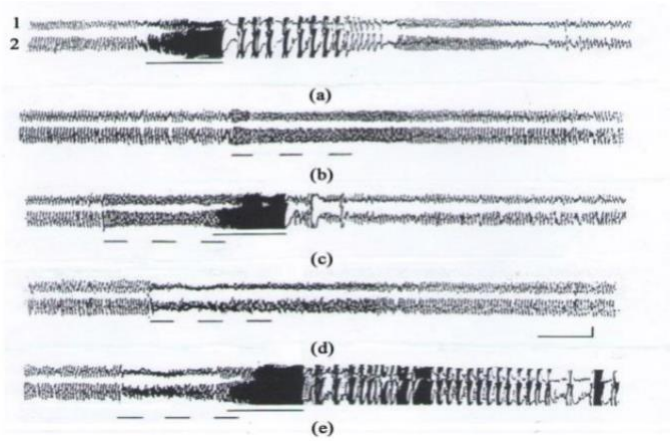

Fig.2. Influence of prior hypothalamic stimulation on the evoked seizure activity. (a) Effects of contralateral hippocampal stimulation. (b) Effects of DMH threshold stimulation); (c) Effects of preliminary hypothalamic threshold stimulation on the seizure activity; (d) Effects of DMH suprathreshold stimulation. (e) Effects of preliminary hypothalamic suprathreshold stimulation on the seizure activity. Stimulation of the hippocampus is indicated by the horizontal line. The bold line indicates stimulation of DMH. Calibration—250 μV, 3 Sec.

It is remarkable that in the case of stimulation of the hypothalamus as well as of the brainstem reticular formation, change in the electrical activity of the hippocampus is dependent on the stimulation parameters. Consequently, these structures have a diverse action on the development of seizure reactions in the hippocampus. In experiments we have examined the effects of experimental induction and/or suppression of the hippocampal theta activity on the evoked hippocampal seizures (Figure 2).

Conclusion

It is assumed that increased inhibition during the main goal of our research is to establish the relationship between emotions and epilepsy and that hippocampal theta rhythm is a physiological state of the hippocampus, which opposes its recruitment into seizures.

References

Davis R. Cerebellar stimulation for cerebral palsy spasticity, function and seizures. Arch Med Res. 2000;31(3):290- 299. doi:10.1016/S0188-4409(00)00065-5

Magdaleno-Madrigal V, Valdes-Cruz A, Martinez-Vargas D. Effect of electrical stimulation of the nucleus of the solitary tract on the development of electrical kindling in the cat. Epilepsia. 2002;43(9):964-969. doi:10.1046/j.1528-1157.2002.05702.x

Chanel S, Westerveld M, Spenser S. Long-term outcome of vagus nerve stimulation for refractory partial epilepsy. Epilepsy Behav. 2003;4(3):302-309. doi:10.1016/S1525-5050(03)00109-4

Buzsáki G, Buhl DL, Harris KD, Csicsvari J, Czéh B, Morozov A. Hippocampal network patterns of activity in the mouse. Neuroscience. 2003;116(1):201-211. doi:10.1016/S0306-4522(02)00669-3

Liberson WT, Akert K. Hippocampal seizure states in guinea pig. Electroencephalogr Clin Neurophysiol. 1955;7(2):211-222. doi:10.1016/0013-4694(55)90036-5

Keywords:
Brain
Epilepsy
Hippocampus
Medical research

ACKNOWLEDGEMENTS
Study was supported by the Georgian National Science Foundation (GNFS) Grant –FR-23-1938)

36. Comparing the Effects of Dorsal Anterior Cingulate Cortex Transcranial Direct Current Stimulation on Patch-Switching Skills

Zeba Fatima[1*], George Zacharopoulos[2]
Affiliations: [1]Psychology Department, Swansea University, Swansea, United Kingdom
*zebafatima2090@gmail.com

INTRODUCTION/MOTIVATION

Reward-based decision making plays a significant role in taking decisions in every aspect of life from starting a business to leaving a job, from purchasing one item to other. From the examples, it is obvious that while taking decisions humans prioritize their choices in order to get more rewards. In other words, staying in one patch and leaving the other leads to changes in patch-switching threshold. All these sets of patterns are linked to neurocomputational model of decision making which entertained with marginal value theorem, in which optimizing the choice in term of time and cost is a basic concept. Following, taking decision and thirst of earning rewards leads to significant learning in humans while making wrong choices known as reinforced learning. Precisely, learning occurs through two pathways that is model-free learning which does not encounter marginal value theorem and second one is the model-based learning, which is directed to error detection, estimating the value of the reward, adaptive the future decision according to the previous learning. Interestingly, the controlling centre of all the process is regarded as dorsal anterior cingulate cortex. However, specific functions are yet to be discovered related to reward-based decision making. Amazingly, it was discovered that reinforced learning leads to neuroplasticity in the anterior cingulate cortex which improves decision making skills of the people suffering from psychiatric disorders including

schizophrenia. Schizotypal personality disorder is linked with impaired decision-making skills and impaired memory which are the essential ingredients of the reward-based decision-making. Previous research supported that stimulating the anterior cingulate cortex results in improving the memory of the people with schizotypal personality disorder which in turn improve the decision-making skills. However, it is not certain which part of anterior cingulate cortex is more active in the reward-based decision making and what aspects of neurocomputational mechanism is involved in this process while adapting patch-switching.

METHODS

Experimental methods involve the stimulation of the dorsal anterior cingulate cortex (dACC) of the participants with schizotypy while they were performing the patch-switching task. In this experiment 37 undergraduates and postgraduate students participated. The parameters used in the study involve the stimulation consisting of two levels (active and sham) and schizotypy involving high and low levels assessed through the SPQ-BR (Schizotypal Personality Questionnaire-Brief Revised) (Cohen et al., 2010). The statistical parameters include the 2-way ANOVA, descriptive statistics calculating mean, median, standard deviation, and correlation between schizotypy and reward as previous research advocating the more biased approach of people focusing on harvesting the local forage ground or in other words immediate rewards. Other correlations also performed among different superordinate subscales of schizotypy and patch-switching parameter that is harvesting frequency (number of harvest).

RESULTS AND DISCUSSION

From the result it is concluded that people having high schizotypy with active and sham stimulation performed equally in the reward based-decision making task. Other findings of correlation of schizotypy with patch switch parameter (number of harvest) provide positive correlation but it was not statistically significant due to some limitations of the sample. From the above findings it is concluded that improvement in the rewards-based decision-making tasks in terms of getting more rewards (number of apples) may be the result of reinforced learning which is the raw ingredient for neuroplasticity in dorsal anterior cingulate cortex.

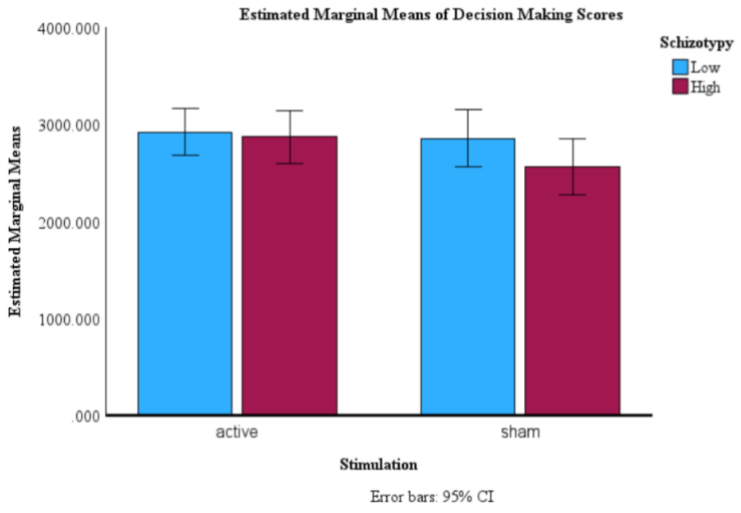

Figure 1. Estimated Marginal Means of Decision-Making Scores

The bar graph depicts the estimated marginal means scores of the active and sham brain stimulations. It is clear from the graph that marginal means of decision-making score for low and high schizotypy under active condition is nearly the same whereas under sham stimulation the means of decision-making score for low and high schizotypy under sham condition show greater marginal means for low schizotypy as compared to high schizotypy.

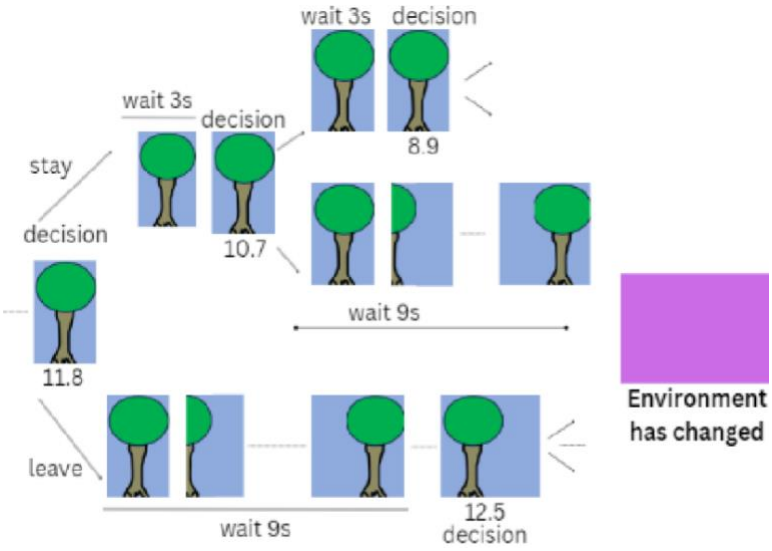

Figure 2. Diagrammatic representation of the Reward-Based Decision-Making Foraging Task

Keywords: Reward-based decision, dACC (dorsal anterior cingulate cortex), neurocomputational, marginal value theorem, schizotypy, neuroplasticity, reinforced learning, tDCS, patch-switching, model-based leaning

ACKNOWLEDGEMENTS

I would like to express my deep gratitude to honourable Dr. George Zacharopoulos for his support to perform this research. I am highly grateful to all the participants who participated in the study.

REFERENCES

1. Blanchard TC, Hayden BY. Neurons in dorsal anterior cingulate cortex signal postdecisional variables in a foraging task. J Neurosci. 2014;34(2):646-655. doi:10.1523/JNEUROSCI.3151-13.2014
2. Cathomas F, Klaus F, Guetter K, et al. Increased random exploration in schizophrenia is associated with inflammation. NPJ Schizophr. 2021;7(1):6. Published 2021 Feb 3. doi:10.1038/s41537-020-00133-0
3. Shi YF, Wang Y, Cao XY, et al. Experience of pleasure and emotional expression in individuals with schizotypal personality features. PLoS One. 2012;7(5):e34147. doi:10.1371/journal.pone.0034147
4. Silvetti M, Alexander W, Verguts T, Brown JW. From conflict management to reward-based decision making: actors and critics in primate medial frontal cortex. Neurosci Biobehav Rev. 2014;46 Pt 1:44-57. doi:10.1016/j.neubiorev.2013.11.003
5. To WT, Eroh J, Hart J Jr, Vanneste S. Exploring the effects of anodal and cathodal high definition transcranial direct current stimulation targeting the dorsal anterior cingulate cortex. Sci Rep. 2018;8(1):4454. Published 2018 Mar 13. doi:10.1038/s41598-018-22730-x
6. Wilson RC, Bonawitz E, Costa VD, Ebitz RB. Balancing exploration and exploitation with information and randomization. Curr Opin Behav Sci. 2021;38:49-56. doi:10.1016/j.cobeha.2020.10.001
7. Zacharopoulos G, Maio G, Linden DEJ. Dissecting the neurocomputational bases of patch-switching. Cereb Cortex. 2023;33(12):7930-7940. doi:10.1093/cercor/bhad088

37. N/A

38. The EBRAINS National Node Network: Connecting European neuroscience for a joint future

Trygve B. Leergaard[1*], Giulia Adembri[2], Andrea Brovelli[3], Paolo Carloni[4,5], Evangelia Drymaliti[6], Mariana de Freitas[7], Jeanette H. Kotaleski[8,9], Jean-François Mangin[7], Evita Mailli[6], Cezary Mazurek[10], Boris Orth[11], Nicola Palomero-Gallagher[4,12], Francesco Pavone[2,13,14], Amaryllis Raouzaiou[6], Aušra Saudargienė[15], Birgit Schaffhausser[16], Bryan Strange[17], Paul H.E. Tiesinga[18], Daniel Vare[19], Guillermo Velasco[20], Lyuba Zehl[21], Jan G. Bjaalie[1], Philippe Vernier[21]

AFFILIATIONS
1. Institute of Basic Medical Sciences, University of Oslo, Oslo, Norway
2. National Institute of Optics of CNR, Sesto Fiorentino (Florence), Italy
3. CNRS, Aux Marseille Universite, Marseille, France
4. Institute for Neuroscience and Medicine, Forschungszentrum Jülich, Germany
5. Department of Physics, RWTH Aachen University, Germany
6. ATHENA Research Center, Athens, Greece
7. CEA, Frederic Joliot Institute for life science, NeuroSpin, Saclay, France
8. Department of Neuroscience, Karolinska Institutet, Stockholm, Sweden
9. Department of Computer Science, KTH Royal Institute of Technology, Stockholm, Sweden
10. Poznan Supercomputing and Networking Center, Institute of Bioorganic Chemistry PAS, Poland
11. Jülich Supercomputing Centre, Forschungszentrum Jülich, Germany
12. C. & O. Vogt Institute of Brain Research, Heinrich-Heine University Düsseldorf, Germany
13. Department of Physics and Astronomy, University of Florence, Italy
14. European Laboratory for Non-Linear Spectroscopy, Sesto Fiorentino (Florence), Italy
15. Lithuanian University of Health Sciences, Kaunas, Lithuania
16. Centre hospitalier universitaire Vaudois (CHUV), Centre de Recherche en Neurosciences Cliniques (CRN), Lausanne, Switzerland
17. Laboratory for Clinical Neuroscience, Center for Biomedical Technology, University Politécnica de Madrid, IdISSC, Madrid, Spain
18. Donders Centre for Neuroscience, Radboud University, Nijmegen, The Netherlands
19. Research Funding Office, Karolinska Institutet, Stockholm, Sweden
20. UPM Neurotech-Translation group, Center for Technology Innovation, University Politécnica de Madrid, Madrid, Spain
21. EBRAINS AISBL, Brussels, Belgium

Corresponding author:
*t.b.leergaard@medisin.uio.no

INTRODUCTION
The EBRAINS Research Infrastructure [1,2] offers an ecosystem of data, tools, and resources for neuroscience research. EBRAINS accommodates heterogeneous, multilevel data that are carefully curated and made findable and interoperable through structured metadata and connected to digital brain atlases and computational resources for exploration and analysis. EBRAINS was delivered by the Human Brain Project (2013-2023) [3], with several follow-up projects contributing to operating, maintaining and developing the core infrastructure and distributed services. Providing novel solutions for sharing, integration and analysis of data [4], EBRAINS has opened new avenues for the field of neuroscience. In 2021 EBRAINS was added to the ESFRI (European Strategy Forum on Research Infrastructures) roadmap, initiating efforts to configure EBRAINS for the future. To establish a

sustainable future for EBRAINS, a scientific, technical, financial, legal and governance framework is now being developed.

METHODS

The hub-node structure of EBRAINS was established in 2019, with seven founding member institutions forming the EBRAINS AISBL as a legal entity. Services are provided through a distributed network of National Nodes offering scientific expertise, software, services, and support. The EBRAINS PREP project (2022-2025) defined an organizational framework with statutes, business plan, technical design, and formal agreements, connecting EBRAINS nodes into a consortium dedicated to providing services and contributing to the development of EBRAINS. The EBRAINS 2.0 project is improving, automating, and monitoring services, as well as onboarding new services.

RESULTS AND DISCUSSION

Through the EBRAINS PREP project, the National Nodes developed governance and financial models formalizing the nodes internally with mandates for signing national node agreements and contributing membership fees. The National Node Agreements, signed in 2025, regulate the collaborative work, to facilitate the operation and development of EBRAINS and expand the pan-European EBRAINS user base to increase scientific exchange and advancement. The EBRAINS PREP project delivered updated formal policy documents regulating activities, as well as updated catalogues of services, tools, and training resources. To ensure seamless operation services, new service onboarding and monitoring routines were developed, defining core services and distributed operational services, together with agreements regulating service levels and commitment to support. The National Node Board serves as a liaison between the EBRAINS and distributed user communities, coordinating the National Nodes to facilitate service onboarding and provisioning, collaborative training efforts and outreach to recruit new users and expand the national node network to new member states. Finally, following the inclusion of EBRAINS in the ESFRI 2021 roadmap, the choice was made to develop EBRAINS towards becoming a European Digital Infrastructure Consortium (EDIC), as a multi-country collaboration delivering an extensive portfolio of digital research tools and services for neuroscience. The EBRAINS hub-node network, with a defined governance structure underpinned by formal agreements, policies, and procedures, provides a foundation for the further development of a financial, legal and governance framework suitable for implementing EBRAINS as an EDIC. To achieve this ambition and secure a longer-term sustainable future for EBRAINS, it is necessary to describe how EBRAINS can operate as an EDIC, with a suitable governance structure and a suite of service offerings needed by the brain research community. The National Nodes are central to this endeavour, connecting national user communities with EBRAINS services, maintaining interoperability with other research infrastructures, and contributing to community engagement and matching services to needs and trends across the European neuroscience landscape.

KEYWORDS

<EBRAINS National Nodes>, <EBRAINS community>, <Open Science>, <EDIC>

ACKNOWLEDGEMENTS

This work has received funding from the European Union's Horizon Europe research and innovation programme under grant agreement No 101079717 (EBRAINS PREP) and No 101147319 (EBRAINS 2.0); the Research Council of Norway, Grant number 350201 (NORBRAIN4), Agencia Estatal de Investigación "Redes Estrategiacas" RED2022-134823-E y RED2023-153668-E Programa Estatal de Tranferencia y Colaboración del Minsterio de Ciencia, Innovación y Universidades de España, Ministerstwo Nauki i Szkolnictwa Wyższego of Poland granted under decision 83/WFSN/2024.

REFERENCES

[1] EBRAINS RRID: https://scicrunch.org/resolver/RRID:SCR_019260

[2] EBRAINS DOI: https://doi.org/10.25504/FAIRsharing.XO6ppp
[3] Pipa G, Newell F, Hulshoff H, Chiappalone M, Soria-Frisch A, Human Brain Project. 10 years assessment. https://digital-strategy.ec.europa.eu/en/library/human-brain-project-10-years-assessment
[4] Amunts K et al., The coming decade of digital brain research: A vision for neuroscience at the intersection of technology and computing. Imaging Neuroscience 2, imag-2-00137, 2024, https://doi.org/10.1162/imag-a-00137

39. Neuroinflammation and disrupted functional connectivity in coma: a graph-theoretical study

Authors. Arturo Cabrera Vazquez[1,2,3], Sophie Achard[1], Michel Dojat[1,2], Stein Silva[3].
1 Univ. Grenoble Alpes, CNRS, Inria, Grenoble INP, LJK, 38000 Grenoble, France.
2 Univ. Grenoble Alpes, Inserm, U1216, Grenoble Institut Neurosciences, 38000 Grenoble, France.
3 INSERM U1214, Toulouse Neuroimaging Center, CHU Purpan, 31059 Toulouse, France.

Introduction. Coma, regardless of etiology, is a major health concern, often leading to lasting cognitive and behavioral deficits.[1] The profiling of structural and functional brain damage underlying coma remains poorly understood.[2] Understanding recovery mechanisms is key for developing outcome biomarkers,[3] requiring a multimodal approach spanning imaging, modeling, and clinical practice.[4] Recent studies using 18^{F}-DPA-714 TSPO PET imaging have revealed substantial neuroinflammation in cortical and subcortical areas corresponding to central nodes of resting-state networks, suggesting new avenues for identifying mechanistic biomarkers.[5] Resting-state functional connectivity (FC) breakdown in coma has been assessed with graph-based measures such as the Hub Disruption Index (HDI), revealing reorganization of functional networks.[6] However, the relationship between neuroinflammation and FC in coma remains unclear.[7]

Methods. A cohort of 11 traumatic and 6 anoxic patients with coma was studied in the University Hospital of Toulouse. Structural, functional, and PET images were acquired 2-30 days post injury, with minimal inter-scan delay. Patients underwent behavioral assessment at admission and 90 days post-injury, allowing classification of outcomes as favorable or unfavorable. Twenty age- and sex-matched healthy controls were also included, as detailed by Sarton et al.[5] FC data were analyzed following Malagurski et al.,[6] using a modified AAL atlas with 89 regions,[8] and applying a 10% threshold to the binarized connectivity matrices. One anoxic and two traumatic patients were excluded due to too few significant edges, leaving 14 coma patients in the analysis. TSPO binding potential maps were converted into graphs by summarizing regional data into subject-level normalized histograms, computing the Bhattacharyya coefficient between region pairs, and thresholding the resulting matrices at 10% density. HDI for the graph metric degree was used to compare populations within the same modality. We constructed nodal equivalent classes (ECs), defined as sets of nodes sharing the same value for a chosen nodal metric.[9] For fMRI graphs, we used clustering coefficient, and for TSPO graphs, we used degree, both metrics selected based on their relevance to our preliminary results. To integrate modalities, we intersected ECs across fMRI and TSPO graphs for each subject, creating multimodal ECs.[7] Cross-modal similarity was then assessed at the group level by comparing these ECs across subjects within the same population using Correspondence Structural Pattern Score (CSPS).[9] Values near 1 indicate strong global correspondence in EC structure across subjects, reflecting population-level consistency. Group differences were assessed with two-tailed t-tests for HDI and Z-tests for CSPS.

Results. fMRI-HDI reproduced results from previous studies, effectively capturing network disruption in the coma population compared to controls ($p=0.0004$). TSPO-HDI showed similar group differences, distinguishing controls from coma patients ($p=5.2\text{x}10^{-7}$). Comparing intersections of ECs

across imaging modalities with CSPS also revealed significant differences between groups (p=0.0099).

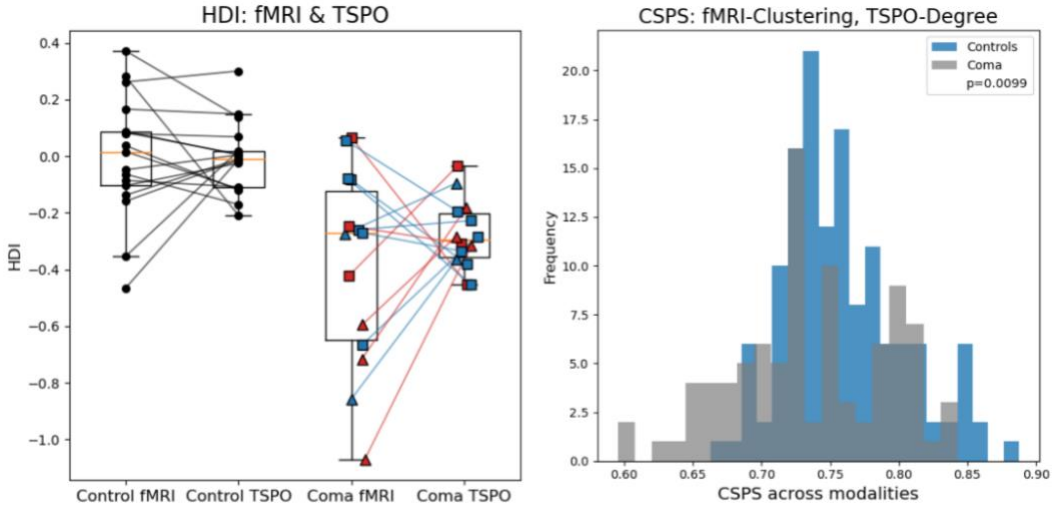

Figure 1 (left). HDI values across imaging modalities. Coma patients: anoxic (triangles), traumatic (squares); 90-day outcomes color-coded (blue=favorable, red=unfavorable).
Figure 2 (right). Within-group CSPS indicating global cross-modal similarity.

Discussion. HDI reveals that neuroinflammation patterns in coma parallel fMRI network disruption, suggesting an association between TSPO expression and FC. CSPS shows a disrupted multimodal relationship in coma, with well-connected regions in fMRI not necessarily aligning with regions of similar TSPO. The statistical significance of this node-metric combination, comparing fMRI connectivity of neighboring regions with TSPO similarity across nodes, shows the complex interplay between brain connectivity and neuroinflammation.

References.

1. Cronberg T, Greer DM, Lilja G, Moulaert V, Swindell P, Rossetti AO. Brain injury after cardiac arrest: from prognostication of comatose patients to rehabilitation. The Lancet Neurology. 2020;19(7):611-622. doi:https://doi.org/10.1016/s1474-4422(20)30117-4
2. Dehaene S, Changeux JP. Experimental and Theoretical Approaches to Conscious Processing. Neuron. 2011;70(2):200-227. doi:https://doi.org/10.1016/j.neuron.2011.03.018
3. Edlow BL, Claassen J, Schiff ND, Greer DM. Recovery from disorders of consciousness: mechanisms, prognosis and emerging therapies. Nature Reviews Neurology. 2021;17(3):135-156. doi:https://doi.org/10.1038/s41582-020-00428-x
4. Luppi AI, Cain J, Spindler LRB, et al. Mechanisms Underlying Disorders of Consciousness: Bridging Gaps to Move Toward an Integrated Translational Science. Neurocritical Care. 2021;35(S1):37-54. doi:https://doi.org/10.1007/s12028-021-01281-6
5. Benjamine Sarton, Tauber C, Fridman E, et al. Neuroimmune activation is associated with neurological outcome in anoxic and traumatic coma. Brain. Published online February 27, 2024. doi:https://doi.org/10.1093/brain/awae045
6. Malagurski B, Péran P, Sarton B, et al. Topological disintegration of resting state functional connectomes in coma. Neuroimage. 2019;195:354-361. doi: https://doi.org/10.1016/j.neuroimage.2019.03.012
7. Vazquez AC, Achard S, Dojat M, Silva S. Graph theory in Disorders of Consciousness: Toward multimodal integration. Halscience. Published online July 8, 2025:1-1. doi:https://hal.science/hal-05153617

8. Termenon M, Jaillard A, Delon-Martin C, Achard S. Reliability of graph analysis of resting state fMRI using test-retest dataset from the Human Connectome Project. NeuroImage. 2016;142:172-187. doi:https://doi.org/10.1016/j.neuroimage.2016.05.062
9. Carboni L, Dojat M, Achard S. Nodal-statistics-based equivalence relation for graph collections. Physical review E. 2023;107(1). doi:https://doi.org/10.1103/physreve.107.014302

Acknowledgments. Arturo Cabrera Vazquez is a recipient of a PhD grant by Inria. Sophie Achard has been partially supported by a French government grant, administered through the MIAI Cluster and managed by the Agence Nationale de la Recherche under the France 2030 program, reference ANR-23-IACL-0006.

Keywords: fMRI, TSPO, graph theory, multimodal imaging, disorders of consciousness, biomarkers

40. Updated EBRAINS curation workflow: A user-friendly path to FAIR neuroscience data sharing

Authors
Signý Benediktsdóttir[1,2], Naz Karadag[1], Archana Golla[1], Maya Kobchenko[1], Eivind Hennestad[1], Eszter A. Papp[1], Sophia Pieschnik[1], Heidi Kleven[1], Maja A. Puchades[1], Camilla H. Blixhavn[1], Ingrid Reiten[1], Ulrike Schlegel[1], Oliver Schmid[3], Andrew P. Davison[4], Lyuba Zehl[2], Trygve B. Leergaard[1], Jan G. Bjaalie[1]

Affiliations:
1. Institute of Basic Medical Sciences, University of Oslo, Norway
2. EBRAINS AISBL, Brussels, Belgium
3. CSCS, ETH Zurich, Zurich, Switzerland
4. Paris-Saclay Institute of Neuroscience, CNRS, Université Paris-Saclay, Saclay, France

INTRODUCTION: Open sharing of scientific results is widely recognized as crucial for advancing neuroscience research, yet the quality and the structure of shared outputs remain inconsistent. While researchers are increasingly willing to share their data, many lack the necessary training, expertise, and support for proper data management practices [1,2]. Additionally, the variety of standards and formats can complicate the adoption of appropriate data and metadata structures, often making data from different sources difficult to compare and combine. To address these challenges, the EBRAINS Research Infrastructure has developed a standardized data curation workflow built on a structured metadata framework, with recent updates aimed at improving usability, accessibility and efficiency for researchers. The workflow ensures that outputs are well-structured, discoverable, interpretable, and reusable, ultimately facilitating better integration across diverse platforms while adhering to FAIR principles.

METHODS: Continuously shaped by researcher needs, the EBRAINS Data Services employ a structured, user-friendly curation workflow to facilitate FAIR-aligned data sharing across a broad range of neuroscience domains. The workflow includes both a human-readable data descriptor to support dataset interpretation, and machine- actionable metadata annotation based on the openMINDS framework (RRID: SCR_023173), ensuring interoperability and reusability. The workflow design has been informed by iterative user feedback. To simplify the metadata integration, an intuitive metadata wizard (https://metadata-wizard.apps.ebrains.eu/) has been developed. This tool assists researchers in submitting metadata that can be readily converted to openMINDS. The improvements to the workflow have been iteratively refined through user feedback and validated across multiple neuroscience subdomains, demonstrating its adaptability and effectiveness.

RESULTS: Here we present recent improvements to the EBRAINS curation workflow designed to enhance metadata quality, usability, and data accessibility. Key updates include enhancements to the Metadata Wizard include dynamic term retrieval from the EBRAINS Knowledge Graph and new features like secure authentication, collaborative editing, a guided data descriptor questionnaire, and enhanced support for metadata collection. To further support researchers, the curation workflow improves the discoverability and interpretability of sensitive data by sharing data descriptors and anonymous metadata. This approach makes sensitive data accessible via sensitive data infrastructures following an application procedure, ensuring compliance with ethical guidelines and regulations. These improvements to metadata quality and accessibility lay the foundation for integrating EBRAINS datasets with external research infrastructures. Building on this foundation, EBRAINS datasets are now connected to the broader ecosystem of neuroscience research outputs in the OpenAIRE Graph through the SciLake Neuroscience pilot which leverages graph- based methods to structure and contextualize scientific information and support analysis of dataset usage, emerging trends, and research visibility.

DISCUSSION: These recent updates strengthen the EBRAINS curation workflow by improving metadata integration, streamlining submission processes, and enabling broader support for diverse and sensitive data types. The improved curation workflow reduces the complexity of data sharing for researchers while ensuring compliance with ethical and technical standards. Integration with SciLake and OpenAIRE further extends the reach of EBRAINS datasets, providing insights into usage and impact that support both service refinement and increased research visibility. As a result, EBRAINS is increasingly positioned as a driving force in open and collaborative neuroscience, with continuous improvements guided by the evolving needs of the research community.

References:
[1] Tenopir C, Rice NM, Allard S, et al. Data sharing, management, use, and reuse: practices and perceptions of scientists worldwide. PLoS One. 2020;15(3):e0229003. doi:10.1371/journal.pone.0229003
[2] Tenopir C, Allard S, Douglass K, et al. Data sharing by scientists: practices and perceptions. PLoS One. 2011;6(6):e21101. doi:10.1371/journal.pone.0021101
[3] Amunts K, Axer M, Banerjee S, et al. The coming decade of digital brain research: A vision for neuroscience at the intersection of technology and computing. Imaging Neurosci. 2024;2:imag–2–00137. doi:10.1162/imag_a_00137

Acknowledgements: This project has received funding from the European Union's Horizon Europe research and innovation programme under Grant Agreement No. 101147319 (EBRAINS 2.0) and Grant Agreement No. 101058573 (SciLake).

Keywords: data curation, data sharing, reusability, interoperability, open science

41. Regulation of the Brain Acetylome by Sirtuin-2 and During Ageing

Authors and Affiliations:
Hatoon M. Alamri[1,2] and Mark O. Collins[3]
1 King Abdullah Medical City, Makkah, KSA
2 The General Directorate of Research and Studies, Ministry of Health, KSA
3 School of Biosciences, University of Sheffield, UK
Emails: Hatoon08@gmail.com, mark.collins@sheffield.ac.uk

Introduction
Non-histone lysine acetylation was recently recognised as a highly enriched PTM in the brain. Lysine acetylation regulates the stability of important synaptic proteins such as the AMPA receptor. Sirt2 is a

NAD-dependent enzyme, expressed highly in the brain and is associated with neurodegenerative diseases and ageing. Sirt2−/− mice exhibit impaired synaptic plasticity, including altered LTP and LTD, as well as significant impairments in spatial and contextual memory. A limited number of Sirt2 substrates have been characterised, and the regulatory role of Sirt2 is poorly understood in the brain. Although the role of acetylation has been recognised in the physiology and pathology of ageing, mostly in relation to Sirtuin enzymes, few studies have investigated the changes in acetylation during ageing. **The objective of this study was to identify novel Sirt2 substrates and characterise changes in the brain acetylome during ageing using quantitative proteomics.**

Methods
Here we identified putative Sirt2 substrates through comparative acetylome analysis of Sirt2 KO and WT mouse brain tissue. A comparative analysis of acetylation in old and young mouse brain tissue was performed to understand how acetylation changes during ageing. These datasets were generated by the analysis of immuno-enriched acetylated peptides from tissue samples using quantitative mass spectrometry.

Results
In Sirt2−/− versus WT brains, we identified 2,054 unique acetylation sites across 818 proteins; 226 sites exhibited significantly higher acetylation in Sirt2−/− mice and are considered putative Sirt2 substrate sites. In aged versus young brains, we identified 2,496 unique sites across 1,091 proteins, with 60 sites showing significant age-associated changes (24 increased, 36 decreased).

Discussion
These results identify novel candidate Sirt2 substrates in the brain and define acetylation changes associated with ageing. Together, they provide mechanistic insight into acetylation pathways linked to synaptic function and neurodegeneration. By highlighting the biological significance of acetylation dynamics in ageing, this work underscores potential therapeutic avenues for age-related neurological disorders.

References:
1. Bayés À, Collins MO, Reig-Viader R, et al. Evolution of complexity in the zebrafish synapse proteome. Nat Commun. 2017;8:14613. doi:10.1038/ncomms14613.
2. Choudhary C, Kumar C, Gnad F, et al. Lysine acetylation targets protein complexes and co-regulates major cellular functions. Science. 2009;325(5942):834-840. doi:10.1126/science.1175371.
3. Lundby A, Lage K, Weinert BT, et al. Proteomic analysis of lysine acetylation sites in rat tissues reveals organ specificity and subcellular patterns. Cell Rep. 2012;2(2):419-431. doi:10.1016/j.celrep.2012.07.006.
4. Svinkina T, Gu H, Silva JC, et al. Deep, quantitative coverage of the lysine acetylome using novel anti-acetyl-lysine antibodies and an optimized proteomic workflow. Mol Cell Proteomics. 2015;14(9):2429-2440. doi:10.1074/mcp.O114.047555.
5. Wang G, Li S, Gilbert J, et al. Crucial roles for SIRT2 and AMPA receptor acetylation in synaptic plasticity and memory. Cell Rep. 2017;20(6):1335-1347. doi:10.1016/j.celrep.2017.07.030.

Keywords:
Lysine acetylation.
Sirtuin-2.
Acetylome.
Brain.
Ageing.
Synaptic Plasticity.
Neurodegeneration.

Acknowledgments
The authors acknowledge the financial support of King Abdullah Medical City (KAMC) and the BBSRC.

42. N/A

43. Supporting Reproducibility in EBRAINS Analysis Workflows for Electrophysiology

Cristiano Köhler[1], Sonja Grün[1,2], Michael Denker[1]

[1] Institute for Advanced Simulation (IAS-6), Jülich Research Centre, Jülich, Germany
[2] Theoretical Systems Neurobiology, RWTH Aachen University, Aachen, Germany

Striving for reproducibility of processes surrounding scientific knowledge discovery is an imperative of scientific research. This goal continues to remain challenging in computational workflows processing data from electrophysiology due to the complexity and heterogeneity of data, and the diversity and volatility of analysis workflows utilizing complementary approaches. The difficulty in providing recipes enabling the precise reproduction of scientific results limits the degree to which data resulting from these processes adheres to FAIR principles, specifically impairing aspects of Findability and Interoperability. Here, we present an approach to support reproducible, shareable electrophysiology research using open-source tools from the EBRAINS ecosystem. We focus on the library Elephant ([1], doi:10.5281/zenodo.1186602; RRID:SCR_003833) and the workflow Cobrawap ([2], doi:10.5281/zenodo.10198748; RRID:SCR_022966), two Python-based approaches designed for building analysis and visualization workflows for electrophysiological data [3]. We address reproducibility and sharing by automatizing in-depth provenance tracking of the workflow operations through the use of Alpaca ([4], doi:10.5281/zenodo.10276510; RRID:SCR_023739) to facilitate the documentation of typical computational analysis workflows based on Elephant and Cobrawap. By linking analysis functions and workflow components to concepts defined by the Neuroelectrophysiology Analysis Ontology (NEAO, [5], purl.org/neao), we introduce a semantic layer that abstracts the underlying code to formalized software-independent descriptions of the analysis workflow. We demonstrate how this construct leads to workflow descriptions that are interpretable by researchers, and expose similarities between different workflows. By integrating these resources, researchers can enhance the transparency, reproducibility, and reusability of their work, fostering collaboration and accelerating discovery in neuroscience.

[1] Denker, M., Yegenoglu, A., Grün, S. (2018) Collaborative HPC-enabled workflows on the HBP Collaboratory using the Elephant framework. Neuroinformatics 2018, P19. https://doi.org/10.12751/incf.ni2018.0019
[2] Gutzen, R., De Bonis, G., Luca, C.D., Pastorelli, E., Capone, C., Mascaro, A.L.A., Resta, F., Manasanch, A., Pavone, F.S., Sanchez-Vives, M.V., Mattia, M., Grün, S., Paolucci, P.S., Denker, M., 2024. A modular and adaptable analysis pipeline to compare slow cerebral rhythms across heterogeneous datasets. Cell Reports Methods 4, 100681. https://doi.org/10.1016/j.crmeth.2023.100681
[3] Unakafova, V.A., Gail, A., 2019. Comparing Open-Source Toolboxes for Processing and Analysis of Spike and Local Field Potentials Data. Front. Neuroinform. 13, 57. https://doi.org/10.3389/fninf.2019.00057
[4] Köhler, C.A., Ulianych, D., Grün, S., Decker, S., Denker, M., 2024. Facilitating the Sharing of Electrophysiology Data Analysis Results Through In-Depth Provenance Capture. eNeuro 11, ENEURO.0476-23.2024. https://doi.org/10.1523/ENEURO.0476-23.2024
[5] Köhler, C.A., Grün, S., Denker, M., 2025. Improving data sharing and knowledge transfer via the

Neuroelectrophysiology Analysis Ontology (NEAO). Sci Data 12, 907. https://doi.org/10.1038/s41597-025-05213-3

Acknowledgements: Helmholtz School for Data Science in Life, Earth and Energy (HDS-LEE). EU Horizon 2020 Framework Programme Grant Agreement No. 945539 (Human Brain Project SGA3), the EU Horizon Europe Programme Grant Agreement No. 101147319 (EBRAINS 2.0 Project), the Ministry of Culture and Science of the State of North Rhine-Westphalia, Germany (NRW-network "iBehave", grant number: NW21049), Joint Lab "Supercomputing and Modeling for the Human Brain."

44. FERES on EBRAINS: Federated, Privacy-Preserving Analysis of European Stroke Registries

Authors: Georges Melissargos[1], Viktoria Bastic Schmid[1], Birgit Schaffhauser[1], Pauline Ducouret[1], Julien Dhallenne[1]. Kostas Filippopolitis[2], Evita Mailli[2], Maria-Olympia Katsouli[2], Thanasis Karampatsis[2], Yannis Ioannidis[2], Philippe Ryvlin[1], Alexander Salerno[3]; Patrik Michel[3].

Affiliations: [1] Neurodigital, Department of Clinical Neurosciences, Lausanne University Hospital (CHUV), Switzerland; [2] ATHENA Research Center, Athens, Greece; [3] Stroke Center, Department of Clinical Neurosciences, Lausanne University Hospital (CHUV) and University of Lausanne, Switzerland.

Keywords: Stroke Registry; Federated analysis; EBRAINS; Medical Informatics Platform; Data Anonymization; FAIR; Data Harmonization; Stroke Common Data Elements; Medical analytics

Introduction

Stroke is a leading cause of death and disability in Europe, yet access to evidence-based therapies (intravenous thrombolysis, endovascular thrombectomy) and organised stroke-unit care remains uneven. Prospective national registries capture real-world practice, but heterogeneity and strict privacy laws keep data siloed, limiting multinational analyses. We present FERES powered by the MIP on EBRAINS, a federated, privacy-preserving platform that enables cross-border analysis of stroke registries without centralising patient-level data, illustrating how EBRAINS services power clinical neuroscience and FAIR health data use.

Methods

Architecture and governance. FERES runs on the EBRAINS Medical Informatics Platform (MIP). Each registry operates a local MIP node behind its firewall; datasets are anonymised at source and kept in situ. Communication with the central orchestrator uses encrypted VPN tunnels. Access is controlled via EBRAINS single sign-on (SSO), role-based permissions and audit logs; activities are governed by DSAs/DTAs and multi-jurisdiction ethics approvals.

Anonymization and harmonization. Anonymisation follows HRO and SPHN guidance: removal of direct identifiers; masking/generalisation of quasi-identifiers; generalising or replacing exact dates with clinically meaningful deltas (e.g., door-to-needle); exclusion of free text; and small-n suppression in outputs. Our stroke experts designed a stroke Common Data Elements (CDE) model (demographics, risk factors, treatments, outcomes). Site-specific data curation pipelines map local exports to CDEs (Figure 1). Hierarchical variables preserve clinical meaning across registries. Quality checks validate ranges and coding prior to federation.

Federated analytics. A code-visits-data paradigm is used: the MIP distributed engine (Exareme2) executes descriptives, regression, ANOVA and clustering at nodes, returning only results for secure

aggregation. A browser-based GUI (Figure 2) supports point-and-click analyses and saves full provenance for reproducibility. Nodes can also be hosted at CSCS under the same governance. User accreditation is handled by a multi-registry governance committee; each institution remains data controller with approval rights on analyses and publications. All queries are logged, and a minimum patients-number threshold is enforced across outputs.

Results

Implementation status. Five national nodes from Austria, Greece, Ireland, Italy and Switzerland, are already connected to FERES. A consensus CDE catalogue is created and each FERES member is harmonizing to it. End-to-end pilots validated the pipeline: centrally authored queries execute locally; only aggregated outputs return (Figure 3); no record-level data are exposed. The federation runs stably across heterogeneous IT environments (on-prem and CSCS-hosted).

Scale and readiness. The Swiss Stroke Registry alone includes ~150,000 records across >10 years; combined analyses are projected to exceed 500,000 cases as additional extracts are harmonised.

Discussion

FERES shows that GDPR-compliant, multi-country registry analytics are feasible without centralising data. By uniting standardised, anonymised datasets under a governed federation, the platform enables pan-European benchmarking of key performance indicators (e.g., thrombolysis/thrombectomy rates, door-to-treatment intervals), comparative effectiveness studies and multivariable risk modelling at scale. The approach respects data sovereignty, lowers legal friction via reusable agreements and establishes a learning network for continuous quality improvement. Near-term use cases include data dashboards and reproducible analysis studies shared within the consortium. With five registries live and SOPs for refresh/validation in place, FERES is poised to onboard new members and deliver generalizable insights unattainable within single-country datasets, in line with FAIR and the EBRAINS mission.

Number of figures: 3

References

1. Hallock H, Marshall SE, ’t Hoen PAC, et al. Federated networks for distributed analysis of health data. Front Public Health. 2021;9:712569. doi:10.3389/fpubh.2021.712569
2. Blacketer C, Schuemie MJ, Moinat M, et al. Advancing Real-World Evidence Through a Federated Health Data Network (EHDEN). J Med Internet Res. 2025;27(8):e59024. doi:10.2196/59024
3. Bienzeisler J, Kombeiz A, Ehrentreich S, et al. Pioneering federated data access for Germany’s National ED Registry. NPJ Digit Med. 2025;8:94. doi:10.1038/s41746-025-01481-w
4. Maas MB, Kumar Y, Merkler AE, et al. National hospital-based stroke registries: strengths and limitations. Int J Stroke. 2023;18(5):555-563. doi:10.1177/17474930221118434
5. Maurer J, Österle S, Armida J, Kiss Blind J, Egli M, Raisaro J-L, et al.; SPHN Data De-identification Project Task Force. Guidance for de-identification of health-related data in compliance with Swiss law requirements. Version 2.0. Bern: SPHN; 2025 Feb 14. https://sphn.ch/wp-content/uploads/2025/02/Data-de-identification-guidance-v2.0_20250214.pdf
6. Filippopolitis, K., Foufoulas, I., Garofalakis, M., Glenis, A., Ioannidis, Y., Karampatsis, T.-M., Katsouli, M.-O., Mailli, E., Papageorgiou-Mariglis, A., Papanikos, G., Pikramenos, G., Sakellariou, J., Simitsis, A., Ducouret, P., Ryvlin, P., & Spuhler, M.-G. (n.d.). MIP: Advanced Data Processing and Analytics for Science and Medicine. 802–805
7. Swiss Federal Council. Ordinance on Human Research with the Exception of Clinical Trials (Human Research Ordinance, HRO; SR 810.301). Published September 20, 2013. Accessed September 28, 2025. https://www.fedlex.admin.ch/eli/cc/2013/642/en

Acknowledgments
This project has received funding from the EU's Horizon 2020 Framework Partnership Agreement No. 650003 (Human Brain Project), European Union's Horizon Europe research and innovation programme under Grant Agreement No. 101147319 (EBRAINS 2.0), the Swiss State Secretariat for Education, Research and Innovation (SERI) under contract No. 23.00638 (EBRAINS 2.0) and EAN support for FERES. We thank the national stroke registries and the EBRAINS/MIP teams for governance, deployment and operations.

It must also be mentioned that the screenshots of the FERES deployment of the MIP, as depicted in figures 2 and 3, are based out of synthetic stroke datasets and do not disclose or analyze real patient data.

IMRaD character count (incl. spaces): 3939

Figures

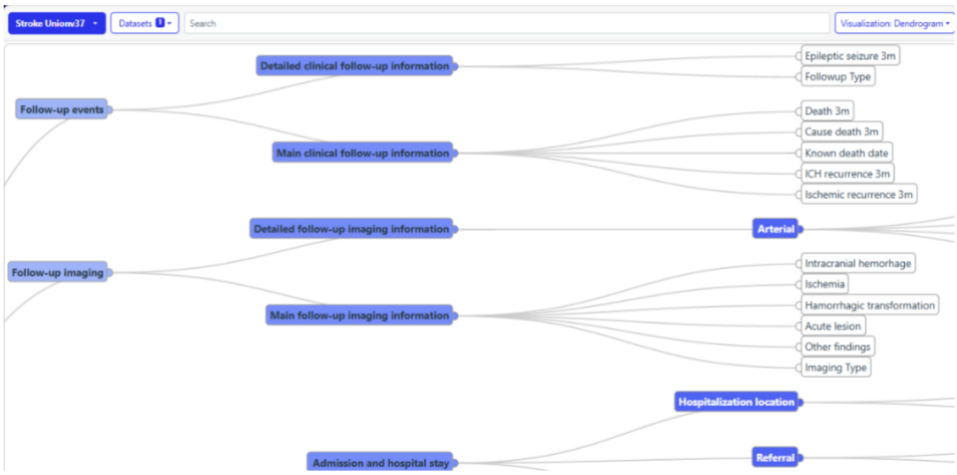

Figure 1. Dendogram visualization (partial) of the FERES Common Data Elements

Figure 2. FERES MIP Graphical User Interface – Choosing stroke variables

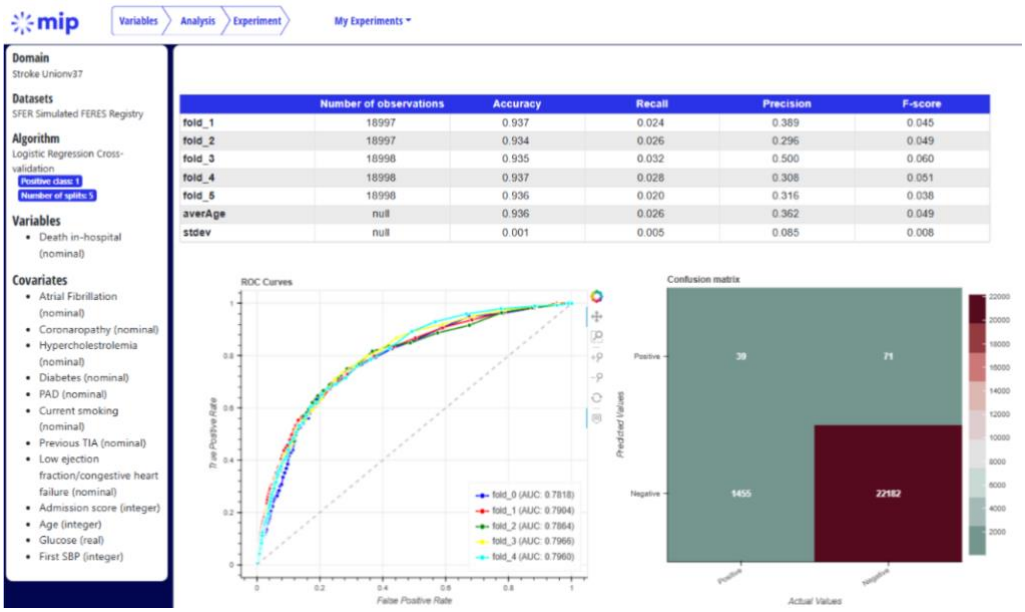

Figure 3. FERES MIP Federated Analytics – Logistic Regression with Cross Validation

45. Merging Services for a Novel Neuroscience Knowledge Graph: Enhancing Data Integration and Tracking Research Impact

Authors
Archana Golla[1*], Maya Kobchenko[1*], Sophia Pieschnik[1*], Ingrid Reiten[1], Serafeim Chatzopoulos[2], César Parra-Rojas[3], Pablo Accuosto[3], Nicolau Duran-Silva[3,4], Nikolay Yakovets[5], Daan de Graaf[5], Miriam Baglioni[6], Jan G. Bjaalie[1], Thanasis Vergoulis[2], Trygve B. Leergaard[1]

Affiliations
1. Institute of Basic Medical Sciences, Faculty of Medicine, University of Oslo, Oslo, Norway
2. Information Management Systems Institute (IMSI), Athena Research Center, Athens, Greece
3. SIRIS Lab, Research Division of SIRIS Academic, Barcelona, Spain
4. LaSTUS Lab, TALN, Universitat Pompeu Fabra, Barcelona, Spain
5. Eindhoven University of Technology, Eindhoven, The Netherlands
6. CNR - ISTI, Pisa, Italy

Abstract
Introduction
As open research data expands, the complexity of neuroscience outputs presents substantial challenges for data collection, organization, and analysis. This often hinders efficient data integration, retrieval, and impact monitoring. Current solutions utilize different Scientific Knowledge Graphs (SKGs) for storing research objects; however, inconsistencies in metadata representation and a lack of interoperability hinder effective connections between information. To tackle these challenges, the Neuroscience pilot of the EU-funded SciLake project developed a novel SKG combining SciLake's analytical capabilities with curated datasets from EBRAINS[1] and the wide range of research products aggregated on OpenAIRE Graph[2].

Methods
We began by creating a neuroscience gateway[3] on OpenAIRE Graph that includes research products from diverse neuroscience journals and repositories. Mapping the metadata of the research products on the OpenAIRE neuroscience gateway and the curated EBRAINS datasets to the SKG- IF

format[4], we created the new SKG. This SKG was integrated into BIP! Finder[5], facilitating the exploration of research products through impact-based ranking.

Subsequently, the SKG was loaded onto AvantGraph[6] to perform advanced analytics and was also imported into Neo4j[7] for efficient visualization and querying of research products and their interconnections. Further, a set of selected controlled terms (Techniques, Preparation Types, UBERON Parcellations, Biological Sex and Species) from openMINDS[8] were loaded as nodes into the SKG, and an entity recognition model[9] was trained to identify and classify mentions of these terms in relevant texts; the mappings between these texts and the identified entities will be incorporated into the graph, thereby enriching the relationships among the research outputs.

Results
The developed SKG enables advanced citation analyses and enriches existing datasets within EBRAINS. During testing, the integrated system effectively supported metadata queries. We executed queries on Neo4j to retrieve citation counts for various research products and even employed the PageRank algorithm[10] in AvantGraph to identify the top 10 influential publications within the SKG. In addition, the BIP! Finder's user interface allows users to access citation metrics that highlight the impact of various research efforts in neuroscience.

Discussion
This neuroscience Scientific Knowledge Graph, fully integrated with the SciLake services, provides researchers with a powerful tool for exploring research uptake, impact, and trends in the neuroscientific research landscape, aiming to optimize research and data sharing efforts. Future work will focus on enhancing the SKG's capabilities and expanding its reach, ultimately ensuring that it remains a valuable resource for neuroscientific research.

Acknowledgement
This work was funded by the EU Horizon Europe projects: SciLake (GA: 101058573) and EBRAINS 2.0 (GA:101147319)

References
1. EBRAINS. EBRAINS Knowledge Graph. Resource Identification Portal. RRID:SCR_017612. See also (accessed 2025-09-29): https://kg.ebrains.eu
2. OpenAIRE. OpenAIRE Graph. Accessed 2025-09-29. https://graph.openaire.eu/
3. OpenAIRE. Neuroscience. Accessed 2025-09-29. https://neuroscience.openaire.eu/
4. SKG-IF. SKG-IF Documentation. Accessed 2025-09-29. https://skg-if.github.io/
5. BIP!Services. Scilake Neuroscience pilot. 2025. Accessed 2025-09-29. https://bip.imsi.athenarc.gr/search/neuroscience-pilot
6. AvantGraph. AvantGraph. Accessed 2025-09-29. https://github.com/avantlab/avantgraph
7. Neo4j. Neo4j. 2025. Accessed 2025-09-29. https://neo4j.com/
8. Open Metadata Initiative. openMINDS metadata framework. Resource Identification Portal. RRID:SCR_023173. See also GitHub repository (published 2023; updated 2025; accessed 2025-09-29): https://github.com/openMetadataInitiative/openMINDS
9. SIRIS-Lab. SciLake-Neuroscience-GLiNER-large. Accessed 2025-09-29. https://huggingface.co/SIRIS-Lab/SciLake-Neuroscience-GLiNER-large
10. Gleich DF, PageRank Beyond the Web. SIAM Review. 2015;57:3. doi:10.1137/140976649

46. Reduced dynamic functional connectivity in higher ages: Are older brains less adaptable?

Natalia Zhukova[2*], Camilla Mendl-Heinisch[1,2], Christiane Jockwitz[1,2*] & Svenja Caspers[1,2*]

Institutions:
[1]Institute of Neuroscience and Medicine (INM-1), Research Centre Jülich, Jülich, Germany
[2]Institute for Anatomy I, Medical Faculty & University Hospital Düsseldorf, Heinrich Heine University Düsseldorf, Düsseldorf, Germany

Email addresses of authors: natalia.zhukova@hhu.de, c.jockwitz@fz-juelich.de, s.caspers@fz-juelich.de

Introduction
A comprehensive understanding of age-related changes in the brain's functional architecture is essential to distinguish healthy from pathological aging, particularly given increasing life expectancy. Static functional connectivity (FC) has revealed key insights into resting-state network organization, including age-related shifts in the balance between network segregation and integration[1]. Building on this, research increasingly highlights the brain's inherently dynamic nature and calls for investigations into how functional network patterns fluctuate at finer temporal scales, particularly to deepen our understanding of cognitive decline and resilience while potentially serving as early biomarkers for cognitive decline[2]. Therefore, the current study set out to systematically investigate age-related alterations in dynamic FC in 817 older males and females (374 females; 55–85 years) from 1000BRAINS[3].

Methods
Data were acquired on a 3T Siemens Tim-TRIO scanner (TR=2.2 s, TE=3.03 ms, flip angle=9°, voxel size=1 mm³). Preprocessing included motion correction, ICA-AROMA, global signal regression, band-pass filtering (0.01–0.1 Hz), and normalization to MNI space[4]. Sliding-window (30 s, non-overlapping) Pearson correlations generated time-resolved connectivity matrices, which were clustered into 4 dynamic FC states using Ward's method of Hierarchical clustering[5]. Temporal metrics (dwell time, transitions) and network properties (integration/segregation, based on the 400-node Schaefer parcellation, 17-network version[6]) were quantified and correlated with age. Additional group comparisons were made, divided by age (young old adults ≤67 y | older old adults ≥68 y) and further categorized based on high and low global cognitive performance.

Results and Discussion
Overall, dynamic FC slowed with age, with older adults showing longer dwell times, fewer transitions, and a higher tendency to remain in a single state. Critically, two out of four states showed robust age effects: the most integrated state became less prevalent, while the most segregated state became more prevalent with age (Fig. 1). Age stratified group analyses replicated the four-state architecture, but only the oldest age group showed an age-related slowing in dynamic FC. In turn, younger old adults exhibited stronger within-network connectivity in both, integrative and segregated states. Further stratification by cognition showed that in younger old adults, higher cognitive performance was associated with greater network integration, while in older old adults, greater segregation and higher dynamic FC were associated with worse cognitive performance.

Current results highlighted a reduced functional adaptability in higher ages (e.g. longer dwell times, fewer transitions), which is consistent with prior works[7]. The dominance of segregated states in older adults suggests a shift toward more stable yet less flexible network configurations with age, potentially to strive for network stability and energy efficiency[8]. Comparing age groups revealed age-related slowing in dynamic FC to be present only in the oldest old age group, stressing the importance of non-linear age trajectories of functional brain dynamics. Furthermore, higher cognitive performance was associated with greater network integration in the younger old group, consistent with the notion of compensatory recruitment to support cognitive functioning[9]. The opposite effect was observed in older old adults, where greater within-network connectivity was associated with

worse cognitive performance. This suggests that the functional significance of integration may change with age, shifting from beneficial compensation to dedifferentiation[10]. These findings underscore the utility of dynamic FC as a sensitive marker of cognitive health, capable of capturing both compensatory and dedifferentiation processes, by adding the time dimension to the static FC approach.

Keywords: aging, dynamic functional connectivity, network architecture, population-based cohort, sliding windows analysis, dFC states.

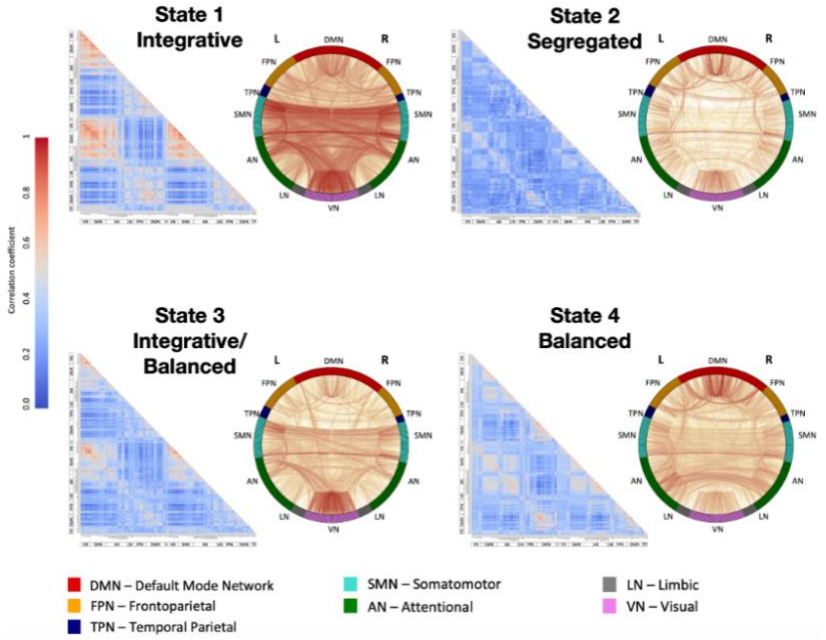

Fig. 1. *Whole-brain functional connectivity patterns across four dynamic connectivity states. Correlation matrices depicting the functional coupling of 400 brain parcels[6] across four states. Positive correlations are shown in red and negative correlations in blue, with intensity representing correlation strength. Corresponding circular connectivity plots illustrating whole-brain functional network organization for each state on the left side of circular plot nodes in the left hemisphere are presented, right side right hemisphere. Brain parcels are color-coded according to the summation of the 17 network parcellation into 7 networks, and only positive correlations are displayed.*

1. Betzel RF, Byrge L, He Y, Goñi J, Zuo XN, Sporns O. Changes in structural and functional connectivity among resting-state networks across the human lifespan. Neuroimage. 2014;102(P2):345-357. doi:10.1016/j.neuroimage.2014.07.067
2. Ourry V, Gonneaud J, Landeau B, et al. Association of quality of life with structural, functional and molecular brain imaging in community-dwelling older adults. Neuroimage. 2021;231. doi:10.1016/j.neuroimage.2021.117819
3. Caspers S, Moebus S, Lux S, et al. Studying variability in human brain aging in a population-based German cohort-rationale and design of 1000BRAINS. Front Aging Neurosci. 2014;6(JUL). doi:10.3389/fnagi.2014.00149
4. Pruim RHR, Mennes M, van Rooij D, Llera A, Buitelaar JK, Beckmann CF. ICA-AROMA: A robust ICA-based strategy for removing motion artifacts from fMRI data. Neuroimage. 2015;112:267-277. doi:10.1016/j.neuroimage.2015.02.064
5. Ward JH. Hierarchical Grouping to Optimize an Objective Function. Vol 58.; 1963.
6. Schaefer A, Kong R, Gordon EM, et al. Local-Global Parcellation of the Human Cerebral Cortex from Intrinsic Functional Connectivity MRI. Cerebral Cortex. 2018;28(9):3095- doi:10.1093/cercor/bhx179

7. Battaglia D, Boudou T, Hansen ECA, et al. Dynamic Functional Connectivity between order and randomness and its evolution across the human adult lifespan. Neuroimage. 2020;222. doi:10.1016/j.neuroimage.2020.117156
8. Weistuch C, Mujica-Parodi LR, Razban RM, et al. Metabolism modulates network synchrony in the aging brain. Published online 2021. doi:10.1073/pnas.2025727118/-/DCSupplemental.y
9. Zhang H, Gertel VH, Cosgrove AL, Diaz MT. Age-related differences in resting-state and task-based network characteristics and cognition: a lifespan sample. Neurobiol Aging. 2021;101:262-272. doi:10.1016/j.neurobiolaging.2020.10.025
10. Viviano RP, Raz N, Yuan P, Damoiseaux JS. Associations between dynamic functional connectivity and age, metabolic risk, and cognitive performance. Neurobiol Aging. 2017;59:135-143. doi:10.1016/j.neurobiolaging.2017.08.003

47. N/A

48. The Virtual Aging Brain: A Scalable Framework of Dopaminergic Modulation

Authors: Amirhossein Esmaeili[1,*], Giacomo Preti[1], Spase Petkoski[1], Marmaduke Woodman[1], Meysam Hashemi[1], Daniele Marinazzo[2,†], Viktor Jirsa[1,†]

1. Aix Marseille University, INSERM, INS, Inst Neurosci Syst, Marseille, France
2. Department of Data Analysis, Ghent University, Ghent, Belguim
* Corresponding author: Amirhossein.Esmaeili@univ-amu.fr
† These authors contributed equally to this work and share senior authorship.

Keywords: Aging, Dopaminergic modulation, Virtual Brain Twins, Whole-brain modelling, Probabilistic inference

Introduction:
Age-related changes in the dopamine (DA) system are considered a key mechanism contributing to cognitive decline in later life, with significant reductions of D1 transporters (DATs) and receptor densities (Rds) across decades [6]. However, much remains to be known with regards to the complex interplay between the components of the DA subsystem, and their contribution to whole-brain
(macroscale) dynamics. We therefore developed a biologically-plausible and scalable whole-brain computational model of D1 which integrates region-specific D1 receptor densities, with a global modulation of DATs, in order to to formally investigate the impact of the aforementioned changes on macroscale dynamics.

Methods:
Our proposed framework builds upon the neural mass-model (NMM) by Gast and colleagues [2] (Figure **1A,B**).

A

$$C\dot{r} = \Delta k^2(v - v_r) + r\Big(k(2v - v_r - v_\theta) - (B_d + M_d)\gamma s_a - g_g s_g\Big)$$

$$C\dot{v} = kv(v - v_r - v_\theta) - \pi Cr\left(\Delta + \frac{\pi Cr}{k}\right) + kv_r v_\theta - u + I + (B_d + M_d)\gamma s_a(E_a - v) + g_g s_g(E_g - v)$$

$$\dot{u} = \frac{b(v - v_r) - u}{\tau_u} + \kappa r$$

$$\dot{s}_a = -\frac{s_a}{\tau_{s_a}} + J_{sa} c_{exc} + J_a r$$

$$\dot{s}_g = -\frac{s_g}{\tau_{s_g}} + J_{sg} c_{inh} + J_g r$$

$$\tau_{D_p}\dot{D}_p = J_{dopa} c_{dopa} - \frac{V_{max} D_p}{K_m + D_p}$$

$$\tau_{M_d}\dot{M}_d = -M_d + \frac{R_d}{1 + \exp\left(S_d \log(D_p + Z)\right)}$$

$$C_{p,i} = w_p \sum_j^N k_{ij} m_{p,ij} r_j$$

B

Parameter	Value	Parameter	Value
C	100.0	k	0.7
Δ	0.5	v_r	−60.0
v_θ	−40.0	B_d	0.9
γ_a	1.0	γ_g	1.0
E_a	0.0	E_g	−50.0
I	46.5	τ_u	33.33
b	−2.0	κ	100.0
τ_{sa}	6.0	τ_{sg}	6.0
J_a	13	J_g	15
J_{sa}	13	J_{sg}	15.0
J_{dopa}	100000	V_{max}	1300.0
K_m	150.0	τ_{D_p}	500.0
R_d	0.1	S_d	−10
Z	0.5	τ_{M_d}	1000

Figure 1: A. Equations of the whole-brain model. B. Parameters of the whole-brain model.

Derived from tractography data and adjusted based on previous research on connectivity, the effects of dopamine are represented via the D1 receptor, which enhances excitatory synaptic currents (AMPA channels) [10], with D1 inputs and re-uptake regulating dopamine concentration at each node (region-specific representation of D1 receptor densities is estimated with the help of PET data, Figure **2A-C**) [1,5]. We use anatomically-informed connectivity masks to define distinct glutamatergic, GABAergic, and dopaminergic projections between brain regions, including key basal ganglia and cortico-striatal circuits [7, 8, 9]. This is implemented as a multiplicative term, (Bd+Md), that modulates a node's excitatory current. Dopamine concentration (Dp) at each node is regulated by dopaminergic inputs and a Michaelis-Menten re-uptake mechanism, while receptor occupancy (Md) follows a sigmoidal dose-response curve dependent on Dp and the number of D1 receptors (Rd). Age-related decline in dopaminergic function is simulated by scaling the D1 receptor density parameter (Rd) with an aging factor, β.

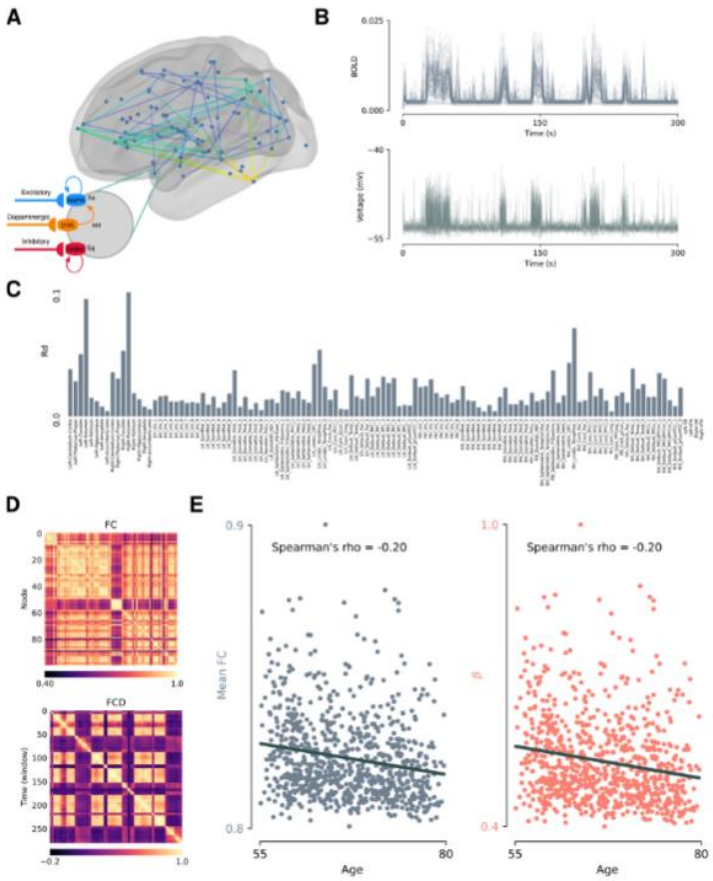

Figure 2. Figure 2: A. Schema of the whole-brain dopaminergic aging model, with nodes operating via three types of inputs: glutamatergic, GABAergic, and dopaminergic. Glutamatergic inputs excite the node, GABAergic inputs inhibit it, and dopaminergic inputs modulate its excitatory drive. B. Sample simulation of model dynamics in the oscillatory regime. C. Implementation of heterogeneous D1 receptor densities in the Schaefer 7Networks parcellation. D. Sample functional connectivity (FC) and functional connectivity dynamics (FCD). E. Preliminary findings of probabilistic inference of receptor density scaling in the 1000BRAINS dataset. A template structural connectivity is used for runnings simulations and training the neural density estimator.

Results:
In order to test the effects of D1 modulation on macroscale dynamics, we ran a probabilistic inference of receptor densities based on simulations obtained through the structural connectivity of one sample participant (i.e. shared connectome across simulations). Sampling randomly from a prior distribution of the parameter β, we obtained a pool of 5000 simulations which we used to train a neural density estimator (via the simulation-based inference package) in order to establish an amortized mapping between said parameter, and mean functional connectivity obtained from the simulations. We observed that reduction in mean functional connectivity across age leads to a corresponding reduction in β (Figure **2D,E**), consistent with the observed trend in the 1000BRAINS cross-sectional dataset, providing support for the validity of the dopaminergic framework of aging outlined here [4].

Discussion:
The virtual aging framework proposed here provides a powerful, computationally efficient means of investigating the trajectory of dopaminergic modulation in aging, bridging the gap between between microscale changes (i.e. modulation of D1 receptor density and re-uptake rates) and macroscale brain dynamics. It is critical to note that while the preliminary results outlined here are promising, its findings should not be extended to a cohort-level investigation. In addition, the reduction in receptor densities is along the same trajectory as the previously observed decrease in interhemispheric connectivity, neither of which provide a suitable candidate for the potential role of D1 dynamics in homeostatic regulation of cognitive function. Thus, our next step is to conduct a fully-personalized cross-sectional probabilistic inference of receptor re-uptake rates in the 1000BRAINS dataset. Nevertheless, we believe that the flexible framework presented here can be used for in-silico hypothesis testing which pertain not only to brain health trajectories, but also with regards to the pathophysiology of neurodegenerative disorders such as Parkinson's disease and potential therapeutic interventions.

Acknowledgments:
This project/research has received funding from the European Union's Horizon Europe Programme under the Specific Grant Agreement No. 101147319 (EBRAINS 2.0 Project), No. 101137289 (Virtual Brain Twin Project).

References:
1. Depannemaecker D., Duprat D., Angiolelli M., Sales Carbonell C., Wang H., Petkoski S., Sorrentino P., Sheheitli H., Jirsa V. (2024). A neural mass model with neuromodulation. BioRxiv, https://doi.org/10.1101/2024.06.23.600260
2. Gast, R., Solla, S. A., & Kennedy, A. (2024). Neural heterogeneity controls computations in spiking neural networks. Proceedings of the National Academy of Sciences, 121(3), e2311885121 https://doi.org/10.1073/pnas.2311885121
3. Handfield-Jones, Nicholas, "Connectomic Analysis of Substantia Nigra Pars Compacta and Ventral Tegmental Area Projections to the Striatum and Cortex" (2019). Electronic Thesis and Dissertation Repository. 6463.https://ir.lib.uwo.ca/etd/6463
4. Jung, K., Eickhoff, S. B., & Popovych, O. V. (2022). Parcellation-based structural and resting-

state functional whole-brain connectomes of 1000BRAINS cohort (v1.1) [Data set]. EBRAINS. https://doi.org/10.25493/8XY5-BH7
5. Kaller, S., Rullmann, M., Patt, M., Becker, G. A., Luthardt, J., Girbardt, J., ... & Sabri, O. (2017). Test–retest measurements of dopamine D1-type receptors using simultaneous PET/MRI imaging. European journal of nuclear medicine and molecular imaging, 44(6), 1025-1032. https://doi.org/10.1007/s00259-017-3645-0
6. Karrer, T. M., Josef, A. K., Mata, R., Morris, E. D., & Samanez-Larkin, G. R. (2017). Reduced dopamine receptors and transporters but not synthesis capacity in normal aging adults: a meta-analysis. Neurobiology of aging, 57, 36-46. https://doi.org/10.1016/j.neurobiolaging.2017.05.006
7. Mallet, N., Delgado, L., Chazalon, M., Miguelez, C., & Baufreton, J. (2019). Cellular and synaptic dysfunctions in Parkinson's disease: stepping out of the striatum. Cells, 8(9), 1005. https://doi.org/10.3390/cells8091005
8. Russo, S. J., & Nestler, E. J. (2013). The brain reward circuitry in mood disorders. Nature reviews neuroscience, 14(9), 609-625. https://doi.org/10.1038/nrn3381
9. Sonne, J., Reddy, V., & Beato, M. R. (2024). Neuroanatomy, substantia nigra. In StatPearls [Internet]. StatPearls Publishing. https://www.ncbi.nlm.nih.gov/books/NBK536995/
10. Surmeier, D. J., Ding, J., Day, M., Wang, Z., & Shen, W. (2007). D1 and D2 dopamine-receptor modulation of striatal glutamatergic signaling in striatal medium spiny neurons. Trends in neurosciences, 30(5), 228–235. https://doi.org/10.1016/j.tins.2007.03.008

49. bids2ebrains: Automating BIDS Dataset Registration into the EBRAINS Knowledge Graph

Renqing Cuomao[1*], Raphaël Gazzotti[2*], Sophia Pieschnik[3], Oliver Schmid[4], Peyman Najafi[5], Andrew P. Davison[5], Cyril Pernet[6], Lyuba Zehl[2*]

[1]EPFL, Lausanne, Switzerland
[2]EBRAINS AISBL, Brussels, Belgium
[3]Institute of Basic Medical Sciences, Faculty of Medicine, University of Oslo, Oslo, Norway
[4]CSCS, ETH Zurich, Zurich, Switzerland
[5]Institut des Neurosciences Paris-Saclay, Université Paris-Saclay, CNRS, Saclay, France
[6]Neurobiology Research Unit, Copenhagen University Hospital, Rigshospitalet, Copenhagen, Denmark
*renqing.cumao@epfl.ch; raphael.gazzotti@ebrains.eu; lyuba.zehl@ebrains.eu

INTRODUCTION/MOTIVATION
The Brain Imaging Data Structure (BIDS) standard [1] and the openMINDS metadata framework [2] are cornerstones for findable, accessible, interoperable, and reusable (FAIR) neuroscience [3]. BIDS ensures consistency in dataset organization, while openMINDS enables explicit, ontology-driven metadata representations within the EBRAINS Knowledge Graph (KG) [4]. However, registering BIDS datasets in EBRAINS remains a mostly manual and error-prone process that requires detailed knowledge of metadata schemas. This hinders the large- scale integration and reuse of neuroscience datasets within EBRAINS. To overcome this obstacle, we first developed the bids2openminds converter [5] which is now complemented with the bids2ebrains [6].

METHODS
bids2ebrains facilitates the registration of BIDS datasets into the EBRAINS KG by providing a semi-automated pipeline for uploading openMINDS compliant metadata formatted as JSON-LD. The tool is available as (1) a command-line interface (CLI), (2) an interactive Streamlit-based graphical user

interface (UI), and (3) a Python library, accommodating both technical and non-technical users. All interfaces enable the following workflow:

- **Conversion module** – relies on the existing prototype of the bids2openminds converter for translating BIDS metadata to openMINDS compliant JSON-LD files.
- **Scan module** – automatically detects and reports missing metadata entries expected by the EBRAINS curation service.
- **Patch module** – enables completion of missing fields either automatically (e.g., for file sizes) or interactively (e.g., for missing controlled vocabulary).
- **Upload module** – authenticates provider for uploading openMINDS compliant metadata of the BIDS dataset into an eligible EBRAINS KG space.

Once uploaded to an eligible EBRAINS KG space, metadata only requires final validation by the EBRAINS curation service before being released.

RESULTS AND DISCUSSION

We validated bids2ebrains using the ds001 open dataset from the BIDS examples repository [7]. Running the conversion module generated the essential set of openMINDS JSON-LD files for the Dataset, DatasetVersion, Subject, and File entities. The scan module identified all missing metadata entries across the detected files and automatically aggregated these entries into prompts. The interface of the patch module enabled the interactive completion of missing controlled vocabularies and free-text fields. Moreover it auto-completes fields that are inferable from the source data. The finally complete set of openMINDS metadata was then pushed into a dedicated EBRAINS KG test space via the upload module, after a dry-run for ensuring safe validation before final submission. Initial testing showed that the tool substantially reduces the effort needed for registration and curation when submitting BIDS compliant datasets to EBRAINS. These findings highlight how bids2ebrains streamlines data sharing and provide the basis for further discussion of its broader impact.

bids2ebrains enables the seamless integration of BIDS datasets into the EBRAINS KG, bridging community standards (BIDS) with infrastructure-level metadata frameworks (openMINDS). By combining automation, validation, and user-friendly interfaces, the tool lowers technical barriers and the required effort for dataset registration and curation. Looking ahead, bids2ebrains will enable both individual BIDS datasets registration and large-scale synchronization with external BIDS-compliant repositories (e.g., publicnEUro), provided that EBRAINS registration requirements are fulfilled, as expected/ensured by the tool's validation workflow. Its modular design enables future extensions to new modalities and metadata classes as BIDS and openMINDS evolve, positioning it as a key infrastructure tool for open and FAIR neuroscience, standardization alignment, and reproducible (meta)data registration and curation.

Keywords: BIDS, openMINDS, FAIR data, EBRAINS, Knowledge Graph, metadata curation, automation, interoperability, neuroinformatics, data integration

ACKNOWLEDGEMENTS

This work was developed as part of the Google Summer of Code 2025 program, under the mentorship of the International Neuroinformatics Coordinating Facility (INCF). This work also received funding from the European Union's Horizon Europe research and innovation programme under grant agreement No 101147319 (EBRAINS2.0).

REFERENCES

[1] Gorgolewski K, Auer T, Calhoun V, et al. The brain imaging data structure, a format for organizing and describing outputs of neuroimaging experiments. Sci Data. 2016;3:160044. https://doi.org/10.1038/sdata.2016.44

[2] Open Metadata Initiative. openMINDS metadata framework. Resource Identification Portal: RRID:SCR_023173. FAIRsharing.org: https://doi.org/10.25504/FAIRsharing.6ac6aa. See also

GitHub repository (published 2023; updated 2025; accessed 2025-08-25): https://github.com/openMetadataInitiative/openMINDS
[3] Wilkinson MD, Dumontier M, Aalbersberg IJ, et al. The FAIR Guiding Principles for scientific data management and stewardship. Sci Data. 2016;3:160018. https://doi.org/10.1038/sdata.2016.18
[4] EBRAINS. EBRAINS Knowledge Graph. Resource Identification Portal. RRID:SCR_017612. See also (accessed 2025-08-26): https://kg.ebrains.eu
[5] Open Metadata Initiative. bids2openminds. (published 2024; updated 2025; accessed 2025-08-26) https://github.com/openMetadataInitiative/bids2openminds
[6] EBRAINS. bids2ebrains. (published 2025; accessed 2025-08-26) https://gitlab.ebrains.eu/ri/projects-and- initiatives/bids2ebrains/bids2ebrains
[7] Brain Imaging Data Structure. bids-examples. (published 2016; updated 2025; accessed 2025-08-26) https://github.com/bids-standard/bids-examples

50. Clinical imaging coregistration for localisation of neuro-electrodes (CiCLONE)

Authors: Carolina **Ciumas**[1], Florian **Sipp**[1], Francesco **Cardinale**[2], Nathalie **Casati**[3], Philippe **Ryvlin**[1]

Affiliations:
[1] Department of Clinical Neurosciences, Centre Hospitalier Universitaire Vaudois, Switzerland
[2] Ospedale Niguarda Ca' Granda: Milano, Lombardia, Italy
[3] Biomedical Data Science Center, Centre Hospitalier Universitaire Vaudois, Switzerland

Introduction
CiCLONE [1] is a newly designed, user-friendly tool that revolutionizes the co-registration of multimodal imaging data in the presurgical evaluation of patients with pharmacoresistant epilepsy. Unlike existing fragmented approaches, CiCLONE delivers a **single, standardized, and automated pipeline** that accelerates image alignment and electrode localization while minimizing operator burden. By embedding this functionality into the Human Intracerebral EEG Platform, HIP [5], CiCLONE transforms a traditionally time-consuming process into a **reliable, reproducible, and clinically impactful workflow**—a major step forward for both patient care and research.

Methods
CiCLONE builds upon the Milano co-registration pipeline from Francesco Cardinale but extends its functionality through a fully integrated architecture. The tool unifies:

- **FSL FEAT** [2] for robust multimodal image alignment
- **FreeSurfer** [3] for cortical surface extraction and atlas-based parcellations
- **3D Slicer** [4] for electrode registration and interactive visualization

Through its intuitive interface, clinicians can rapidly select a reference image, align multiple modalities into a common native space, and transform outputs into standardized spaces such as MNI. Electrode localization is streamlined by incorporating clinical implantation schema, with user input limited to essential electrode parameters.

Results
CiCLONE enables **fast, reliable, and standardized multimodal co-registration** and delivers **precise electrode localization** (tip and skull entry point) with full compatibility for visualization in 3D Slicer. Data are automatically stored in both native and MNI spaces, supporting **patient-level precision** while also enabling **group-level aggregation** for translational research. Validation on 15 patients (CHUV dataset, Seizure Database Project on the HIP) demonstrated 100% successful processing, with end-to-end execution—including co-registration, surface extraction, and electrode

marking—completed in hours rather than days. The seamless integration with 3D Slicer further enriches the workflow, allowing direct use of cortical reconstructions and parcellations without additional preprocessing.

Discussion:
CiCLONE represents a **step-change in presurgical epilepsy imaging**. By unifying multimodal image alignment, electrode localization, and standardized space transformation into a **single reproducible pipeline**, it reduces complexity, improves efficiency, and strengthens data quality. Its dual focus on clinical usability and research scalability positions CiCLONE as a **critical new tool** for advancing surgical planning and enabling large-scale, data-driven discoveries in epilepsy.

Acknowledgements:
This work was supported by the European Union's Horizon Europe research and innovation programme under Grant Agreement No. 101147319 (EBRAINS 2.0) and the Swiss State Secretariat for Education, Research and Innovation (SERI) under contract No. 23.00638 (EBRAINS 2.0).

References:
1. CiCLONE Command-line tool for CT image registration and 3D electrode localization https://github.com/NeuroTech-Platform/CiCLONE
2. FSL FMRIB Software Library https://fsl.fmrib.ox.ac.uk/fsl/docs/#/
3. Freesurfer Software Suite https://surfer.nmr.mgh.harvard.edu/
4. 3D Slicer image computing platform https://www.slicer.org/
5. Human Intracerebral EEG Platform, HIP https://thehip.app/apps/hip/about

Keywords:
CiCLONE, Human Intracerebral EEG Platform (HIP), multimodal co-registration, electrode localization, presurgical evaluation, 3D Slicer, FreeSurfer, FSL FEAT, standardized pipeline

51. Limit-cycle dynamics and MEG functional connectivity dynamics best explain empirical brain activity

Masanori Ue[1, 2*], Okito Yamashita[2, 3]
[1]Department of Science and Technology, Nara Institute of Science and Technology, Ikoma, Japan
[2] Department of Computational Brain Imaging, Advanced Telecommunications Research Institute International, Soraku-gun Seika-cho, Japan
[3] RIKEN Center for Advanced Intelligence Project, RIKEN, Wako, Japan
* m.ue@atr.jp

INTRODUCTION/MOTIVATION
How macroscale brain dynamics described as functional connectivity (FC) and functional connectivity dynamics (FCD) emerge from structural connectivity (SC) is still unresolved[1]. While various mathematical models address this structure-function relationship, model parameters crucially determine behavior and mechanistic interpretation[2,3]. Most studies fix parameters based on assumptions, potentially limiting comprehensive understanding. Furthermore, parameter fitting typically assumes all metrics and modalities contribute equally to optimization, despite distinct temporal-spatial resolutions[4,5]. We test whether fitting a whole-brain neural-mass model to multi-modal targets—fMRI and MEG with static FC and dynamic FCD metrics—can identify regime-specific parameters and clarify which targets most effectively constrain model selection.

METHODS

Data. Human Connectome Project[6] data (S1200) included: structural connectivity from 1113 subjects via diffusion MRI with probabilistic tractography (5000 samples/voxel), averaged across subjects; resting-state fMRI from 1003 subjects (469 male, 534 female; 994 subjects aged 22-35 years, 9 subjects aged >36 years; TR=720ms, 2mm isotropic) band-pass filtered 0.01–0.08 Hz; MEG from 87 subjects (46 male, 41 female; all aged 22-35 years; 248 magnetometers) preprocessed with band-pass filtering (0.4–50 Hz), artifact rejection, and LCMV beamforming to project onto AAL cortical regions. Envelope timeseries were computed per frequency band (delta: 0.4–4 Hz, theta: 4–8 Hz, alpha: 8–13 Hz, beta: 13–30 Hz, gamma: 30–50 Hz).
Modeling. A 78-region Wilson–Cowan network coupled by empirical SC[7]. Following Siu et al. [8], we probed three node dynamics regimes: fixed point, hysteresis, and limit cycle, while jointly sweeping global coupling and excitatory threshold parameters. Simulations lasted 14 minutes; hemodynamic response functions generated fMRI-comparable signals.
Metrics. FC was computed as Pearson correlations between regional timeseries compared via Spearman's correlation. FCD employed sliding windows (60s fMRI; 30s MEG, 80% overlap) compared via Kolmogorov–Smirnov distance[9]. Additional metrics included similarity rank, log-power spectra (0.4–50 Hz) metastability (standard deviation of Kuramoto order parameter) and criticality via generalized Ising model simulations.

RESULTS AND DISCUSSION

Aggregating similarity scores across four metrics (fMRI-FC, fMRI-FCD,MEG-FC, MEG-FCD), we summarize the regime-wise fits (Figure 1). The limit-cycle dynamics yielded a significantly better empirical fit than the fixed-point and hysteresis regimes (Wilcoxon rank-sum, $p < 0.001$). Within the limit-cycle regime, MEG-derived FCD provided greatest explanatory power for detrended log-power spectra ($r = 0.655$), metastability and criticality compared to other metrics. Bootstrap comparisons confirmed MEG-FCD superiority ($p < 0.001$), suggesting high-temporal-resolution dynamics most effectively constrain model parameters.

Multi-metric, multi-modal optimization successfully identifies physiologically plausible operating regimes for cortical dynamics. MEG-FCD prominence highlights temporal resolution importance in capturing brain dynamics. Key limitations include exclusive cortical focus while subcortical structures remain crucial[10]; fixed biophysical properties (e.g., cell density[8]). Future investigations incorporating subcortical regions and richer biophysical heterogeneity may refine parameter identifiability and mechanistic interpretation.

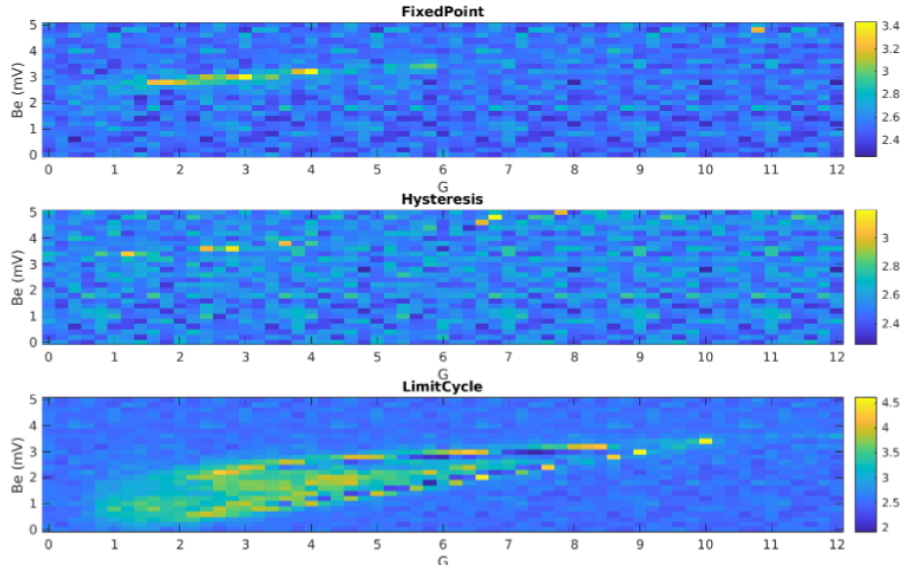

Figure 1. Limit-cycle dynamics show higher empirical fit than other regimes.

Keywords: Whole-brain modeling, Wilson–Cowan model, Limit-cycle dynamics, Functional connectivity (FC), Functional connectivity dynamics (FCD), Magnetoencephalography (MEG), Functional MRI (fMRI), Structural connectivity (SC), Metastability, neural mass model

ACKNOWLEDGEMENTS

Data were provided by the Human Connectome Project, WU-Minn Consortium (Principal Investigators: David Van Essen and Kamil Ugurbil; 1U54MH091657) funded by the 16 NIH Institutes and Centers that support the NIH Blueprint for Neuroscience Research; and by the McDonnell Center for Systems Neuroscience at Washington University.

REFERENCES

1. Suárez LE, Markello RD, Betzel RF, Misic B. Linking Structure and Function in Macroscale Brain Networks. Trends Cogn Sci. 2020;24: 302–315. doi:10.1016/j.tics.2020.01.008
2. Breakspear M. Dynamic models of large-scale brain activity. Nat Neurosci. 2017;20: 340–352. doi:10.1038/nn.4497
3. Sanz-Leon P, Knock SA, Spiegler A, Jirsa VK. Mathematical framework for large-scale brain network modeling in The Virtual Brain. Neuroimage. 2015;111: 385–430. doi:10.1016/j.neuroimage.2015.01.002
4. Endo H, Hiroe N, Yamashita O. Evaluation of Resting Spatio-Temporal Dynamics of a Neural Mass Model Using Resting fMRI Connectivity and EEG Microstates. Front Comput Neurosci. 2019;13: 91. doi:10.3389/fncom.2019.00091
5. Kong X, Kong R, Orban C, Wang P, Zhang S, Anderson K, et al. Sensory-motor cortices shape functional connectivity dynamics in the human brain. Nat Commun. 2021;12: 6373. doi:10.1038/s41467-021-26704-y
6. Van Essen DC, Smith SM, Barch DM, Behrens TEJ, Yacoub E, Ugurbil K, et al. The WU-Minn Human Connectome Project: an overview. Neuroimage. 2013;80: 62–79. doi:10.1016/j.neuroimage.2013.05.041
7. Wilson HR, Cowan JD. Excitatory and inhibitory interactions in localized populations of model neurons. Biophys J. 1972;12: 1–24. doi:10.1016/S0006-3495(72)86068-5
8. Siu PH, Müller E, Zerbi V, Aquino K, Fulcher BD. Extracting Dynamical Understanding From Neural-Mass Models of Mouse Cortex. Front Comput Neurosci. 2022;16: 847336. doi:10.3389/fncom.2022.847336
9. Cabral J, Kringelbach ML, Deco G. Functional connectivity dynamically evolves on multiple time-scales over a static structural connectome: Models and mechanisms. Neuroimage. 2017;160: 84–96. doi:10.1016/j.neuroimage.2017.03.045
10. Müller EJ, Munn B, Hearne LJ, Smith JB, Fulcher B, Arnatkevičiūtė A, et al. Core and matrix thalamic sub-populations relate to spatio-temporal cortical connectivity gradients. Neuroimage. 2020;222: 117224. doi:10.1016/j.neuroimage.2020.117224

52. CHORUS.HIP: A Secure, Evolving Collaborative Environment for Multimodal Epilepsy Data and Beyond

Authors and Affiliations

Florian Sipp[1], Carolina Ciumas[1], Jonathan Haab[1], Julien Dhallenne[1], Birgit Schaffhauser[1], Viktoria Bastic Schmid[1], Jean Louis Raisaro[2], Nathalie Casati[2], Manuel Spuhler[2], Sami Perrin[2], Jeremie Frei[2], Philippe Ryvlin[1]

[1] Department of Clinical Neurosciences, Lausanne University Hospital (CHUV), Lausanne, Switzerland
[2] Biomedical Data Science Center, Lausanne University Hospital (CHUV), Lausanne, Switzerland

Abstract

Introduction
Epilepsy affects an estimated 50 million people worldwide, with approximately one-third resistant to medication. Understanding brain dynamics in drug-resistant epilepsy requires multimodal datasets — including intracranial EEG (iEEG), neuroimaging, and clinical information — that are scarce, fragmented, and difficult to share under strict privacy regulations. The Human Intracerebral EEG Platform (HIP) was developed to address these challenges by providing a secure, browser-based Trusted Research Environment (TRE) for data storage, curation, analysis, and controlled sharing.

HIP is now evolving into CHORUS.HIP, a next-generation, secure, and scalable environment powered by the CHORUS open-source TRE, supporting modern biomedical and AI-development.

Methods
Initially designed for iEEG data, the platform has since been expanded to support additional epilepsy data types such as MRI/CT neuroimaging, demographic variables, and biosignal data. Data are organized using the Brain Imaging Data Structure (BIDS/iEEG-BIDS) standard to enable harmonized and reproducible workflows. The platform currently provides two workspaces:

- Personal Space – for private uploading, storage, and analysis of pseudonymized data
- Collaborative Space – for sharing curated data with authorized partners on project-specific initiatives
- Public Space – for open data sharing is planned for future releases

Integrated applications like Anywave, Brainstorm, 3D Slicer and MRtrix3, enable signal processing, time-frequency analysis, co-registration of electrodes, and multimodal visualization.

Results
To date, 31 European centers and 2 U.S. centers have been onboarded and provided with HIP accounts, with most institutions currently in the testing and evaluation phase. Eight collaborative projects have been initiated on the platform, with one example here:

> Heartbeat and Sound Processing in Epilepsy – Using SEEG to investigate how interoceptive signals shape auditory perception during wakefulness and sleep. This is a collaborative project between Hospices Civils de Lyon (HCL), France and Lausanne University Hospital (CHUV), Switzerland.

These projects are establishing reproducible, multicenter workflows for integrating iEEG, imaging, and biosignal data within platform.

Discussion
CHORUS.HIP represents the next step in the evolution of HIP: a secure, flexible, and sustainable TRE deployment dedicated to neuroscience. Built on the CHORUS infrastructure (www.chorus-tre.ch), it provides greater scalability, expanded multimodal support, advanced governance, and improved collaborative capabilities.

As neuroscience datasets grow and AI becomes more central to research, CHORUS.HIP offers the robust technical and governance framework required for large-scale, privacy-preserving, multicenter epilepsy and iEEG research.

Figures
Figure 1. CHORUS platform.

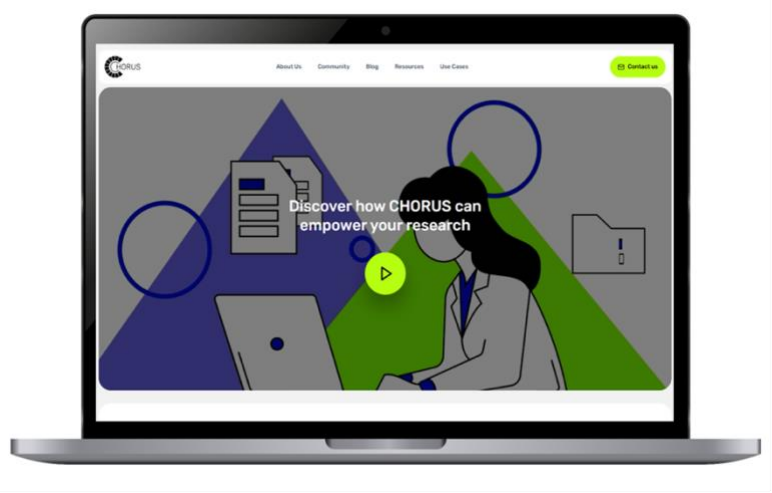

Figure 2. CHORUS.HIP in action. Using 3dSlicer and Brainstorm for data analysis.

References
1. CHORUS website: https://www.chorus-tre.ch
2. CHORUS demo: https://www.chorus-tre.ch

Keywords
iEEG, epilepsy, neuroimaging, SEEG, SUDEP, Trusted Research Environment, BIDS, CHORUS, data sharing, multicenter collaboration, AI development

Acknowledgments
This work was supported by the European Union's Horizon 2020 Research and Innovation Programme under grant agreement No. 945539 (Human Brain Project SGA3), the Horizon Europe Grant No. 101147319 (EBRAINS 2.0) and the Swiss State Secretariat for Education, Research and Innovation (SERI) under contract No. 23.00638 (EBRAINS 2.0).

53. N/A

54. Unveiling the Relationship Between Functional and Effective Connectivity through spontaneous sEEG and CCEPs

Alessandra Calcagno[1], Serena Valenzano[2,3,4], Marta Porro[3,5], Giulia Furregoni[2,3], Flavia Zauli[3,4], Ivana Sartori[4], Ezequiel Mikulan[6,$], Andrea Pigorini[1,$*]

[1]Department of Biomedical, Surgical and Dental Sciences, Università degli Studi di Milano, Milano, Italy
[2]School of Advanced Studies, Center of Neuroscience, University of Camerino, Camerino, Italy
[3]Department of Biomedical and Clinical Sciences "L. Sacco", Università degli Studi di Milano, Milano, Italy
[4]Center of Epilepsy Surgery "C. Munari", Niguarda Hospital, Milano, Italy
[5]Department of Philosophy "Piero Martinetti", Università degli Studi di Milano, Milano, Italy
[6]Department of Health Sciences, Università degli Studi di Milano, Milano, Italy

[$]equally contributing last authors
*andrea.pigorini@unimi.it

INTRODUCTION/MOTIVATION
Functional connectivity (FC) can be estimated through various methods and is increasingly used to investigate large-scale brain interactions in health and disease. Although functional links often mirror structural architecture [1], their precise relationship with structural connectivity and the unique information conveyed by FC remain unclear. Stereo-EEG (sEEG) provides direct access to brain activity, enabling the investigation of these dynamics at the cortical level. Cortico-cortical evoked potentials (CCEPs) offer a direct measure of effective connectivity and consistently align with structural pathways [2]. Comparing FC with CCEPs therefore represents a valuable approach to elucidate the specific contribution of FC.

METHODS
We analyzed sEEG recordings from 50 patients with intracranial electrodes. Resting-state functional connectivity was quantified using the Phase Locking Value (PLV) [3], while effective connectivity was derived from cortico-cortical evoked potentials (CCEPs). PLV was computed across Delta (1-4 Hz), Theta (4-8 Hz), Alpha (8-13 Hz), Beta (13-30 Hz), and Gamma (50-150 Hz) bands and compared with CCEPs. Moreover, to interpret results at the network level, electrodes were mapped onto the seven canonical Yeo functional networks [4]. Finally, we examined how phase relationships at rest across frequency bands relate to the CCEP responses elicited between the same electrode pairs.

RESULTS AND DISCUSSION
PLV revealed connectivity patterns that closely mirrored CCEPs across frequency bands (Fig. 1), and this similarity was preserved when electrodes were grouped into canonical networks. Crucially, the phase–CCEP relationship showed that electrode pairs with significant cortico-cortical interactions at rest were predominantly synchronized either in-phase (0°) or in anti-phase (180°) within the Delta and Theta bands. Moreover, CCEP amplitude increased as the resting-state phase difference approached 0° or 180°, indicating that stronger evoked responses are associated with near in-phase or anti-phase synchronization (Fig. 2).

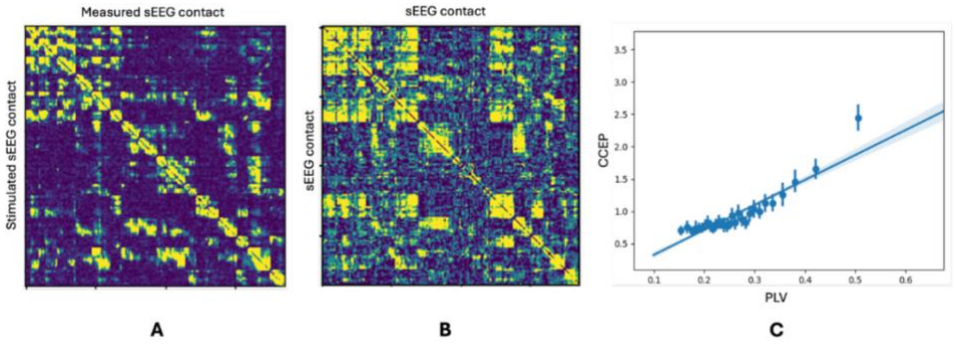

Fig. 1. Agreement between effective and functional connectivity in a single subject. (A) CCEP connectivity matrix. (B) PLV connectivity matrix in the Theta band. (C) Linear correlation between Theta-band PLV and CCEP amplitudes for electrode pairs separated by >2.5 cm.

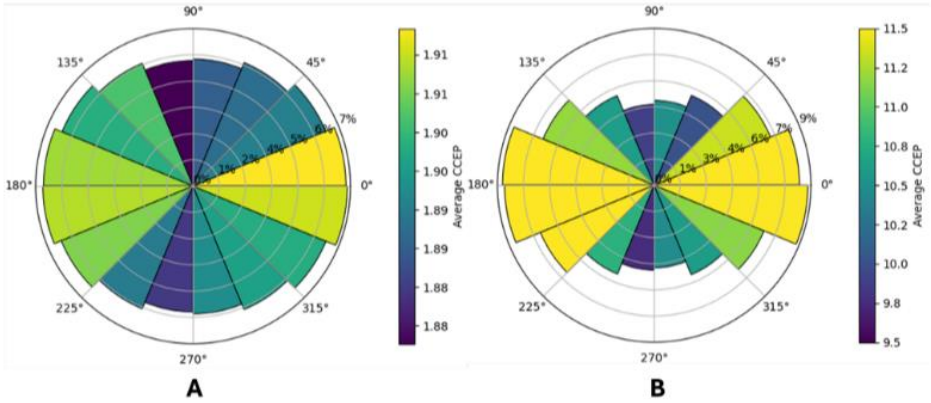

Fig. 2. Phase–CCEP relationship across the full cohort. (A) Distribution of resting-state phase differences for all electrode pairs (distance > 2.5 cm) showing no significant cortico-cortical connection. (B) Distribution of phase differences for electrode pairs (distance > 2.5 cm) with significant cortico-cortical connections. Color maps indicate the average CCEP amplitude within each phase bin.

These results may indicate that resting-state functional connectivity best approximates effective connectivity when zero-phase coupling is accounted for. A possible interpretation is that cortico-cortical connected regions mainly engage in-phase communication during spontaneous activity at rest. Future directions include testing whether task-related conditions reveal distinct, frequency-specific functional interactions beyond those observed at rest. Finally, a similar framework could be applied to pathological conditions to test whether similar phase/ FC–CCEP relationships are preserved or altered.

Keywords: functional connectivity, effective connectivity, sEEG

REFERENCES

[1] Honey CJ, Sporns O, Cammoun L, et al. Predicting human resting-state functional connectivity from structural connectivity. Proc Natl Acad Sci U S A. 2009;106(6):2035-2040. doi:10.1073/pnas.0811168106.
[2] Keller CJ, Bickel S, Honey CJ, et al. Intrinsic functional architecture predicts electrically evoked responses in the human brain. Proc Natl Acad Sci U S A. 2014;111(36): E4678-E4687. doi:10.1073/pnas.1019750108

[3] J.-P. Lachaux, E. Rodriguez, J. Martinerie, F. J. Varela, Measuring phase synchrony in brain signals, Human Brain Mapping, 8(4), 194–208, 1999. doi:10.1002/(SICI)1097-0193(1999)8:4<194::AID-HBM4>3.0.CO;2-C
[4] Yeo BT, Krienen FM, Sepulcre J, et al. The organization of the human cerebral cortex estimated by intrinsic functional connectivity. J Neurophysiol. 2011;106(3):1125-1165. doi:10.1152/jn.00338.2011

55. A modular, end-to-end framework for modelling neural state-spaces and deriving interpretable descriptors of whole-brain dynamics

Julian Kędys[1*], Cezary Mazurek[1]
[1]Department of Digital Medicine, Poznan Supercomputing and Networking Center, Polish Academy of Sciences, Poznan, Poland
* jkedys@man.poznan.pl

INTRODUCTION/MOTIVATION
Understanding distributed brain function and complex neurodevelopmental phenotypes demands tools that model population-level neural state-spaces with precision, interpretability, and cross-subject comparability. We present a standalone, modular pipeline that meets these needs by combining energy-landscape analysis[1,2] (ELA) and phase-diagram analysis[3,4] (PDA) with a full stack of “ELA-secure” preprocessing, multi-subject alignment/dimensionality reduction, and population-aware summarisation—each stage usable independently or as an end-to-end workflow. The pipeline exposes all internal choices, supports parameter sweeps and automatic, data-driven optimisation, and is engineered for numerical stability and parallel/HPC execution.

METHODS
Backbone methods: Neural dynamics are modelled with Ising/Pairwise Maximum Entropy Model[5] (PMEM) estimators (exact/pseudo-likelihood[6]/variational Bayes), yielding landscapes, disconnectivity graphs, basin structure, and kinetic descriptors (MFPTs, committor fields, relaxation spectra). We provide fast QC via null-simulation thresholds on moment-matching errors, and Numba-accelerated MCMC for transition analyses and rich visualisations (e.g., basin timecourses).

ELA-secure preprocessing and imputation: The toolkit includes adaptive despiking, IQR-based outlier repair with local percentile replacements, linear/polynomial/moving-average detrending, and population-universal detrending via an automatically selected LOESS/linear/quadratic model that promotes residual stationarity—guarding against landscape distortions. We also implement guarded concatenation of recording sessions with similarity checks, alignment, and optional final QC. Neuro-aware imputation and audited binarisation ensure downstream PMEM fits remain valid and comparable across subjects/runs.
Multi-subject alignment and dimensionality reduction: We provide Shared Response Model[7] (SRM), Multiset Canonical Correlation Analysis[8] (MCCA), group PCA/ICA[9], and a consensus option that aligns component spaces (Hungarian + neuro-Procrustes), evaluates cross-subject consistency and RSA/Procrustes metrics, and reports explained variance—delivering shared, low-dimensional latents while preserving subject-specific features. These latents feed directly into ELA/PDA, enabling population-level comparisons of regimes.

RESULTS AND DISCUSSION
Scope and applicability: The pipeline accepts any modality with meaningfully binarisable dynamics (rows=ROIs, columns=time), supports resting-state or task data, and scales to whole-brain recordings. It was developed and tested on resting-state fUS from eight cre-lox mouse lines (one

control, seven ASD models across four symptomatic subtypes), but the submission is method/tool-oriented and modality-agnostic.

Impact and contributions: By delivering transparent, reproducible, and population-comparable landscape descriptors—together with open, modular building blocks for preprocessing, alignment, inference, kinetics, and visualisation—this framework advances cross-subject, cross-modal neuroscience and is EBRAINS-ready for large datasets and HPC workflows. It directly supports open-science reuse and method benchmarking while enabling rigorous, interpretable comparisons of brain-dynamics regimes across subjects, conditions, and tasks. >

Keywords: Brain dynamics, Neural state-spaces, Multi-subject, Comparability, Whole-brain, Ising, Criticality, Phase transitions

REFERENCES

[1] Masuda N., Islam S., Aung S. T., Watanabe T. Energy landscape analysis based on the Ising model: Tutorial review. PLOS Complex Systems (2025) [https://doi.org/10.1371/journal.pcsy.0000039]
[2] Watanabe T. et al. Energy landscapes of resting-state brain networks. Frontiers in Neuroinformatics (2014) [https://doi.org/10.3389/fninf.2014.00012]
[3] Ezaki T. et al. Closer to critical resting-state neural dynamics in individuals with higher fluid intelligence. Communications Biology (2020) [https://doi.org/10.1038/s42003-020-0774-y]
[4] Sherrington D., Kirkpatrick S. Solvable model of a spin glass. Phys. Rev. Lett. (1975) [https://doi.org/10.1103/PhysRevLett.35.1792]
[5] Schneidman E. et al. Weak pairwise correlations imply strongly correlated network states in a neural population. Nature (2006) [https://doi.org/10.1038/nature04701]
[6] Ravikumar P., Wainwright M., Lafferty J. High-dimensional Ising model selection using ℓ1-regularized logistic regression. Ann. Stat. (2010) [https://doi.org/10.48550/arXiv.1010.0311
[7] Chen P.-H. C. et al. A reduced-dimension fMRI shared response model. NeurIPS (2015) [https://proceedings.neurips.cc/paper_files/paper/2015/file/b3967a0e938dc2a6340e258630febd5a-Paper.pdf]
[8] Correa N. M. et al. Multi-set canonical correlation analysis for the fusion of concurrent single-trial ERP and fMRI. NeuroImage (2010) [https://doi.org/10.1016/j.neuroimage.2010.01.062]
[9] Calhoun V. D., Adali T., Pearlson G. D., Pekar J. J. A method for making group inferences from functional MRI data using independent component analysis. Hum. Brain Mapp. (2001) [https://doi.org/10.1002/hbm.1048]

56. BraVa: Integration of brain vasculature into the EBRAINS Human Brain Atlas

Nerea González[1], Xabier Urra[2], Emma Muñoz-Moreno[1]*
[1]MRI Core Facility, Institut d'Investigacions Biomèdiques August Pi i Sunyer (IDIBAPS), Barcelona, Spain

INTRODUCTION/MOTIVATION

Neurovascular disease is a significant cause of death and disability, related to alterations of the vasculature supplying or within the brain [1]. Therefore, the characterization of brain vascular morphology associated with disease is essential to understand the underlying pathological mechanisms. Likewise, vasculature is related to brain function and structure, being angiogenesis and neurogenesis closely related [2]. However, while several brain atlases provide detailed information about anatomy and function, only some have described vascular architecture [3, 4], and they are based on small cohorts of healthy population.

In this abstract, we introduce the BraVa project (Brain vasculature diversity underlying vascular disease: integrating vascular architecture into the EBRAINS Human Brain Atlas), funded by the EBRAINS 2.0 Open Call. It aims to generate group-wise probabilistic maps of brain vascular architecture, associated with specific diagnostic features. Likewise, models of 3D reconstructions of the vasculature for each category will be provided in a reference space. This will represent a beneficial tool for neurovascular research, encouraging the implementation of more realistic blood flow computational models, essential to simulate disease and treatment effects.

METHODS

The project is based on a database of 4000 patients with a suspected stroke that arrive at the Hospital Clinic of Barcelona (HCB). Each patient underwent a computed tomography (CT) scan at admission (including both anatomical and angiography images). Besides, about 40% of the cases were also scanned during the first week using magnetic resonance imaging (MRI), also including anatomical (T1-weighted) and angiography image (time-of-flight acquisition). Together with the images, clinical and demographic data was compiled, that will be used to obtain group-specific patterns of vasculature.

CT and CT angiography (CTA) consists of sagittal, axial and coronal acquisitions, that are combined to obtain a higher resolution 3D image, using SVRTK [5]. Both MRA and the 3D reconstructed CTA are processed to automatically segment vasculature. An automatic thresholding method based on maximum entropy has been applied, although further improvements will be developed to capture more detailed vasculature.

To obtain the probabilistic model, images are registered into the EBRAINS Human Brain Atlas template. For that, elastic diffeomorphic registration was performed between patient MR images and the template was applied using ANTs Registration toolkit [6]. ANTs was also applied to perform intra-patient affine registration to ensure inter-modality matching. The estimated transformations are applied to the vessel segmentation on the corresponding modality, so they are aligned with the template. Thus, at each voxel of the template, the probability of the presence of a vessel can be easily determined.

RESULTS AND DISCUSSION

A pipeline to create a probabilistic atlas of the brain vasculature has been developed. It has been tested in a small subset of the dataset that will be further analysed to characterize the variability of the vasculature under different conditions. A scheme of the pipeline can be shown in figure 1. A key step of the atlas development is the segmentation of vasculature in either CTA or MRA. In Figure 2, an example of 3D visualization of the resulting vascular tree obtained after segmentation is shown.

The developed pipeline will be applied to the whole dataset, and groupwise average performed to obtain group-wise probabilistic maps of vasculature. Such generated data will be integrated into the EBRAINS Human Brain Atlas to make them available to the community. The atlas could contribute to a better understanding of changes occurring during a neurovascular accident, providing a set of morphological architecture maps for specific diagnostic features.

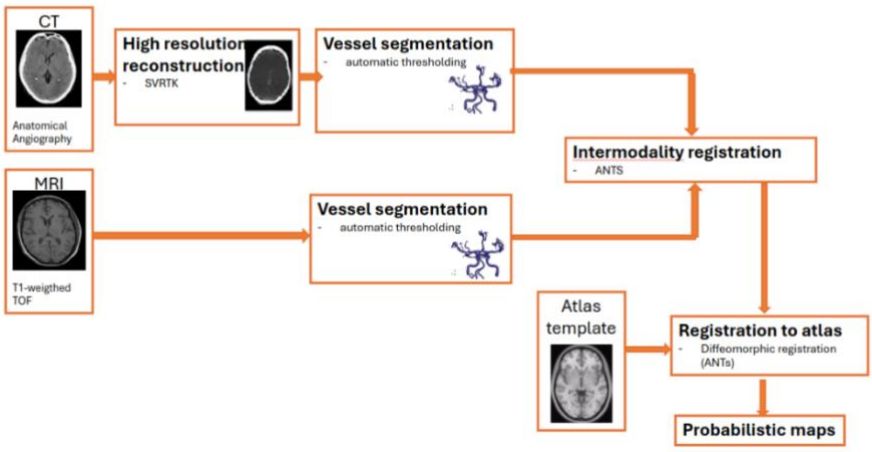

Figure 1. Processing pipeline scheme for a patient. After registration to atlas template of the patients in the dataset, group-wise averaging will be performed to obtain probabilistic maps of vasculature.

Figure 2. 3D reconstruction of the vascular tree after vessel segmentation.

Keywords: Brain atlases, Neurovascular morphology, Angiography, Stroke, Magnetic Resonance Imaging, Computed Tomography, EBRAINs Human Brain atlas

ACKNOWLEDGEMENTS
This work is funded by the EBRAINS 2.0 Open Call.

REFERENCES
[1] Feigin VL, et al. Global, regional, and national burden of stroke and its risk factors, 1990–2019: a systematic analysis for the Global Burden of Disease Study 2019. Lancet Neurology 2021; 20: 795–820. doi: 10.1016/S1474-4422(21)00252-0
[2] Crouch EE, et al. Disentangling brain vasculature in neurogenesis and neurodegeneration using single-cell transcriptomics. Trends Neurosci. 2023 Jul;46(7):551-565. doi:10.1016/j.tins.2023.04.007
[3|Bernier M, et al. The morphology of the human cerebrovascular system. Hum Brain Mapp. 2018; 39(12):4962-4975. doi: 10.1002/hbm.24337
[4] Viviani R. A Digital Atlas of Middle to Large Brain Vessels and Their Relation to Cortical and Subcortical Structures. Front Neuroanat. 2016; 10:12. doi: 10.3389/fnana.2016.00012
[5] Kuklisova-Murgasova M, et al. Reconstruction of fetal brain MRI with intensity matching and complete outlier removal. Med Image Anal. 2012;16(8):1550-64. doi: 10.1016/j.media.2012.07.004.

[6] Avants BB, et al. Symmetric diffeomorphic image registration with cross-correlation: evaluating automated labeling of elderly and neurodegenerative brain. Med Image Anal. 2008;12(1):26-41. doi:10.1016/j.media.2007.06.004…

57. Cerebellar compensation breakdown underlying deep nuclei overdrive in schizophrenia

Alberto A Vergani[1,2,*], Pawan Faris[1], Marialaura De Grazia[1], Claudia Casellato[1], Egidio U D'Angelo[1,3]

[1]Department of Brain and Behavioral Sciences, University of Pavia, Pavia, Italy
[2]Sant'Anna School of Advanced Studies, Institute of BioRobotics and Department of Excellence in Robotics and AI, Pisa, Italy
[3]Digital Neuroscience Center, IRCCS Mondino Foundation, Pavia, Italy
Email: *albertoarturo.vergani@unipv.it

Keywords: Schizophrenia, Cerebellar Reserve, Purkinje Cells, Deep Cerebellar Nuclei, Computational Modeling, Digital Physiology

Objectives
Schizophrenia (SZ) affects approximately 1% of the global population and has been associated with cortical, subcortical, and cerebellar dysfunctions, particularly impacting cognitive-affective processes (McCutcheon, Reis Marques, et al., 2020). An emerging hypothesis suggested that SZ is a glutamatergic synaptopathy (Coyle, 2006; McCutcheon, Krystal, et al., 2020) extending to cerebellar circuits and contributing to "cognitive dysmetria" effects (Andreasen et al., 1998; Argyropoulos et al., 2020), ultimately interacting with cerebellar reserve (Herrero et al., 2020; Mitoma et al., 2020). Building on these observations, we computationally investigated baseline network dynamics in a cerebellar model embedded with structural alterations typical of SZ.

Material and Methods
We developed a digital cerebellum model to simulate the continuum of SZ-associated neurodegeneration, ranging from healthy (0% atrophy) to severe impairment (40% atrophy). To this aim, we implemented the schizophrenia atrophy algorithm (SZA, Figure 1), which systematically applied structural alterations at synaptic, cellular, and network levels from a canonical cerebellar model by using Brain Scaffold Builder framework (BSB) (De Schepper et al., 2022). The SZA progressively induced morphological shrinkage, dendritic pruning, and radius reduction, while at the network level neuronal density and cortical thickness declined. These alterations were quantified through measures of cell complexity and network connectivity. In line with the glutamatergic hypothesis in SZ, excitatory synaptic weights were selectively reduced, whereas inhibitory synapses were preserved. Moreover, the algorithm integrated the cerebellar reserve, modeled via differential resilience profiles (high vs low) defined by probability-of-cell-life curves given SZ degeneration. We translated these alterations in a spiking neural network and simulated it in NEST under baseline conditions.

Results
This analysis quantified firing rate alterations across cerebellar populations along the SZ continuum (Figure 2). In high resilience, granule cells and Golgi cells showed a more gradual decline, whereas in low resilience they dropped earlier and more steeply. Molecular layer interneurons exhibited a gradual reduction in high resilience, while in low resilience their activity persisted abnormally. We then focused on Purkinje cells (PCs) and deep cerebellar nuclei projection neurons (DCN-P), as their interaction critically determined network output. In high resilience, PCs displayed a transient compensatory increase before declining, buffering DCN-P and generating a silent zone where output

remained indistinguishable from healthy up to ~30% SZ Factor. In low resilience, by contrast, PCs were suppressed from the earliest stages, leading to premature DCN-P overdrive already at ~5% SZ Factor. Crucially, the ΔFR DCN-P vs PC relationship revealed that a 1 Hz change in PC firing translated into a highly non-linear amplification in DCN output, with gains of ~1:6 in high resilience and ~1:16 in low resilience, demonstrating that cerebellar reserve not only delayed pathology but also modulated its amplification.

Discussion

The emergence of PC-DCN imbalance and consequent DCN overdrive offered a plausible mechanism for the abnormally high functional connectivity to the midbrain that had recently been reported in SZ patients (Faris et al., 2024). These findings highlighted that the progressive breakdown of cerebellar reserve could accelerate the shift from compensatory to dysfunctional network states. Beyond the baseline condition, we envisioned cerebellar stimulation incorporating sensory-driven stimulation paradigms, thereby probing cognitive dysmetria (Myles et al., 2017). Studies are planned to validate computational scenarios by fitting them against recorded activity from multielectrode arrays in SZ mouse models.

Acknowledgements

Work supported by #NEXTGENERATIONEU (NGEU) and funded by the Ministry of University and Research (MUR), National Recovery and Resilience Plan (NRRP), project MNESYS (PE0000006) – A Multiscale integrated approach to the study of the nervous system in health and disease (DN. 1553 11.10.2022). The Virtual Brain Twin Project has received funding from the European Union's Research and Innovation Program Horizon Europe under grant agreement No 101137289.

References

Andreasen, N. C., Paradiso, S., & O'Leary, D. S. (1998). «Cognitive dysmetria» as an integrative theory of schizophrenia: A dysfunction in cortical-subcortical-cerebellar circuitry? Schizophrenia Bulletin, 24(2), 203–218. https://doi.org/10.1093/oxfordjournals.schbul.a033321

Argyropoulos, G. P. D., van Dun, K., Adamaszek, M., Leggio, M., Manto, M., Masciullo, M., Molinari, M., Stoodley, C. J., Van Overwalle, F., Ivry, R. B., & Schmahmann, J. D. (2020). The Cerebellar Cognitive Affective/Schmahmann Syndrome: A Task Force Paper. Cerebellum (London, England), 19(1), 102–125. https://doi.org/10.1007/s12311-019-01068-8

Coyle, J. T. (2006). Glutamate and Schizophrenia: Beyond the Dopamine Hypothesis. Cellular and Molecular Neurobiology, 26(4), 363–382. https://doi.org/10.1007/s10571-006-9062-8

De Schepper, R., Geminiani, A., Masoli, S., Rizza, M. F., Antonietti, A., Casellato, C., & D'Angelo, E. (2022). Model simulations unveil the structure-function-dynamics relationship of the cerebellar cortical microcircuit. Communications Biology, 5(1), 1–19. https://doi.org/10.1038/s42003-022-04213-y

Faris, P., Pischedda, D., Palesi, F., & D'Angelo, E. (2024). New clues for the role of cerebellum in schizophrenia and the associated cognitive impairment. Frontiers in Cellular Neuroscience, 18. https://doi.org/10.3389/fncel.2024.1386583

Herrero, P., Contador, I., Stern, Y., Fernández-Calvo, B., Sánchez, A., & Ramos, F. (2020). Influence of cognitive reserve in schizophrenia: A systematic review. Neuroscience & Biobehavioral Reviews, 108, 149–159. https://doi.org/10.1016/j.neubiorev.2019.10.019

McCutcheon, R. A., Krystal, J. H., & Howes, O. D. (2020). Dopamine and glutamate in schizophrenia: Biology, symptoms and treatment. World Psychiatry, 19(1), 15–33. https://doi.org/10.1002/wps.20693

McCutcheon, R. A., Reis Marques, T., & Howes, O. D. (2020). Schizophrenia—An Overview. JAMA Psychiatry, 77(2), 201–210. https://doi.org/10.1001/jamapsychiatry.2019.3360

Mitoma, H., Buffo, A., Gelfo, F., Guell, X., Fucà, E., Kakei, S., Lee, J., Manto, M., Petrosini, L., Shaikh, A. G., & Schmahmann, J. D. (2020). Consensus Paper. Cerebellar Reserve: From Cerebellar Physiology to Cerebellar Disorders. The Cerebellum, 19(1), 131–153. https://doi.org/10.1007/s12311-019-01091-9

Myles, J. B., Rossell, S. L., Phillipou, A., Thomas, E., & Gurvich, C. (2017). Insights to the schizophrenia continuum: A systematic review of saccadic eye movements in schizotypy and biological relatives of schizophrenia patients. Neuroscience and Biobehavioral Reviews, 72, 278–300. https://doi.org/10.1016/j.neubiorev.2016.10.034

58. Building discoverability for clinical data: the EBRAINS ecosystem for sharing sensitive data

Eszter A. Papp[1*], Sophia Pieschnik[1], Geneviève Richard[1], Archana Golla[1], Signý Benediktsdóttir[1,2], Naz Karadag[1], Lyuba Zehl[2], Birgit Schaffhauser[3], Michael Schirner[4], Petra Ritter[4], Ainar Drews[5], Trygve B. Leergaard[1], Jan G. Bjaalie[1]

[1] Institute of Basic Medical Sciences, University of Oslo, Norway
[2] EBRAINS AISBL, Brussels, Belgium
[3] Lausanne University Hospital, CHUV, Switzerland
[4] Berlin Institute of Health at Charité – Universitätsmedizin Berlin, Germany
[5] Research Platforms, IT Department, University of Oslo, Norway
*e.a.papp@medisin.uio.no

INTRODUCTION/MOTIVATION
Brain disorders and associated care costs represent a major societal challenge in Europe and worldwide. To build a better understanding of the brain in health and disease, research data from healthy human subjects, patients, and their digital twins need to be shared on a large scale, across multiple areas of neuroscience, and beyond national borders. Such collaborative efforts require well-annotated research data that are findable, accessible, interoperable, and reusable [1]. In addition, special considerations must be taken to safeguard sensitive human data and metadata in compliance with the GDPR.

METHODS
The EBRAINS 2.0 project has built a data sharing ecosystem to support collaborative research on sensitive data collected from human subjects. Together with partners of the eBRAIN-Health project, we have conducted a pilot involving several research groups with clinical data stored in different repositories for sensitive data, to build a standardized representation of anonymous metadata, and make these discoverable on EBRAINS. Metadata provided by each partner have been curated following the EBRAINS curation workflow [2] streamlined for clinical data based on the needs of data owners and researchers interested in reusing the data.

RESULTS AND DISCUSSION
We have curated and published 12 new dataset versions and one new software submission from eBRAIN-Health via the EBRAINS Knowledge Graph [3, RRID:SCR_017612]. During the metadata curation process, we have built openMINDS [RRID:SCR_023173] metadata representations that are

harmonized across datasets, clarified legal responsibilities, extended our documentation, and implemented new technical solutions to better adapt the curation workflow to sharing of clinical data.

To promote research collaborations that reuse GDPR-sensitive datasets discoverable via EBRAINS, the project has established a network of Trusted Research Environments [4] that offer secure data sharing and processing options, and data protection by design and by default. The Health Data Cloud [5], the Medical Informatics Platform, the Human Intracerebral EEG Platform, and the TSD Services for Sensitive Data provide services and resources for analyzing a variety of data types and modalities in a secure environment. As a part of their data sharing journey through EBRAINS, we guide researchers interested in sharing clinical data to these platforms to ensure compliance with regulatory requirements.

Keywords: sensitive data, human data, GDPR, data sharing, trusted research environment

ACKNOWLEDGEMENTS
This project has received funding from the European Union's Horizon Europe research and innovation programme under grant agreement No. 101058516 (eBRAIN-Health) and No. 101147319 (EBRAINS 2.0), and from the University of Oslo (SHAREbrain Hub/Node).

REFERENCES
[1] Wilkinson, M., Dumontier, M., Aalbersberg, I. et al. The FAIR Guiding Principles for scientific data management and stewardship. Sci Data 3, 160018 (2016). https://doi.org/10.1038/sdata.2016.18
[2] https://wiki.ebrains.eu/bin/view/Collabs/data-curation
[3|https://search.kg.ebrains.eu/?category=Dataset&keywords[0]=eBRAIN-Health
[4] https://wiki.ebrains.eu/bin/view/Collabs/trusted-research-environments
[5] https://www.healthdatacloud.eu/

59. Towards MEBRAINS, a Multilevel Macaque Brain Atlas

***Giacometti C**[1,2], Niu M[2], Rapan L[1,2], Nora Eilis Fitzgerald[3,4], Qi Zhu[3,5], Vanduffel W[3,4], Palomero-Gallagher N[1,2]*

[1] Cécile & Oskar Vogt Institute of Brain Research, Medical Faculty and University Hospital Düsseldorf, Heinrich Heine University Düsseldorf, Germany.
[2] Institute of Neuroscience and Medicine (INM-1), Research Centre Jülich, Jülich, Germany.
[3] Dept. of Neurosciences, Lab. For Neuro-and Psychophysiology, KU Leuven, Leuven, Belgium
[4] Leuven Brain Institute, KU Leuven, Leuven, Belgium
[5] Cognitive Neuroimaging Unit, INSERM, CEA, Université Paris-Saclay, NeuroSpin Center, Gif/Yvette, France

Introduction

Understanding the full organizational complexity of the brain requires an integrative approach that bridges multiple modalities (molecular, structural, and functional)[1]. Such integration enables a more comprehensive characterization of brain architecture, providing critical insights into the anatomical foundation that underlies functional specialization. Yet, the majority of atlases present in the literature remain confined to a single modality, limiting their ability to capture the multidimensional nature of brain organization[1].

Animal models are essential in neuroscience because they enable experimental approaches impossible in humans. The macaque's close evolutionary and cortical similarity to humans make it an ideal bridge species. A detailed brain atlas will provide the critical reference needed for robust cross-species comparisons and interpretation of experimental findings.

We present the first macaque brain atlas that integrate cyto-, myelo-, receptor-architecture and retinotopic parcellations. This multimodal framework enables the detection of previously unresolved cortical boundaries[2] and, importantly, provides a refined areal parcellation of the macaque brain.

Methods

The brains of 3 male Macaca fascicularis were deep-frozen and sectioned into coronal slices of 20µm thickness. Alternating sections were incubated with tritiated ligands for receptor visualization, or stained for cell bodies or myelin. After digitization and color-coding of the receptor autoradiographs, we obtained a brain-wide visual representation of the areal and laminar distribution of cell bodies, myelin, and 15 different receptors[3]. These modalities were used to identify the borders between cortical areas which were statistically validated by an observer-independent method[3]. Each of the identified areas was then manually drawn on the MEBRAINS template[4] to create a parcellated 3D volume. Additionally, retinotopic maps[5] have been integrated into the MEBRAINS atlas. They were created as surface flat maps and then both transformed and registered to fit inside the MEBRAINS template volume.

Results

The atlas populates the MEBRAINS template[4] and currently incorporates previously published cyto- and receptor architectonically informed maps[6–9] (Figure 1.A), as well as retinotopic data[5] (Figure 1.B). To date, maps of 105 architectonically distinct cortical areas of the occipital, parietal, and frontal lobes have been completed. In addition, six ongoing projects are focused on the cingulate cortex (28 areas), temporal lobe (52 areas), insular lobe (23 areas), hippocampal, entorhinal cortices, basal ganglia, striatum and claustrum.

Discussion

The aim for this atlas is to become a reference for integrative, comparative and clinical neurosciences.

The MEBRAINS Atlas will serve as a crucial resource for advancing integrative neurosciences, aiming to resolve the microscopic-macroscopic gap in brain organization by providing high-quality anatomical data[6–9], including information of cortical and subcortical receptor densities. This offers novel opportunities for neuroimaging researchers to integrate molecular underpinnings of functional activity observed in-vivo[10].

Plus, the refined parcellation of the macaque brain will provide a more efficient structure for detailed comparative analyses with the human brain. Its purpose is to facilitate studies that aim to identify corresponding areas in macaques and humans based on their unique multimodal fingerprints.

Finally, building a precise atlas of animal models is critical for clinical studies. The MEBRAINS atlas will provide new support for the identification and testing of novel therapeutic targets; and, in association with comparative studies, it will enable the effective translation of such interventions to humans.

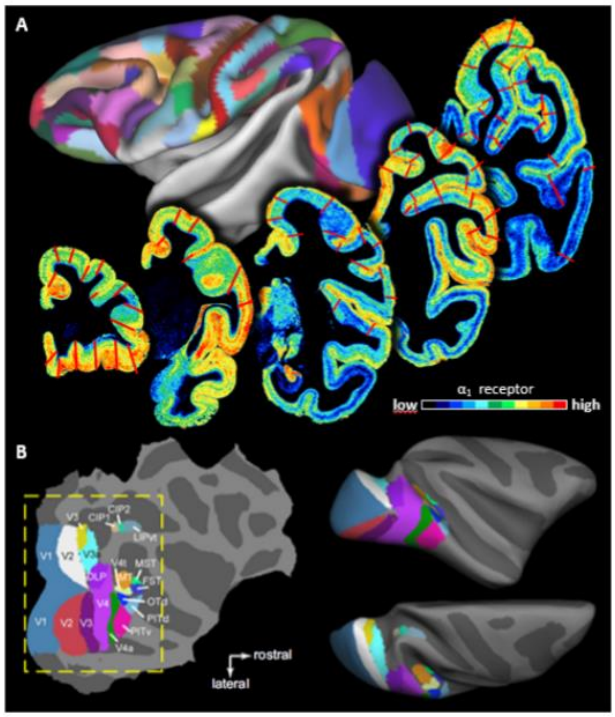

Figure 1. **MEBRAINS atlas areal population.** (A) 3D surface atlas representation of 105 cortical areas. As an example, five coronal sections of the α1 receptor distribution are shown along the anterior-posterior axis. (B). Retinotopic maps extracted5 represented as a surface flat map (left) have been transformed to fit into MEBRAINS 3D volume space (right).

References:

1. Mars RB, Jbabdi S, Rushworth MFS. A Common Space Approach to Comparative Neuroscience. Annu Rev Neurosci. 2021;44(1):69-86. doi:10.1146/annurev-neuro-100220-025942
2. George Paxinos, Petrides, Michael, Xu-Feng Huang, Arthur W. Toga. The Rhesus Monkey Brain in Stereotaxic Coordinates.; 2008. Accessed August 8, 2025. https://shop.elsevier.com/books/the- rhesus-monkey-brain-in-stereotaxic-coordinates/paxinos/978-0-12-373619-2
3. Palomero-Gallagher N, Zilles K. Cyto- and receptor architectonic mapping of the human brain. Handb Clin Neurol. 2018;150:355-387. doi:10.1016/B978-0-444-63639-3.00024-4
4. Balan PF, Zhu Q, Li X, et al. MEBRAINS 1.0: A new population-based macaque atlas. Imaging Neurosci. 2024;2:1-26. doi:10.1162/imag_a_00077
5. Arcaro MJ, Livingstone MS. On the relationship between maps and domains in inferotemporal cortex. Nat Rev Neurosci. 2021;22(9):573-583. doi:10.1038/s41583-021-00490-4
6. Niu M, Impieri D, Rapan L, Funck T, Palomero-Gallagher N, Zilles K. Receptor-driven, multimodal mapping of cortical areas in the macaque monkey intraparietal sulcus. eLife. 2020;9:e55979. doi:10.7554/eLife.55979
7. Niu M, Rapan L, Funck T, et al. Organization of the macaque monkey inferior parietal lobule based on multimodal receptor architectonics. NeuroImage. 2021;231:117843. doi:10.1016/j.neuroimage.2021.117843
8. Rapan L, Froudist-Walsh S, Niu M, et al. Multimodal 3D atlas of the macaque monkey motor and premotor cortex. NeuroImage. 2021;226:117574. doi:10.1016/j.neuroimage.2020.117574
9. Rapan L, Froudist-Walsh S, Niu M, et al. Cytoarchitectonic, receptor distribution and functional connectivity analyses of the macaque frontal lobe. eLife. 2023;12:e82850. doi:10.7554/eLife.82850

10. Froudist-Walsh S, Xu T, Niu M, et al. Gradients of neurotransmitter receptor expression in the macaque cortex. Nat Neurosci. 2023;26(7):1281-1294. doi:10.1038/s41593-023-01351-2

Key words: macaque, brain, atlas, multimodal, receptors, cytoarchitecture, myeloarchitecture, retinotopy

Acknowledgements
This project has received funding from the European Union's Horizon 2020 Research and Innovation Programme under the Specific Grant Agreement 945539 (Human Brain Project SGA3, from the European Union's Horizon Europe Programme under the Specific Grant Agreement No. 101147319 (EBRAINS 2.0 Project), from the Federal Ministry of Education and Research (BMBF) under project number 01GQ1902 and from the Helmholtz Association's Initiative and Networking Fund through the Helmholtz International BigBrain Analytics and Learning Laboratory (HIBALL) under the Helmholtz International Lab grant agreement InterLabs-0015.

60. Atrophy Network Mapping Across Tauopathies: Convergent Networks but Limited Diagnostic Utility

Silvia Saglia[1,†], Emma Maria Sole Tosato[2,†], Lorenzo Pini[2,3], Giorgio Dolci [1,4], Lorenza Brusini[1], Chiara Tuzzato[5], Ilaria Boscolo Galazzo[1,*], **Gloria Menegaz[1,*]**

1: Department of Engineering for Innovation Medicine, University of Verona, 37134 Verona, Italy;
2: Padova Neuroscience Center, University of di Padova, 35121 Padova, Italy;
3: Department of Neuroscience, University of Padova, 35121 Padova, Italy;
4: Department of Computer Science, University of Verona, 37134 Verona, Italy
5: Department of General Psychology, University of Padova 35129, Italy;
†: The authors contributed equally to this work.
*: The authors jointly supervised this work.

Keywords: tauopathy, Alzheimer's disease, corticobasal syndrome, progressive supranuclear palsy, functional connectivity, machine learning, transdiagnostic biomarkers, precision medicine

Introduction
Tauopathies such as Alzheimer's disease (AD), corticobasal syndrome (CBS), and progressive supranuclear palsy (PSP) share abnormal tau levels but differ clinically/anatomically, with overlap and co-pathology complicating diagnosis[1-3]. Misfolded tau propagates along functional/structural connections[4-6] and tau-driven neuronal loss produces grey matter (GM) atrophy that reflects both local vulnerability and network-mediated spread. By projecting patient atrophy onto a normative resting-state connectome, atrophy network mapping (ANM) infers the functional networks (FNs) implicated by the structural damage. Such indirect connectivity mapping has been used to capture specific neuropsychological and neuropsychiatric symptoms[7-9]. We applied ANM in AD, CBS, and PSP patients to test whether it can be used for classifying individuals across tauopathies, holding potential as biomarkers, and capturing disease severity.

Methods
234 participants from the ADNI and the 4RTNI database were selected: 58 cognitively normal (CN 71±8 years [yrs], 67% female [F]), 72 AD (74±9 yrs, 51% F), 44 CBS (67±7 yrs, 52% F), and 60 PSP (71±8 yrs, 58% F). T1-weighted scans were processed using SPM12 following the VBM pipeline[10] for extracting individual normalized GM maps: segmentation, study-specific geodesic SHOOT template, MNI normalization with jacobian modulation, 5-mm FWHM smoothing. GM atrophy was quantified with W-score maps (Z-scores adjusted for covariates). In CN, we fit linear models on GM maps (GM

~ age + sex + education) to obtain, for each voxel, the expected GM for a given demographic profile and the residual SD, and by applying the CN β-weights to each patient's demographics, we derived the expected GM. For each patient, we computed W = expected GM − observed GM) / SD, then thresholded W>2 to define the individual atrophy mask. To generate ANM maps, each mask was first seeded into a normative resting-state functional connectome (Human Connectome Project, n=173, 7T), and the resulting seed-based whole-brain correlations Fisher z- transformed and averaged across HCP to yield a single ANM map per patient. We derived two sets of ANM features: (i) atlas-based FNs summaries averaged within the Yeo 7 cortical parcellation and a subcortical composite, (ii) voxelwise z-maps. Atlas-level features entered a Random Forest (RF) classifier, while a 3D DenseNet was applied to ANM maps for performing binary classifications. Clinical associations were tested with OLS models of CDR-SB and MMSE (covariates: age, sex, education). Voxelwise inference used FSL randomise (5,000 permutations; TFCE), additionally controlling for atrophy-seed size.

Results

ANM reduced heterogeneous atrophy into convergent temporo-occipital/fronto-parietal FN, yet diagnostic separation remained limited. Atlas-based RF yielded modest pairwise performance: AD–CBS (accuracy [ACC]=.63; F1=.56), AD–PSP (ACC=.62; F1=.61), PSP–CBS (ACC=.52 F1=.51). The 3D CNN on voxelwise ANM maps performed similarly or worse: AD–CBS (ACC=.60; F1=.47), AD–PSP (ACC=.47; F1=.36), PSP–CBS (ACC=.56; F1=.67). Clinical associations were significant ($p<.001$) but low, with atlas-based metrics explaining CDR with $R^2=.270$ and MMSE $R^2=.281$. Voxelwise regression localized severity-related connectivity to bilateral ventro and dorsomedial and right dorsolateral prefrontal cortex, thalamus/striatum, and bilateral cerebellum.

Discussion

ANM aligns heterogeneous atrophy with shared FNs, but this convergence across clinical groups limits diagnostic separability. Neither atlas-based RF nor voxelwise CNN achieved robust discrimination. Clinical associations were significant yet explained modest variance, indicating limited standalone prognostic utility. ANM is therefore best positioned as a transdiagnostic scaffold linking structural damage to FNs dysfunction. Improved stratification will likely require integrating ANM with molecular biomarkers, subject-specific connectomes, and longitudinal data.

Acknowledgments:

This study was in part funded by FSE project ANTIAGING: "Artificial intelligence for healthy aging" (project-reference code B31J23000910002).

REFERENCES

1. Garcia-Cordero I, Anastassiadis C, Khoja A, et al. Evaluating the Effect of Alzheimer's Disease- Related Biomarker Change in Corticobasal Syndrome and Progressive Supranuclear Palsy. Ann Neurol. 2024;96(1):99-109. doi:10.1002/ana.26930
2. Zhang Y, Wu KM, Yang L, Dong Q, Yu JT. Tauopathies: new perspectives and challenges. Mol Neurodegener. 2022;17(1):28. Published 2022 Apr 7. doi:10.1186/s13024-022-00533-z
3. Phan TX, Mullins WA, Tetrault AM, et al. Transdiagnostic Network Localization of Social, Language, and Motor Symptoms in Patients With Frontotemporal Lobar Degeneration. Neurology. 2024;103(12):e210108. doi:10.1212/WNL.0000000000210108
4. Mudher A, Colin M, Dujardin S, et al. What is the evidence that tau pathology spreads through prion-like propagation?. Acta Neuropathol Commun. 2017;5(1):99. Published 2017 Dec 19. doi:10.1186/s40478-017-0488-7
5. de Bruin H, Groot C, Barthel H, et al. Connectivity as a universal predictor of tau progression in atypical Alzheimer's disease. Brain. Published online August 14, 2025. doi:10.1093/brain/awaf279

6. Franzmeier N, Brendel M, Beyer L, et al. Tau deposition patterns are associated with functional connectivity in primary tauopathies. Nat Commun. 2022;13(1):1362. Published 2022 Mar 15. doi:10.1038/s41467-022-28896-3
7. Fox MD. Mapping Symptoms to Brain Networks with the Human Connectome. N Engl J Med. 2018;379(23):2237-2245. doi:10.1056/NEJMra1706158
8. T Tetreault AM, Phan T, Orlando D, et al. Network localization of clinical, cognitive, and neuropsychiatric symptoms in Alzheimer's disease. Brain. 2020;143(4):1249-1260. doi:10.1093/brain/awaa058
9. Chu M, Jiang D, Li D, et al. Atrophy network mapping of clinical subtypes and main symptoms in frontotemporal dementia. Brain. 2024;147(9):3048-3058. doi:10.1093/brain/awae067
10. Ashburner J, Friston KJ. Diffeomorphic registration using geodesic shooting and Gauss-Newton optimisation. Neuroimage. 2011;55(3):954-967. doi:10.1016/j.neuroimage.2010.12.049

61. NeuroWorkflow: A Node-Based Framework for Scalable Computational Neuroscience with AI-Ready Infrastructure

Authors and Affiliations:
Carlos Enrique Gutierrez (1), Henrik Skibbe (2), Kenji Doya (1)
1 - Okinawa Institute of Science and Technology Graduate University, 2- RIKEN Center for Brain Sciences.

Abstract:
Introduction
Computational neuroscience faces significant challenges in model development, reproducibility, and scalability across diVerent simulation platforms. Current tools typically focus on single simulation environments, limiting cross-platform compatibility and collaborative research. We present NeuroWorkflow, a node-based framework that addresses these limitations through a unified, extensible architecture supporting multiple neural simulation paradigms including spiking neural networks (SNNs) and mean-field models. Additionally, the emerging potential of Large Language Model (LLM) agents in scientific workflows remains largely untapped due to the absence of well-structured, AI-ready computational neuroscience code components for AI-augmented and assisted brain modeling. Our well-documented nodes, enabled by our schema system, establish the foundation for organizing computational neuroscience functions, algorithms and tools, ready for AI few-shot learning via protocols such as MCP, enabling future AI-augmented computational neuroscience systems

Methods
NeuroWorkflow implements a modular node-based architecture with three core components: (1) A comprehensive schema system defining standardized node interfaces with input/output ports, parameters, and method definitions; (2) An AI-ready infrastructure featuring machine-readable node designed for LLM comprehension, enabling future integration with Model Context Protocol (MCP) servers where AI agents can autonomously understand, compose, and execute neuroscience workflows; (3) Specialized node libraries including SNNbuilder for detailed spiking neural network construction in NEST and TVB (The Virtual Brain) nodes for brain modeling. The framework employs a port-based connection system enabling type-safe data flow between heterogeneous components. Each node contains structured metadata, semantic descriptions, and usage examples formatted for LLM interpretation, positioning the system as a foundation for AI-augmented scientific computing. We developed automated code generation capabilities that transform high-level workflow descriptions into executable simulation code. The system includes comprehensive validation mechanisms and error handling, designed to support both human users and AI agents.

Results
We successfully developed NeuroWorkflow with specialized nodes across multiple domains, each equipped with comprehensive machine-readable documentation. The framework operates as a standalone Python library enabling direct node instantiation, port-based connections, parameter configuration, and programmatic workflow execution. SNNbuilder nodes enable construction of detailed cortical microcircuits in NEST. MFbuilder nodes provide seamless access to mean-field models and simulation capabilities in TVB. Nodes communicate through both traditional I/O mechanisms and eVicient in-memory object passing, enabling high-performance data flow between components. We developed a comprehensive graphical user interface for intuitive workflow construction and testing, supported by a backend system for workflow management. The system operates in both local standalone mode and distributed client-server configurations, facilitating collaborative research environments. The structured node schema system successfully enables programmatic workflow composition. Preliminary testing with LLM-based workflow generation demonstrates the system's readiness for AI agent integration, with structured node descriptions enabling accurate workflow composition in test scenarios.

Discussion
NeuroWorkflow represents a paradigm shift toward AI-augmented computational neuroscience, enabling both researchers without extensive programming backgrounds and future AI agents to construct sophisticated neural models. The node-based approach with machine-readable schemas facilitates rapid prototyping, systematic parameter exploration, and positions the framework as a foundational component for MCP servers in computational neuroscience. Key innovations include the LLM-comprehensible node documentation system, standardized schema ensuring type safety and AI interpretability, and the unified interface bridging traditionally separate simulation environments. The framework addresses needs for standardization, accessibility, and AI-readiness in computational neuroscience, potentially enabling a new era of AI-augmented brain modeling research where human expertise is amplified by intelligent agents capable of understanding and manipulating complex neuroscience workflows.

Keywords: computational neuroscience, workflow management, spiking neural networks, brain modeling, AI-ready infrastructure, LLM agents, MCP server, node-based programming, automated workflow composition, AI-augmented research

Acknowledgments:
This work was supported by Brain/MINDS 2.0 project, AMED.

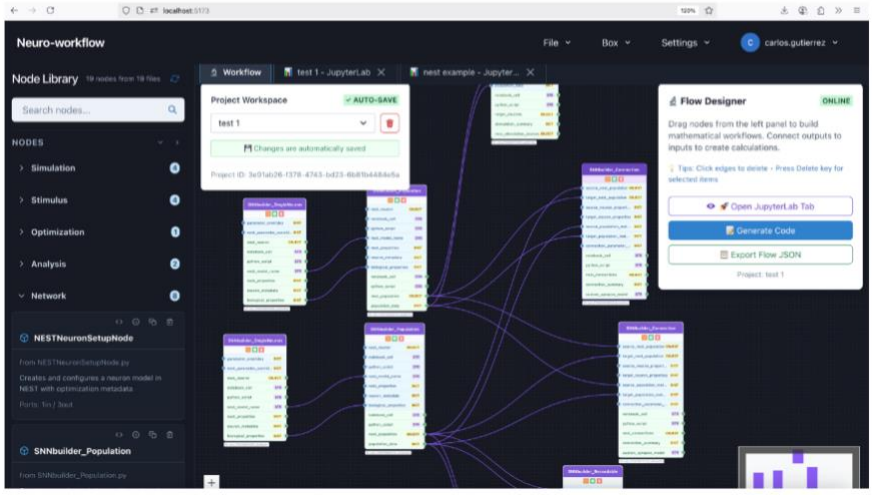

Figure 1. Neuroworkflow includes a graphical user interface for intuitive workflow construction and testing.

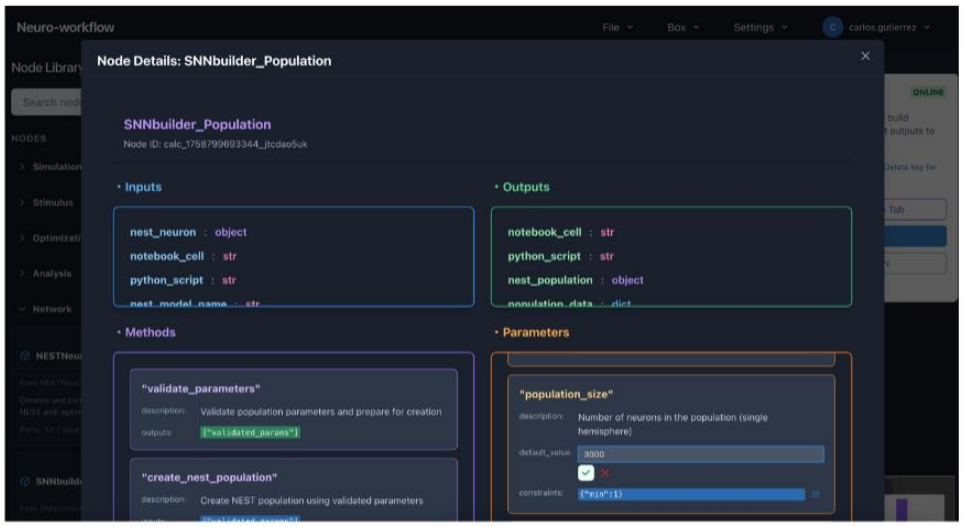

Figure 2. Schema defining standardized node interfaces with input/output ports, parameters, and method definitions.

62. Epidemiological Trends of Schizophrenia in the Salé-Rabat Region, Morocco: A 14-Year Retrospective Study at Ar Razi Psychiatric Hospital (2011–2024)

Fatima Zahra Kessam[1], Basma Qasbi[1], El Hassan Ouanouche[1], Soukaina Stati[2], Ouanass Abderrazak[2], Abdelhalem Mesfioui[1]

[1]Laboratory of Biology and Health, Neurosciences, Neuro-immunology and Behaviour Unit, Faculty of Science, Ibn Tofail University, Kenitra, Morocco
[2]Arrazi University Psychiatric Hospital, Faculty of Medicine and Pharmacy, Mohammed V University, Rabat, Morocco

Abstract :

Introduction: According to the World Health Organization, schizophrenia is a mental disorder characterized by significant impairments in how the individual perceives reality, and changes in behavior related to delusions, hallucinations, experiences of influence, and more. People with schizophrenia experience difficulties with their cognitive and thinking skills, such as memory, attention, and problem-solving. The World Health Organisation's report in 2022 revealed that Schizophrenia affects approximately 24 million people, or 1 in 300 people, worldwide. This rate is 1 in 222 among adults. It's less common than other mental disorders, and the onset is often during late adolescence and the twenties [2] and the onset tends to happen earlier among men than among women. In Morocco, A national survey has shown that Mental disorders are common in the Moroccan general population, with a prevalence of more than 40% [3]. Nonetheless, in Morocco, epidemiological studies on mental health disorders and schizophrenia remain rare, limiting a comprehensive understanding of their burden within the Moroccan context.

Objective: Our study aims to analyze the epidemiological trends of schizophrenia in the province of

Sale-Rabat, Morocco, by examining the distribution of cases at the Ar Razi Psychiatric Hospital from 2011 to 2024 and assessing variation in prevalence based on age and sex, and identifying potential fluctuations over time.

Methods: A retrospective descriptive study was conducted at Ar Razi University Psychiatric Hospital (Salé, Morocco) from 2011 to 2024. Medical archives of 13,337 patients diagnosed with schizophrenia were analyzed for demographic variables (age, sex). Descriptive statistics and sex ratios were calculated using IBM SPSS Statistics 25.0.

Results: Over the study period, males accounted for 77% of cases (n = 10,261) and females for 23% (n = 3,076), with a male-to-female ratio ranging from 2.32 to 4.51. The most affected age group was 15–60 years (95.6% of cases), with minimal cases in children (1.7%) and older adults (2.68%). Temporal trends showed fluctuations, with marked declines in 2013 and 2020 (COVID-19 pandemic), followed by a sharp increase peaking in 2023.

Conclusion: Schizophrenia in the Salé-Rabat region predominantly affects males in early to middle adulthood. The observed fluctuations highlight the impact of social, cultural, and external factors such as the COVID-19 pandemic on hospitalization rates. Findings underscore the need for targeted mental health policies addressing stigma, gender disparities, and accessibility to care in Morocco.

Keywords: Schizophrenia, Epidemiology, Morocco, Sex distribution, Age distribution, Mental health trends

Acknowledgments: The author gratefully acknowledges the support of the Centre Hospitalo-Universitaire Ibn Sina and the staff of Hôpital Ar-Razi for granting access to the data and facilitating this research.
The author also acknowledges the Centre National pour la Recherche Scientifique et Technique (CNRST, Morocco) for providing a PhD scholarship under the PhD-Associate Scholarship – PASS program.

References:
(1) World Health Organization. Schizophrenia [Internet]. 2022 Jan 10 [cited 2025 Aug 30]. Available from: https://www.who.int/news-room/fact-sheets/detail/schizophrenia
(2) Miettunen J, Immonen J, McGrath JJ, Isohanni M, Jääskeläinen E. The age of onset of schizophrenia spectrum disorders. In: Age of onset of mental disorders: Etiopathogenetic and treatment implications. 2019. p. 55-73.
(3) Kadri N, Agoub M, Assouab F, Tazi MA, Didouh A, Stewart R, et al. Moroccan national study on prevalence of mental disorders: a community-based epidemiological study. Acta Psychiatr Scand. 2010;121(1):71-4.

63. Dynamic Causal Modelling to infer connectivity from MEG high-gamma activity: a Markov-Chain Monte Carlo approach

Pedro García-Rodríguez[*1], Matthieu Gilson[1], Jean-Didier Lemaréchal[1] and Andrea Brovelli[1]

[1]CNRS UMR 7289, Institut de Neurosciences de la Timone, Campus Santé Timone, Marseille, France
*pedro.garcia-rodriguez@univ-amu.fr

INTRODUCTION/MOTIVATION

Bayesian inference in Dynamic Causal Modelling (DCM) has been widely applied to resting-state data, but rarely to the case of non-monotonic task-related brain activity profiles. Model inversion traditionally considers the application of Bayesian variational schemes, i.e. quadratic approximations in the vicinity of minima in the parameters space [1]. On the other hand, more general Markov-Chain-Monte-Carlo methods (MCMC) opt for an intense use of random numbers to sampling posterior probability distributions. The successful application of either of them highly depend on the correct choice of prior distributions.

METHODS

Here we propose an automated workflow combining MCMC with more conventional optimization Gradient-Descent (GD) techniques. Following the bi-linear model [2], a simpler DCM is considered with a matrix A for effective connectivity and a matrix C for sensory driving inputs. Alpha and Gamma functions for input profiles complete the modeling scenario.

Model's parameters are estimated in three parts. Firstly, the matrix A is initialized from a Gaussian distribution with null-mean and variance given by the observer-specific Granger Causality (GC) computed from the data. Next, GD algorithms implement a constraint bounded optimization to keep input parameters within plausible (positive) intervals. The adequacy of the parameters values found are further tested through a Levenberg-Marquardt GD form. Finally, a MCMC Bayesian scheme incorporates the covariance of the observation noise in a Multivariate Gaussian likelihood model. A Generative Model is so completed with parameter's prior distributions based on the GD optimizations mentioned above. Normal or Log-Normal distributions are alternatively used, the latter to ensure positive values after sampling when needed.

A detailed computational study with synthetic data shows that the workflow is able to recover the original (ground-truth) connectivity matrix, given that an accurate version of GC matrix is used to initialized the model, and data from hundred of trials with a moderate signal-to-noise ratio are available.

RESULTS AND DISCUSSION

The approach is successfully applied to High-Gamma Activity induced responses during visuo-motor transformation tasks executed by 8 subjects, as reported in [3]. Methods were applied to hundred of trials for each subject, providing a handy data-driven DCM framework to evaluate the plausibility of various model configurations. Observation noise is empirically estimated from the pre-stimulus periods in original trials. Model inversion pipeline tends to support the most realistic model configuration tested, containing inputs to both sensory areas.

Comparison of prior and posterior distributions can help distinguish informative from non-informative parameters. Alternative initializations of matrix A with linear correlation or unitary matrices were also tested.

Keywords: Dynamic Causal Modelling, Markov-Chain Monte Carlo, effective connectivity, high-gamma activity, MEG

ACKNOWLEDGEMENTS

A.B. and P.G-R were supported by EU's Horizon 2020 Framework Programme for Research and Innovation under the Specific Grant Agreements No. 101147319 (EBRAINS 2.0 Project).

REFERENCES

[1] Zeidman P, Friston K, Parr T. (2023) A primer on Variational Laplace (VL). Neuroimage 279:120310. doi: 10.1016/j.neuroimage.2023.120310.

[2] Chen CC, Kiebel SJ, Friston KJ (2008). Dynamic causal modelling of induced responses. Neuroimage 41(4):1293-1312. DOI: 10.1016/j.neuroimage.2008.03.026. PMID: 18485744.

[3] Brovelli A., Chicharro D., Badier J-M., Wang H., Jirsa V. (2015). Characterization of Cortical Networks and Corticocortical Functional Connectivity Mediating Arbitrary Visuomotor Mapping. J. Neuroscience 35(37):12643-12658. doi: 10.1523/JNEUROSCI.4892-14.2015.

64. Streamline-based lesion-symptom mapping (SLSM), a new eBRAINS technique

Ema Vaidelyte, Marco Reisert*, Felix Hertel, Emiel van den Hoven, Michel Rijntjes, Cornelius Weiller

Depts.of Neurology and Radiology/Stereotactic Neurosurgery (*), University hospital and Faculty of Medicine, Freiburg i.Br., Germany

Introduction: Studying the brain's connections may contribute more readily to understanding its function than examining cortical parcellations [1,2]. Accordingly, relating patients' symptoms to affected tracts may improve understanding the disease. Most current concepts superimpose lesion masks onto templates of known tracts and calculate the affection. However, canonical tracts cover only a minor part of all fibres. Furthermore, attribution of streamlines to tracts is arbitrary and follows no convention [3]. Lastly, a single tract can be affected more than once in its course. We therefore developed a new technique, streamline based lesion symptom mapping (SLSM). Like VLSM, SLSM is a whole brain analysis, however on a single stream line basis, rather than voxels.

Methods: For SLSM, first a normative connectome is constructed using a global tracking approach (GT). Global tracking avoids the inherent bias of predetermined start and end points or binary tract definitions, thus enables an unbiased analysis [4]. We used data from the human connectome project to obtain a normative connectome (see [5] for detailed methodology). Once the normative connectome is established, the extent of overlap (expressed as a percentage) between the lesion mask of each patient and the normative connectome is calculated as an anatomical marker at the streamline level, forming the individual disconnectome. As use case we utilized 493 acute stroke patients from the Freiburg Large Scale Project, a prospective study of currently > 1100 acute stroke patients with a single ischemic lesion. We performed a whole-connectome, streamline-level statistical analysis, using the modified Rankin Scale at follow up (mRSFU) > 3 months after the stroke, an established scale for disability after stroke, as the independent variable in a non-parametric multiple regression model. The outcome is a disconnectome map that identifies the streamlines associated with the mRSFU.

Results: SLSM identified the streamlines affected by the acute lesions that related to disability after stroke (mRSFU). For both hemispheres, afferent and efferent (cortico-spinal tract) projection fibres were found, interhemispheric transcallosal fibres, as well as three bundles of association fibres (Fig. 1).

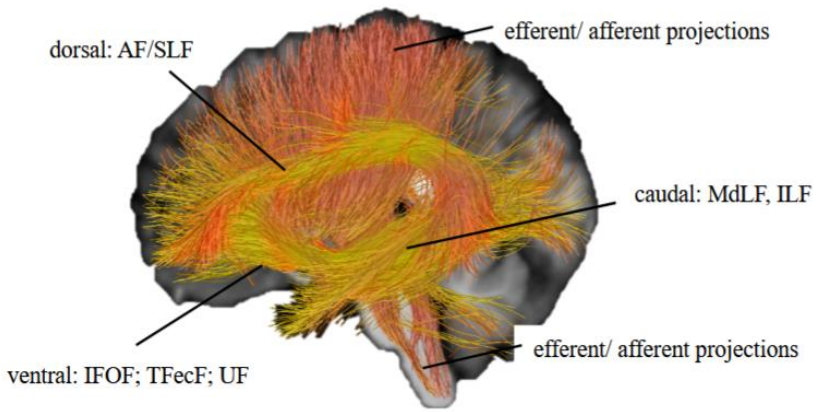

Fig. 1: mRSFU disconnectome map (left hemisphere, n=263), showing afferent and efferent projection fibres, a dorsal bundle comprising AF/SLF (arcuate fascicle/ superior longitudinal fascicle), a ventral bundle comprising IFOF, TFecF and UF (inferior fronto-occipital fascicle, temporo-frontal extreme capsule fascicle, uncinate fascicle) and a caudal bundle related to the MdLF/ILF (middle longitudinal fascicle/ inferior longitudinal fascicle). The normative connectome was used for classification.

Discussion:
SLSM is new technique using no a priori tract definitions or ROIs to construct whole brain connectomes of patients on a single streamline level, which can be correlated with clinical variables. In stroke, disability at the chronic state as measured by the mRS is related to lesioning of afferent and efferent projection fibres, which was expected, and to the lesioning of three large association tract systems. Dorsal and ventral pathways are known to conjugate in network nodes, “hubs” in frontal and posterior cortex, constituting the dual-loop model 6. The dual-loop facilitates flexible categorization, abstraction, generalization and counterfactual inference, extending concepts to new contexts, even those unlinked to perceptual entities [7]. These capabilities are not only needed for a wide range of significant cognitive functions [8,9], they are also crucial when confronted with new situations, when lacking retrievable specifications forces the brain to resort to analogy. That is what stroke patients need to adapt by using the remaining physical abilities.

References:
1. Goldstein K. Das Symptom, seine Entstehung und Bedeutung für unsere Auffassung vom Bau und von der Funktion des Nervensystems. Archiv für Psychiatrie. 1925;76:84-108.
2. Weiller C, Rijntjes M. Should concepts of brain functions be based on psychology or anatomy? An echo from Kurt Goldstein. Brain. Published online March 10, 2023:awad081. doi:10.1093/brain/awad081
3. van den Hoven E, Weiller C, Reisert M, Rijntjes M. Inferring the “functions” of tracts: a cautionary note. Brain. 2025;148(5):1447-1450. doi:doi:%2010.1093/brain/awaf114
4. Reisert, M, Mader, I, Anstasopoulos, C, Weigel, M, Schnell, S, Kiselev, V. Global fiber reconstruction becomes practical. Neuroimage. 2011;15(54):955-962.
5. Weiller C, Reisert M, Peto, I, et al. The ventral pathway of the human brain: A continuous association tract system. Neuroimage. 2021;234(1):117977. doi:10.1016/j.neuroimage.2021.117977
6. Weiller, C, Reisert, M, Glauche, V, Musso, M, Rijntjes, M. The dual-loop model for combining external and internal worlds in our brain. Neuroimage. 2022;263(11):119583. doi:10.1016/j.neuroimage.2022.119583
7. Weiller, C, Reisert, M, Levan, P, Hosp, J, Coenen, V, Rijntjes, M. Hubs and interaction: the brain’s meta-loop. Cerebral Cortex. 2025;35(3):bhaf035. doi:10.1093/cercor/bhaf035
8. Dehaene S, Al Roumi F, Lakretz Y, Planton S, Sablé-Meyer M. Symbols and mental programs: a hypothesis about human singularity. Trends Cogn Sci. 2022;26(9):751-766. doi:10.1016/j.tics.2022.06.010
9. Mitchell M. Abstraction and analogy-making in artificial intelligence. Ann N Y Acad Sci. 2021;1505(1):79-101. doi:10.1111/nyas.14619

Keywords: Streamline-based lesion-symptom mapping, MRI, Stroke, Disability, Outcome

Acknowledgments:
FH, EvdH, MR are supported by EBRAINS2.0 (funded from the European Union's Horizon Europe research and innovation program under grant agreement No 101147319 (EBRAINS 2.0)). HCP data were provided by the HCP, Wu–Minn Consortium (principal Investigators D. Van Essen and K. Ugurbil; no. 1U54MH091657) funded by the 16 NIH Institutes and centers that support the NIH Blueprint for Neuroscience Research, and by the McDonnell Center for Systems Neuroscience at

Washington University. This work was supported by the MASSIVE HPC facility, Sylvia and Charles Viertel Foundation grant no. 2017042 to A.F., National Health and Medical Research Council grant nos. 1197431 and 1146292 to A.F., Australian Research Council grant nos. FL220100184 and DP200103509 to A.F., National Health and Medical Research Council grant no. 2008612 to M.B., Australian Research Council Laureate Fellowship no. FL140100025 to P.A.R. and Australian Research Council Center of Excellence no. CE1401000.

65. EBRAINS Italy - The inNuCE Research Infrastructure

Gianvito Urgese, Vittorio Fra, Andrea Pignata, Giuseppe Fanuli, Walter Gallego Gomez, Riccardo Pignari, Michelangelo Barocci, Benedetto Leto, Salvatore Tilocca, Nicola Cassetta, Enrico Macii

The Industry 5.0 and AIoT sectors increasingly demand low-power, low-latency, and privacy-preserving computation. Neuromorphic hardware (HW) provides a brain-inspired, energy-efficient paradigm but remains costly, fragmented, and difficult to access [1-3]. To address this barrier, we developed the inNuCE Research Infrastructure (RI), a two-level facility that integrates (i) the Heterogeneous Prototyping Platform (HPP), a cloud-based Prototype-as-a-Service for neuromorphic/digital co-design, and (ii) a dedicated laboratory hosting neuromorphic sensors and dev boards for direct experimentation.

The HPP supports a wide range of devices and development frameworks, including Brainchip Akida, SynSense Speck/Xylo, and SpiNNaker neuromorphic boards, as well as Nvidia Jetson and GPU servers. These are containerized with their respective SDKs to ensure reproducible development environments. The workflow encompasses model definition, training, simulation, hardware deployment, and results analysis. Both expert-oriented tools (VSCode, Jupyter, Kubeflow pipelines) and simplified interfaces (drag-and-drop pipelines) are available.
Two use cases were implemented:

1) SNN Sudoku Solver [4]: A spiking stochastic neural network for constraint satisfaction problems deployed on neuromorphic simulators. Performance was benchmarked in terms of solution accuracy, speed, and energy consumption.
2) 2) Braille Letter Neuromorphic Reading [5]: A tactile sensing application using event-driven encoding and classification networks for Braille characters. Accuracy and HW energy consumption were compared across heterogeneous devices.

The Sudoku solver achieved robust performance on constraint satisfaction tasks with energy-delay product (EDP) improvements up to two orders of magnitude compared to digital baselines, while maintaining comparable accuracy. The Braille reader application achieved >85% classification accuracy on a 27-class dataset, with activation sparsity >95% and significant reductions in multiply-accumulate operations, demonstrating suitability for embedded edge devices. Comparative benchmarks across neuromorphic and GPU-based systems validated that the HPP enables transparent cross-platform evaluation.

These results demonstrate that the inNuCE-RI lowers the entry barrier for neuromorphic computing by providing scalable cloud access and physical laboratory integration. By enabling direct comparison of algorithms across diverse HW, it accelerates prototyping and supports reproducibility. Integration with EBRAINS-Italy ensures sustainability, nationwide access, and alignment with the European EBRAINS ecosystem. The infrastructure thus represents a key enabler for bridging neuroscientific insights with industrial AIoT applications.

References

[1] Urgese, Gianvito, et al. "Powering the next-generation IoT applications: new tools and emerging technologies for the development of Neuromorphic System of Systems." FiN 17 (2023): 1197918. DOI: 10.3389/fnins.2023.1197918
[2] Muir, Dylan Richard, and Sadique Sheik. "The road to commercial success for neuromorphic technologies." NC 16.1 (2025): 3586. DOI 10.1038/s41467-025-57352-1
[3] Kudithipudi, Dhireesha, et al. "Neuromorphic computing at scale." NC 637.8047 (2025): 801-812. DOI: 10.1038/s41586-024-08253-8
[4] Pignari, Riccardo, et al. "Efficient solution validation of constraint satisfaction problems on neuromorphic hardware: the case of Sudoku puzzles." IEEE Transactions on Artificial Intelligence (2025). DOI: 10.1109/TAI.2025.3536428
[5] Müller-Cleve, Simon F., et al. "Braille letter reading: A benchmark for spatio-temporal pattern recognition on neuromorphic hardware." FiN 16 (2022): 951164. DOI: 10.3389/fnins.2022.951164

Acknowledgments
We acknowledge a contribution from the Italian National Recovery and Resilience Plan (NRRP), M4C2, funded by the European Union – NextGenerationEU (Project IR0000011, CUP B51E22000150006, “EBRAINS-Italy”).

66. Layer-specific cell counts in BigBrain – decomposing cortex-wide numbers based on cytoarchitectonics

Sebastian Bludau[1,*], Timo Dickscheid[1,2,3,*], Anna Steffens[1], Christian Schiffer[1,3], Eric Upschulte[4], Katrin Amunts[1,4]

[1] Institute of Neuroscience and Medicine (INM-1), Forschungszentrum Julich GmbH, Germany
[2] Faculty of Mathematics and Natural Sciences - Institute of Computer Science, Heinrich Heine University Düsseldorf, Germany
[3] Helmholtz AI, Research Center Jülich, Germany
[4] Cecile and Oskar Vogt Institute for Brain Research, Düsseldorf, Germany

Introduction: Cell counts of the cerebral cortex represent one of the most fundamental characteristics of brain organization, and serve as the basis for studying evolution, development and disease (e.g., [1, 2]). However, the total number of cells in the brain or cerebral cortex does not reflect the variation between layers and cortical areas, which is related to the functional heterogeneity of the human brain. Therefore, we investigated layer- specific cell counts in 94 cytoarchitectonic cortical areas in the anatomical BigBrain model [3].

Methods: The study is based on cell counts and cortical thickness measurements in high- resolution 2D scans (1 µm in-plane resolution), most of which are already publicly available [4]. In total, 940 patches were analyzed across 94 areas of the Julich Brain Atlas [5] (Fig. 1), with 10 patches sampled per area, ensuring a >65% probability of region being present at each location. Using siibra-python [6], patches were assigned to Julich Brain cytoarchitectonic probabilistic maps by transforming their locations to MNI space [7]. These were chosen to be perpendicular to the cortical surface. Manual layer annotations were performed by anatomical experts and independently verified. Cells were segmented using a novel deep learning approach [8, 9] including correction for truncated cells (Fig1). Cell numbers were corrected for histological shrinkage [10]. To cross-validate data and capture intersubject variability among brains, patches from frontal pole area Fp1, motor area 4a, and visual area hOc1of ten Julich- atlas brains were analyzed using the same counting approach and compared to the BigBrain data.

Results: Comprehensive data sets of 940 image patches were obtained including the 1 µm images with manual annotation of cortical layers, the cell counts, cell sizes, and cortical as well as layer thicknesses (Fig1, Fig 2). The analysis revealed a considerable regional variations in cell counts across layers and areas as illustrated in Fig. 2. E.g., areas of the insula showed up to 15% variance. After shrinkage correction and adjusting for truncated cells, the corrected total cell count of the human cortex has been estimated to be approximately 33.9 billion. Based on a neuron-to-glia ratio of 1:1.5 [1], this corresponds to 13.6 billion neurons and 20.3 billion glial cells. The average cortical thickness across all regions was 2667.15 µm. Quantitative measures of areas Fp1 of the BigBrain (Fig. 2) and of the other two areas were in the range of variation of the ten brains from Julich Brain Atlas. The data will be shared as part of a growing dataset collection [11] in accordance with the FAIR principles via the EBRAINS infrastructure.

Discussion: This study has introduced a new, comprehensive dataset with detailed area- and layer specific cell counts of the human cerebral cortex, supplementing previous data at whole- cortex level [1]. It extended our knowledge on cytoarchitectonic differences, e.g., between granular, dysgranular and granular areas and further quantified regional differences at laminar level. The considerable differences between areas within the insular cortex, as one example, confirms the hypothesis that macroanatomically defined regions do not adequately reflect the microstructural organization of the brain; they may lump together structurally and functionally different areas. Data on cortical thickness correspond to earlier histological and MR-based findings [2, 12, 13]. We will continuously supplement the data together with new releases of Julich Brain Atlas areas. Cell counts based on cytoarchitectonics may serve as reference for comparative and disease studies, and inform modeling and simulation, and AI, highlighting the value of high-resolution atlases for capturing details of microscopical brain organization.

References:

1. von Bartheld, C.S., et al., The search for true numbers of neurons and glial cells in the human brain: A review of 150 years of cell counting. J Comp Neurol, 2016. **524**(18): p. 3865-3895.
2. von Economo, C.F., et al., Die Cytoarchitektonik der Hirnrinde des erwachsenen Menschen. 1925: J. Springer.
3. Amunts, K., et al., BigBrain: an ultrahigh-resolution 3D human brain model. Science, 340(6139): p. 1472-5.
4. Schiffer, C., Lepage, C., Omidyeganeh, M., Mohlberg, H., Brandstetter, A., Bludau, S., Heuer, K., Toussaint, P.-J., Wenzel, S., Dickscheid, T., Evans, A. C., & Amunts, K. , Selected 1 micron scans of BigBrain histological sections (v1.0) 2022.
5. Amunts, K., et al., Julich-Brain: A 3D probabilistic atlas of the human brain's cytoarchitecture. Science, 2020. **369**(6506): p. 988-992.
6. Dickscheid, T., Gui, X., Simsek, A. N., Koehnen, L., Marcenko, V., Schiffer, C., Bludau, S., & Amunts, K., siibra-python (Zenodo). https://zenodo.org/records/14184565.
7. Lebenberg, J., et al., A framework based on sulcal constraints to align preterm, infant and adult human brain images acquired in vivo and post mortem. Brain Struct Funct, **223**(9): p. 4153-4168.
8. Ma, J., et al., The multimodality cell segmentation challenge: toward universal solutions. Nat Methods, 2024. **21**(6): p. 1103-1113.
9. Upschulte, E., et al., Contour proposal networks for biomedical instance segmentation. Med Image Anal, 2022. **77**: p. 102371.
10. Amunts, K., et al., Gender-specific left-right asymmetries in human visual cortex. J Neurosci, 2007. **27**(6): p. 1356-64.
11. Dickscheid, T., Bludau, S., Paquola, C., Schiffer, C., Upschulte, E., & Amunts, K., Layer-specific distributions of segmented cells in different cytoarchitectonic regions of BigBrain iso cortex. EBRAINS project: https://search.kg.ebrains.eu/instances/f06a2fd1-a9ca-42a3-b754-adaa025adb10.

12. Frangou, S., et al., Cortical thickness across the lifespan: Data from 17,075 healthy individuals aged 3-90 years. Hum Brain Mapp, 2022. **43**(1): p. 431-451.
13. Wagstyl, K., et al., BigBrain 3D atlas of cortical layers: Cortical and laminar thickness gradients diverge in sensory and motor cortices. PLoS Biol, 2020. **18**(4): p. e3000678.

Fig 1:

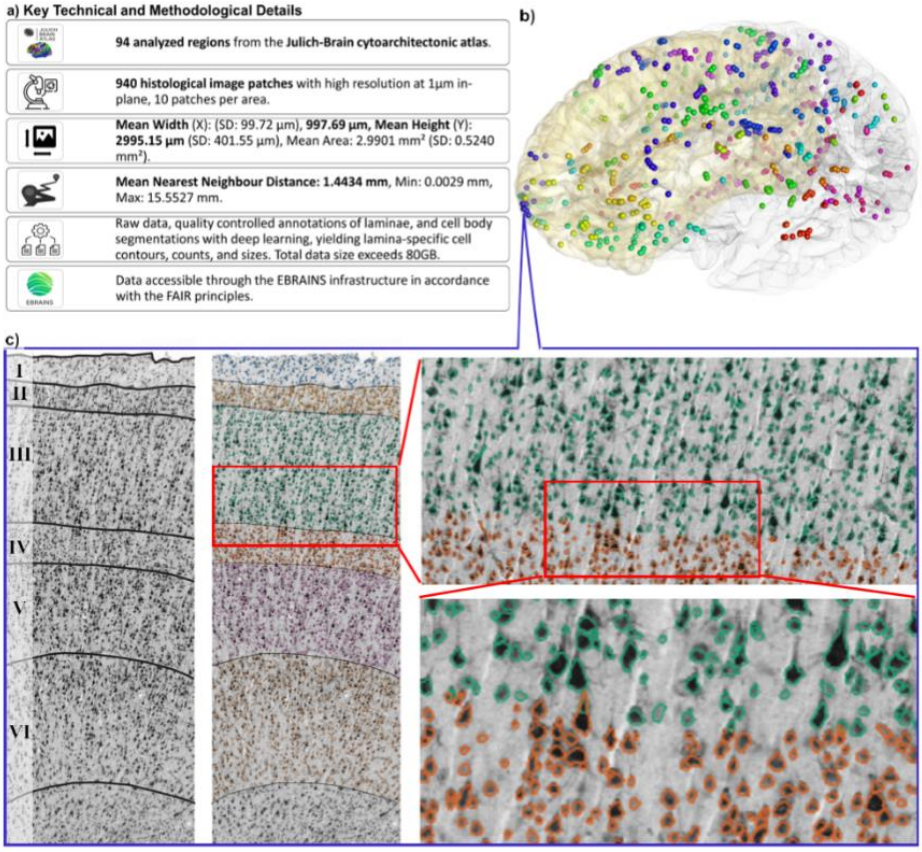

Figure 1: a) Summary of key methodological details, including analyzed regions, high-resolution histological image patches, and dataset characteristics. **b)** Illustrates the spatial distribution of the 940 analyzed histological image patches within the BigBrain reference space. Each patch position is represented as a sphere, with colors indicating the assignment to the 94 analyzed areas of the Julich-Brain atlas (4). **c)** Presents representative histological images included for each of the 940 patches: the first image displays manually annotated layer marked by black lines, while the subsequent images highlight segmented cells in different colors, representing their layer assignment: blue (Layer I), yellow (Layer II), green (Layer III), orange (Layer IV), pink (Layer V), and light brown (Layer VI), emphasizing layer-specific cellular organization. In addition to the raw data, the dataset includes segmented data, corresponding layer masks, and fully aggregated text files containing information such as cell counts, cell sizes, thickness, and coordinates in the supported reference spaces.

Fig 2:

a)

Cortical Layer	Measured Thickness (µm) (Mean ± SD)	Literature Thickness (µm) (Mean ± SD)			Measured Relative Cell Counts (cells/mm³)	Literature Cell Counts
		Von Economo u Koskinas (1925)	Wagstyl et al. (2020)	Frangou et al. (2022)		von Bartheld CS, Bahney J, Herculano-Houzel S (2016, Review)
Layer I	**267 ± 79**	280 ± 150	290 ± 30		**57,306**	
Layer II	**181 ± 54**	160 ± 110	240 ± 30		**114,855**	
Layer III	**863 ± 209**	740 ± 330	740 ± 80		**88,273**	
Layer IV	**163 ± 112**	210 ± 190	200 ± 80		**112,054**	
Layer V	**515 ± 153**	460 ± 160	570 ± 110		**89,212**	
Layer VI	**678 ± 227**	880 ± 330	630 ± 90		**82,176**	
Overall	**2667 ± 430**	2680 ± 710	2670 ± 700	2667 ± 430	Neuron/Glia ratio estimate **13.6 billion neurons, 20.3 billion glia cells**	Neuron/Glia ratio estimate 10-20 billion neurons, 15-30 billion glial cells

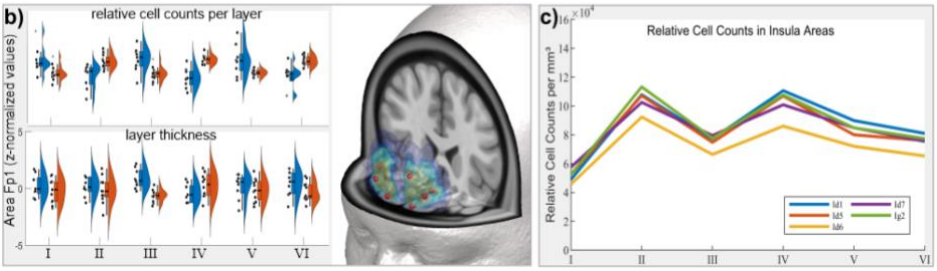

Figure 2: Cortical Layer Properties
a) Measured cortical thickness (µm) and cortical cell counts (cells/mm³) are shown alongside reference values from the literature. Thickness values are compared to von Economo and Koskinas (1925) (2), Wagstyl et al. (2020) (10), and Frangou et al. (2022)(9). Measured cell counts are compared to estimates from von Bartheld et al. (2016) (1).**b)** Violin plots display the distribution of thickness and relative cell counts across cortical layers based on area Fp1in 10 different human brains, which are part of the Julich Brain Atlas project (blue), and the newly described and analyzed BigBrain patches (orange).**c)** Line plot illustrate relative cell counts (cells/mm³) across cortical layers (Layer I–VI) for different cortical areas of the Insula. The insula region show characteristic area- and layer-specific differences. These findings highlight the distinct layer organization in these cortical areas and emphasize that, on a microstructural level, differences exist even between these defined regions. These microstructural variations establish an important link between structure and function in the human brain.

67. <Acceptability and usability of home telemonitoring SmartMe&You videogames to monitor cognitive functions in Alzheimer's and Parkinson's disease patients>

<Mina De Bartolo[1], Roberta Lizio[1], Giuseppe Noce[1], Susanna Lopez[1], Matteo Carpi[1], Claudio Del Percio[1], Claudio Babiloni[1*]>

<Affiliations: [1]Department of Physiology and Pharmacology "V. Erspamer", Sapienza University of Rome, Rome, Italy>
*e-mail address of corresponding author: claudio.babiloni@uniroma1.it.

INTRODUCTION/MOTIVATION
<The SmartMe&You program is part of a smart home telemonitoring environment (https://smartme.cloud.garr.it/) designed to monitor cognitive and motor functions, general stress levels, and
sleep-wake cycle for one week in older adults at risk of cognitive impairment or already diagnosed with cognitive disorders. Here, we tested the usability, acceptability, and validity of the SmartMe&You serious video games for assessing cognitive status in cognitively unimpaired older adults (Healthy) and patients with mild cognitive deficits or mild dementia due to Alzheimer's (ADCD) and Parkinson's (PDCD) diseases. The validity was assessed using the Mini-Mental State Examination (MMSE) score as the gold standard>

METHODS
< As part of the Italian Rome Technopole and European eBRAIN-Health projects, clinical and demographic data were collected from 40 healthy individuals, 58 ADCD patients, and 54 PDCD patients. All participants were involved in the SmartMe&You program. SmartMe&You's serious video games included 7 unsupervised cognitive tasks (including Posner's and Go-NoGo tests), implying the

quick evaluation of visual stimuli in a grid and finger motor responses on a commercial tablet monitor. The MMSE score and performance (i.e., accuracy and reaction time) of the serious video games were acquired. Statistical analyses were performed using the freeware tool Jamovi version 2.3.>

RESULTS AND DISCUSSION

< All participants accepted the SmartMe&You serious video games. All Healthy people (100%), 81% (N = 47) of ADCD patients, and 91% (N = 49) of PDCD patients were able to complete the SmartMe&You task battery. The ADCD and PDCD patients demonstrated significantly lower accuracy and slower reaction times in their video game performances compared to the Healthy group (Rank transformation ANCOVAs, $p < 0.05$; Figure 1). Finally, a statistically significant positive association was found between the MMSE score and task performances in the Healthy, ADCD, and PDCD participants as a whole group (GLMs; $p < 0.001$; Figure 2)>

Figure 1

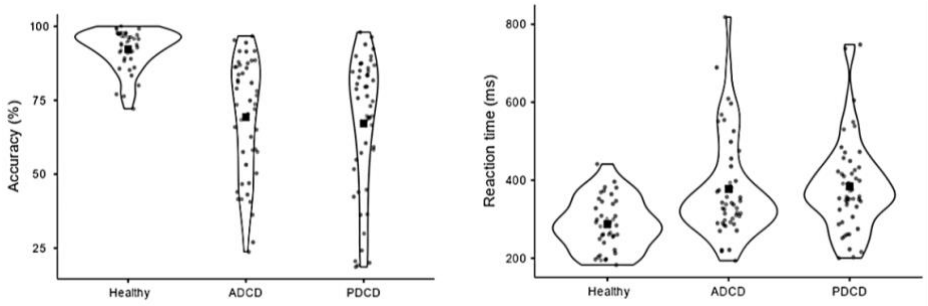

Figure 1. Individual values of the overall ("global") SmartMe&You performance (i.e., accuracy and reaction time) in the Healthy, ADCD, and PDCD groups. Abbreviations: Healthy = cognitively unimpaired older adults; ADCD = patients with cognitive deficits due to Alzheimer's disease; PDCD = patients with cognitive deficits due to Parkinson's disease.

Figure 2

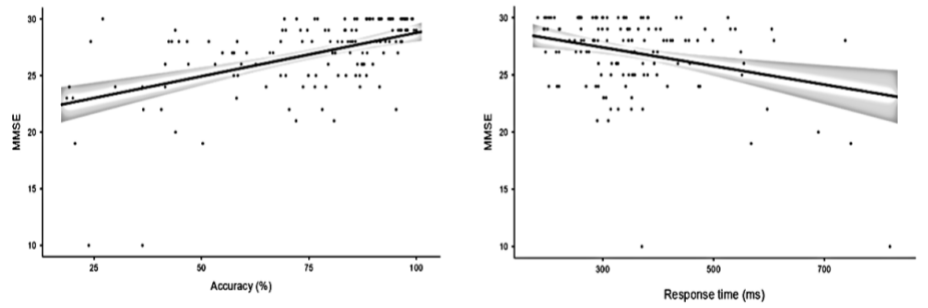

Figure 2. Scatterplots showing the association between the overall ("global") SmartMe&You serious video games performance (i.e., accuracy and response time) and the global cognitive status (i.e., MMSE score) in the Healthy, ADCD, and PDCD participants as a whole group. Abbreviations: MMSE = Mini-Mental State Evaluation; Healthy = cognitively unimpaired older adults; ADCD = patients with cognitive deficits due to Alzheimer's disease; PDCD = patients with cognitive deficits due to Parkinson's disease.

Keywords: <Home Telemonitoring of Dementia Risk Factors>, <Serious Video Games>, <Electroenceaphalography>, <Alzheimer's Disease>, <Parkinson's Disease>

68. < ANTERIOR-POSTERIOR GRADIENT IN THE JOINT PROCESSING OF MOVEMENT DIRECTION AND DEPTH IN CORTEX>

<Kostas Hadjidimitrakis[1*], Marina De Vitis[1], Matteo Filippini[1], Francesco Vaccari[1], Patrizia Fattori[1]>

< [1]Department of Biomedical and Neuromotor Sciences, University of Bologna, Bologna, Italy>
* kon.chatzidimitrakis@unibo.it

INTRODUCTION/MOTIVATION
Accurate performance of arm movements depends on the integrity of a network of areas located in the parietal cortex that integrate visual information about the location of objects in space with visual and proprioceptive information about hand position, to guide arm movements. An unsettled question in Neurosciences is how the various parameters of movements that unfold in real, 3D space are encoded in the primate cortex. The traditional view is that the direction and distance information (i.e., how far the effector moves) are processed by distinct circuits in the brain as reviewed by Crawford et al.[1] . This view derives mainly from psychophysical evidence and there is sparse neurophysiological evidence without consensus on this issue.

METHODS
We studied the strength, timing and integration of direction and depth/distance signals during arm movements in 3D space in a large dataset of neurons from three distinct parietal areas of the reaching network (areas V6A, PEc and PE; Galletti and Fattori[2]). We used both parametric and nonparametric, information theoretic and singular value decomposition methods in single neurons and population-level dimensionality reduction approaches as detailed by Hadjidimitrakis et al.[3].

RESULTS AND DISCUSSION
We found that in all parietal areas direction of movement processing preceded the coding of information about depth. In addition, we found the convergence of direction and depth information increased going from anterior (PE) to posterior (V6A) parietal cortex i.e., the two components were processed by largely separate populations in PE, as per the classical view by Crawford et al.[1]. In the same antero-posterior fashion we found a hierarchical processing of depth information with stronger and earlier effects in V6A then in PEc and lastly in PE. These findings suggest a significant degree of sequential direction and depth processing that supports behavioral evidence. In addition, they reveal a gradient-like organization of joint versus independent control of reach parameters in parietal cortex that could be viewed in light of its role in visuomotor transformations during actions. Knowing how the activity of cells in different areas encodes different aspects of movements (e.g. direction and or amplitude of the arm movements) has the potential of helping optimize of brain-machine interfaces for the control of prosthetic arms. To ensure the transparency and reproducibility of our findings and promote future studies that integrate neural data recorded in different labs with similar tasks from different cortical areas and species, we have recently made publicly available the present study's dataset via the EBRAINS initiative.

Keywords: <cortex>, <arm movement>, <3D space>

ACKNOWLEDGEMENTS
< H2020-EIC-FETPROACT-2019-951910-MAIA >, <NEXTGENERATIONEU (NGEU) >, <Ministry of University and Research (MUR), National Recovery and Resilience Plan (NRRP), MNESYS (PE0000006) >, <Ministry of University and Research (MUR), PRIN2022-2022BK2NPS >

REFERENCES

[1] Crawford et al. 2011. Three dimensional transformations for goal-directed action. Annu Rev Neurosci. 34:304-331. https://doi.org/10.1146/annurev-neuro-061010-113749
[2] Galletti and Fattori 2018 The dorsal visual stream revisited: Stable circuits or dynamic pathways? Cortex 98, 203–217 doi: 10.1016/j.cortex.2017.01.009.
[3| Hadjidimitrakis et al. 2022 Anterior-posterior gradient in the integrated processing of forelimb movement direction and distance in macaque parietal cortex.Cell Rep 2022 ;41(6):111608. doi: 10.1016/j.celrep.2022.111608.

69. Toward Patient-Specific Brain Models in Parkinson‘s Disease

Gabriele Casagrande[1*], Augustinas Fedaravicius[2,3*], Vytautas Kucinskas[2*], Mariana Angiolelli[1*], Gustavas Davidavicius[2,4*], Marmadooke Woodman[1], Spase Petkoski[1], Andrius Radziunas[3], Ieva Puleikyte[3], Karolina Reinyte[2], Viktor Jirsa[1+], Pierpaolo Sorrentino[1+], Damien Depannemaecker[1+], Ausra Saudargiene[2,4,+]

[1]Institut de Neurosciences des Systèmes, Aix-Marseille Université, Marseille, France
[2]Neuroscience Institute, Lithuanian University of Health Sciences, Kaunas, Lithuania
[3]Department of Neurosurgery, Medical Academy, Lithuanian University of Health Sciences, Kaunas, Lithuania
[4]Department of Informatics, Vytautas Magnus University, Kaunas, Lithuania
*equally contributing first author
+equally contributing last author

Introduction
Parkinson's disease, the second most common neurodegenerative disorder, is marked by progressive loss of dopaminergic neurons. Dopaminergic disruption causes severe motor symptoms (resting tremor, rigidity, bradykinesia, postural instability), cognitive deficits, and reduced quality of life in aging. While incurable, treatments such as deep brain stimulation can alleviate symptoms. We aim to develop personalized virtual brain models for Parkinson's patients that explicitly incorporate dopaminergic modulation. Building on our earlier work, we now refine these models by integrating individual structural connectivity, advanced neural mass formulations, and EEG-derived biomarkers, enabling more precise characterization of patient-specific dynamics.

Methods
We introduced a modular framework to capture dopaminergic regulation at the neural mass scale (Depannemaecker, 2024; Casagrande, 2025). Targeting D1-type receptor dynamics, it enables investigation of how fluctuations in dopamine availability shape population responses. The framework adopts a mean-field formulation (Chen & Campbell, 2022), providing a tractable yet biologically plausible description of macroscopic activity, well-suited to study dopamine-mediated modulation of basal ganglia circuits in health and disease.To identify biomarkers of brain dynamics in Parkinson’s disease (PD), we analyzed resting-state EEG acquired before and after DBS electrode implantation. Preoperatively, patients were tested ON and OFF L-DOPA; postoperatively, six months later, they were assessed with DBS ON and OFF, under both medication conditions. EEG features—Amplitude Envelope Correlation (AEC) and Phase Locking Value (PLV)—were extracted, and significant effects identified with permutation ANOVA.

Results
Our framework reveals that dopaminergic modulation critically reshapes the dynamical repertoire of neural mass models. By systematically varying dopamine input levels, we identified transitions between qualitatively distinct regimes, including fixed-point convergence, sustained oscillatory activity (limit cycles), and bursting dynamics. Progressive increases in dopaminergic tone induced a marked expansion of quiescent states, accompanied by reduced oscillatory frequencies across both fast

spiking and inter-burst domains. Importantly, these model-derived regimes correspond to electrophysiological features observed in EEG and DBS recordings from Parkinsonian patients, thereby providing a mechanistic account of dopamine-dependent neural dynamics. Analysis of EEG data showed that the most significant changes were found in the reduction in the Beta band for both PLV and AEC features, as reported in previous studies.

Discussion
Our results show that dopaminergic tone critically shapes neural mass dynamics, inducing transitions between quiescent, oscillatory, and bursting regimes. The observed reduction in oscillatory frequency and expansion of quiescent states parallel electrophysiological signatures in Parkinsonian EEG and DBS data, particularly in the Beta band. Next, we will integrate model-derived features with empirical connectivity into a unified framework, extending earlier approaches (Angiolelli, 2025) by incorporating DBS effects. This strategy advances toward personalized dynamical models to guide understanding and optimization of neuromodulation therapies.

Acknowledgment
The project has received funding from the Excellence Initiative of Aix-Marseille Université - AMidex, a French “Investissements d’Avenir programme” AMX-21-IET-017. This research has received funding from the European Union’s Horizon Europe Programme under the Specific Grant Agreement No. 101147319 (EBRAINS 2.0 Project); the European Union’s Horizon Europe Programme under the Specific Grant Agreement No. 101137289 (Virtual Brain Twin Project), and No. 101057429 (project environMENTAL); a government grant managed by the Agence Nationale de la Recherche (ANR) under the France 2030 program, reference ANR-22-PESN-0012; the grant "Personalised brain models of Parkinson's disease patients", "Modèle de cerveau personnalisé pour les patients atteints de la maladie de Parkinson", Lithuanian-French programme Gilibert, project No 2024-PRO-00148/ P-LZ-24-6, 2025-2026.

References
Casagrande, G., Fedaravičius, A., Duprat, C., McIntosh, A. R., Sorrentino, P., Petkoski, S., Saudargiene, A., Jirsa, V., & Depannemaecker, D. (2025). Next generation neural mass model with dopamine modulation mediated by D1-type receptors. bioRxiv. https://doi.org/10.1101/2025.09.01.673498

Depannemaecker, D., Duprat, C., Angiolelli, M., Carbonell, C. S., Wang, H., Petkoski, S., Sorrentino, P., Sheheitli, H., & Jirsa, V. (2024). A neural mass model with neuromodulation. bioRxiv (Cold Spring Harbor Laboratory). https://doi.org/10.1101/2024.06.23.600260

Chen, L., & Campbell, S. A. (2022). Exact mean-field models for spiking neural networks with adaptation. Journal of Computational Neuroscience, 50(4), 445– 469. https://doi.org/10.1007/s10827-022-00825-9

Angiolelli, M., Depannemaecker, D., Agouram, H., Régis, J., Carron, R., Woodman, M., Chiodo, L., Triebkorn, P., Ziaeemehr, A., Hashemi, M., Eusebio, A., Jirsa, V., & Sorrentino, P. (2025). The Virtual Parkinsonian patient. NPJ Systems Biology and Applications, 11(1), 40. https://doi.org/10.1038/s41540-025-00516-y

70. Towards a foundation model for causal inference of functional anatomy

Authors
Bey, Patrik[1]; Pombo, Guilherme[1]; Ruffle, James[1]; Nachev, Parashkev[1]

Affiliations

[1] High-Dimensional Neurology Group, Department of Translational Neuroscience & Stroke, Queen Square Institute of Neurology, University College London, London, United Kingdom

KEYWORDS
AI, focal lesions, causal inference, semi-supervised learning, foundation model, MRI

INTRODUCTION
Lesion-based studies have laid the foundation for causal inference in neuroscience, and considerably enhanced our understanding of how the brain shapes behaviour[1,2]. Yet we are still lacking an adequate framework for capturing the complex relationship between a patient's functional deficit and the underlying pathology. Here we advance towards a foundation model of causal functional anatomy by establishing a highly expressive synthetic prior of lesion-deficit causal relations within a deep representational model, jointly of lesions and deficits, based on variational autoencoding.

Biologically plausible ground-truth neural substrates are used in combination with large-scale synthetic lesion data to generate a wide range of complex associations (Fig. 1 (**A**&**E**)), creating a prior distribution of possible lesion-deficit relations. Our model both successfully reconstructs unseen lesion maps, demonstrating command of pathological lesion structure, and infers unseen ground-truth substrates with high-fidelity.

METHODS
We created 22000 synthetic lesions masks, based on random spheroids confined within MNI152 template space. Masks were subsequently adjusted by applying a tissue probability map as well as removing random voxel clusters to embody realistically complex pattern of brain lesions (Fig. 1 (**A**)). The dataset was split into reconstruction pretraining subset (*rec-set*; 20K lesions), fine tuning subset (*ft-set*; 1K lesions), and zero-shot inference subset (*inf-set*; 1K lesions). A previously described NeuroQuery based motor task activity map[3] served as ground-truth neural substrate. Lesion-deficit relations were computed by creating a binary vector representing the overlap of each lesion and each substrate, and a vector of ratios of overlapping voxels with added Gaussian noise using three different sigma values (0.1,0.5,1). The inference target synthetic deficit used for validating the model's ability to deduce the spatial representation for complex previously unseen lesion-deficit associations was computed as the Euclidean distance between centre-of-gravities of substrates and masks.

The presented model extends upon previous work[4] introducing deep variational lesion-deficit mapping (DLM) with two decoding modules (Fig. 1 (**B**)) capturing the joint spatial distribution of lesions and functional deficits. Here we introduce a synthetic pre-training regime that establishes a highly expressive prior. First, we employ semi-supervised learning[5] to ensure the accurate reconstruction of the lesion masks by pre-training the corresponding layers (Fig. 1 (**B**) blue shape) using the *rec-set*. Subsequently, the full model is fine-tuned on the *ft-set* (Fig. 1 (**B**) orange shape) to learn multiple complex associations of pathology and behaviours, before inferring, in a zero-shot approach, the neural substrate for the previously unseen deficit associations of the *inf-set*. Our proof-of-concept 2D model was trained for 200 epochs with a batch size of 256 and 32x32 dimensionality of both lesion masks and neural substrate using a single NVidia RTX 4090 GPU.

RESULTS
Our findings show a high accuracy of the lesion reconstruction task of the model with a mean dice-score of 0.665 for training and 0.668 for the validation data set. The prediction of the unseen ground-truth neural substrate resulted in a mean dice score of 0.81 over the last 50 training epochs.

DISCUSSION
We first showed that our model learns a shared representation of spatial lesion masks and behavioural deficits, providing a single causal model from pathology to varying deficits. Critically we could further show the models capacity to infer such patterns based on unseen associations,

highlighting the broad learned context of the model beyond provided deficit scores, a critical milestone towards a foundational model of brain pathology.

FIGURES

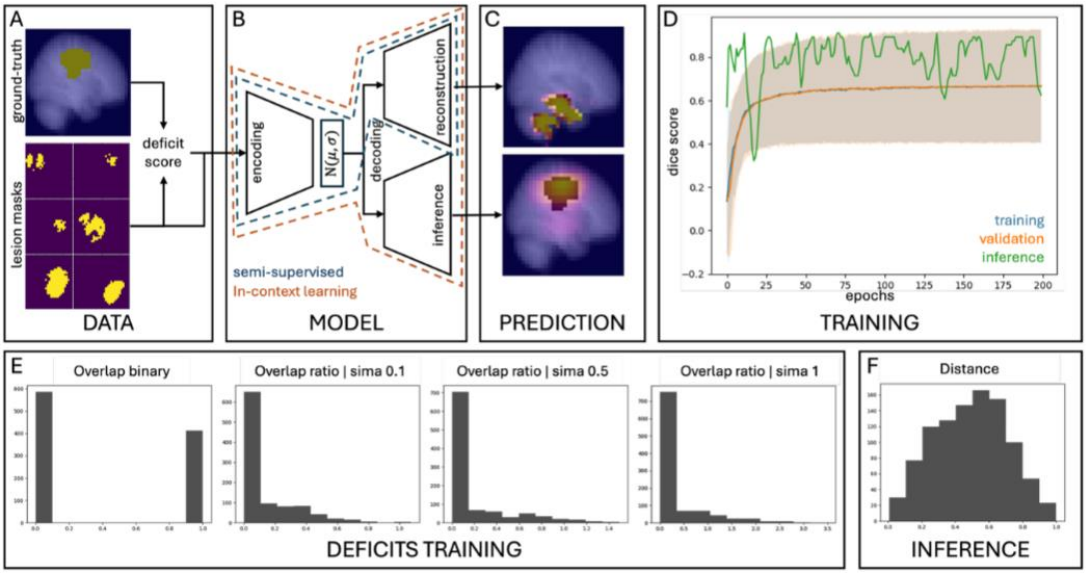

Figure 1 Project summary (**A**) The estimation of deficit scores is based on associations between individual lesion masks and a ground-truth neural substrate. The deep VAE model (**B**) takes masks and deficit scores predicting lesion reconstruction and inferring substrate from a single latent space (**C**). The training dynamic (**D**) shows the ability of the model to reconstruct both training (blue) and validation (orange) data sets and accurately infer the neural substrate (green line). The underlying deficits scores used during fine-tuning (**E**) highlight the ability of the model to infer complexity with significantly different distributions as given in the inference data set deficit score (**F**).

REFERENCES

1. Vaidya AR, Pujara MS, Petrides M, Murray EA, Fellows LK. Lesion Studies in Contemporary Neuroscience. Trends Cogn Sci. Published online 2019. doi:10.1016/j.tics.2019.05.009
2. Siddiqi SH, Kording KP, Parvizi J, Fox MD. Causal mapping of human brain function. Nat Rev Neurosci. 2022;23(6):361-375., doi:10.1038/s41583-022-00583-8
3. Giles D, Gray R, Foulon C, et al. Individualized prescriptive inference in ischaemic stroke. arXiv [q-bioQM]. Published online January 25, 2023. https://arxiv.org/abs/2301.10748
4. Pombo G, Gray R, Nelson APK, Foulon C, Ashburner J, Nachev P. Deep variational lesion-deficit mapping. arXiv [csLG]. Published online May 27, 2023. http://arxiv.org/abs/2305.17478
5. Kingma DP, Rezende DJ, Mohamed S, Welling M. Semi-supervised learning with deep generative models. arXiv [csLG]. Published online June 20, 2014. Accessed September 24, 2025. http://arxiv.org/abs/1406.5298
6. Brown TB, Mann B, Ryder N, et al. Language Models are Few-Shot Learners. ArXiv [csCL]. Published online May 28, 2020. http://arxiv.org/abs/2005.14165

71. Inferring Human Connectome Directionality from Macaque Tracer Data and Its Dynamical Impact

Nan Huang[1*], Huifang Wang[1], Claudia A.M. Gandini Wheeler-Kingshott[2], Alain Destexhe[3], Egidio D'Angelo[4], Nigel P Pedersen[5], Viktor Jirsa[1]

[1] Institut de Neurosciences des Systèmes (INS), UMR1106, Aix-Marseille Université, Marseille, France
[2] NMR Research Unit, Queen Square MS Centre, Department of Neuroinflammation, UCL Institute of Neurology, Faculty of Brain Sciences, University College London, WC1B 5EH, London, UK
[3] Paris-Saclay University, CNRS, Paris-Saclay Institute of Neuroscience (NeuroPSI), Saclay, France.
[4] Department of Brain and Behavioral Sciences, University of Pavia, Via Forlanini 6, 27100, Pavia, Italy
[5] Department of Neurology, and UC Davis Comprehensive Epilepsy Center, University of California, Davis School of Medicine, Center for Neuroscience, Davis, CA 95618, USA
* nan.HUANG@univ-amu.fr

Introduction
Human whole-brain models typically rely on diffusion-weighted MRI (DWI)–derived structural scaffolds that provide undirected estimates of connection strength but omit axonal directionality. Directed projections—feedforward, feedback and recurrent loops—profoundly shape network stability, information flow and causal propagation[1,2]; therefore, undirected scaffolds limit a model's ability to capture direction-sensitive phenomena. Invasive tracing in non-human primates remains the gold standard for mesoscale directionality. Given practical and ethical constraints on analogous human data, cross-species inference from macaque tracer datasets provides a principled route to impute putative directionality onto human connectomes, while recognizing species-specific differences in topology.

Keywords: *connectivity; directed graph; brain dynamics; whole brain simulation*

Methods
We constructed a directed human structural scaffold by mapping macaque tracer evidence (CocoMac)[3] to a human parcellation (HCPex) via correspondences defined through 42 homologous white-matter tracts[4]. For each ordered region pair we estimated a projection probability from macaque tracer presence and retained directed edges in the top 20% as a putative directional backbone. Group-average diffusion weights from 100 HCP-YA subjects were assigned to these directed edges to yield a weighted, directed human network. As a control, we generated a symmetrized variant of the directed scaffold (Aij=Aji) to dissociate orientation effects from topology/weight changes. Whole-brain dynamics were simulated with The Virtual Brain (TVB) across three substrates (undirected, directed, symmetrized), sampling global coupling (G) and noise amplitude (σ) to identify parameter regimes that reproduce empirical resting-state signatures.

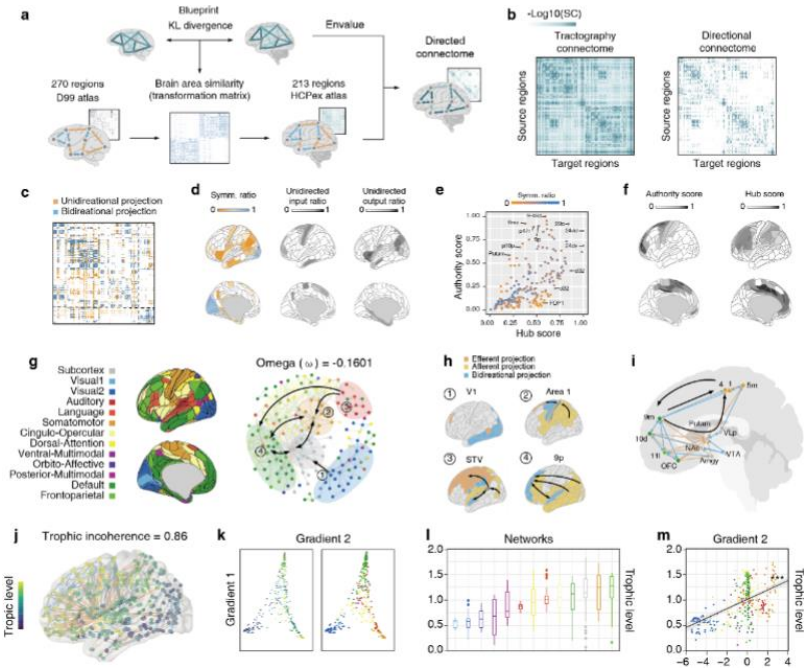

Figure.1: Inferred human brain directed connectome and its network characteristics

Results

The tracer-informed network displays spatially heterogeneous asymmetries: parietal and portions of frontal cortex are relatively incoming-dominated, whereas insular and occipital sectors are more outgoing-biased. Hub regions exhibit distinct in/out strength profiles. Topologically, the network retains small-world organization (ω = −0.16) and reproduces canonical projection motifs (e.g., visual/auditory → prefrontal; prefrontal → basal ganglia → motor). Trophic-level analysis of the directed graph reveals hierarchical ordering that correlates more strongly with the second cortical gradient reported by Margulies et al. [5] than with the principal gradient. Although numerous unidirectional edges are introduced, global trophic incoherence and other measures indicate the network does not reduce to a strictly feedforward architecture; reciprocal loops persist. TVB simulations show that inclusion or removal of directed edges potentially shifts the network dynamic; however, as the work is not yet complete, further experimental evidence is currently required.

Discussion

Macaque-guided directionality systematically alters structural properties of human whole-brain models. Cross-species inference is a pragmatic, biologically grounded strategy to enrich human connectomes, but it carries limitations: thresholding choices, sample size, tract correspondence accuracy, modality mismatches between tracer presence and tractography weights, and cell-type specificity. Future work should prove robustness to thresholding, validate predictions with causal perturbations and subject-specific fits, and incorporate laminar/scale priors. Overall, tracer-informed directionality is a valuable addition for probing direction-sensitive neural dynamics and refining mechanistic interpretations of whole-brain activity. We predict that this approach will enhance virtual brain twin performance and whole-brain modeling, supporting applications in multiple brain disorders and clinical decision-making.

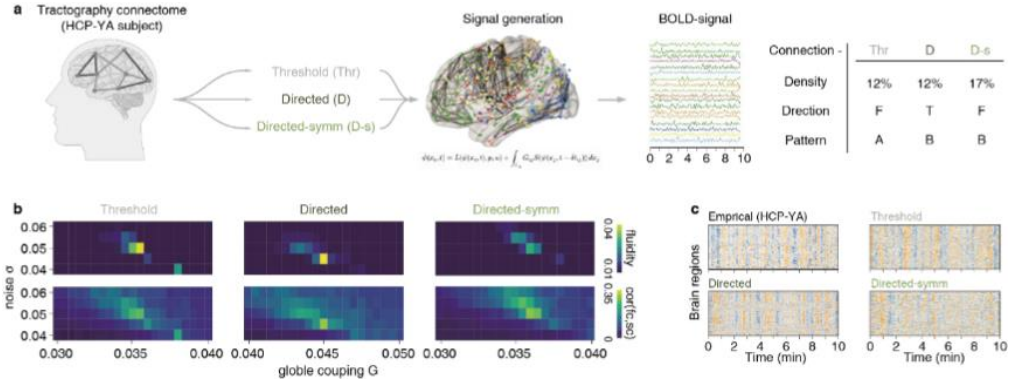

Figure.2: Differentiated resting-state brain dynamics arising from directionality of connectome

References:
1. Johnson S. Digraphs are different: why directionality matters in complex systems. J Phys Complex. 2020;1(1):015003. doi:10.1088/2632-072X/ab8e2f
2. Nartallo-Kaluarachchi R, Kringelbach ML, Deco G, Lambiotte R, Goriely A. Nonequilibrium physics of brain dynamics. arXiv. Preprint posted online April 16, 2025. doi:10.48550/arXiv.2504.12188
3. Modha DS, Singh R. Network architecture of the long-distance pathways in the macaque brain. Proc Natl Acad Sci. 2010;107(30):13485-13490. doi:10.1073/pnas.1008054107
4. Mars RB, Sotiropoulos SN, Passingham RE, et al. Whole brain comparative anatomy using connectivity blueprints. eLife. 2018;7:e35237. doi:10.7554/eLife.35237
5. Margulies DS, Ghosh SS, Goulas A, et al. Situating the default-mode network along a principal gradient of macroscale cortical organization. Proc Natl Acad Sci. 2016;113(44):12574-12579. doi:10.1073/pnas.1608282113

72. Co-simulation framework combining detailed CA1 point neuron model with high- resolution virtual brain model

Tartarini L.[1*], Triebkorn P.[2], Gandolfi D.[3], Wang H.[2], Jirsa V.[2], Mapelli J.[1**]

1. Department of Biomedical, Metabolic and Neurosciences, University of Modena and Reggio Emilia, Italy
2. Aix Marseille Univ, INSERM, INS, Inst Neurosci Syst, Marseille, France.
3. Department of Engineering "Enzo Ferrari," University of Modena and Reggio Emilia, Italy

* lorenzo.tartarini@unimore.it
** jonathan.mapelli@unimore.it

Background. The human brain is a fascinating complex system expressing behavioral and cognitive functions that result from the interplay of multiple mechanisms occurring at different temporal and spatial scales [1]. Addressing the multiscale dynamics of the human brain is challenging and requires the development of advanced computational models, implementing mechanistic hypotheses about neural dynamics spanning multiple spatiotemporal scales [1,2]. Methods. In this work, a co-simulation framework has been designed, implemented and tested, combining a microscopically detailed spiking neural network model using the NEST framework [3] with macroscopic whole-brain models using The Virtual Brain (TVB) simulator [4]. The specific brain region simulated in NEST is the CA1 region of the human hippocampus [5]. We used a downsampled version of the right CA1 which has been scaled from the original 5.28 million neurons and 40 billion synapses to 110 000 neurons and 4.3 million connections. Each neuron is simulated with the Hill-Tononi model [6] and Tsodyks [7] synaptic connections. The macroscopic brain model in TVB was based on the surface mesh and

corresponding connectivity of the right hemisphere hippocampal regions, fusiform gyrus, para-hippocampal gyrus and entorhinal cortex, as extracted from MRI data, resulting in a total of 16 636 neural masses. The dynamics of each neural mass is governed by the Spatial Epileptor Model (SEM) [8] which consists of rapid-discharges (DS) states, spike-and-wave events (SWE) states and, a permittivity state which drives the system between ictal and non- ictal periods. The conversion from SEM states to spiking activity has been carried out based on the spiking synchronization due to slow (SWE) dynamics seen in [9]. The transfer function consists of a Rectified Linear Unit like approximation of the instantaneous SEM activity with two main components, driven by DS and SWE states. The conversion has been tuned to reproduce the behavior from [9]. For each CA1 neural mass, the rate coded activity is coupled to a corresponding NEST subpopulation through the Message Passing Interface protocol. Such subpopulations have been clustered by computing geodesic Laplace coordinates of both NEST neurons and TVB nodes along the Anterior-Posterior and Proximal-Distal axes of the hippocampal surfaces, as computed by the HippUnfold toolbox [10]. The rate-coded TVB activity of each node is thus received by custom designed Poisson generators, integrated in the NEST C++ codebase, which stimulates homogeneously the corresponding NEST subpopulation. Tests were carried out by setting excitability parameters to reproduce epileptic CA1 region in the TVB model, and perturbating a few CA1 nodes to start a seizure. Then, synchronicity between the two spatiotemporal scales was analyzed with the phase-locked histogram (PLH) between each TVB node SEM rate-coded activity phase and the corresponding NEST subpopulation spike histogram (Fig. 2K).

Results and discussion. Preliminary tests validated the system by keeping both simulations in a steady state and perturbing the neural-mass-models side of the co-simulation to verify seizure propagation to the finer scale. The high resolution TVB embedded with SEM neural mass models exhibit seizure-like activity in the theta-gamma bands, propagating across the brain surface (Fig 2G). NEST simulation activity synchronization with the whole brain model subset results in corresponding active regions (Fig. 2A-F, I) and phase-locked histogram centered at 0 degrees of the SEM derived driving signals (figure 2I). The proposed framework represents a step forward in integrating microscopically detailed networks with whole-brain models, enabling the study of dynamic interactions across multiple scales. Future efforts will focus on large-scale simulations on both ends, conducting deeper analysis of meso- and macro-scale emergent features across different frequency bands and investigating the long-range effects of local phenomena.

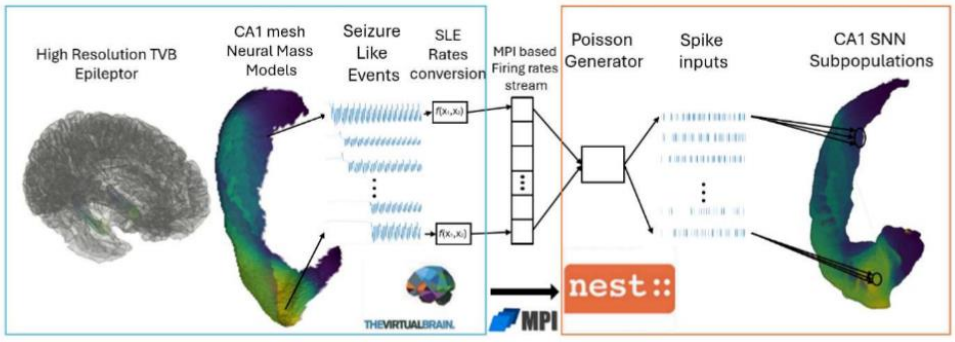

Figure 1. From left to right, High Resolution TVB region around the right hippocampus CA1, the CA1 region neural masses with ids color coded, Spatial Epileptor Model Seizure Like Events propagating from an onset site, conversion to spiking rates, synchronized communication using the MPI protocol of the computed rates to the NEST simulation, conversion to spike events using a custom designed poisson generator, corresponding spikes trains, 3D plot of the NEST population with corresponding TVB ids color coded.

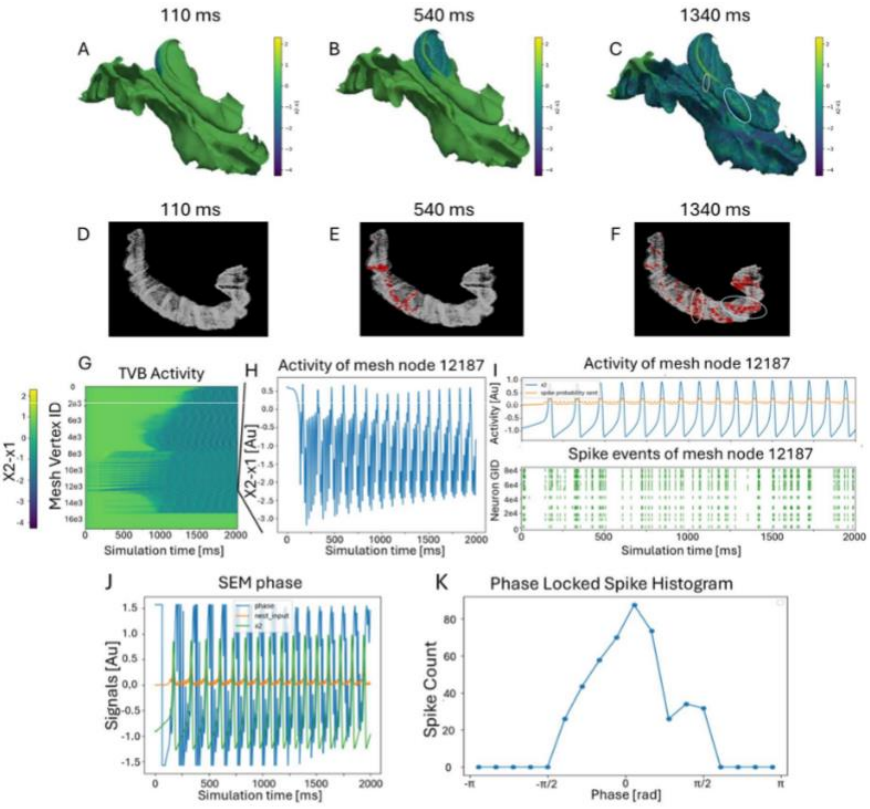

Figure 2. (A-C) Temporal evolution of the TVB SEM showing the propagation of seizure-like events at three different time points. The onset site of the seizure comprises a subset of CA1 vertices. (D-F) Temporal evolution of the NEST spiking neural network showing coherent activity (red dots) between TVB vertices and CA1 point neurons. Circled regions in C and F highlight the same regions in the two models. (G) Propagation of TVB node activity (x2-x1) as a time series across 16636 vertices. (H) Timeseries of a single TVB node. (I) Comparison between TVB node x2 driving signal (upper panel, blue), the activity converted spike probability sent to the NEST model (upper panel, yellow) and generated spike activity in the NEST model (lower panel). (J) The phase of the spike probability sent from TVB to Nest Simulator computed using the Hilbert transform and (K) average phase locked spike histogram across CA1 vertices and corresponding spiking subpopulations.

Keywords. Multiscale co-simulation, Human Hippocampus, Spiking Neural Networks, High Resolution Virtual Brain, Spatial Epileptor, Neural Mass Models

Acknowledgements

Data were provided in part by the Human Connectome Project, WU-Minn Consortium (Principal Investigators: David Van Essen and Kamil Ugurbil; 1U54MH091657) funded by the 16 NIH Institutes and Centers that support the NIH Blueprint for Neuroscience Research; and by the McDonnell Center for Systems Neuroscience at Washington University."

PRJ-0408-FAR2024-UNIMORE-EPICURE-D.GANDOLFI (E93C24002030005)

References:

1. D'Angelo E, Jirsa V. The quest for multiscale brain modeling. Trends Neurosci. 2022 Oct;45(10):777-790. doi:10.1016/j.tins.2022.06.007. Epub 2022 Jul 27. PMID: 35906100.
2. Kusch L, Diaz-Pier S, Klijn W, Sontheimer K, Bernard C, Morrison A and Jirsa V (2024) Multiscale co- simulation design pattern for neuroscience applications. Front. Neuroinform. 18:1156683. doi: 10.3389/fninf.2024.1156683

3. Gewaltig M-O, Diesmann M, NEST (Neural Simulation Tool), Scholarpedia 2(4):1430, (2007)
4. Sanz-Leon P., Knock S. A., Spiegler A., Jirsa V. K., Mathematical framework for large-scale brain network modeling in The Virtual Brain, NeuroImage, Volume 111, 2015.
5. Gandolfi, D., Mapelli, J., Solinas, S.M.G. et al. Full-scale scaffold model of the human hippocampus CA1 area. Nat Comput Sci 3, 264–276 (2023). https://doi.org/10.1038/s43588-023-00417-2
6. Hill S., Tononi G., Modeling Sleep and Wakefulness in the Thalamocortical System, J Neurophysiol 93, 2005. doi:10.1152/jn.00915.2004
7. Tsodysk M. V., Markram H., The neural code between neocortical pyramidal neurons depends on neurotransmitter release probability. PNAS 94(2), 719–723. https://doi.org/10.1073/pnas.94.2.719 (1997).
8. Proix, T., Jirsa, V.K., Bartolomei, F., Guye, M., & Truccolo, W. (2018). Predicting the spatiotemporal diversity of seizure propagation and termination in human focal epilepsy. Nature Communications, 9, 1088. https://doi.org/10.1038/s41467-018-02973-y
9. Truccolo, W., Ahmed, O.J., Harrison, M.T., Eskandar, E.N., Cosgrove, G.R., Madsen, J.R., Blum, A.S., Potter, N.S., Hochberg, L.R., & Cash, S.S. (2014). Neuronal ensemble synchrony during human focal seizures. Journal of Neuroscience, 34(30), 9927–9944. https://doi.org/10.1523/JNEUROSCI.4567-13.2014
10. DeKraker, J., Haast, R. A., Yousif, M. D., Karat, B., Lau, J. C., Köhler, S., & Khan, A. R. (2022). Automated hippocampal unfolding for morphometry and subfield segmentation with HippUnfold. Elife, 11, e77945

73. Accelerating Brain Simulations using High Performance Computing

Maren Frings[1*], Han Lu[1**], Ekaterina Zossimova[1], Sinovia Fotiadou[1], Thorsten Hater[1], Michiel van der Vlag[1], Sandra Diaz[1***]

[1]Forschungzentrum Jülich GmbH
* m.frings@fz-juelich.de
** ha.lu@fz-juelich.de
*** d.siaz@fz-juelich.de

Keywords: Brain Simulations; High-Performance Computing; EBRAINS Base Infrastructure; Arbor; TVB; NEST; Co-Simulation

Abstract
High-performance computing (HPC) has become an indispensable tool for scientific research, enabling the simulation, analysis, and visualization of complex systems across a wide range of disciplines. In neuroscience, HPC empowers researchers to explore the intricate mechanisms of brain functions, from single-cell dynamics to whole-brain network interactions. Our team develops different tools and EBRAINS infrastructure components to serve this purpose at the microscopic, mesoscopic, and macroscopic levels. The poster shows a few examples of the studies we conducted and showcases how the EBRAINS RI can be used to solve scientific questions. By developing tools like Arbor and TVB, the Arbor-TVB co-simulation framework, and by coupling NEST with AI tools, we have enabled neuroscientists to explore brain dynamics in health and disease across multiple scales. The EBRAINS research infrastructure hosts these tools, enables interoperability, and provides users with access to a vast range of open-source neuroscience datasets. These efforts help to bridge the gap between neuroscience and HPC.

74. Global white-matter disruption in postherpetic neuralgia indexed by PSMD

Daeseok Oh[1*], Kang Min Park[2]

[1] Department of Anesthesiology and pain medicine, Inje University Haeundae Paik Hospital, Busan, Republic of Korea
[2] Department of Neurology, Inje University Haeundae Paik Hospital, Busan, Republic of Korea
* h00508@paik.ac.kr

INTRODUCTION/MOTIVATION
Postherpetic neuralgia (PHN) is increasingly linked to central white-matter (WM) alterations, yet voxel- or ROI-based diffusion tensor imaging (DTI) may miss diffuse injury. We evaluated whether peak width of skeletonized mean diffusivity (PSMD)—a histogram-based, fully automated global DTI marker—captures PHN-related WM burden and offers superior case–control discrimination compared with conventional DTI metrics.

METHODS
In a university-hospital case–control cohort (PHN n=42; age/sex-matched healthy controls n=41), we acquired 3T DTI and computed PSMD from skeletonized MD histograms (FSL-TBSS framework), alongside FA/MD/AD/RD. Group differences were tested with general linear models (covariates: age, sex), receiver-operating-characteristic (ROC) curves compared discrimination, and multivariable logistic regression assessed independent predictors of PHN status. Exploratory analyses examined hemispheric PSMD versus rash laterality and correlations with age, DN4, pain intensity/interference, and disease duration.

RESULTS AND DISCUSSION
The PSMD was significantly higher in patients with PHN compared to healthy controls ($2.862 \pm 0.436\times10^{-4}$ vs. $2.369 \pm 0.407\times10^{-4}$ mm^2/s, $p < 0.001$). Additionally, the MD and AD were higher in patients with PHN compared to healthy controls (0.854 ± 0.035 vs. 0.836 ± 0.030, $p = 0.012$; 1.292 ± 0.036 vs. 1.264 ± 0.033, $p < 0.001$; respectively). PSMD showed the highest diagnostic accuracy, with an area under the curve (AUC) of 0.816 ($p < 0.001$). A binary logistic regression model was performed with PSMD, AD, and MD as independent variables to distinguish patients with PHN from healthy controls, and among the predictors, PSMD was a significant independent factor ($p = 0.002$), whereas MD ($p = 0.667$) and AD ($p = 0.136$) did not reach statistical significance.

PHN shows a widespread, non-lateralized white-matter burden that is efficiently summarized by PSMD. Its superior discrimination over conventional DTI indices suggests a diffuse rather than tract-specific signal, where histogram-based metrics avoid spatial dilution and multiple-comparison penalties. The lack of associations with DN4, pain intensity, or duration—despite clear group differences—implies PSMD indexes a trait-like substrate (aging/chronic-disease–related microstructural compromise) rather than momentary symptoms, consistent with prior links between PSMD and global WM integrity in older adults. Clinically, PSMD's automation and portability make it attractive for trial screening/stratification and, pending longitudinal validation, as an auxiliary outcome. Limitations include the cross-sectional design (vulnerability vs. consequence), and PSMD's sensitivity without biological specificity; future work should benchmark against free-water correction, NODDI/SMT, and fixel-based metrics. Potential confounds (small-vessel disease, motion, comorbidities, medications) require systematic control, and harmonization will be important for multi-site studies. Although PSMD did not track symptom severity here, it may capture staging or recovery; longitudinal and interventional cohorts integrating network-level graph metrics and cognitive endpoints are needed to test responsiveness and mechanisms.

In summary, PSMD emerges as a practical, harmonizable biomarker of diffuse WM involvement in PHN, complementing tract/network analyses and enabling standardized, cross-site phenotyping and biologically informed enrichment in future trials.

Keywords: postherpetic neuralgia; diffusion tensor imaging; white matter

REFERENCES

[1] Baykara E, Gesierich B, Adam R, et al. A novel imaging marker for small vessel disease based on skeletonization of white matter tracts and diffusion histograms. Ann Neurol. 2016;80(4):581-592. doi:10.1002/ana.24758.
[2] Low A, Mak E, Stefaniak JD, et al. Peak width of skeletonized mean diffusivity as a marker of diffuse cerebrovascular damage. Front Neurosci. 2020;14:238. doi:10.3389/fnins.2020.00238.
[3| Raposo N, Remer J, Boulouis G, et al. Peak width of skeletonized mean diffusivity is altered in cerebral amyloid angiopathy and associates with processing speed. AJNR Am J Neuroradiol. 2021;42(6):1130-1136.
doi:10.3174/ajnr.A7042.
[4] Wu Y, Gu L, Hong S, et al. Altered white matter microstructure in herpes zoster and postherpetic neuralgia determined by automated fiber quantification. Brain Sci. 2022;12(12):1668. doi:10.3390/brainsci12121668.
[5] Qiu J, Yi M, Zhang M, et al. The brain's structural differences between postherpetic neuralgia and low back pain. Sci Rep. 2021;11(1):22455. doi:10.1038/s41598-021-01915-x.

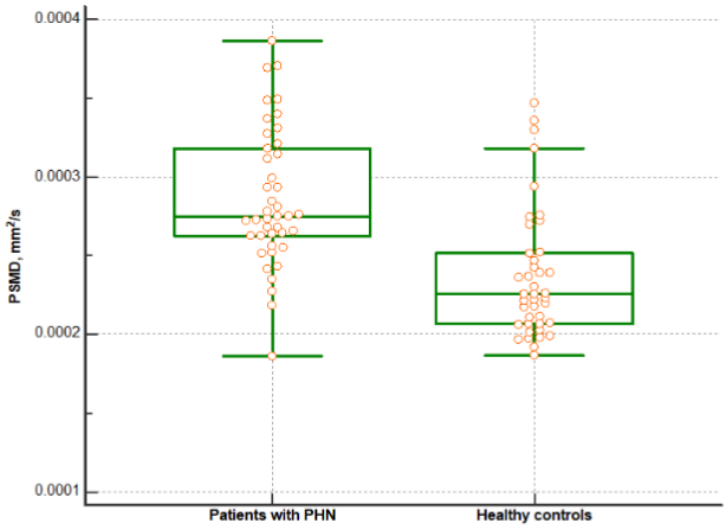

Figure 1. Comparison of PSMD between patients with postherpetic neuralgia and healthy controls
The figure shows that the PSMD is significantly higher in patients with PHN compared to healthy controls ($2.862 \pm 0.436 \times 10^{-4}$ vs. $2.369 \pm 0.407 \times 10^{-4}$ mm^2/s, $p < 0.001$).

PSMD: Peak Width of Skeletonized Mean Diffusivity, PHN: Postherpetic neuralgia

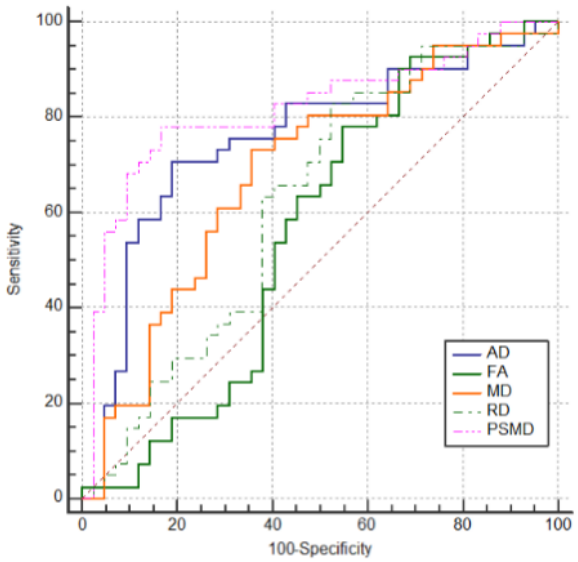

Figure 2. ROC curve analysis
The figure represents that PSMD shows the highest diagnostic performance with an AUC of 0.816 (95% CI: 0.716-0.893, p < 0.001). In contrast, FA (AUC = 0.562, 95% CI: 0.448-0.670, p = 0.347) demonstrates poor discriminative ability, while MD (AUC = 0.685, 95% CI: 0.573-0.782, p = 0.001), AD (AUC = 0.754, 95% CI: 0.648-0.842, p < 0.001), and RD (AUC = 0.621, 95% CI: 0.508–0.726, p = 0.053) show moderate performance.

PSMD: peak width of skeletonized mean diffusivity, FA: fractional anisotropy, MD: mean diffusivity, AD: axial diffusivity, RD: radial diffusivity

75. Spatial Clustering of Excitatory Synapses Enhances Computational Efficiency in CA1 Pyramidal Neurons

Simone Tasciotti[1,2], Daniel Maxim Iascone[3], Spyridon Chavlis[2], Luke A. Hammond[3,#], Yardena Katz[3], Attila Losonczy[3,4], Franck Polleux[3,4], Panayiota Poirazi[2,5]

[1] Department of Biology, University of Crete, Heraklion, Greece
[2] Institute of Molecular Biology and Biotechnology, Foundation for Research and Technology-Hellas, Heraklion, Greece
[3] Mortimer B. Zuckerman Mind Brain Behavior Institute, Columbia University, New York, NY, USA
[4] Department of Neuroscience, Columbia University, New York, NY, USA
[5] Lead contact
[#]Present address: Department of Neurology, The Ohio State University, Wexner Medical School, Columbus, Ohio, USA

Introduction
The hippocampus, and particularly its CA1 region, plays a crucial role in spatial navigation and memory formation through the activity of spatially tuned neurons known as place cells. These cells encode specific locations within an environment, forming a cognitive map that supports navigation and memory recall[1]. Although numerous studies have investigated how the properties of CA1 pyramidal neurons (PNs) shape their computation, the influence of the spatial and temporal organization of synaptic inputs on information processing remains unclear. Given that dendritic nonlinearities and active conductances can profoundly modulate neuronal output[2,3], understanding

how the spatial arrangement of synapses affects computation is essential for elucidating the biophysical basis of place cell formation and function.

Methods

To examine how synaptic spatial distribution modulates computation in CA1 PNs, we performed a multimodal investigation combining high-resolution morphological reconstructions, biophysical modeling, and large-scale simulations. We labeled individual CA1 PNs via single-cell electroporation of tdTomato in acute hippocampal slices from adult mice. Using Vaa3D-based automated tracing[4] followed by manual verification, we reconstructed dendritic trees with submicron precision, annotating the location and size of both excitatory and inhibitory synapses[5]. These CA1 PNs reconstructions, first ever with a complete synaptic mapping, served as templates for the generation of multicompartmental, biophysically neuron models using an automated Python-based pipeline built upon the NEURON simulation environment[6]. Ionic channel distributions and kinetics were implemented to ensure physiological accuracy. We then simulated place-tuned input patterns mimicking realistic synaptic activation sequences, approximating the proportion of synaptic clustering and dispersion observed experimentally[7]. Input-output transformations were quantified through spike timing, dendritic voltage propagation, local calcium dynamics, and quantitative measures of place field quality[8].

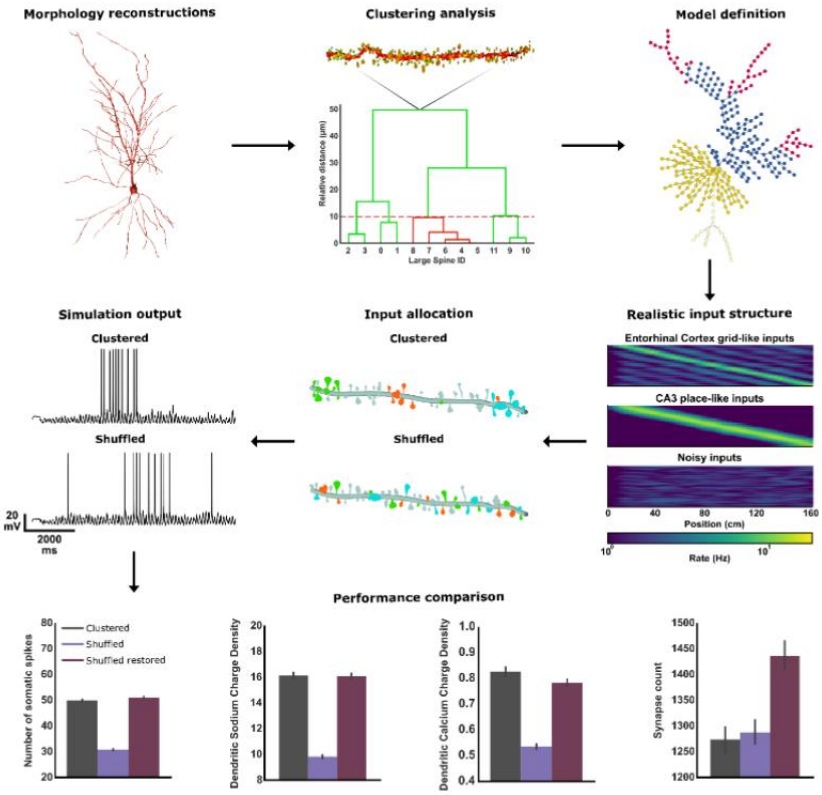

Study Pipeline: Hyperdetailed morphological reconstructions of CA1 PNs are used as a scaffold to build biophysical models and analyzed to extract the synaptic distribution data. Biologically relevant inputs are used to stimulate synapses in Clustered and Shuffled configurations, comparing then the somatic and dendritic outputs. Shuffled performances are then restored by increasing the number of activated synapses.

Results

Morphological reconstruction analysis revealed a non-uniform distribution of excitatory synapses across the dendritic arbor, in contrast to the more uniform organization of inhibitory synapses. Terminal dendrites in both apical and basal domains exhibited higher spine densities than

intermediate segments, resulting in a greater likelihood of large, closely spaced spines (i.e., spine clustering).

Additionally, model simulations predicted that the spatial clustering of excitatory inputs substantially enhanced the computational efficiency of CA1 PNs. Neurons receiving clustered excitatory inputs exhibited enhanced dendritic spike initiation, leading to stronger, place-tuned somatic firing compared to neurons with uniformly distributed inputs. Such clustered arrangements optimized local nonlinear integration, enabling the formation of sharply tuned place fields with fewer active synapses. In contrast, dispersed configurations yielded weaker depolarization spread and reduced dendritic nonlinearity, requiring roughly 15% more active synapses to achieve performance comparable to that of the clustered condition.

Conclusions

This study provides direct evidence that the spatial organization of synaptic inputs is a key determinant of neuronal computation in CA1 PNs. By combining detailed morphological reconstructions with biophysical simulations, we demonstrate that realistic, non-uniform, clustered synaptic activation patterns enhance neuronal selectivity and efficiency, enabling the generation of robust place fields with fewer active synapses. These findings support the view that dendritic processing acts as a form of subcellular parallel computation[3,9], where spatially constrained synaptic ensembles encode localized information with high efficiency[10].

Acknowledgments

We thank all members of the PoiraziLab for their valuable feedback on the project. This project has received funding from the European Union's Horizon 2020 research and innovation programme under the Marie Skłodowska-Curie grant agreement No.860949; Stavros Niarchos Foundation (SNF) and the Hellenic Foundation for Research and Innovation (H.F.R.I.) under the 5th Call of "Science and Society" Action Always strive for excellence – Theodoros Papazoglou" (Project Number: 28056); H.F.R.I call "Basic research Financing (Horizontal support of all Sciences)" under the National Recovery and Resilience Plan "Greece 2.0" funded by the European Union – NextGenerationEU (Project Number: 014941); COFLEX 14941 HFRI P.N. 80147/17.1.24; NIH grant No 1R01MH124867 to P.P.; NIH grants F31NS101820 and F32MH125600 to D.M.I.; NIH-NINDS (R35 NS127232) (FP), and an award from the NOMIS Foundation (FP). A.L. is supported by National Institute of Mental Health (NIMH) R01MH124047 and R01MH124867; National Institute on Aging (NIA) RF1AG080818; National Institute of Neurological Disorders and Stroke (NINDS) Brain Initiative U01NS115530; NINDS R01NS121106, NINDS R01NS131728, and NINDS Brain Initiative R01NS133381

References

1. O'Keefe J, Dostrovsky J. The hippocampus as a spatial map. Preliminary evidence from unit activity in the freely- moving rat. Brain Res. 1971;34(1):171-175. doi:10.1016/0006-8993(71)90358-1
2. Losonczy A, Magee JC. Integrative properties of radial oblique dendrites in hippocampal CA1 pyramidal neurons. Neuron. 2006;50(2):291-307. doi:10.1016/j.neuron.2006.03.016
3. Poirazi P, Brannon T, Mel BW. Arithmetic of subthreshold synaptic summation in a model CA1 pyramidal cell. Neuron. 2003;37(6):977-987. doi:10.1016/s0896-6273(03)00148-x
4. Peng H, Bria A, Zhou Z, Iannello G, Long F. Extensible visualization and analysis for multidimensional images using Vaa3D. Nat Protoc. 2014;9(1):193-208. doi:10.1038/nprot.2014.011
5. Iascone DM, Li Y, Sümbül U, et al. Whole-Neuron Synaptic Mapping Reveals Spatially Precise Excitatory/Inhibitory Balance Limiting Dendritic and Somatic Spiking. Neuron. 2020;106(4):566-578.e8. doi:10.1016/j.neuron.2020.02.015
6. Hines ML, Carnevale NT. The NEURON simulation environment. Neural Comput. 1997;9(6):1179-1209. doi:10.1162/neco.1997.9.6.1179

7. Adoff MD, Climer JR, Davoudi H, Marvin JS, Looger LL, Dombeck DA. The functional organization of excitatory synaptic input to place cells. Nat Commun. 2021;12(1):3558. doi:10.1038/s41467-021-23829-y
8. Skaggs W, McNaughton B, Gothard K. An Information-Theoretic Approach to Deciphering the Hippocampal Code. In: Advances in Neural Information Processing Systems. Vol 5. Morgan-Kaufmann; 1992. Accessed May 28, 2025. https://proceedings.neurips.cc/paper/1992/hash/5dd9db5e033da9c6fb5ba83c7a7ebea9-Abstract.html
9. Bittner KC, Grienberger C, Vaidya SP, et al. Conjunctive input processing drives feature selectivity in hippocampal CA1 neurons. Nat Neurosci. 2015;18(8):1133-1142. doi:10.1038/nn.4062
10. Karbowski J, Urban P. Cooperativity, Information Gain, and Energy Cost During Early LTP in Dendritic Spines. Neural Comput. 2024;36(2):271-311. doi:10.1162/neco_a_01632

76. Stimulation of the Medial Prefrontal Cortex Alters Inhibitory Control Dynamics

Ahsan Khan[1*], Raymond Kai-Yu Tong[2]

[1]Department of Education and Psychology, Academy of Wellness and Human Development, Hong Kong Baptist University, Hong Kong, China
[2]Department of Biomedical Engineering, The Chinese University of Hong Kong, Hong Kong, China
*ahsankhan@hkbu.edu.hk

INTRODUCTION
The prefrontal cortex plays a pivotal role in inhibitory control, enabling the brain to detect and suppress competing or irrelevant information during episodic memory retrieval. These control processes rely on coordinated activity across distributed brain networks. Non-invasive brain stimulation offers a powerful approach to causally modulate these mechanisms by targeting key nodes within these networks.

METHODS
In this study, we examined how transcranial direct current stimulation (tDCS) over the medial prefrontal cortex (mPFC) influences inhibitory control during memory retrieval using a retrieval-induced forgetting (RIF) paradigm. RIF occurs when selectively recalling target memories leads to the subsequent forgetting of related, non-target information a hallmark of inhibitory control at work. We utilized electroencephalography (EEG) to understand stimulation induced changes in brain circuitry.

RESULTS
Stimulation of the mPFC produced a selective reduction in RIF indicating weakened inhibitory control processes while leaving memory facilitation effects unchanged. Moreover, stimulation disrupted performance on a flanker interference task, suggesting overlap between inhibitory control mechanisms engaged during memory retrieval and those involved in resolving response conflict. The decrease in memory inhibition was associated with stronger beta-band (15–17 Hz) desynchronization in the left dorsolateral prefrontal cortex (DLPFC) during an early retrieval phase and sustained beta desynchronization in the parietal cortex during later stages, potentially reflecting retrieval of less competitive memories.

DISCUSSION

These findings demonstrate that direct current stimulation of the mPFC disrupts inhibitory control during memory retrieval by inducing network-level desynchronization across fronto-parietal regions. The results further indicate that active forgetting of competing memories and successful retrieval are functionally independent processes. Beta-band desynchronization in the left DLPFC emerged as a key neural predictor of reduced inhibition, highlighting a causal role of mPFC-mediated network dynamics in controlling memory interference.

Keywords: Inhibitory Control, Episodic Memory, Medial Prefrontal Cortex, tDCS, Retrieval-Induced Forgetting

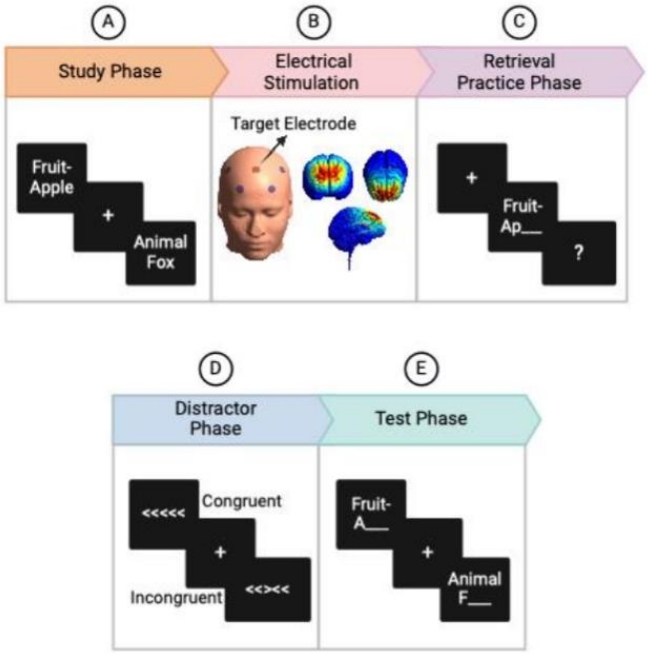

Figure 1. ***Experimental Design.*** *(A) During the study phase, participants learned word–category pairs for a later test. (B) A 15-min stimulation period followed, with electrodes arranged in a ring configuration (target: Fz; returns: AF3, AF4, FC3, FC4; SimNIBS model shown). (C) Immediately after stimulation, participants completed three retrieval-practice trials for selected exemplars (RP+ items). (D) A 5-min distractor task preceded (E) the final memory test assessing recall for all studied items.*

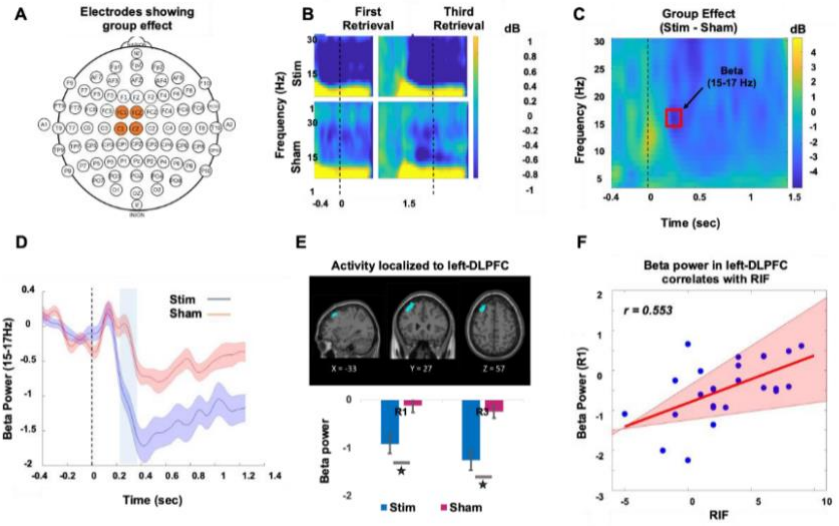

Figure 2. ***Beta desynchronization in the left DLPFC predicts modulation of RIF.*** *(A) Electrodes showing a significant group effect. (B) Time–frequency plots from the first (R1) and third (R3) retrieval sessions reveal stronger beta (15–17 Hz) desynchronization in the stimulation group. (C) Group differences (stimulation – sham) were significant within 0.24–0.32 s, highlighted in red. (D) Mean beta power (15–17 Hz) in significant channels shows greater desynchronization for stimulation across R1 and R3. Shaded regions denote ± SEM; blue shading marks the significant window. (E) Source localization identified the effect in the left DLPFC, driven by stronger beta desynchronization in the stimulation group ($p < 0.01$). (F) Beta desynchronization during R1 correlated with RIF magnitude in the stimulation group.*

77. Single-cell transcriptional analysis of long non-coding RNAs during visual imprinting memory in chicks

Vincenzo Lagani[1,2 #], Lela Chitadze[2], Ana Cecilia Gonzalez Alvarez[1], Teimuraz Bokuchava[2], Giulia Sansone[1], Veriko Bokuchava[2], Lia Tsverava[2,3], Aragorn Jones [4], Steven Lisgo[4], Xabier Martinez De Morentin[1], Robert Lehmann[1], Jesper Tegner[1,5,6,7], Leena Ali Ibrahim[1], Brian J. McCabe [8], Zaza Khuchua[2], David Gomez Cabrero[1,9 #], and Revaz Solomonia[2,3 #]

[1] Biological and Environmental Sciences and Engineering Division (BESE), King Abdullah University of Science and Technology (KAUST), Thuwal, Saudi Arabia.
[2] School of Natural Sciences and Medicine, Institute of Chemical Biology, Ilia State University, Tbilisi, Georgia
[3] Iv. Beritashvili Centre of Experimental Biomedicine, Tbilisi, Georgia
[4] Biosciences Institute, Newcastle University, Newcastle upon Tyne, United Kingdom
[5] Electrical and Mathematical Sciences and Engineering Division, King Abdullah University of Science and Technology (KAUST), Thuwal, Saudi Arabia.
[6] Department of Medicine, Center for Molecular Medicine, Karolinska Institutet, Karolinska University Hospital, Stockholm, Sweden.
[7] Science for Life Laboratory, Solna, Swede
[8] Department of Zoology, University of Cambridge, Cambridge, United Kingdom
[9] Translational Bioinformatics Unit, Navarrabiomed, Fundacion Miguel Servet, Universidad Publica de Navarra (UPNA), IdiSNA, Pamplona, Spain
[#]Correspondence: vincenzo.lagani@kaust.edu.sa, david.gomezcabrero@kaust.edu.sa, revaz_solomonia@iliauni.edu.ge

A comprehensive understanding of the fundamental mechanisms of learning and memory remains elusive to neuroscientists. Visual imprinting in domestic chicks is a rapid and robust form of learning that underlies recognition memory formation. Converging evidence indicates that the intermediate medial mesopallium (IMM), serves as the primary storage site for information about the imprinting stimulus[1]. The different types of IMM cells undergo distinct learning and memory-related molecular changes during visual imprinting, however, the cell type, memory related specific changes are poorly studied. For further understanding the molecular mechanisms of memory, it is crucial to understand in more detail in which cell type learning-related changes occur. We conducted single nuclei RNA-SEQ analysis, and initially, we have: (i) characterized approximately >54,000 IMM cells and identified four major populations of neuronal and non-neuronal cells, each spanning several different clusters, using well-established marker genes; (ii) revealed differences in gene expression patterns according to these defined cell groups between good learners and untrained chicks 24h h after imprinting training which is a time period when learning-related molecular changes are typically more strongly expressed in the left IMM[2,3]. For each cell cluster, virtually 50% of the significantly changed transcripts were lncRNAs.

Using real-time polymerase chain reaction (RT-PCR), we also examined whether the observed changes for the following two lncRNAs were specific to imprinting memory: (1) ENSGALG00010007489 – expressed only in cluster 2, which constitutes only 4% of glutamatergic neurons and (2) ENSGALG00010026609 - ubiquitously expressed candidate. Moreover, fluorescence in situ hybridization (FISH) experiments were conducted to study the putative expression of ENSGALG00010007489 in the glutamatergic neurons of the IMM.

The results show a significant correlation between ENSGALG00010007489 expression and preference score (Pearson's correlation = 0.64, p = 0.03, Figure 2-A). The observed positive correlation directly results from learning during training. However, a positive correlation between ENSGALG00010026609 and preference score (r = 0.63, P = 0.037; Figure 2-B) was driven by a predisposition to learn. No significant learning-related changes were evident in other brain regions.

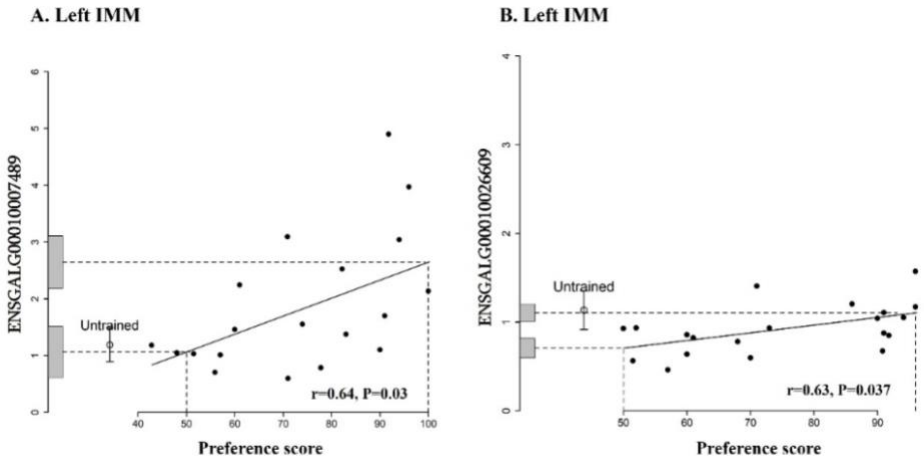

Figure 2. Standardized relative amount of lncRNA ENSGALG00010007489 (A) and ENSGALG00010026609 (B) in the left IMM plotted against preference score. For both lncRNA the correlations are significant (P=0.03 and P=0.037 respectively).

The tissue distribution and subcellular localization of both lncRNAs was analyzed using quantitative RT-PCR. ENSGALG00010007489 expression was detected only in brain. In contrast, ENSGALG00010026609 is detected across all studied tissues (heart, muscle, liver, lung and brain). ENSGALG00010007489 levels were found to be over 100-fold higher in the nuclear fraction while ENSGALG00010026609 is present both in the nuclear and cytoplasmic fractions. Furthermore, the triple FISH experiments unequivocally confirm the specific localization of ENSGALG00010007489 in the cluster of glutamatergic cells and increase associated with memory.

Overall, the present study, for the first time (i) provides compelling evidence for a previously unrecognized role of long non-coding RNAs (lncRNAs) in long-term memory; and (ii) uncovers a molecular signature of visual imprinting in chicks at single-cell resolution.

Keywords:
visual imprinting, learning, memory, Single-cell transcriptomic, IMM, long non-coding RNAs,

REFERENCES

1. Horn G. Nat Rev Neurosci. 2004;5(2):108-120. doi:10.1038/nrn1324
2. Solomonia RO, McCabe BJ. doi:10.1016/j.neubiorev.2014.09.013
3. Chitadze L et al., PLoS One. 2024;19(1):e0297166. doi:10.1371/journal.pone.0297166

78. Association of Early Hyperthermia With Infarct Expansion and Blood–Brain Barrier Dysfunction After Ischemic Stroke

Crhistian-Mario Oblitas, Pablo Hervella, Ramón Iglesias-Rey

Neuroimaging and Biotechnology Laboratory (NOBEL), Clinical Neurosciences Research Laboratory (LINC), Health Research Institute of Santiago de Compostela (IDIS), Santiago de Compostela, 15706 A Coruña, Spain

Introduction: Early hyperthermia, occurring within the first 24 hours after ischemic stroke (IS), has consistently been linked to worse neurological outcomes [1-3]. However, the underlying mechanisms contributing to this relationship remain unclear. One possible explanation involves increased blood–brain barrier (BBB) permeability, which could exacerbate secondary injury and promote infarct expansion. This study aimed to explore whether BBB disruption contributes to the association between early hyperthermia and early infarct growth (EIG) after IS.

Methods: We performed a retrospective analysis based on a prospective ischemic stroke biobank. Early infarct growth (EIG) was defined as the percentage increase between the infarct volume (mL) measured by diffusion-weighted Magnetic Resonance Imaging at admission and the volume (mL) observed in the control Computed Tomography scan performed between days 4 and 7. Hyperthermia was defined as an axillary body temperature ≥ 37.5 °C within the first 24 h post-stroke. Serum soluble tumor necrosis factor-like weak inducer of apoptosis (sTWEAK) concentrations were determined by ELISA as a biomarker potentially reflecting BBB dysfunction.

Results: Among 519 patients (45.6% women), 102 (19.7%) presented early infarct growth. Axillary body temperature correlated linearly with EIG (Pearson's $r = 0.46$; $p < 0.001$), indicating that higher early temperatures were associated with greater infarct expansion. Elevated sTWEAK levels also showed predictive value for EIG (c-statistic = 0.74; 95% CI 0.69–0.79), with an optimal cutoff > 3000 pg/mL. Moreover, microalbuminuria correlated strongly with sTWEAK concentrations (Pearson's $r = 0.75$; $p < 0.001$), suggesting a link between systemic endothelial dysfunction and BBB permeability. In the multivariate analysis, hyperthermia (adjusted OR 24.21; 95% CI 12.03–39.12), sTWEAK > 3000 pg/mL (adjusted OR 16.43; 95% CI 3.71–72.70), leukoaraiosis (adjusted OR 10.42; 95% CI 2.68–39.08), and microalbuminuria (adjusted OR 1.02; 95% CI 1.00–1.12) were independently associated with early infarct growth.

Discussion: In this cohort, hyperthermia within the first 24 h after ischemic stroke was independently associated with early infarct growth. The concurrent association of EIG with microalbuminuria, leukoaraiosis, and elevated sTWEAK levels suggests that increased BBB permeability may mediate the link between elevated body temperature and infarct expansion.

Ref:

1. Oblitas C-A, Sampedro-Viana A, Fernández-Rodicio S, et a. Hyperthermia and Early Growth of Cerebral Infarct: The Potential Role of Blood-Brain Barrier Permeability. Transl Stroke Res. 2025 Oct;16(5):1783-179
2. Kim SM, Kwon SU, Kim JS, et al. Early infarct growth predicts long-term clinical outcome in ischemic stroke. J Neurol Sci. 2014;347:205–9.
3. Rigual R, Fuentes B, Díez-Tejedor E. Management of acute ischemic stroke. Med Clin (Barc). 2023;161:485–92.

Keywords: Blood–brain barrier; Early infarct growth; Hyperthermia; MRI; Stroke

Acknowledgments: Instituto de Salud Carlos III (ISCIII) (PI17/01103, PI22/00938, ISCIII/PI21/01256/Co-financed by the EU). C Amodeo-Oblitas from the Rio Hortega Program of ISCIII (CM23/00173), and R. Iglesias-Rey (CP22/00061) from the Miguel Servet Program and Co-financed by the EU. EBRAINS 2.0 A Research Infrastructure to Advance Neuroscience and Brain Health

79. Fine-Grained Cytoarchitectonic Parcellation of Broca's Region Supports Functional Differentiation — In Julich-Brain Atlas (EBRAINS)

Nataliia Fedorchenko (C&O Vogt Institute for Brain Research University Hospital Duesseldorf),
Sabine Ruland (Institute for Neuroscience and Medicine (INM-1) Research Centre Juelich),
Hartmut Mohlberg (Institute for Neuroscience and Medicine (INM-1) Research Centre Juelich),
Sebastian Bludau (Institute for Neuroscience and Medicine (INM-1) Research Centre Juelich),
Christian Schiffer (Institute for Neuroscience and Medicine (INM-1) Research Centre Juelich),
Kai Benning (Institute for Neuroscience and Medicine (INM-1) Research Centre Juelich)
Patrick C. Trettenbrein (Max Planck Institute for Human Cognitive and Brain Sciences, Leipzig; Experimental Sign Language Laboratory (SignLab), Department of German Philology, University of Göttingen, Göttingen)
Angela D. Friederici (Max Planck Institute for Human Cognitive and Brain Sciences, Leipzig)
Katrin Amunts (C&O Vogt Institute for Brain Research University Hospital Duesseldorf; Institute for Neuroscience and Medicine (INM-1) Research Centre Juelich);

n.fedorchenko@fz-juelich.de

Introduction
Broca's region plays a key role in language and action processing, yet its classical subdivision into areas 44 and 45 does not fully capture its functional heterogeneity. Existing anatomical maps often lack sufficient granularity and do not adequately reflect interindividual variability. To address this, we performed a detailed cytoarchitectonic parcellation of Broca's region, complemented by 3D reconstruction and layer-specific cell segmentation approaches. The resulting maps will be integrated into the EBRAINS infrastructure to facilitate neuroimaging and brain modelling research.

Methods
Ten post-mortem human brains (5 female, 5 male; age range 30–80 years) were analyzed using an observer-independent, quantitative cytoarchitectonic mapping method (Bludau et al., 2014). This approach identified four subdivisions—44p, 44a, 45p, and 45a—arranged along the anterior-posterior axis of Broca's region. 3D probability maps (PMs), and maximum probability maps (MPMs) were generated in MNI Colin27 and MNI152 stereotaxic reference spaces to capture interindividual spatial variability. Ultra-high-resolution 3D reconstructions were performed using the BigBrain (Amunts et all., 2013) dataset at 1 µm isotropic resolution following the methods of (Schiffer et al., 2021). Layer-specific cell segmentation was conducted using Contour Proposal Networks (CPN), a state-of-the-art object instance segmentation method for biomedical images (Upschulte et al., 2022); quantitative cell counts are pending. Lateralization was quantified by calculating Euclidean distances between left and right homologous subdivisions. Structural relationships with adjacent cortical areas were explored via hierarchical clustering and multidimensional scaling. Functional relevance was assessed by mapping fMRI activation peaks reported in key studies (Goucha & Friederici, 2015; Zaccarella & Friederici, 2015; Papitto et al., 2024). Furthermore, a meta-analysis using MPMs of the four subdivisions as speed regions identified brain areas consistently co-activated during various cognitive and sensorimotor tasks.

Results
The four subdivisions—44p, 44a, 45p, and 45a—were robustly identified and exhibited distinct cytoarchitectonic features. Probabilistic maps showed stable spatial distributions with measurable interindividual variability. BigBrain-based reconstructions provided detailed visualization of microstructural anatomy. Layer-specific cell segmentation delineated cortical layers, with quantitative analysis ongoing. Lateralization analysis revealed left-right spatial asymmetries, with median Euclidean distances of approximately 1.5–2.5 for key subdivisions, supporting known left-hemisphere dominance in language processing. Functional mapping linked 44p primarily with action and syntax,

44a with syntax, and 45p/45a with semantic processing. The meta-analysis further confirmed differential co- activation patterns across the four subdivisions, highlighting their functional specialization.

Conclusions
This work offers a refined cytoarchitectonic parcellation of Broca's region with probabilistic 3D maps, supporting its functional differentiation. Integration with high-resolution 3D reconstructions and layer-specific segmentation advances the microstructural understanding of this critical language areas. Lateralization results align with known hemispheric specialization. All data and maps will be made publicly available via the Julich-Brain Atlas (Amunts et al., 2020) on the EBRAINS platform, promoting FAIR data access and supporting future neuroimaging, brain modeling, and structure-function investigations.

Anknowledgements
This work was in part funded by Max Planck School of Cognition, Leipzig, Germany, as well received a funding from European Union's Horizon 2020 Research and Innovation Programme under ´Grant Agreement No. 101147319 (EBRAINS 2.0 Project) as well as from the Helmholtz Association's Initiative and Networking Fund through the Helmholtz International BigBrain Analytics and Learning laboratory (HIBALL) under the Helmholtz International Lab grant agreement InterLabs-0015

References
1. Bludau, S., Eickhoff, S. B., Mohlberg, H., Caspers, S., Laird, A. R., Fox, P. T., Schleicher, A., Zilles, K., & Amunts, K. (2014). Cytoarchitecture, probability maps and functions of the human frontal pole.
NeuroImage, 93 Pt 2(Pt 2), 260–275. https://doi.org/10.1016/j.neuroimage.2013.05.052
2. Amunts, K., Lepage, C., Borgeat, L., Mohlberg, H., Dickscheid, T., Rousseau, M. É., Bludau, S., Bazin, P. L., Lewis, L. B., Oros-Peusquens, A. M., Shah, N. J., Lippert, T., Zilles, K., & Evans, A. C. (2013). BigBrain: an ultrahigh-resolution 3D human brain model. Science (New York, N.Y.), 340(6139), 1472–1475. https://doi.org/10.1126/science.1235381
3. Christian Schiffer, Hannah Spitzer, Kai Kiwitz, Nina Unger, Konrad Wagstyl, Alan C. Evans, Stefan Harmeling, Katrin Amunts, Timo Dickscheid, Convolutional neural networks for cytoarchitectonic brain mapping at large scale, NeuroImage, Volume 240, 2021, https://doi.org/10.1016/j.neuroimage.2021.118327
4. Upschulte, E., Harmeling, S., Amunts, K., & Dickscheid, T. (2022). Contour proposal networks for biomedical instance segmentation. Medical image analysis, 77, 102371. https://doi.org/10.1016/j.media.2022.102371
5. Goucha, T., & Friederici, A. D. (2015). The language skeleton after dissecting meaning: A functional segregation within Broca's Area. NeuroImage, 114, 294–302. https://doi.org/10.1016/j.neuroimage.2015.04.011
6. Zaccarella, E., & Friederici, A. D. (2015). Merge in the Human Brain: A Sub-Region Based Functional Investigation in the Left Pars Opercularis. Frontiers in psychology, 6, 1818. https://doi.org/10.3389/fpsyg.2015.01818
7. Papitto G, Friederici AD, Zaccarella E. Distinct neural mechanisms for action access and execution in the human brain: insights from an fMRI study. Cereb Cortex. 2024 Apr 1;34(4):bhae163. doi: 10.1093/cercor/bhae163. PMID: 38629799; PMCID: PMC11022341.
8. Amunts, K., Mohlberg, H., Bludau, S., & Zilles, K. (2020). Julich-Brain: A 3D probabilistic atlas of the human brain's cytoarchitecture. Science (New York, N.Y.), 369(6506), 988–992. https://doi.org/10.1126/science.abb458Z

Keywords
Julich-Brain Atlas, Broca's region, EBRAINS, BigBrain; Language

80. „Anxiety like behaviours during periadolescence in mice prenatally treated with levetiracetam and valproic acid“

Podgorac J.

Department of Neurophysiology, Institute for Biological Research „Siniša Stanković“

Introduction: Long run follow-up studies of childrens whose mothers were treated with one or more antiepileptics are insufficient. It’s not only neccessary to evaluate the early psychomotor develepment, adolescence represent the very critical period which demand to be assesse, in particular whereas children were prenatally exposed to neurotropic drug. Treatment of seizures sometimes is challenging task. Eventhough the monotherapy is imperative, especially during gestation, in some cases and conditions, epilepsy demand to be controlled with combinations of two or more antiepileptics. Valproic acid (VPA) has been used for 50 years and if it’s known as teratogen, in treatment of particular seizures couldn’t be replaced. On the other side, levetiracetam (LEV) is relatively new age antiepileptic and belong to category „C“ drugs. In some cases, the combination of these two antiepileptics provide additional effect in seizure treatment. Continuous application of these two antiepileptics during prenatal period should be estimated in descendants, during early development and adolescence.

Aim: According to this, the aim of present study was to assesse anxious/ anxiolytic activity during periadolescence in mice whose mothers were treated with combination of VPA and LEV (ratio 1:1) during breeding and whole gestation.

Method and results: Adult 8-weeks old females, NMRI mice, were used in this study. Two groups of animals were formed: group (8 females) treated with combination of LEV in dose of 211mg/kg/day (LEV-1000) and VPA in dose of 200mg/kg/day (VPA-1000) and control group (10 females) which received corresponding volume of saline (CTR). Performed doses correspond to human doses of 1000mg/day for both antiepileptics. All animals were treated subcutaneously into the skin on the back of the neck twice daily. The treatment was started when males and females were paired and continued during whole gestation period till the females gave birth. After delivery, each female with its litter was housed separately. Animals were separated by sex at day 20. The anxious/ anxioloytic behaviour has been tested in elevated plus maze test (EPMT) on PND37.

Discussion: Offspring exposed to combination of VPA+LEV favored risk assesement behavior in EPMT. Namely, males in group prenatally treated with VPA+LEV, expressed stastistically significant number of digging and streaching corresponding to control, while in female offspring prenatally exposed to combination of antiepileptics statistically observed was the number of digging. Considering positive correlation between hyperactivity and some specific behavioral characteristics of periadolescence, early identification and correction of different behavioural patterns in youngs prenatally treated with antiepileptic combinations.

This study was supported by the Ministry of Science, Technological Development and Innovation of the Republic of Serbia (Contract No. 451-03-136/2025-03/200007).

The results presented in this manuscript are in line with Sustainable Development Goal 3 (Good Health and Well-being) of the United Nations 2030 Agenda.

81. Sleep Quality And Cognitive Performance In Smartme&You Games In Alzheimer’s And Parkinson’s

Veronica Henao Isaza[1], Mina De Bartolo[1], Matteo Carpi[1], Roberta Lizio[1], Claudio Del Percio[1], Susanna Lopez[1], Burcu Bolukbas[1], Antonio Pio Afragola[1], Filippo Carducci[1], Giuseppe Noce[2], Paolo Barone[2,3], Arianna Cappiello[3], Angelo Barone[3], Angelo Antonini[4], Simone Cauzzo[4], Fabrizio Stocchi[5], Chiara Coletti[5], Francesco Infarinato[5], Giacomo Maria Russo[6], Cristina Ranallo[6], Michela Bonaccorsi[6], Andrea Rosati[7], Andrea Baldas[7], Vittorio Luigi Diana[7], Delia Passalaqua[8], Sabrina Tommassini[8], Eleonora Fiorenzato[4], Claudio Babiloni[1,9]

[1] Department of Physiology and Pharmacology "Vittorio Erspamer", Sapienza University of Rome, Rome, Italy, [2] IRCCS Synlab SDN, Naples, Italy, [3] Center for Neurodegenerative Diseases-CEMAND, UNISA, Salerno, Italy, [4] Parkinson and Movement Disorders Unit, Study Center for Neurodegeneration (CESNE), Center for Rare Neurological Diseases (ERN-RND), Department of Neuroscience, University of Padua, Padua, Italy, [5] IRCCS San Raffaele, Rome, Italy, [6] Sentech S.r.L., Rome, Italy, [7] Sogetel S.r.L., Rome, Italy, [8] Consortium GARR, Rome, Italy, [9] Hospital San Raffaele Cassino, Cassino, Italy

Introduction:
Sleep disturbances are common in neurodegenerative disorders and may exacerbate cognitive decline. We hypothesized that sleep quality, objectively measured by smartwatches during home telemonitoring, would be associated with performance in unsupervised serious video games assessing cognitive function in patients with mild cognitive deficits or mild-to-moderate dementia due to Alzheimer's disease (ADCD) and Parkinson's disease (PDCD).

Methods:
Data were collected from 11 healthy controls (Healthy), 37 participants with ADCD, and 47 with PDCD. All participants underwent standard clinical, neuropsychological, and instrumental assessments, including EEG and MRI, in hospital settings. They also completed one week of home telemonitoring using the SmartMe&You platform, which included seven unsupervised cognitive video games administered via tablet and continuous sleep monitoring with Samsung Galaxy Watch6 smartwatches. Global cognition was evaluated using the Mini-Mental State Examination (MMSE). Between-group comparisons were performed using t-tests, Mann–Whitney U, or Fisher's exact tests, and associations between sleep quality and performance accuracy were assessed using general linear models.

Table 1

DEMOGRAPHIC AND CLINICAL DATA				
	Healthy	**ADCD**	**PDCD**	**Statistical analyses**
N	11	37	47	-
Age (years)	70.5 ± 7.3	75.0 ± 6.5	74.0 ± 7.2	t-test PDCD vs ADCD: p=0.946 PDCD vs Healthy: p=0.169 ADCD vs Healthy: p=0.161
Sex (M/F)	3/8	21/16	34/13	Fisher's test PDCD vs ADCD: p = 0.040* PDCD vs Healthy: p = 0.005* ADCD vs Healthy: p = 0.182
Educat-ion (years)	14.7 ± 3.3	11.2 ± 5.5	11.1 ± 4.4	t-test PDCD vs ADCD: p = 0.416 PDCD vs Healthy: p = 0.007* ADCD vs Healthy: p = 0.053
MMSE Score	29.2 ± 1.0	21.4 ± 6.6	26.0 ± 3.4	Mann-Whitney PDCD vs ADCD: p < 0.001* PDCD vs Healthy: p < 0.001* ADCD vs Healthy: p < 0.001*

Quality Sleep	76.1 ± 14.2	67.2 ± 14.7	54.3 ± 16.2	t-test PDCD vs ADCD: $p < 0.001$* PDCD vs Healthy: $p < 0.001$* ADCD vs Healthy: $p = 0.066$

Table 1. Mean values (± SD) of demographic and clinical data, and results of statistical comparisons ($p < 0.05$) between Healthy participants and patients with ADCD and PDCD. Abbreviations: Healthy = cognitively unimpaired older adults; ADCD = patients with mild cognitive impairment and mild-moderate dementia due to Alzheimer's disease; PDCD = patients with mild cognitive impairment and mild-moderate dementia due to Parkinson's disease; MMSE = Mini-Mental State Examination; SD = standard error; n.s. = not significant ($p > 0.05$).

Results:
Sleep quality was significantly reduced in patients with PDCD (54.3 ± 16.2) compared to ADCD (67.2 ± 14.7) and Healthy controls (76.1 ± 14.2; $p < 0.001$). Across all participants, higher sleep quality was positively correlated with better average accuracy across all SmartMe&You games ($r = 0.229$, $p < 0.05$). However, the association between sleep quality and MMSE scores did not reach significance ($p > 0.05$).

Discussion/Conclusions:
Our findings demonstrate that sleep quality, objectively monitored through wearable technology, is linked to cognitive performance in unsupervised home-based tasks in older adults with and without neurodegenerative disease. The *SmartMe&You* telemonitoring platform provides a feasible, low-cost, and ecologically valid approach for assessing sleep and cognition remotely. This integrated system holds promise for both early detection of cognitive decline and tertiary prevention strategies in patients with ADCD and PDCD.

Figure 1. Scatterplots illustrating the relationship between night sleep quality and mean performance accuracy (%) in the serious video games of the SmartMe&You home telemonitoring platform for Healthy participants and patients with ADCD and PDCD. Sleep quality was measured over one week using the Samsung Galaxy Watch6 smartwatches. SmartMe&You's serious video games are implemented on commercial tablets. Abbreviations: Healthy = cognitively unimpaired older adults; ADCD = patients with mild cognitive impairment and mild-moderate dementia due to Alzheimer's disease; PDCD = patients with mild cognitive impairment and mild-moderate dementia due to Parkinson's disease; MMSE = Mini-Mental State Examination.

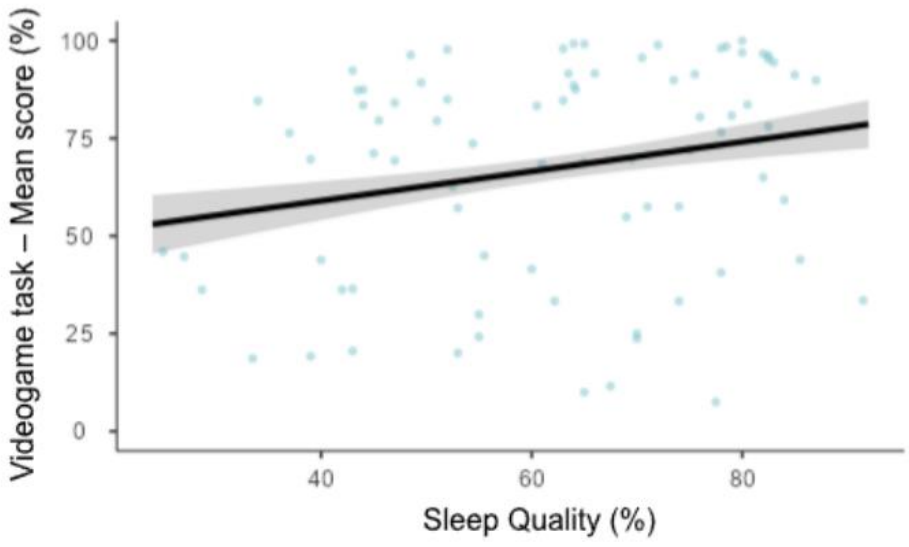

Acknowledgments: We thank all the participating institutions for their collaboration: Sapienza University of Rome, IRCCS Synlab SDN, University of Salerno (CEMAND), University of Padua, IRCCS San Raffaele Rome, Sentech S.r.L., Sogetel S.r.L., Consortium GARR, and Hospital San Raffaele Cassino. This work was supported by the EBRAINS Research Infrastructure.

82. High-resolution 3D Mapping of the Human Hypothalamus:Towards a Comprehensive Cytoarchitectonic Atlas

Alexey Chervonnyy[1*], Christian Schiffer[2], Eric Upschulte[1,2], Sebastian Bludau[2], Hartmut Mohlberg[2], Katrin Amunts[1,2]

Affiliations: [1]Cécile and Oskar Vogt Institute of Brain Research, Heinrich Heine University Düsseldorf, Germany, [2]Institute of Neuroscience and Medicine (INM-1), Research Centre Jülich, Germany
*Alexey.Chervonnyy@hhu.de

INTRODUCTION/MOTIVATION

The hypothalamus is crucial for maintaining homeostasis, regulating sleep-wake cycles, appetite, circadian rhythm, and thermal regulation[1]. Despite its importance, its structural organization, precise boundaries, and functional differentiation of nuclei remain incompletely understood. Existing anatomical maps of the hypothalamus do not reflect interindividual variability in 3D space; they often lack the spatial resolution and morphological detail to provide a comprehensive understanding of this complex region and to inform neuroimaging studies about the microstructure. Therefore, we aimed to develop probabilistic cytoarchitectonic maps to address intersubject variability and provide a high-resolution 3D map of the hypothalamus to neuroimaging studies of the living human brain.

METHODS

Using every 15th cell body stained brain section (1 µm resolution) from 10 postmortem brains (5 female), including the BigBrain dataset[2], we delineated the hypothalamus and its nuclei. For the BigBrain dataset, a deep learning–based tool[3] was employed to delineate the remaining sections and create a continuous high-resolution 3D model. Delineated nuclei were 3D-reconstructed and superimposed in standard reference space[4], and corresponding probability maps were generated to quantify intersubject variability in their size and spatial location.

To further characterise cytoarchitectonic features of nuclei, we performed texture analysis[5] on 6,709 regions of interest derived from the initial delineations, employing the Gray Level Co-occurrence Matrix method[6] to quantify local spatial relationships and intensity distributions in grayscale images. Differences between hypothalamic subdivisions were assessed using the independent-samples Kruskal-Wallis test. In parallel, neurons were segmented using a Contour Proposal Network based on Fourier Descriptors[7], enabling precise measurements of neuron number, size, and morphology.

RESULTS AND DISCUSSION

We generated a high-resolution 3D map of 23 nuclei of the human hypothalamus, that show their shapes and neighbourhood relationships with high precision (Fig. 1). Intersubject variability was reflected in the probabilistic maps, which will be made openly available as part of the Julich-Brain Atlas[4] and accessible via EBRAINS and other platforms.

Principal Component Analysis (PCA; SPSS v.29) identified four main components explaining 87.27% of the total variance. Significant differences in at least one main component were observed between all adjacent nuclei, supporting their delineation. For visualisation, we generated a heatmap (Fig.2) indicating levels of cytoarchitectural difference: a score of 0 showed no significant differences, while a score of 4 indicated pronounced disparities across all components. In addition, some more distant nuclei, such as the uncinate and suprachiasmatic nuclei, showed no significant differences in the

PCA components. These cytoarchitectural similarities may suggest functional connectivity between distant nuclei and warrant further investigation of their interactions. The contour proposal network enabled pixel-level labeling of cells in microscopic images, facilitating the identification of individual neurons. Using the extracted data, such as the number of neurons and their size, we calculated the cell packing density and observed the highest density in the supraoptic nucleus and the lowest in the lateral tuberal nucleus, which was three times less dense.

In summary, the new maps of the hypothalamus with its 23 nuclei provide highly detailed reference data on its structure, intersubjective variability and localization in the standard reference space. This resource will support the identification of microstructural correlates of functional and connectivity data in both healthy individuals and patients.

Figure 1

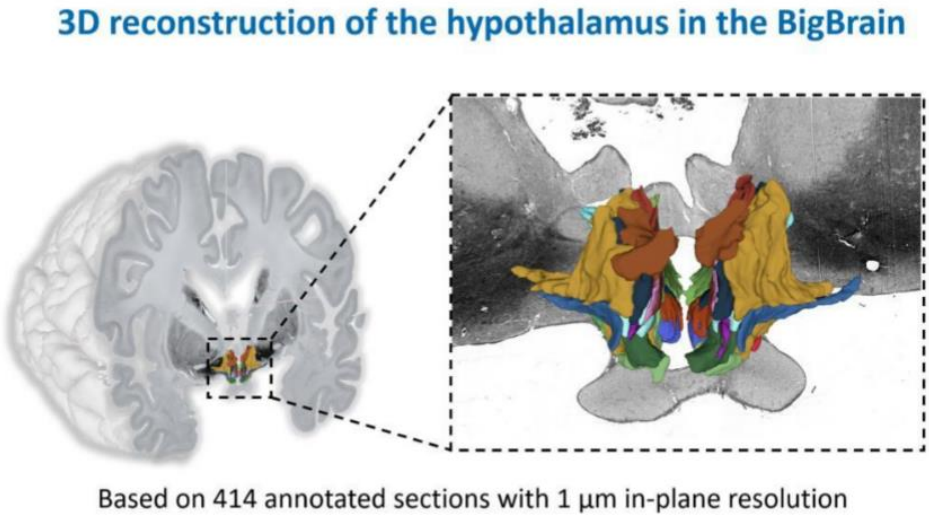

Figure 2

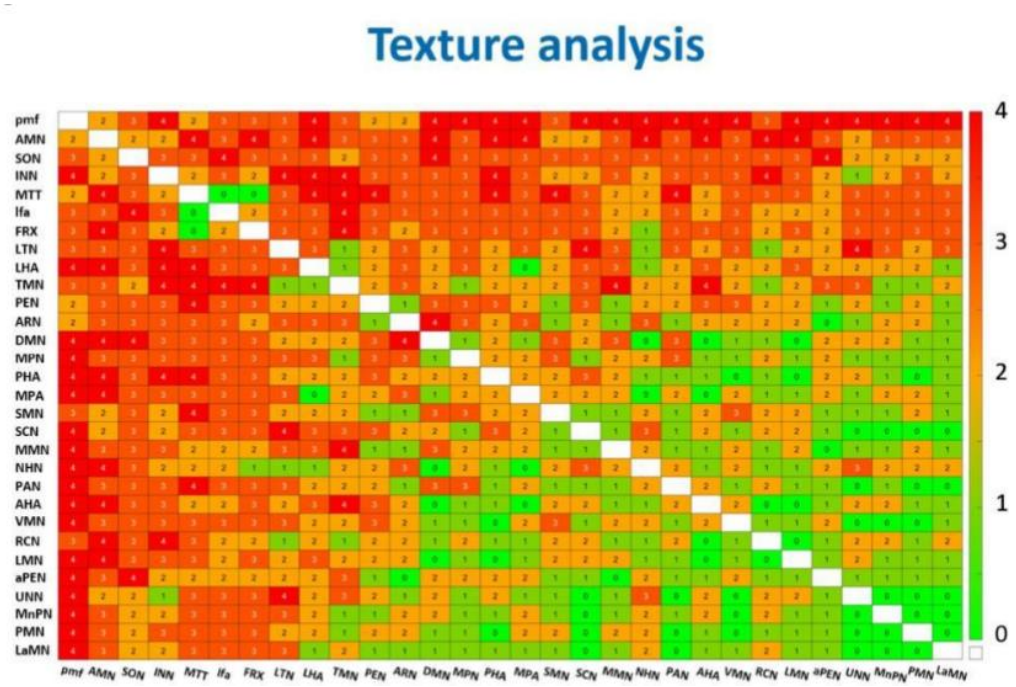

Keywords: <hypothalamus>, <cytoarchitecture>, <probabilistic mapping>, <3D reconstruction>, <BigBrain>, <texture analysis>, <cell segmentation>, <Julich-Brain atlas>

REFERENCES
1. Nieuwenhuys, R., Voogd, J., van Huijzen, C., & Papa, M. (2010). The Human Central Nervous System. Springer-Verlag Italia. https://doi.org/10.1007/978-88-470-1140-3
2. Amunts, K., Lepage, C., Borgeat, L., Mohlberg, H., Dickscheid, T., Rousseau, M. É., Bludau, S., Bazin, P. L., Lewis, L. B., Oros-Peusquens, A. M., Shah, N. J., Lippert, T., Zilles, K., & Evans, A. C. (2013). BigBrain: an ultrahigh-resolution 3D human brain model. Science (New York, N.Y.), 340(6139), 1472–1475. https://doi.org/10.1126/science.1235381
3. Schiffer, C., Spitzer, H., Kiwitz, K., Unger, N., Wagstyl, K., Evans, A. C., Harmeling, S., Amunts, K., & Dickscheid, T. (2021). Convolutional neural networks for cytoarchitectonic brain mapping at large scale. NeuroImage, 240, 118327. https://doi.org/10.1016/j.neuroimage.2021.118327
4. Amunts, K., Mohlberg, H., Bludau, S., & Zilles, K. (2020). Julich-Brain: A 3D probabilistic atlas of the human brain's cytoarchitecture. Science, 369(6506), 988–992. https://doi.org/10.1126/SCIENCE.ABB4588
5. Kedo, O., Bludau, S., Schiffer, C., Mohlberg, H., Dickscheid, T., & Amunts, K. (2024). Cytoarchitectonic Analysis and 3D Maps of the Mesial Piriform Region in the Human Brain. Anatomia, 3(2), 68-92. https://doi.org/10.3390/anatomia3020007
6. Löfstedt T, Brynolfsson P, Asklund T, Nyholm T, Garpebring A (2019) Gray-level invariant Haralick texture features. PLoS ONE 14(2): e0212110. https://doi.org/10.1371/journal.pone.0212110
7. Upschulte, E., Harmeling, S., Amunts, K., & Dickscheid, T. (2022). Contour proposal networks for biomedical instance segmentation. Medical image analysis, 77, 102371. https://doi.org/10.1016/j.media.2022.102371

83. A 3D brain atlas of Pogona vitticeps for investigating sleep regulation

Authors and Affiliations
Hsing-Hsi Li[1], Takehito Tomita[1], Anja Arends[1], Michaela Klinkmann[1], Jennifer Knop[1], Christina Thum[1], Florian Vollrath[1], Friedrich Kretschmer[1], Gilles Laurent[1]

1 Max Planck Institute for Brain Research, Frankfurt am Main, Germany

Abstract
Introduction
Brain atlases are essential for understanding neural organization and function [1]. While 2D histology provides cellular detail, it lacks spatial context, highlighting the need for 3D representations. The bearded dragon (*Pogona vitticeps*) exhibits a two-stage sleep pattern resembling simplified slow-wave and REM sleep in mammals, alternating in ~80 sec cycles [2], making it a tractable model to study neural mechanisms underlying sleep-state transitions. However, detailed anatomical and functional information on sleep-related brain structures and circuits in *Pogona* is lacking.

Methods
To address this gap, we applied neuronal markers identified in mammalian studies to map homologous brain regions in *Pogona* using immunohistochemistry (IHC) and fluorescence in situ hybridization (FISH) [3]. We constructed a multimodal 3D brain atlas integrating four complementary datasets: whole-brain µCT for structural reference, serial 2D Nissl-stained sections for cytoarchitecture, and HCR FISH with iDISCO clearing to visualize modulatory systems. All datasets were co-registered in 3D Slicer [4] using landmark-based thin-plate spline alignment to the CT volume. Immediate early gene (*EGR1*) expression mapping was used to assess functional differentiation across regions.

Results

The integrated atlas delineates over 25 distinct regions, including forebrain, hypothalamic, and brainstem nuclei that share features with mammalian systems, suggesting conserved regulatory mechanisms. *EGR1* mapping revealed neural activity during wakefulness and sleep as either intermingled or clustered into functional domains; the claustrum exemplifies such localized activity patterns (Figure 2). These data indicate diverse neuron types, connectivity motifs, and local circuits contributing to sleep-state regulation.

Discussion

This study provides the first structural and functional maps of the *Pogona* brain, bridging a critical gap between reptilian and mammalian sleep research. Although the atlas remains incomplete in regional delineation and functional coverage, it establishes a multimodal 3D framework for future mapping of neural activity, connectivity, and gene expression dynamics. Beyond evolutionary neuroscience, this resource offers a scalable platform for comparative and functional studies, supporting broader efforts to link brain structure to behavioral state regulation across vertebrates.

Keywords: *Pogona vitticeps*, 3D brain atlas, Multimodal imaging, Neuroanatomy / Functional mapping, Comparative neuroscience, Sleep-state regulation

Reference

1. Amunts K, Mohlberg H, Bludau S, Zilles K. Julich-Brain: A 3D probabilistic atlas of the human brain's cytoarchitecture. Science 2020;369(6506):988-92 doi: doi:10.1126/science.abb4588.
2. Shein-Idelson M, Ondracek JM, Liaw HP, Reiter S, Laurent G. Slow waves, sharp waves, ripples, and REM in sleeping dragons. Science 2016;352(6285):590-5 doi: 10.1126/science.aaf3621.
3. Norimoto H, Fenk LA, Li H-H, et al. A claustrum in reptiles and its role in slow-wave sleep. Nature 2020;578(7795):413-18 doi: 10.1038/s41586-020-1993-6.
4. Fedorov A, Beichel R, Kalpathy-Cramer J, et al. 3D Slicer as an image computing platform for the Quantitative Imaging Network. Magnetic Resonance Imaging 2012;30(9):1323-41 doi: https://doi.org/10.1016/j.mri.2012.05.001.

Figures

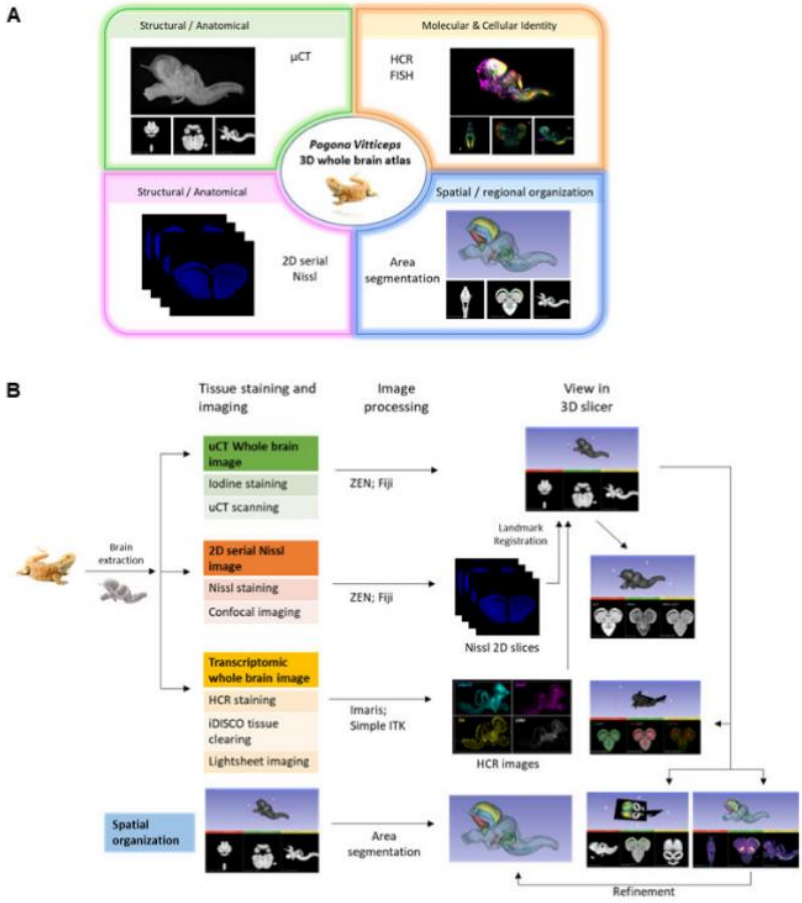

Figure 1 Workflow for constructing a multimodal 3D atlas of the *Pogona* brain.
(A) Four datasets integrated into the 3D atlas: whole-brain µCT, serial Nissl sections, HCR FISH with iDISCO clearing, and the organization of identified anatomical areas. **(B)** Workflow illustrating tissue preparation, imaging, and processing steps. Serial Nissl sections and HCR-cleared whole-brain images were aligned and registered to the µCT volume. Brain region boundaries were delineated using segmentation functions in 3D Slicer and refined based on HCR FISH gene expression patterns.

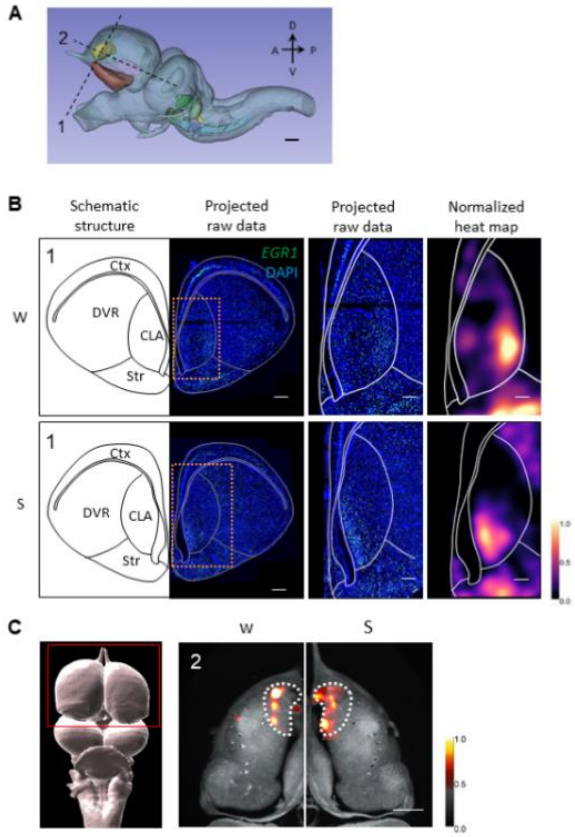

Figure 2 Anatomical and functional mapping in the claustrum (CLA).
(A) Sagittal view of the Pogona brain showing identified areas. The dashed line indicates the cutting level and angle for panels B and C. Scale bar: 1 mm. **(B)** *EGR1* expression in the CLA. Left: schematic of anterior forebrain regions; right: *EGR1* expression during wakefulness (W, top) and sleep (S, bottom). Scale bar: whole slice, 500 µm, magnified view: 200 µm. **(C)** Representative 3D reconstructed EGR1 heatmap of the CLA from one lizard during W (left) and S (right). Left panel: cropped region corresponding to the right panel. The number "2" indicates the transverse section in panel A. White dashed line marks the CLA boundary. Scale bar: 1 mm. Calibration bars in panels B and C show normalized EGR1 density.
Abbreviations: CLA, claustrum; Ctx, cortex; DVR, dorsal ventricular ridge; Str, striatum.

84. Going 3D with AI: Full 3D Reconstructions of Cytoarchitectonic Maps in BigBrain

Authors: Kimberley Lothmann[1,3], Christian Schiffer[1,2], Timo Dickscheid[1,2], Katrin Amunts[1,3]

Affiliations:
1 Institute of Neuroscience and Medicine (INM-1), Research Centre Jülich, Jülich, Germany
2 Helmholtz AI, Research Centre Jülich, Jülich, Germany
3 Cécile and Oskar Vogt Institute for Brain Research, University Hospital Düsseldorf, Düsseldorf, Germany

Abstract:

Introduction:
As part of the Julich-Brain Atlas (Amunts et al., 2020), the BigBrain dataset (Amunts et al., 2013) provides the first ultrahigh-resolution 3D model of the human brain at 20 µm isotropic resolution,

reconstructed from 7,404 histological sections. It enables cytoarchitectonic mapping at a level of detail that bridges microscopic organization with macroscale imaging. Traditionally, areas have been delineated on 2D sections, limiting their integration into 3D brain reference spaces.

Methods:
We developed a hybrid workflow combining expert identification of cortical areas with deep learning-based 3D reconstruction. Using the ATLaSUI interface (Schiffer et al., 2021), neuroscientists annotated every 10th – 15th histological section, providing training data for the CytoNet model (manuscript in preparation). CytoNet infers cortical layer continuity and areal boundaries between annotated sections, avoiding geometric interpolation and preserving cytoarchitectonic detail. Large-scale model inference and reconstruction were performed on the JURECA-DC supercomputer (Jülich Supercomputing Centre).

Results:
Currently, 33 cortical BigBrain areas are publicly available through the siibra tool suite and EBRAINS Knowledge Graph. An additional 56 cortical areas, including eight newly mapped regions, were reconstructed at 20 µm resolution, expanding the Julich-Brain Atlas to a total of 98 BigBrain areas. All maps will be openly accessible via EBRAINS, enabling interactive and programmatic exploration within a unified reference framework.

Discussion:
Since areas were reconstructed independently, minor overlaps can occur at region borders, especially in highly folded cortical zones. Sampling every 10th – 15th section may also introduce interpolation artifacts in regions with steep cytoarchitectonic transitions. Future work will focus on multi-area optimization to reduce boundary inconsistencies and improve 3D continuity. These ongoing developments advance the integration of microstructural and macroscale brain data within a coherent human brain reference space.

Keywords: BigBrain, Julich Brain Atlas, Cytoarchitecture, 3D Reconstruction, Deep Learning, Human Brain Atlas, EBRAINS

References
Amunts K, Lepage C, Borgeat L, et al. BigBrain: An ultrahigh-resolution 3D human brain model. Science. 2013;340(6139):1472-1475. doi:10.1126/science.1235381

Amunts K, Mohlberg H, Bludau S, Zilles K. Julich-Brain: A 3D probabilistic atlas of the human brain's cytoarchitecture. Science. 2020;369(6506):988-992. doi:10.1126/science.abb4588

Schiffer C, Spitzer H, Kiwitz K, et al. Convolutional neural networks for cytoarchitectonic brain mapping at large scale. Neuroimage. 2021;240:118327. doi:10.1016/j.neuroimage.2021.118327

Acknowledgments:
This project received funding from the European Union's Horizon 2020 Research and Innovation Programme, grant agreement 101147319 (EBRAINS 2.0 Project), the Helmholtz Association port-folio theme "Supercomputing and Modeling for the Human Brain", the Helmholtz Association's Initiative and Networking Fund through the Helmholtz International BigBrain Analytics and Learning Laboratory (HIBALL) under the Helmholtz International Lab grant agreement InterLabs-0015, from HELMHOLTZ IMAGING, a platform of the Helmholtz Information \& Data Science Incubator [X-BRAIN, grant number: ZT-I-PF-4-061], and from the Deutsche Forschungsgemeinschaft (DFG, German Research Foundation) under the National Research Data Infrastructure – NFDI 46/1 – 501864659.

85. Medical Informatics Platform (MIP) Infrastructure as Code: From Virtual Machine based deployments to managed Kubernetes for secure, federated neuro-statistical analyses

Julien Dhallenne[1*], Konstantinos Filippopolitis[2], Evita Mailli[2*], Thanasis Karampatsis[2], Yannis Ioannidis[2], Philippe Ryvlin[1]

AFFILIATIONS

1. Centre hospitalier universitaire Vaudois (CHUV), Centre de Recherche en Neurosciences Cliniques (CRN), Lausanne, Switzerland
2. ATHENA Research Center, Athens, Greece Corresponding authors:

*julien.dhallenne@chuv.ch, e.mailli@athenarc.gr

INTRODUCTION

Collaborative neuroscience requires infrastructures that let hospitals keep data on-site while still participating in cross-site studies. The first-generation Medical Informatics Platform (MIP) (https://mip.ebrains.eu), built on Virtual Machines, highlighted challenges around deployment speed, operational resilience, and scalability. We present 'MIP Infrastructure as Code (IaC)', a new version running on a managed Kubernetes cluster and leveraging modern IaC practices, designed to make federation setup faster, more reliable, and more secure.

METHODS

Instead of manual server configuration, all deployments are now handled automatically through GitOps – continuous deployment for cloud native applications - tools ArgoCD [1] and Helm [2]. Each federation runs in its own dedicated namespace - a separate, self- contained workspace - ensuring clear isolation and easy reproducibility. Each federation runs in its own secure environment, with hospital sites able to connect from lightweight clusters with the use of Submariner [3]. To keep everything safe and reliable, we use strong access control, continuous image scanning, and regular security audits. In practice, this is implemented with EBRAINS Keycloak for access control, EBRAINS Harbor for container image scanning, and periodic checks against security benchmarks. Additional hardening follows the CIS Kubernetes Benchmark, using kube-bench and OS-level Ansible playbooks from https://github.com/NeuroTech-Platform/linux-server-management.

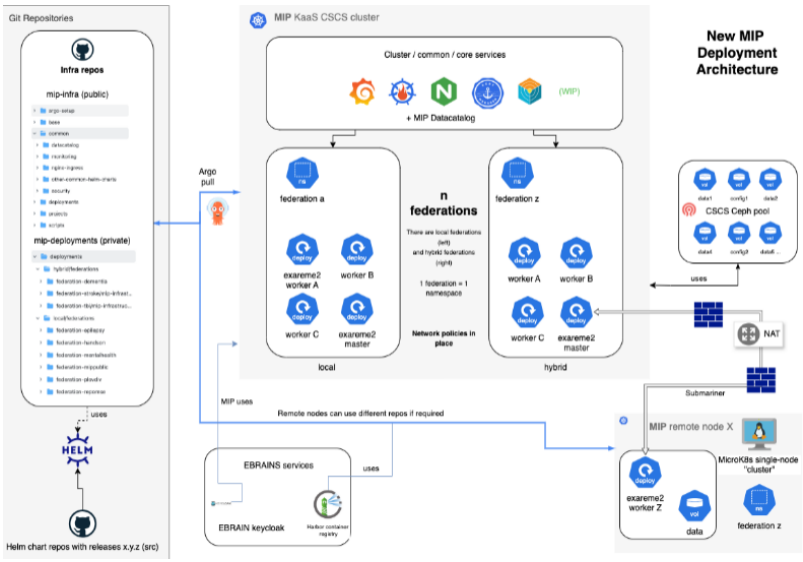

Figure 1: Overview of the new MIP deployment architecture integrating GitOps

RESULTS AND DISCUSSION

The shift from VMs to managed Kubernetes has reduced deployment time from days to under thirty minutes. New sites can join with a single configuration step, and the cluster automatically recovers from node failures, ensuring uninterrupted service. By distributing workloads more efficiently, the infrastructure not only minimizes wasted resources but also moves toward a sustainable, demand-driven model where resource usage closely follows actual workload needs.

Aspect	*Legacy VM-based Setup*	*MIP IaC on Managed Kubernetes*
Deployment time	Days, manual setup	< 30 minutes, automated via GitOps
Deployment ease	Manual SSH access, error-prone	Automated, infrastructure-agnostic
Resilience	Node failure disrupted services	Self-healing: workloads automatically recover
Resource utilisation	Static, inefficient	Dynamic, balanced workloads
Security & auditing	Limited, manual	Integrated (ECK, CIS checks)

Figure 2: Legacy VM setup vs. IaC, highlighting faster deployment, resilience, efficiency, and built-in security.

In practice, the infrastructure already supports six local federations and one hybrid federation, with hospital partners joining through simple, one-node clusters. The infrastructure code is available at https://github.com/NeuroTech-Platform/mip-infra. MIP IaC integrates security and reproducibility through EBRAINS services, while ongoing work addresses SATRE [4] specification Trusted Research Environment security requirements, enhanced encryption, and supply chain security. This approach demonstrates how cloud-native infrastructure can meet hospital-grade research requirements and scale up to enable large, federated neuroscience research. We invite additional clinical centres to evaluate the platform and contribute to its roadmap.

KEYWORDS

Federated analytics, Kubernetes, Infrastructure-as-Code, GitOps, Exareme2, neuroinformatics, security, FAIR, EBRAINS, HPC, CIS, SATRE

ACKNOWLEDGEMENTS

This project has received funding from the EU's Horizon 2020 Framework Partnership Agreement No. 650003 (Human Brain Project) and Horizon Europe Grant No. 101147319 (EBRAINS 2.0). It is co-funded by the Swiss SERI (Contract No. 23.00638).

REFERENCES

[1] Argo CD. (n.d.). Argo CD – Declarative GitOps Continuous Delivery for Kubernetes. Retrieved September 29, 2025, from: https://argo-cd.readthedocs.io/en/stable/

[2] Helm. (n.d.). Helm – The package manager for Kubernetes. Retrieved September 29, 2025, from: https://helm.sh/

[3] Submariner. (n.d.). Submariner – Cross-cluster networking for Kubernetes. Retrieved September 29, 2025, from: https://submariner.io/

[4] Johnston, J., Sheane, S., Almond, E., Whiting, A., Higgins, D., Nadin, R., Hagen, J.-A., & Billins, T. (2025). SATRE Centric Control Alignment Table for Trusted Research Environments. TRE Community, Leeds. Zenodo. https://doi.org/10.5281/zenodo.16837077